Design Optimisation of Steel Portal Frames Using Modified Distributed Genetic Algorithms

Honar Khoshavi Issa

A thesis submitted in partial fulfilment of the requirements of the Nottingham Trent University for the degree of Doctor of Philosophy

March 2010

Dedicated To:

My parents who have taught me how to be, have let me do what I love, and love me just the way that I am. My wife who has understood the situation. The soul of 'Mustafa Barzani', the father of Kurds, who in spite of his pivotal role in the development and recognition of Kurds sense of identity, had lived a modest life. Those innocent lives, whose hopes and dreams were brutally taken away from them during the notorious 'Anfal Campaign' in Kurdistan of Iraq, and savagely cut short in 'Halabja' by chemical bombardment.

Copyright Statement

Acknowledgements

It would not have been possible to write this doctoral thesis without the help and support of the kind people around me, to only some of whom it is possible to give particular mention here.

Above all, I would like to thank my charming wife, Samira, for her personal support and great patience at all times. My parents, brothers, and friends have given me their unequivocal support throughout, as always, for which my mere expression of thanks likewise does not suffice.

This research would have not been possible without the moral and material support of his Excellency the prime minister for Kurdistan Regional Government, kak Nechirvan Barzani. My special thanks go to his active advisors, kak Ijra Saeid, kak Nazat Salih, and kak Fahmi Mohammd-faqe for their wonderful support and encouragement.

This thesis would not have been possible without the help, support and patience of my director of study, Dr. Fouad Mohammad, not to mention his priceless advice and insightful knowledge of structural optimisation. The good advice, support and friendship of my second supervisor, Dr. Mark Breach, and third supervisor, Dr. Anton Ianakiev have been invaluable on both an academic and a personal level, for which I am extremely grateful.

I would like to acknowledge the academic and technical support of the Nottingham Trent University, School of Architecture, Design, and the Built Environment, in particular the support of staff in the Research Studies Office.

And finally, I would like to express special thanks to my fellow PhD students in the Research Studies office especially Guy Birkin, a PhD student in Art and Design and Mathew Malpass, a PhD student in Product Design, for their invaluable support and help during this study.

Abstract

Distributed genetic algorithms have been modified in this study to improve their quality, performance, and convergence to the optimum solution for structural steel frames. This was achieved by introducing some novelties of the main algorithm of distributed genetic algorithms and applying them in structural optimisation. Among these are the creation of new mutation schemes, adding a crossover scheme, definition of a penalty function, properties of twins, and definition of the reproduction scheme.

Many optimisation problems have been designed to minimise the weight of a steel structure and are well documented in the literature. However, having a frame controlled by displacement will necessitate choosing a different approach for the objective function. In addition to weight minimisation, attempts have been made to investigate displacement maximisation and this also forms part of the novelty of this study. Various steel frames in terms of geometry and loading conditions are considered during the optimisation process and they are assumed to have rigid and/or semi-rigid connections. The design optimisations are conducted according to the requirements of both BS 5950 and EC3 codes of practice. A stiffness matrix is developed for a non-prismatic member that is involved in the analysis process.

A program DO-DGA, written in Visual Basic 6.0, has been developed to include all aspects of the modified distributed genetic algorithms as well as the decided terms for the analysis, such as the types of connections, the geometry of members, and the type of design problem; minimisation or maximisation. The performance of the developed algorithm is validated by comparing the optimum solutions obtained with the results published in the literature.

The results of tests indicate that the developed algorithm is robust and efficient in seeking the optimum solutions within a reasonable time. They also reveal that the weight minimisation outperforms the displacement maximisation and the haunched-rafter steel portal frame with rigid connections yields a lighter frame than one with semi-rigid connections. In general, the design optimisation according to EC3

demonstrates that a lighter frame can be achieved comparing with the design optimisation according to BS 5950.

Key words: Steel Portal Frames, Structural Optimisation, Distributed Genetic Algorithms, Weight Minimisation, Displacement Maximisation

List of Contents

List of Figures

List of Tables

Nomenclatures

Chapter 2

A_1	cross sectional area of one end of member
A_2	cross sectional area of the other end of member
a_0, a_1, and a_2	constants
E	modulus of elasticity
I_1 and I_2	moments of inertia of the member ends
k	stiffness of the member due to the axial force
T	symbol of transpose
u_m	final axial displacement of the member
x_i	independent variable
y_i	dependent variable
$\{D\}$	global displacement vector
$\{d\}$	displacement vector
$\{F\}$	global force vector
$\{f\}$	member force vector
$[k]$	member stiffness matrix
[K]	global stiffness matrix and can be formulated as:
$[T]$	transformation matrix
Δd	difference between the depths of member ends
δu_m	axial displacement of the member
ε_x	axial strain

Chapter 3

A_s	bolt net area
b	vertical distance between the centre of tension bolts and the centre line of beam tension flange
b_{fb}	flange width of beam
b_p	width of end plate
C_1, C_2, and C_3	parameters obtained by curve fitting

d	depth of beam section
d_a	height of single end plate
d_b	depth of the beam
d_b	diameter of bolts
d_{bolt}	nominal bolt diameter
d_g	distance between the far tension and compression bolts
dp	depth of plate in the header plate connections
E	modulus of elasticity
EI	bending rigidity of the connected beam
g	distance between the centre of bolts in the same row
h_b	beam section height
h_{wb}	web height of beam
I	second moment of area of the member cross-section
K	standardization parameter
$K_{eq\text{-}endplate}$	end plate equivalent initial stiffness in bending
$K_{eq\text{-}plate}$	bolt equivalent initial stiffness in bending
k_i	stiffness coefficient of the basic joint component i
k_σ	buckling factor
L	length of beam
l_a	width of end plate
L_{bolt}	length of bolt
M	applied bending moment
M_{Fi} and M_{Fj}	fixed end moments
M_i and M_j	bending moment at ends i and j
M_p	plastic moment capacity of the connected beam
M_{SRi} and M_{SRj}	semi-fixed end moments
M_u	ultimate bending moment capacity of connection
m	horizontal distance between the centre of the tension bolt and beam web-effective fillet weld
n	shape parameter
R_k	slope of the M-θ_r curve naming as initial stiffness
R_{ki} and R_{kj}	initial connection stiffness of the member ends
t	thickness of the top seat angle section
t_a	gap between the beam end and the face of column

t_c	thickness of web angle
t_{fb}	flange thickness of beam
t_p	thickness of end plate
t_w	web thickness of beam
t_{wb}	web thickness of beam
z	vertical distance between the centre of tension bolts and centre line of the compression flange
α_1, α_2, …, and α_8	dimensionless coefficients
Δ	relative lateral displacements of ends A and B
θ_A	slope angle of member end A
θ_B	slope angle of member end B
θ_r	rotation of the connection
θ_{ri} and θ_{rj}	rotations at the member ends

Chapter 4

A	gross cross-sectional area
$A_{c,eff}$	effective area of a flat compression element
A_e	effective area of the section
A_{eff}	effective area of the section
A_g	gross area of the section
A_n	net area of the section
A_v	shear area of the section
A_x	cross-sectional area at the section considered
A_y	area of the cross-section
a	distance between transverse stiffeners
B_f	breadth of the flange
$\bar{b}$	appropriate width depending on the cross-section element
C_1	coefficient which takes into account the moment gradient along the beam
c	coefficient
D	total depth of section
d	depth of the web
d_w	depth between the fillet

E	effect of actions
E	modulus of elasticity
E_{d}	design value of effect of actions
e_{Ny}	distance between the neutral axis of gross cross-section and neutral axis of effective cross-section.
F_c	applied compressive force
F_t	applied tensile force
F_{v}	applied shear force
f	reduction coefficient
f_u	ultimate tensile stress
f_y	yield stress
f_{yf}	yield strength of the flange
G	shear modulus
$G_{\mathrm{k,j}}$	characteristic value of permanent action j
h	clear height of the column
h_{r}	height of the apex above the top of columns
h_w	height of web
I	moment of inertia of the whole cross-section
I_w	warping constant
I_z	second moment of inertia about the minor axis
i	radius of gyration about the axis whose the buckling plane is located on
K_{e}	factor and depends on the grade of the steel
k	lateral bending coefficient
$\mathrm{k_c}$	correction factor depend on bending moment
k_w	warping coefficient
k_{yy} and k_{zy}	interaction factors
k_τ	buckling coefficient
L	span of the steel portal frame
L	length of the member
L	distance between lateral supports
L_E	effective length of the member between two restraints
L_{eff}	segment length between two restraints (buckling length) in the buckling plane considered

M	applied bending moment
M_2	value of the moment at the one-quarter point of the segment
M_3	value of moment at the mid-point of the segment
M_4	value of moment at the three-quarter point of the segment
M_A, M_B & M_C	bending moments at the L/4, L/2 and 3L/4 of the steel members respectively
M_b	buckling resistance moment
$M_{b,Rd}$	design buckling resistance moment
$M_{cl,Rd}$	design elastic resistance bending moment of cross-section
$M_{c,\ Rd}$	design resistance for bending moment about one principal axis of a cross-section
M_{cr}	elastic critical moment for lateral torsional buckling
M_{cx}	bending moment capacity about the major axis
$M_{f,Rd}$	bending moment resistance of flange
M_{Ed}	design value of bending moment
M_{equ}	equivalent uniform moment
M_m	maximum moment of the segment between two lateral restraints
$M_{pl,Rd}$	design plastic resistance bending moment of cross-section
M_x	maximum major axis moment in the segment
m_{LT}	equivalent uniform factor
$N_{b,Rd}$	design buckling resistance of the compression member
$N_{c\ Rd}$	design uniform compression resistance of cross-section
N_{cr}	elastic critical buckling force due to Euler's formula
N_{Ed}	design value of the compression force
N_{Sd}	axial member force
$n\varphi$	total of number of holes in the cross-section
P	relevant representative value of a pre-stressing action
P_c	compression resistance of the member' cross-section
P_{cx}	compression resistance of the member about the major axis
P_{cy}	compression resistance of the member about the minor axis
P_v	shear capacity of the section
p_b	bending strength
p_{cs}	value of p_c for a reduced slenderness

p_y	design strength
$Q_{k,1}$	characteristic value of the leading variable action 1
$Q_{k,i}$	characteristic value of the accompanying variable action *i*
q_{cr}	critical shear strength
q_w	shear buckling strength
r	root radius
r_y	radius of gyration about the minor axis of the member's
S	first moment of area about the centroidal axis of that portion between the boundary of the cross-section and the point at which the shear is required
S_x	plastic section modulus
$S_{x,eff}$	effective plastic section modulus
S_v	plastic modulus of shear area, A_v
t	thickness at the required point
t	thickness of web or flange
t_f	thickness of the flange
t_w	thickness of web
u	torsional index
$V_{b,Rd}$	buckling shear resistance
$V_{bf,Rd}$	buckling shear resistance of the flange
$V_{bw,Rd}$	buckling shear resistance of the web
V_{Ed}	design value of shear force
V_{cr}	shear resistance
$V_{pl,Rd}$	plastic design shear resistance
v	slenderness factor
$W_{el,min}$	minimum elastic section modulus of cross-section
$W_{pl,\ min}$	minimum plastic section modulus of cross-section
W_y	section modulus
Z_x	elastic section modulus
$Z_{x,eff}$	effective elastic section modulus
α	linear thermal expansion
α	coefficient measured as the height of the compression area
α	imperfection factor and depends on the buckling curve
α_{LT}	imperfection factor

$\gamma_{G,j}$	partial factor for permanent action *j*
γ_{M0}	partial factor equals 1.0 as given by EC3
γ_P	partial factor for pre-stressing actions
$\gamma_{Q,1}$	partial factor for variable action 1
$\gamma_{Q,i}$	partial factor for variable action *i*
ε	relative stress coefficient
η	factor for shear area
λ	slenderness ratio
λ_1	slenderness value to determine the relative slenderness, $\overline{\lambda}$
λ_{LT}	slenderness ratio for lateral torsional buckling
$\overline{\lambda}$	non-dimensional slenderness
$\overline{\lambda}_p$	stress ratio factor
$\overline{\lambda}_w$	modified web plate slenderness
ξ	reduction factor for unfavourable permanent actions G
ρ	reduction factor
ρ	shear effect reduction factor
$\sum$	implies "the combined effect of"
σ_a	axial stress
τ_{cr}	critical elastic local buckling stress
τ_{Ed}	design shear stress
υ	Poisson's ratio of steel
Φ	value to determine the reduction factor, χ
χ	reduction factor due to the relevant buckling mode
χ_{LT}	reduction factor due to torsional-flexural buckling
χ_w	factor for the contribution of the web to shear buckling
χ_y	reduction factors due to flexural buckling about the major axis
χ_z	reduction factors due to flexural buckling about the minor axis
ψ	stress ratio of the extreme fibre
ψ_0	factor for combination value of a variable action
"+"	implies "to be combined with"

Chapter 5

A_{gj}	gross section area of member j
B_{fbk} & B_{fck}	width of the beam and column at the intersection joint respectively.
C	penalty value
C_i	penalty value accrued on the individual i
C_p	penalty coefficient
c_1	limiting percentage for constraint violation
F_i	original fitness value of string i in the current generation
F_i'	scaled fitness value of string i
F_i^{New}	new fitness value of the individual i
F_j	value of the objective function
F_j	axial member force of member j
$F_{\max}$	maximum value of the fitness in the current generation
$F_{\min}$	minimum value of the fitness in the current generation
G_C	number of current generation
$g_i(x)$	calculated value of the i^{th} constraints
$\overline{g}_i(x)$	limited value of the i^{th} constraints
g_p	summation of the violation
k_1 and k_2	violation rates
k_3	quadratic penalty rate
k_j	penalty scaling multiplier
k_{xx} & k_{yx}	interaction factors depend on equivalent moment factor
M_{bj}	lateral torsional buckling resistance moment
M_{cxj}	bending moment capacity of member j
M_{LTj}	maximum bending moment in the segment j
M_{xj}	maximum bending moment about major axis
m	number of existing stresses for interactions
m	total number of limitations
m_j	equivalent moment factor for member j
m_{LTj}	equivalent moment factor for segment j
nm	number of members in a group
N_G	number of predetermined generations

n	number of existing constraints
n	penalty scaling exponent
np	population size
nbc	number of beam-column connections
nc	total number of constraints
ng	number of member groups
nj	total number of joints in frame
np	total number of population
P_{bxj} & P_{byj}	buckling capacity of member j about major and minor axes respectively
p_{cj}	compressive strength of member j
p_{cyj}	compressive strength about the minor axis
P_i	selection probability for string i
P_j	axial member force of member j
P_m^{Gc}	mutation probability of the current generation
P_m^{max}	maximum mutation probability
P_m^{min}	minimum mutation probability
p_i	structural parameter or response (deflection, stress, etc)
p_i	scaled constraint violation
$p_{\max}$	maximum allowable value of p_i.
p_y	design strength
q_j	scaling switch
u_j	horizontal displacement of the joint j
V_j	volume of member j
v_i	violation coefficient
v_j	vertical displacement of joint j
W	total weight if frame
W_i	weight of the frame represented by individual i
Z_j	section modulus of the member j
α	constant slightly larger than 1 (typically 1.01).
Δ_j	maximum deflection of member j
Δ_{ju}	maximum allowable deflection
∂	total lateral displacements of joints
δ_i	horizontal and vertical displacements of joint i

δ_{iu}	upper limit of displacements
γ_m	unit weigh of the member group
Φ	penalty multiplier
Φ_i	penalty value for constraint i

Chapter 1: Introduction

1.1 Steel

Steel is a general nomenclature for iron containing small amounts of carbon, manganese and other elements (Salmon and Johnson, 1990). Nowadays, steel is broadly used as the main material in the construction of many buildings around the world. Its high strength to weight ratio and durability has made steel a suitable material for structures which are required to have large space without intermediate columns. The steel members of the frames are manufactured in different forms and cross-section shapes depending on their functions and characteristics.

1.2 Characteristics of steel portal frames

Steel Portal Frames (SPFs) are generally used in single storey buildings. It is estimated that 50% of the all steelwork constructed in the UK is in the primary framework of single-storey buildings (Salter, 2004). Because of its economy and versatility for large spans construction, such as shopping centres, warehouses, barns, retail shops, pools, factories, etc, the SPF has become the structure most often used within this sector. The SPF can be the option for single storey buildings in countries which are at a reconstruction stage. After the war, Iraq and specifically the Kurdistan Region has stepped into a new stage of reconstruction which will require more buildings with SPFs; essentially a demand for factories, warehouses and modern retail parks.

Although SPFs appear to be simple structures, there are more limitations imposed by the codes of practice than for complex structures. The non-prismatic shape of the members used in SPFs requires checking of more limitations than are considered in multi-storey buildings. The major applied loads to a SFP are the combination of dead load, imposed load and wind load. Due to the large area of cladding in a SPF, the wind load has a great impact on the behaviour of the entire structure.

1.3 Types of SPFs

A number of low-rise structures can be classified as portal frames. The most popular types are pitched roof and arched SPF as they give a pleasant appearance in terms of the architectural design view point.

1.3.1 Pitched Roof

A single-span pitched-roof SPF is depicted in Fig. 1-1. This type of SPF has typically a span of between 10 and 30m, and an eaves height of between 5 and 10m, a pitched roof between 5° and 10° and has haunches in the rafters at the eaves and in the apex. The existence of the haunches reduces the depth of the rafters and provides an efficient resistance to the bending moment at the connections (Salter, 2004).

1.3.2 Propped SPF

This type of frame is used where a relatively large span is required and the existence of an intermediate column does not adversely affect the function of the intended building. The frame is constructed to include a column connected to the apex. The intermediate column is conventionally called a prop and has a great impact on reducing the depth of the rafter. This type of frame apparently refers to a single span SPF, but realistically it is a two-span frame in terms of its structural behaviour. Fig. 1-2 shows the general geometrical layout of propped SPF.

1.3.3 Tied SPF

This type of frame is similar to a structural truss but the difference is that the rafters and columns are considered as moment resisting members. As shown in Fig. 1-3, a tie is constructed and connects the two columns. Hangers are sometimes used to connect the tie to the rafters. This kind of the frame erection will tremendously reduce the horizontal movement of the frame and hence improves lateral suitability for using a crane. However, the rafters and columns of this type of SPF are under a significant heavy load which needs careful attention during the design.

1.3.4 Mansard SPF

In a Mansard SPF, the rafters are split up into smaller elements having hunches at the connections (Fig. 1-4). This type of the frame is used where the construction of a relatively large span is in demand. However, the eaves height has to be minimised to control the large displacement. On the other hand, using a tie provides an economical solution (Salter 2004).

1.3.5 Curved Rafter SPF

Various shapes of curved SPF have been constructed in recent years. As the shape of those frames is pleasant, it has drawn the architects' attention to design this kind of frame. The rafter is constructed either as one curved element or as a series of small straight elements as shown in Figs. 1-5 and 1-6.

1.4 Haunches

A haunch is like an arm used at the eaves and apex as shown in Fig. 1-7 in order to strengthen the connection for resisting a large applied moment. The eaves haunch can be prepared by cutting a hot rolled section or built-up steel plate (Salter 2004). It is common practice to use the same cross section as the rafter. Build-up of the haunch is for the purposed of providing an adequate section to resist the applied heavy bending moment and displacement. Despite its advantage, use of the haunch necessitates checking more limitations given in the codes of practice. The non-prismatic nature of the haunch should be taken into consideration during the analysis process for more accurate results. However, this might involve some mathematical complication as will be shown in chapter 2.

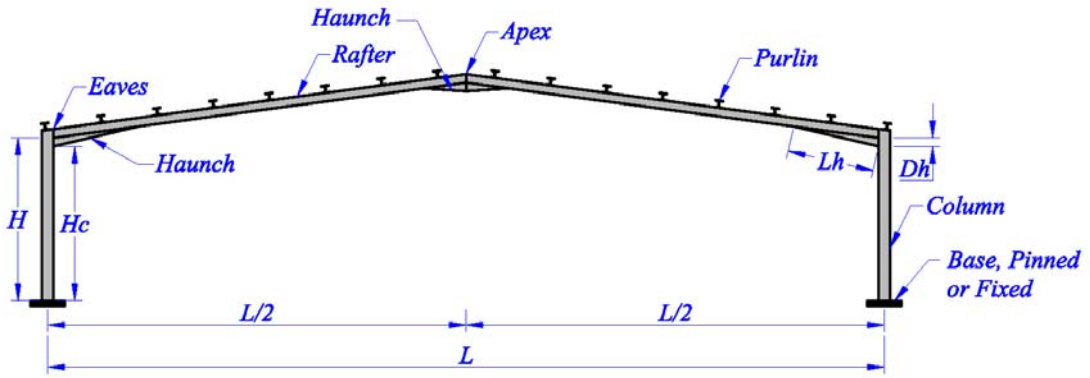

Figure 1-1: Typical type of pitched roof steel portal frame

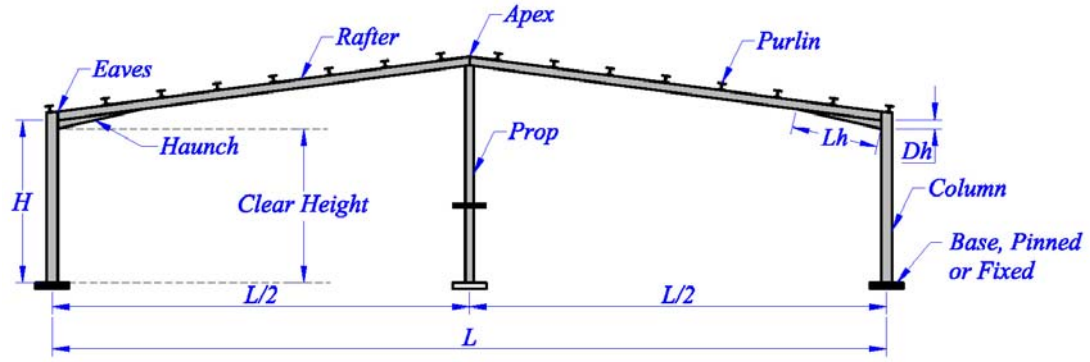

Figure 1-2: General shape of propped steel portal frame

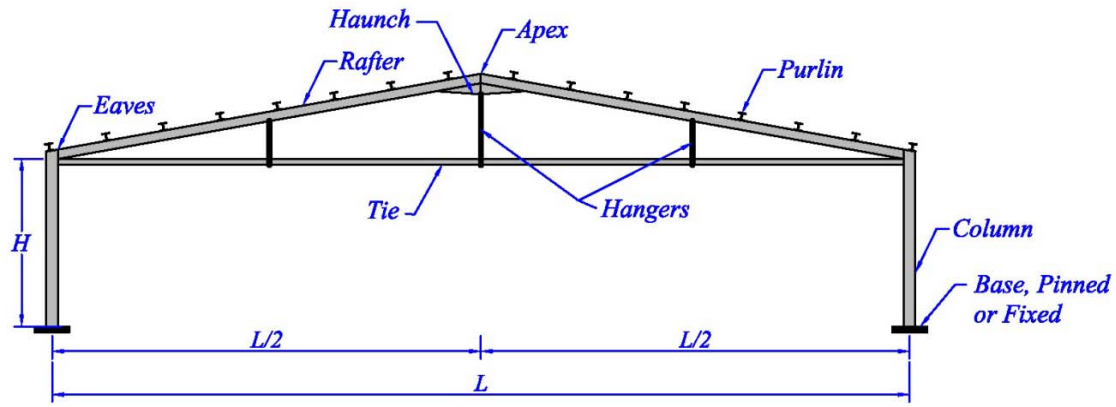

Figure 1-3: A tied steel portal frame

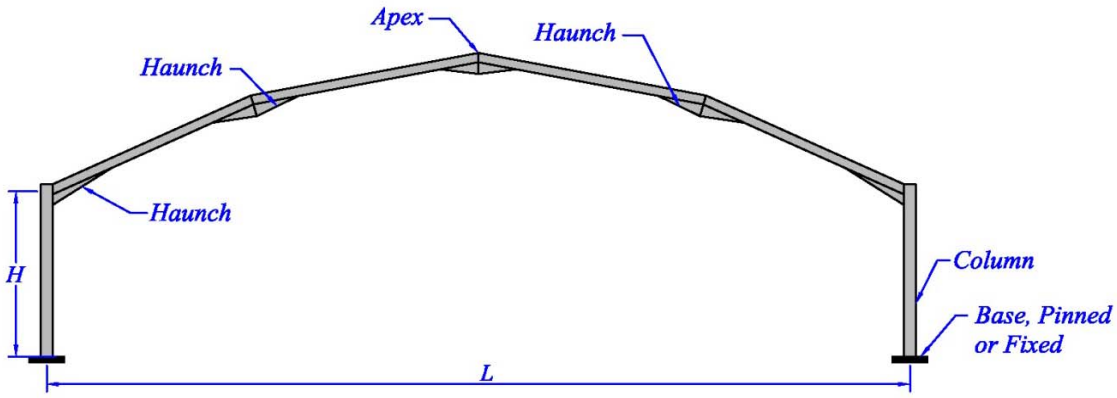

Figure 1-4: Mansard steel portal frame

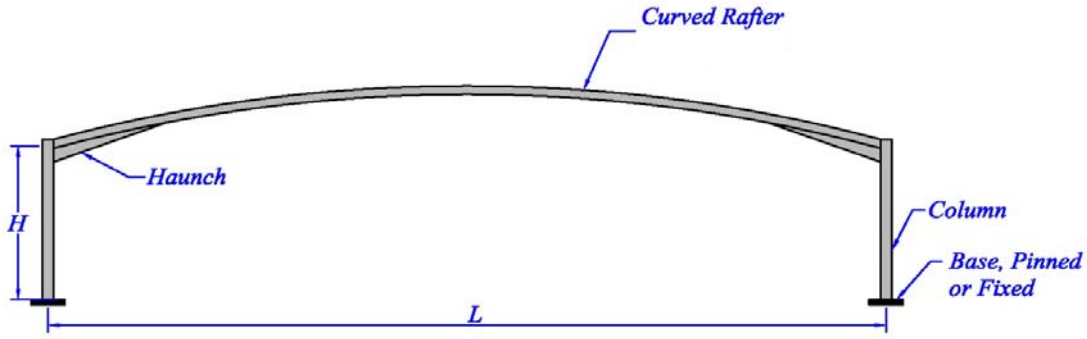

Figure 1-5: A curved rafter SPF

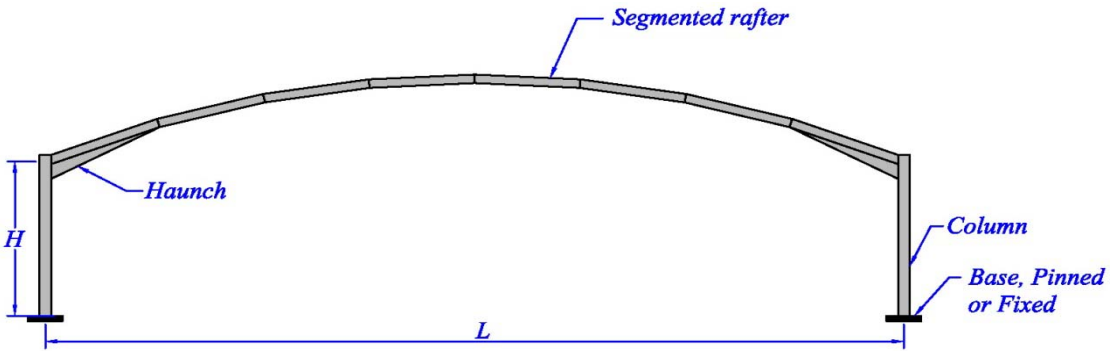

Figure 1-6: A quasi-curved SPF

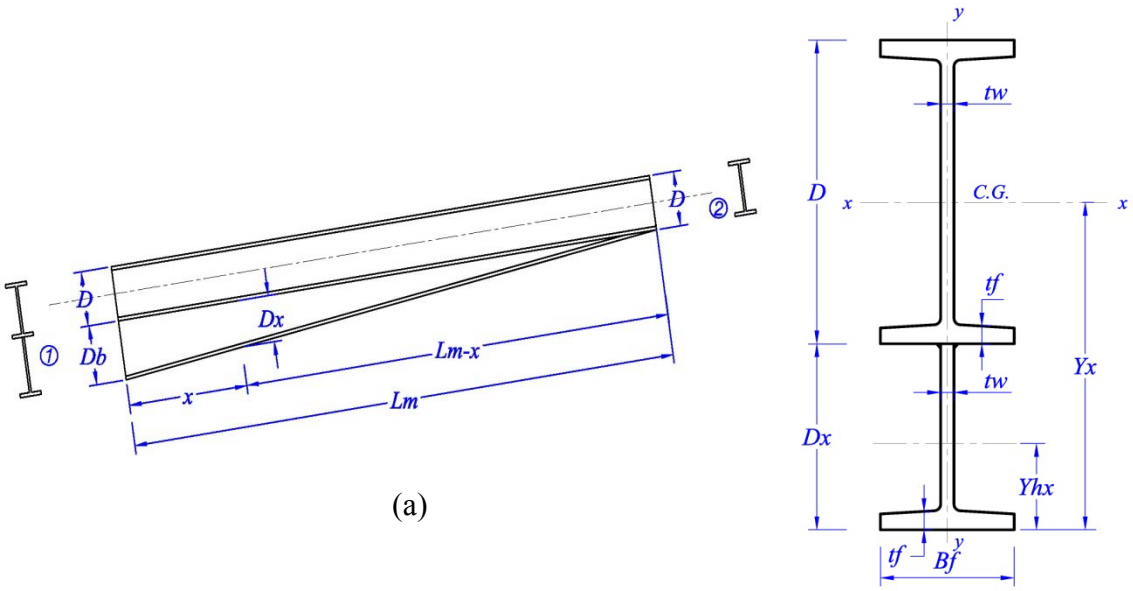

Figure 1-7: Haunch member (a) and its cross section (b)

1.5 The need for optimisation

The design process makes sure that a given structure fulfils the architectural requirement, on one hand, and is safe, serviceable and durable for a cost-effective design, on the other hand (McKenzie, 1998). For a simple structure which is meant to be designed, it is common practice to use the experience and intuition of the structural engineer. Due to the complexity of large structures, it is somewhat difficult to achieve an economical design solution just by using the designer's experience, particularly when the structure experiences various load case scenarios. This is because there are so many criteria which should be considered during the design and all of them have influences on the response of the structure if the member's properties are slightly changed. On the other hand, there is an obvious gap between the progress of optimisation techniques and their practical applications in structural engineering. This is because the complexity of available optimisation techniques represents major obstacles for the design even though the designer is keen to use optimisation techniques (Cohn and Dinovitzer 1994). There is a reluctance to use optimisation techniques in practice because of the difficulty of formulating a comprehensive set of equations for the design problem so that it could be easily used by anyone. This is very true when the technique which is supposed to be used is a mathematical programming method, as they are based on gradient and a derivative has to be taken.

In recent years, the world has witnessed a number of novel and innovative techniques which have had various degree of success. Most of them involve a stochastic search and they use the idea of simulation of natural phenomena. They are structurally and functionally simple to use in practice. However, they are slow-process techniques and some changes need to be addressed to speed up their performance. In addition, rapid development of the domestic personal computer over the past years has increased the motivation to formulate design problems using one of the stochastic optimisation techniques and implement them in the practical field of structural engineering. Nevertheless, efforts should be made to reduce the computation time and make the optimisation technique robust to obtain global optimum and cost-effective solutions for design problems. To achieve this, consequently, it is necessary to investigate more studies to modify the available optimisation techniques so that they will be capable of handling real life design problems in the offices of structural engineers.

1.6 Literature Survey

Structural optimisation has been an interesting topic for more than 100 years. It was begun by the early works of Maxwell (1890; cited in Akin and Arjona-Baez, 2001) and Mitchell (1904; cited in Akin and Arjona-Baez, 2001). After that, considerable analytical works had been done on component optimisation in the 1940s and early the 1950s. The work on optimisation extended to the 1970s and in that time some of researchers offered a comprehensive statement for the use of mathematical programming methods to solve the non-linear and inequality constrained problem of designing structure under a multiplicity of the loading conditions. Among them were Schmit and Farshi (1974; cited in Akin and Arjona-Baez). The work on mathematical programming extended to the 1980s when some algorithms were developed to use the finite element analysis approach to optimise the structural design.

1.6.1 Mathematical Programming Methods

Mathematical programming (MP) methods have been extensively used to solve optimisation problems since the 1940s. Essentially MP methods are divided into two main categories; linear programming and non-linear programming methods. In linear programming methods the objective function and the constraints are linear functions

of the variables. Whereas in non-linear programming methods, this relationship turns to be non-linear and errors will be likely to happen if there is an attempt to express non-linear relations in terms of linear ones. However, the majority of structural optimisation problems are somehow non-linear. Many problems in structural optimisation may conveniently be solved by various techniques in MP. The advent and rapid growth of computers have increased implementation of MP methods for solving cumbersome and complex optimisation problems. Such efforts have stimulated further research on new methods. As a result, various MP emerged during the past decades, such as linear and non-linear programming, integer and mixed integer programming, sequential linear and quadratic programming. These techniques are based on the gradient of the problem's function where the solution starts at a single point and then proceeds toward the optimum one along the direction of the gradient.

A very early attempt to minimise the weight of a structure was done by Bigelow and Gaylord (1967). They used linear programming to find the minimum weight of frameworks up to two-bay and four-storey. Majid and Elliot (1971) applied an elastic design to minimise the weight of a two-bay four-storey structure. They were among the first group of researchers who used non-linear programming. Arora and Govil (1977) proposed a partitioning technique whereby the structure is subdivided into several substructures and the optimisation process is performed for all substructures simultaneously. However, the process could only handle small design changes. Vanderplaats and Sugimoto (1986) developed a technique based on sequential linear and quadratic programming methods to obtain the minimum weight of a steel structure. They concluded that the technique is efficient and robust to explore the optimum solution.

Chang and Liu (1989) developed a computer code based on the optimality criterion to find the minimum designed weight of a plane frame. This was the first attempt to bring the optimisation technique into office-use. The optimality criteria they used was a combination of indirectly applying the Cohn-Tucker conditions of non-linear programming with Lagrangian multipliers (Arora, 1989). The latter are used to include related constraints into an optimisation problem. Saka and Hayalioglu (1991) developed an algorithm to demonstrate the optimum design of various steel frames.

They considered both geometrical and material non-linearlties. As they allowed for the occurrence of a plastic hinge, they excluded stress constraints from the design problem. They used the optimality criteria method to develop a relationship between the design variables taking into consideration displacement constraints. Most of the computation time was used by the iteration process when geometrical non-linearity is taken into account. At the initial stage the developed algorithm required 21 iterations to obtain the non-linear response of the frame. Later it rose to 77 in the final stage of the design cycles. Erbatur and Al-Hussainy (1992) used linear programming to minimise the weight of steel portal frames and compared the result with those reported in the literature where the same portal frames had been analysed using other mathematical techniques. While implementing the available steel section in AISC, they used the theorem of structural variations as the analysis part of the algorithm and concluded that the proposed methodology gives faster and better convergence to the optimum solution.

The design optimisation was then for large scale tall steel structures. Grierson and Park (1993) developed a method designed to obtain the minimum weight of tall steel structures. The structures were laterally loaded and the constraints were the stresses and inter-storey drifts according to the specified limits. Chan *et al*. (1994) developed an optimisation technique based on optimality criteria method. They applied the technique to three-dimensional, tall, steel structures to minimise the weight of steel. Saka and Kameshki (1998) studied the optimum design of rigid frames by using optimality criteria method. The approach was used to reduce the member of non-linear equations of design variables.

1.6.2 Genetic Algorithms and Heuristic Search Techniques

The next generation of optimisation methods were heuristic search techniques which began to be applied from early 1990s. There are various techniques which were developed during recent years. Among them are simulated annealing, genetic algorithms (GA), ant colony, tabu search (TS), and harmony search. After emergence of the heuristic search techniques and simulation of natural phenomena, GA could have a wide role in structural optimisation. It has been the subject of many researches since 1990s and its capability has been recognised along with its robustness. GA are inspired by the Darwinian ‘Survival of the Fittest’ theory and natural selection.

Essentially, GA have three main operators; reproduction, crossover, and mutation. In reproduction, the fittest individuals of the current generation are randomly selected and dropped into a mating pool. Then a pair of individuals is randomly picked as parents for crossover. In crossover, a part of parents' genes are swapped, depending on the crossover probability, resulting in production of two offspring for the next generations. The mutation is a character based operator. A number is randomly generated for each character (gene) of the offspring and compared to the mutation probability which is normally very small. If the number generated is less than the mutation probability, then the binary character of gene is flipped up from '1' to '0' or vice versa. The generation continues until an individual dominates the population or a predetermined maximum number of generations is reached. Since the process is probabilistic, the best individuals may be lost during the genetic operations. For this reason, the best individuals of each generation are saved and secured for the next generation without undergoing the genetic operations. The strategy of preserving the fittest individuals is called elitism.

As one of the first groups of the GA application, Adeli and Cheng (1993) integrated a GA with a penalty-function method to carry out the optimisation of space steel trusses. They minimised the weight of three space trusses; a twelve-bar truss, a twenty five-bar truss, and a seventy two-bar truss. While using the one-point, two-point and mask as crossover schemes, they used constant values for the crossover and mutation probabilities. They concluded that the two-point crossover yields a better convergence tendency than the other two methods. In addition, they found that a bigger population can outperform as the smaller one in the convergence to the global optimum solution. Two years later, Adeli and Kumar (1995) implemented GA to examine their relationships to computer systems. Without stating the reason, they decided to use a different value for the constant mutation probability than in the previous work. They employed two-point crossover as GA operator to minimise the weight of a seventeen-bar truss and of a fifty-storey mega-structure. They used the penalty-function method and augmented Lagrangian approach to transform a constrained optimisation to an unconstrained optimisation. They compared the speed up value of both penalty-function method and augmented Lagrangian approach and concluded that augmenting the Lagrangian value has a lower speed up value than the penalty-function method.

Cohn and Dinovitzer (1994) surveyed nearly 500 published optimisation examples to investigate the possibility of incorporating them into practice. They concluded that although GA is started to be applied in structural engineering, it has shown great potential compared to MP and optimality criteria methods. In the later stage, attempts were made to apply a multi-objective function to structural optimisation. Rajeev and Krishnamoorthy (1997) developed GA-based methodologies to solve the optimisation problem by considering simultaneously topology, configuration, and member cross-section sizes. They used two different set of variables; discrete variables which were used for the cross-section sizes and continuous variables for configuration (position of joints). They checked the suitability of the algorithm by implementing the method on a ten-bar truss, an eighteen-bar truss, and a Microwave Antenna Tower. Having applied constant values for the crossover and mutation probabilities, they used a scale factored penalty for the fitness in case there was any violation by an individual. The scale factor was set to 0.5 in the earlier generation, and was increased after every generation by 5%. They found out that the proposed methodologies gave better solutions to those obtained from the classical optimisation methods based on MP methods.

Development of the personal computer inspired the researchers to start thinking about integration of finite element packages with the optimisation algorithms. Camp *et al*. (1998) developed FEAPGEN as a module in the Finite Element Analysis Program (FEAP). One of the aspects of the algorithm was the use of three reproduction schemes; inverse, partitioning, and generation-dependent distribution. While using the constant values for the mutation and crossover probabilities, they employed fixed, flexible, and uniform crossover schemes with a maximum of three crossover points. They examined the program by using three benchmark examples and compared the results with what had been achieved using optimality criteria method developed by other researchers. While using a ten-bar truss, a one-bay ten-storey frame, and a three-bay three-storey frame, they realised that the optimum design obtained by FEAPGEN using GA can give 4.5 to 23% lighter frames than the design obtained by optimality criteria and gradient methods.

The GA modification inspired the researchers to break down the population of individuals into several sub-populations. Easton and Mansour (1999) used distributed

genetic algorithms (DGA) to minimise the labour expenses and expected opportunity costs. They compared the outcomes of the approach with the other alternative solution procedures such as a simulated annealing (SA) and a tabu search (TS). They came up with the results that DGA found many more least-cost solutions as those found by SA and TS. Also, DGA outperformed the competing alternatives in terms of mean error, maximum error, and percentage of least-cost solution.

The development of computers makes it possible to consider geometric non-linearity behaviour of frames. Pezeshk *et al*. (2000) studied the design of non-linear framed structures using GA. They examined the algorithm which had been developed by implementing three benchmark examples; two examples of a two-bay three-storey frames and a one-bay ten-storey frame. They incorporated the algorithm which had been developed with a finite element package and adopted an adaptive crossover scheme developed by Spears (1994, cited in Pezeshk *et* al., 2000). Constant crossover and mutation probabilities were used in their study. Using thirty runs to find out the best solution, they realised that application of non-linear analysis results in a 4% heavier frame than linear analysis of a two-bay three-storey steel frame. However, it gives a 20% increase in strength with the same post limit load-carrying capacity. They concluded through two design examples that the optimised designs are not significantly affected by the P-Δ effects. In another investigation to include the effect of P-Δ on the structural optimisation, Kameshki and Saka (2001) developed a GA based optimum design method for unbraced multi-storey frames with semi-rigid beam-to-column connection. They showed that lateral displacements in the frames are much more than those of a rigid frame due to its flexible joints. They adopted constant values for the crossover and mutation probabilities and found out that the members are fully stressed in case of rigid connections.

In a study designed to enhance the performance of GA, Toropov and Mahfouz (2001) modified GA to improve its rate of convergence. The modified GA was linked to a system of structural design rules, interacting with a finite element package in order to obtain minimum-weight designs for plane structural steel frames. They examined the algorithm that had been developed using two benchmark examples; a five-bay five-storey and a four-bay four-storey. When incorporating the ANSYS package, they concluded that the algorithm can accurately determine the effective

buckling length of structural members. They applied constant mutation and crossover probabilities.

Two years later, Saka (2003) studied the optimum design of pitched-roof SPF using GA. He used four design variables for one benchmark example with different loads; column, rafter, depth and length of the haunch. The range of the haunch depth varied from 100mm to 740mm with the increment of 20mm whereas the range of haunch length varied from 500mm to 5000mm by the increment of 50mm. He subdivided a frame of 4 members into 24 smaller elements. He ran the program ten times. Each run he called as a 'seed' and used it to reach the optimum solution of the benchmark example. He adopted a non-prismatic stiffness matrix developed by Matheson *et al*. (1959; cited in Saka 2003). On adopting the constant values for mutation and crossover probabilities, it was noticed that the lateral torsional buckling constraints for columns were at their upper bounds while the displacement constraints did not reach to their upper bounds. Continuing to modify the GA, Gero *et al.* (2006) developed an elitist GA and compared it to solutions for complex structural optimisation obtained by common commercial software. They modified different operators and processes to develop an elitist GA. The main modifications carried out were the implementation of a new crossover operator called 'phenotype crossover' which was capable of exchanging real sections obtained from a commercial catalogue, a new selection operator called 'aptitude', a new codification of the design variables, and a modified objective function. They programmed an optimisation module in Visual C++ using 'Galib library' and then integrated the module in the Escal3D software to search for minimum weight of a steel structure. Adopting constant mutation and crossover probabilities, they examined the developed algorithms using 2D and 3D steel frames. They did not consider the node displacement constraints in the design optimisation. They concluded that making a group of beams with the same cross-section gives better results than when each beam is individually assigned with a cross-section.

Using a different heuristic search technique, Kargahi *et al.* (2006) employed a TS method to minimise the weight of steel structures. They developed an algorithm using FORTRAN computer language which performed search, structural analysis and constraints checks in an iterative procedure. They believed that TS like other

heuristic search methods gives a near optimum solution. Like some MP methods, the evident shortcoming of the TS method is that it usually converges to a local optimum as the final solution. They evaluated the developed algorithm using three different case studies; three-bay three-storey, five-bay nine-storey, and five-bay twenty-storey. The results showed that except for the five-bay twenty-storey steel framework, which was controlled by displacement, the rest were mostly controlled by stresses.

Boyd *et al.* (2007) proposed parametric variations and an optimisation method using GA while employing single and multi-objective functions for the optimisation of a structural steel-composite connection. The results indicated that the use of GA provided an efficient method of searching the complex design space of a structural connection. Furthermore, the single objective function provided a substantial reduction in the weight. They adopted a constant value for the mutation probability.

Degertekin *et al*. (2008) implemented GA to investigate the optimal load and resistance factor design. They found that population size has significant influence on computation time. A large population yields an increase in the number of generations and consequently the computation time. However, it slightly reduces the weight of the whole structure. They made comparison between GA and TS and found out that the drift produced by GA is smaller than the one produced by the TS method when the design problem is that of weight minimisation. They applied constant values for the crossover and mutation probabilities and concluded that a mutation probability of 0.002 causes significant divergence from the optimum solution. In another attempt to compare different heuristic search techniques, Saka (2009) presented a harmony search method based optimum design algorithms for the steel sway frames. The algorithm imposed behavioural and performance constraints in accordance with limitations described in BS 5950 code of practice. He evaluated the algorithm by comparing three different frames already designed using simple a GA technique; one-bay single-storey, two-bay six-storey, and three-bay fifteen-storey frames. All frames were subjected to lateral applied loads to model the sway behaviour of frames. The results in case of two-bay six-storey frames showed that there is not a considerable difference between the optimum weights found using the harmony search algorithm and GA. In contrast, there was a substantial difference in optimum weight of three-bay fifteen-storey frame which showed that harmony search

outperformes the GA. However, he stated that it is not possible to judge the performance of the harmony search algorithms from two examples and more investigations are needed.

Krajnc and Beg (2009) implemented heuristic search in the form of GA to minimise the weight of steel planar frames. They compared the outcomes of the design optimisation by GA with the design solution by a MP method called the sequential unconstrained minimisation technique. They concluded that although sometimes the problem of using the GA fell into the local optimum due to premature convergence, GA outperforms the MP method in obtaining the lighter frame; a 2.5% reduction in frame weight was achieved. They also expected that MP methods will fail to handle the rolled steel section due to dealing with continuous variables so that the fact will leave any one GA as an important option.

There are some other researchers that have implemented GA in structural optimisations. Among them are Ghasemi *et al.* (1999), Gutkowski *et al.* (2000), Hasançebi & Erbatur (2000), Pyrz and Zawidzka (2001), Foley and Schinler (2003), Balling *et al.* (2006), Park *et al.* (2006), Wang and Arora (2006), Kripakaran *et al.* (2007), Liu *et al.* (2007), and Joghataie and Asbmarz (2008). They have commonly used constant mutation and crossover probabilities with different values as the genetic operators. None of them has stated the reason for using these constant values. With the results of those investigations, they demonstrated the capability of the GA to search the global optimum in structural optimisation.

1.6.3 Semi-rigid connections

A structure's response is very much affected by the behaviour of its connections. This necessitates more investigations about the actual behaviour of connections and how they affect the design of different frames. In recent years, semi-rigid connections have been investigated by a remarkable number of researchers in different fields of structural engineering; partly because of the development of personal computers, and partly for investigating the real behaviour of connections. All the investigations were conducted to depict the moment-rotation relationship of connections. This results in obtaining the initial stiffness of connections, which is the

preliminary requirement for measuring the structural response against the applied loads.

Machaly (1986) applied an optimisation technique proposed by previous researchers to determine the rigidity percentage of the semi-rigid connection which gives the minimum weight of the structure. Furthermore, he investigated the exact percentage saving of steel when the structural elements are connected semi-rigidly compared to those that are connected assuming rigid connections. He found out that if values of 0.6 and 0.7 are used as rigidity ratios of column and girder, the value of negative and positive member moments will be the same. This is the optimum value when semi-rigid connections are considered. He achieved a 28% saving of weight in SPF and realised that the saving almost occurs in the girders but not in columns. He did not consider the non-linear behaviour of the connection in his study.

Since each type of connection has a different behaviour, Bjorhovde *et al*. (1990) have made attempts to categorise the connections according to stiffness behaviour. They demonstrated that for the connection design, the ultimate moment is $0.9M_p$, $0.6M_p$ and $0.2M_p$ for rigid, semi-rigid and pinned connections respectively, where M_p is the plastic moment of the member. They showed the difficulty of categorising the connections in the sense of both serviceability and ultimate limit states. In the same year, Kishi and Chen (1990) developed a semi-analytical procedure to predict the moment-rotation characteristics of the angle connection type by determining the initial stiffness of the connection, the ultimate moment of the connection and optimum shape parameter. Initial stiffness was formulated in terms of the variables associated with the angles used for connection such as thickness and length of the web angle.

Approaches to finite elements were witnessed in some studies in the early 1990s. Sibai and Frey (1993) proposed a model for semi-rigid connection based on a finite element model. They conducted their study by addressing the problem of full scale frames in the laboratory, considering both sway and non-sway steel frames. They concluded that joint flexibility reduces the structural strength capacity and increases sway displacement in sway frames. Later on, Bahaari and Sherbourne (1994) used finite element analysis to determine the complete moment-rotation relationship for an extended end-plate connection and compared the results with experimental results.

They concluded that the thickness of the end-plate has a large influence on the behaviour of the connection.

In addition to the use of static loads, the behaviour of connections under dynamic loads was investigated. Chui and Chan (1996) presented an incremental-iterative displacement-based computer method for non-linear dynamic analysis and connection non-linearity. They concluded that the displacement response of a semi-rigid frame is considerably larger than that of a rigid frame as the stiffness values of semi-rigid connections are smaller than those of rigid ones. They also noted that the positive displacement response is larger than the negative one because of the presence of the permanent rotational deformation at connections.

Attempts to classify connections continued. Goto and Miyashita (1998) proposed a new classification system for beam-to-column connections in terms of the boundary between rigid and semi-rigid connection. They also determined the rotation capacity for connections. In this classification they took into account not only the ultimate limit state behaviour but also serviceability limit state. They obtained the empirical shape parameter equation for the connection with extended end plate and flush end plate. They estimated the boundaries between rigid and semi-rigid connections in terms of initial stiffness and ultimate moment capacity.

Application of different connection models to compute the initial stiffness of connections went on. Dhillon and O'Malley III (1999) developed a computer oriented analysis and design method for unbraced steel frames with semi-rigid connections. A second order non-linear approach was adopted to include both geometric non-linearity and connection flexibility. The design was based on the Frye-Morris (Frye and Morris, 1975) polynomial connection model. The produced results that compared semi-rigid joints with the rigid ones, showed a 19% increase in drift of the whole structure with a 7% saving in the weight of the structure. Kameshki and Saka (2001) also used the polynomial model of moment-to-rotation relationship proposed by Fry and Morris (1975) to minimise the weight of steel frameworks. They concluded that the semi-rigid connection will produce 11% saving of the frame weight compared to one with the rigid connections. Using again the Frye-Morris polynomial model, Degertekin and Hayalioglu (2004) investigated the design of non-linear semi-rigid steel frames. They considered both beam-to-column and column-to-

base connections as semi-rigid. They concluded that with semi-rigid connections they have a lighter frame of between 3.5% and 19.7%, depending on the type of the connection they used. An end-plate connection leads to the lightest frame compared with other types of connections in three-storey two-bay frame. They also concluded that a reduction in connection stiffness causes an increase in both the frame's weight and sway. They offered a solution that controls the sway by testing the various stiffness values for the joints.

Del Savio *et al*. (2005) carried out a study to evaluate the influence of initial stiffness variation on the joints of the Vierendeel girder type beam, including analyses of semi-rigid portal frames. They used the FTOOL/SRC program to model semi-rigid joints by means of a simple and parametric analysis. They used linear elastic analysis to consider varied joint stiffness conditions to model bending moment versus axial force interaction in Vierendeel steel beam. The results showed that semi-rigid consideration could considerably reduce the initial stiffness from 10^{12} kN.m/rad as for rigid joints to 6000 kN.m/rad.

Castro *et al*. (2007) used the finite element program, ANSYS to analyse and simulate the structural behaviour of SPF with semi-rigid connections. With reference to the literature, they concluded that the model that had been developed is adequate to simulate the semi-rigid joint with a non-linear rotational spring joint element. de Andrade et al (2007) studied semi-rigid connections in a composite frame to develop an efficient and cost-effective building system for steel construction leading to a semi-rigid composite system. They constructed a full-scale semi-rigid composite portal frame to evaluate the proposed system's structural response. They employed two composite connection design models developed by Kishi and Chen (1990) and the EC3 component method. The results demonstrated that the model based on Kishi and Chen (1990) overestimated the connection's initial stiffness because it did not consider all the connection components, disregarding terms related to the column, beam and bolt deformations. The EC3 proposed model was close to the experimental results.

The use of finite element method to model connection behaviour has proved to be more popular recently. Mohamadi-shooreh and Mofid (2008) implemented finite element method to study moment-rotation relationship of a bolted end-plate

connection. They also focussed on obtaining initial stiffness values of the connection. They implemented finite element method to formulate the initial stiffness of a bolted flush end-plate connection. Based on substantial finite element and statistical analyses, they found that, in some cases, EC3 overestimates the initial stiffness of bolted flush end-plate beams by up to 15% and in some other cases, it is likely to underestimate by almost 31%. As a consequence, more investigation should have been carried out to unify the initial stiffness formula of the bolted flush end-plate connection.

In addition to the aforementioned studies, there are a number of researchers that made attempts to model the behaviour of connections and find the values of initial stiffness. Among them are Jones *et al*. (1980), Masik and Dunai (1995), Fang *et al*. (1999), Aristizábal-Ochoa (2001), Law *et al* (2001), and Al-khatab and Bouchaïr (2007). They have either used different models to obtain the initial stiffness values of connections, or modelled the connection's behaviour by different methods.

1.6.4 Difference between optimisation techniques

As stated earlier, structural optimisation has had various techniques for finding the best possible solution of the design problem. The main techniques which can be pointed here are MP methods and heuristic search techniques. The major difference between these two groups of optimisation methods is in the way of defining the relations between the design variables, objective functions, and constraints. Many mathematical linear and nonlinear programming methods have emerged for solving optimisation problems during the last few decades. However, no single method has been found to be robust and efficient for seeking the optimum solution for different kinds of problems (Adeli and Cheng, 1993). All of the constraints are used in the optimisation process are non-linear and non-convex and some of them are even non-continuous (Kargahi *et al.*, 2006). The derivative based MP methods need continuous functions. As a result, the constraints have to be modified to satisfy the continuous function demand. In contrast, heuristic search techniques can deal with discontinuous functions which do not need any modification of constraints (Krajnc and Beg, 2009). Another problem associated with MP methods is that of being complex in their formulation and that solutions may be trapped into local optimum. On the other hand heuristic methods use experience and rule-of-thumb rather than rigorous and

cumbersome mathematical formulation (Hegazy and Kassab, 2003). Many researchers believe that the MP methods should be widely used for structures of moderate size where constraints can be linearised or approximate techniques used. Optimality criteria methods in later generation of MP methods are appropriate for solving large or complex problems whereas heuristic search techniques show great potential in different structural optimisation problems.

Heuristic search techniques are probabilistic techniques which possess transition rules that do not rely only on the current design point but also on probabilities. Their ability to deal with discrete design variables is highlighted as the main advantage of these methods. On the other hand, the MP methods are almost deterministic methods that are able to seek the optimum solution using continuous design variables for large scale problems. However, their inability to deal with discrete design variables has forced structural designers to collate the final results into standard sizes (Ghasemi *et al*. 1999). In structural steel design, however, the design variables are discrete as they are selected from standard steel tables. To overcome and escape from the possibility of only finding a local optimum, stochastic method would be better.

Mathematical optimisation algorithms seek a solution in the neighbourhood of the starting point. If more than one solution exists, the global optimum cannot be found as the solution may be trapped into a local one due to the gradient nature of the algorithms used depending on the choice of starting point (Adeli and Cheng, 1993). Such “hill-climbing” algorithms are extremely efficient when the starting point is close to the optimum solution in the design space. (Hajela, 1990). Nevertheless, the majority of heuristic search techniques start with a population of points at various locations in a problem function. This makes it more likely that you will reach the global optimum.

1.7 Aims and Objectives

The main aim of this research is to select a heuristic search technique for structural optimisation and enhance its performance. GA, as the simulation of survival of the fittest theory, is modified by some changes in its operators, mainly in mutation. This research is directed to parallel operation instead of using a conventional GA. In this operation, conventional GA adopts the migration idea and comes down into DGA

that will be discussed in due course. The optimisation process will be applied to some popular and commonly used steel frameworks, mainly pitched-roof, haunched-rafter, SPFs, and the suitability of the developed algorithm will be examined with respect to various benchmark examples and compared to work in other literature. The objective for the developed algorithm has been established and are designed to achieve the following goals in developing the algorithms:

1) Develop, implement, and fully test the algorithm to examine the suitability, robustness, and capability of it to handle the optimisation problems, particularly those associated with structural engineering.

2) Change in the nature of the genetic operators to show the algorithm's performance in converging to the optimum solution within a reasonable short period of time. The most changes are associated with reproduction, crossover, mutation, and penalty function.

3) Find well-defined relations between the algorithm's operators and the design variables in order that it can deal with different types of structures that have different number of design variables.

4) Develop a program designed to optimise any type of plane steel structure. The program is to involve all aspects of the developed and modified algorithm. It should interact with structural analysis and be compatible with available personal computer so that it may be used by structural engineers.

5) Develop graphs and tables to reduce time and effort of obtaining the required parameters for design of SPF.

The optimisation problem is set to satisfy the requirements of both available codes of practice, EC3 and BS 5950. Since the EC3 is supposed to replace the BS 5950 by April 2010 in the UK, an attempt is made to compare between these two codes of practice. With that, the problem is constructed for both rigid and semi-rigid connections to measure the response of the structure against the applied loads. The question of whether the semi-rigid connection, despite of being a large displacement at SPF, gives the most cost-effective frame or not, will be investigated. The algorithm will have two different objective functions. Since it is believed that the

majority of the steel structural cost is in the self-weight, an attempt is made to minimise the weight in the design of steel frames. On the other hand, SPFs are normally controlled by vertical displacement of the apex and/or lateral displacement due to large applied lateral loads. As a result, one of the objective functions will be devoted to maximise the displacement in both vertical and lateral directions. This might be a potential response to the question of whether weight minimisation is an efficient optimisation or whether focus should be somewhere else in steel structure optimisation.

1.8 Organisation of the thesis

The structure of this thesis is planned to include eight chapters. In the first chapter, called 'introduction', different types of SPF are introduced with their functions and characteristics. After a thorough survey of literature, application of different optimisation techniques is reviewed. In chapter two, titled 'Development of stiffness matrix', the method of direct stiffness is introduced and the stiffness matrix required for a non-prismatic member is derived. Then the method of regression analysis designed to develop a practical stiffness matrix for non-prismatic members is discussed. In chapter three, called 'Connections in steel structure', the models to obtain the initial stiffness of different connections are reviewed while introducing types of connections. The constraints imposed by both BS 5950 and EC3 codes of practice is stated and discussed in chapter four titled 'Design Procedures According to BS 5950 and EC3'. These constraints include the ultimate and serviceability limit states. Chapter five is the core of the thesis and is where the contribution to the knowledge is developed. The process by which GA and DGA work will be explained. In this chapter all aspects that have been considered and used to modify DGA is stated. The program developed to handle the DGA is also introduced. In chapter six, entitled 'Evaluation of Modified DGA', a number of design problems is formulated and results are compared with the results obtained in literature to validate the developed algorithm, In chapter seven, a comprehensive investigation is carried out on different SPFs using all aspects of the modified DGA and developed program. Furthermore, statistical analyses are carried out to show the relationships between the parameters of the structures. Finally, chapter eight summarises the findings and draws the conclusions from the results. Recommendations for future work are made.

1.9 Summary

A number of different types of SPFs with their details were introduced and their functions were addressed thoroughly. The reason why a SPF should undergo the structural optimisation was highlighted. The literature survey was divided into two main categories (structural optimisation and semi-rigid connections) to choose an efficient optimisation technique and a model suitable to calculate the initial stiffness of semi-rigid connections. Also, the comparison was made between the two major group of the optimisation technique; MP methods and heuristic search techniques. The survey indicates that GA are robust and efficient in dealing with structural optimisation problems. The well-known Fry-Morris model is validated and easy to apply for semi-rigid connections.

Chapter 2: Development of Stiffness Matrices

2.1 Introduction

Analysis of a structure is a procedure designed to investigate the balance between external actions on the structure as whole and the internal response of the structure's elements. Since the 1700s, many methods and theorems have been developed to achieve more accurate and practical methods of analysis. The developed methods are categorised as Flexibility (force) and Stiffness (displacement) Methods. The internal and external unknown actions in Flexibility Methods are not directly determined by knowing the displacement while the internal and external unknown actions can be calculated by figuring out the displacement in Stiffness Methods. In 1868, Otto Mohr, a German researcher presented a method of elastic weights whereby the deflection of a beam could be calculated. For this purpose, the beam was imaginary loaded with bending moments with elastic weights. The method was later named as Conjugated-Beam Method. Mohr also developed Mohr's circle to determine the internal principal stresses of the structure's elements. In the same year an Italian railroad engineer, Alberto Castigliano developed his theorem of the least work. This was known as Castigliano's second theorem in 1876 (Willems and Lucas, 1978).

A significant development emerged when Maney presented the Slope Deflection Method of analysis in 1915. This method provided powerful techniques for analysis of continuous frames. However, for a complex structure, the method was not efficient. It was necessary to apply, manually, lots of equations to solve simultaneously. The Moment Distribution Method, developed by Cross in 1924, made a revolution in analysis of structures by hand, which unlike to Slope Deflection Method, no simultaneous equations were required. Computer development raised the idea of using the technology for the analysis of structures. It necessitated finding a method of analysis to be suitable for programming. The ideal method could either be the flexibility method or the stiffness method. It is generally easier to formulate the necessary matrices for computer operation by the stiffness method because

constructing the matrices by the stiffness method depends on the geometry of the structure not the external action. The principle of the slope deflection was used to develop a stiffness matrix for each member of the structure within the member's local coordinate system. Then the stiffness matrices of all the members of structures are assembled and transformed into a global stiffness matrix for whole structure. The global stiffness matrix represents the load-displacement relationship of the whole structures. The way of determining the unknown displacements and forces is called the Matrix Analysis Method which nowadays is applied to analysis of structures using computer programs.

Depending on the shape and geometry, the member of steel frames are categorised into prismatic and non-prismatic members. Each of those has its own member stiffness matrix which should be involved in measuring total response of steel frames.

2.2 Prismatic members

The term of prismatic is assigned to structural members that have a constant cross-sectional area along their length. The slope deflection method is used to derive stiffness matrices for prismatic members. A prismatic member as shown in Fig. 2-1 has six degrees of freedom; horizontal displacement (u), the vertical displacements (v) and rotations (θ) at each end of the member. The corresponding forces to these displacements are axial force, shear force, and bending moment respectively. The forces and displacements shown in Fig. 2-1 all have positive signs.

To derive the stiffness matrix, each displacement and rotation should be considered separately and their effects on the member force components are determined by virtual work and slope deflection methods. First, assume a positive displacement occurs in the direction of x for each member's end separately, while the other displacements and rotations are prevented. By displacing of the near node, the far node is assumed fixed and vice versa (Fig. 2-2). Then using the virtual work method, the axial stiffness coefficient of the member is obtained.

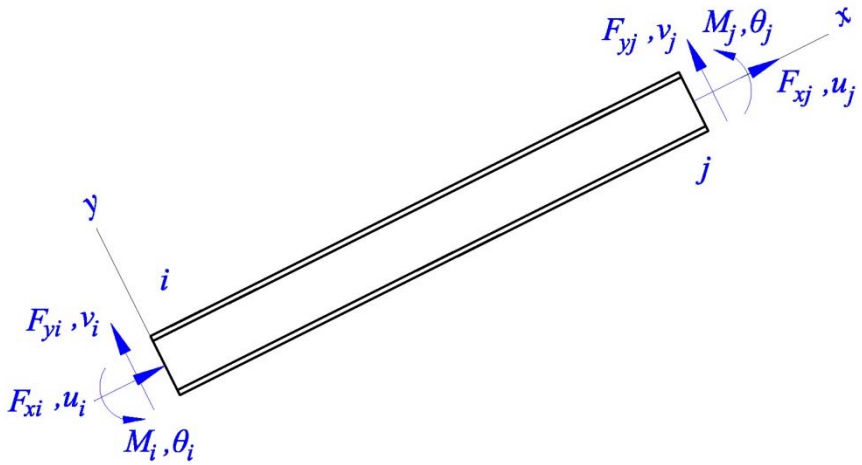

Figure 2-1: The internal forces and displacement of a structural member

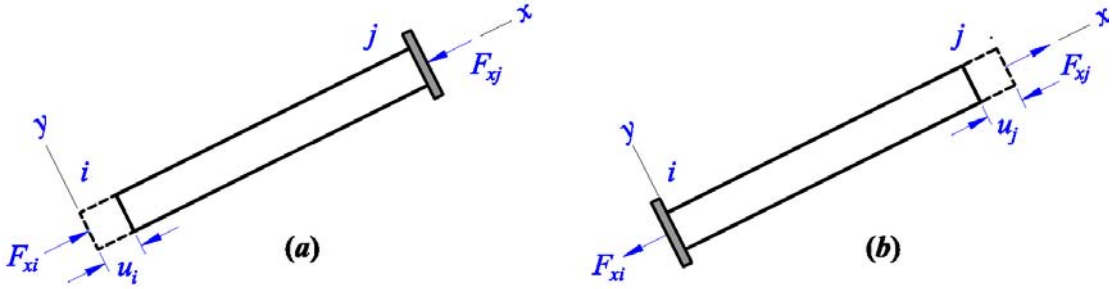

Figure 2-2: x displacement at near node (a) and far node (b) – y displacement and θ rotation are prevented

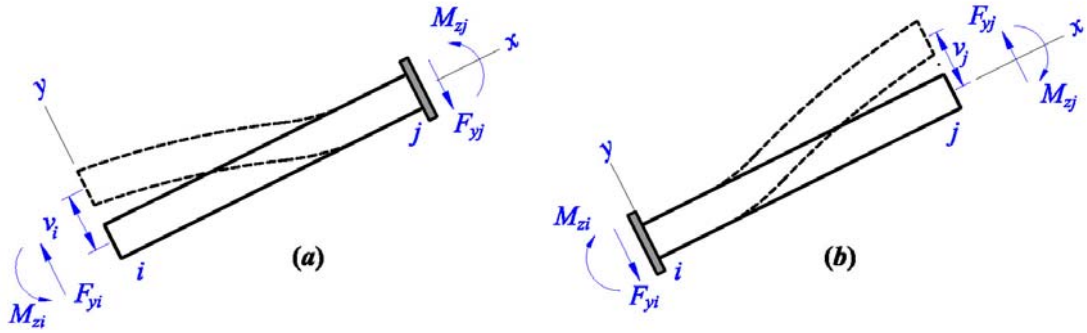

Figure 2-3: y displacement at near node (a) and far node (b) – x displacement and θ rotation are prevented

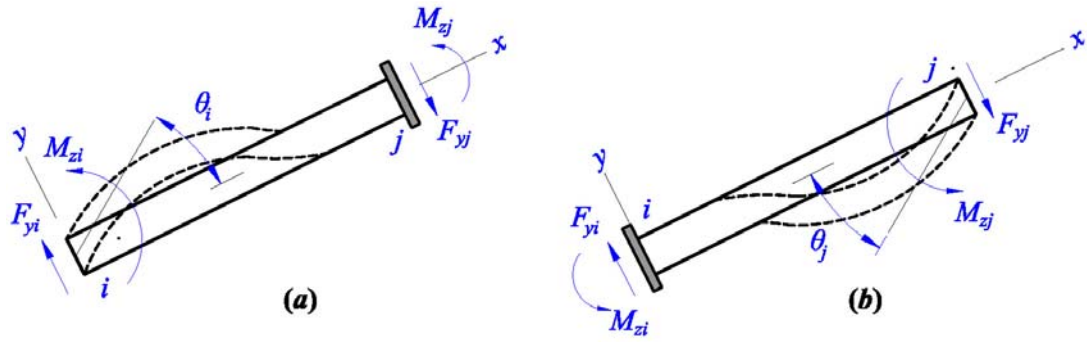

Figure 2-4: θ rotation at near node (a) and far node (b) – x and y displacements are prevented

Second, assume positive vertical displacements take place at each member's end while the other displacement and rotation are prevented (Fig. 2-3). Implementing the slope deflection method, the shear effect in the stiffness matrix will be derived.

Third, assume positive rotations (counter clockwise) occur at both ends of the member, the other displacements are prevented (Fig. 2-4). By using the slope deflection method, the effect of the rotation on the stiffness matrix will be found.

By superposition, the resulting six load-displacement relations for the member can be expressed in the matrix form below:

$$\begin{bmatrix} F_{xi} \\ F_{yi} \\ M_{zi} \\ F_{xj} \\ V_{yj} \\ M_{zj} \end{bmatrix} = \begin{bmatrix} \frac{AE}{L} & 0 & 0 & -\frac{AE}{L} & 0 & 0 \\ & \frac{12EI}{L^3} & \frac{6EI}{L^2} & 0 & -\frac{12EI}{L^3} & \frac{6EI}{L^2} \\ & & \frac{4EI}{L} & 0 & -\frac{6EI}{L^2} & \frac{2EI}{L} \\ & & & \frac{AE}{L} & 0 & 0 \\ & Symmetry & & & \frac{12EI}{L^3} & -\frac{6EI}{L^2} \\ & & & & & \frac{4EI}{L} \end{bmatrix} \times \begin{bmatrix} u_i \\ v_i \\ \theta_i \\ u_j \\ v_j \\ \theta_j \end{bmatrix} \quad (2\text{-}1)$$

The equation can be written in abbreviated form such as:

$$\{f\} = [k]\ \{d\} \quad (2\text{-}2)$$

Where:

$\{f\}$ is the member force vector

$[k]$ is the member stiffness matrix

$\{d\}$ is the local displacement vector

It is clear from the Eq. 2-2 that the stiffness matrix represents the load-displacement relationships. The formation of the stiffness matrix is well documented in a number of textbooks such as Weaver and Gere (1980), Sack (1989), Grawley and Dillon (1993), McGuire *et al*. (2000), Ghali *et al.* (2003), and McCormac (2007)

In order to study the effect of the member displacement on the whole structure, Eq. 2-2 has to be transformed to a global coordinate system. For this purpose, both force and displacement of the members should be expressed in terms of a global coordinate system not a local coordinate system (x and y). Consider the member depicted in Fig. 2-5 which shows the relationship between the global and local coordinate systems.

Assuming $\gamma_x = \cos \alpha_x$ and $\gamma_y = \cos \alpha_y$ represent the cosine direction of the member, the following relation can be expressed between global and local displacements:

$$\begin{bmatrix} u_i \\ v_i \\ \theta_i \\ u_j \\ v_j \\ \theta_j \end{bmatrix} = \begin{bmatrix} \gamma_x & \gamma_y & 0 & 0 & 0 & 0 \\ -\gamma_y & \gamma_x & 0 & 0 & 0 & 0 \\ 0 & 0 & 1 & 0 & 0 & 0 \\ 0 & 0 & 0 & \gamma_x & \gamma_y & 0 \\ 0 & 0 & 0 & -\gamma_y & \gamma_x & 0 \\ 0 & 0 & 0 & 0 & 0 & 1 \end{bmatrix} \times \begin{bmatrix} U_i \\ V_i \\ \theta_i \\ U_j \\ V_j \\ \theta_j \end{bmatrix} \tag{2-3}$$

It can be abbreviated as:

$$\{d\} = [T]\ \{D\} \tag{2-4}$$

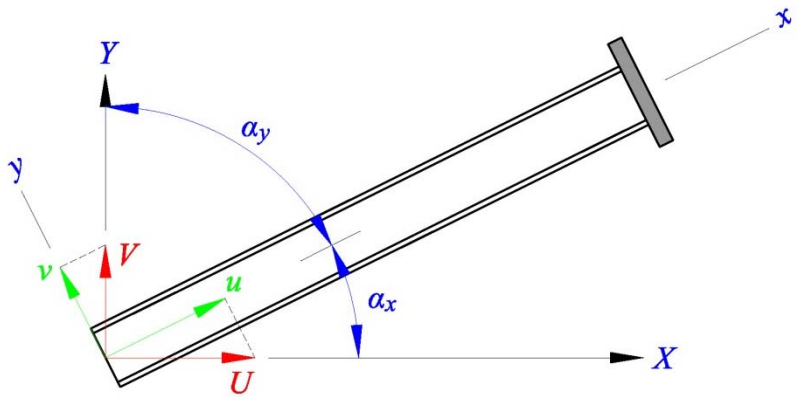

Figure 2-5: Relationship between global and internal displacements

where:

$[T]$ is the transformation matrix

$\{D\}$ is the global displacement vector

The same procedure is repeated to demonstrate the relationship between global and local forces at the two ends (nodes) of the member. Hence,

$$\begin{bmatrix} F_{Xi} \\ V_{Yi} \\ M_{Zi} \\ F_{Xj} \\ V_{Yj} \\ M_{Zj} \end{bmatrix} = \begin{bmatrix} \gamma_x & -\gamma_y & 0 & 0 & 0 & 0 \\ \gamma_y & \gamma_x & 0 & 0 & 0 & 0 \\ 0 & 0 & 1 & 0 & 0 & 0 \\ 0 & 0 & 0 & \gamma_x & -\gamma_y & 0 \\ 0 & 0 & 0 & \gamma_y & \gamma_x & 0 \\ 0 & 0 & 0 & 0 & 0 & 1 \end{bmatrix} \times \begin{bmatrix} F_{xi} \\ F_{yi} \\ M_{zi} \\ F_{xj} \\ F_{yj} \\ M_{zj} \end{bmatrix} \tag{2-5}$$

The load transformation matrix as formed in Eq. 2-5 is the transpose of the displacement transformation matrix $[T]$, i.e.:

$$\{F\} = [T]^{\mathrm{T}} \{f\} \tag{2-6}$$

Where:

$[T]^{\mathrm{T}}$ is the transpose of the transformation matrix

$\{F\}$ is the global force vector

Eqs. 2-1, 2-3, and 2-5 are now combined to derive the global stiffness matrix which represents the factor expressing the relationship between the global loads and displacements. By substituting Eq. 2-4 into Eq. 2-2 the following equation can be formed:

$$\{f\} = [k]\,[T]\,\{D\} \tag{2-7}$$

And substituting Eq. 2-7 into Eq. 2-6 will result in:

$$\{F\} = [T]^{\mathrm{T}}\,[k]\,[T]\,\{D\} \tag{2-8}$$

or simply:

$$\{F\} = [K]\,\{D\} \tag{2-9}$$

Where:

[K] is global stiffness matrix and defined as:

$$[K] = [T]^{T} [k] [T] \tag{2-10}$$

2.3 Non-prismatic members

Generally, a non-prismatic member is subdivided into smaller elements in the structural analysis process. For each element, a stiffness matrix must be constituted using its geometric properties. However, this approach leads to a large global stiffness matrix, and involving it in measuring the response of the structural against the applied load is to some extent cumbersome and time consuming. To eliminate having more members' stiffness matrices, it is necessary to construct a stiffness matrix for each non-prismatic member. In this study, a Virtual Work Method has been implemented to derive a stiffness of axial force and column analogy (Ghalli *et al*, 2003) has been the guideline to constitute the stiffness matrix for bending and shear effects. The virtual work is the work done by real forces acting through virtual displacement (White, 1978; Willems and Lucas, 1978; Bhatt, 1986; Gere and Timoshenko, 1999; Li and Li, 2007). The concept is that of the equality of external and internal work. The principle of virtual work is

$$\delta W_{\text{int}} = \delta W_{ext}$$

where

$$\delta W_{\text{int}} = \int_0^L \delta\varepsilon_x EA\varepsilon_x dx \tag{2-12}$$

and

(2-11)

$$\delta W_{ext} = F_x \delta u \tag{2-13}$$

Where:

W_{int} is the internal work

W_{ext} is the external work

F_x is the axial force at the length x section

ε_x is the axial strain

A is the cross-sectional area

E is the modulus of elasticity

With reference to Fig. 2-6 the stiffness coefficient for axial force can be derived according to following procedure:

The relationship between A_x, A_1 and A_2 with constant width can be defined as:

$$(A_1 - A_2)(\frac{L-x}{L}) = (A_x - A_2)$$

or

$$A_x = A_1(1-\frac{x}{L}) + A_2(\frac{x}{L}) \tag{2-14}$$

Similarly, the member displacement at distance x can be expressed as:

$$\delta u = \frac{x}{L}\delta u_m \tag{2-15}$$

Where

δu_m is the axial displacement of the member

A_1 is the cross sectional area of one end of member

A_2 is the cross sectional area of the other end of member

Since,

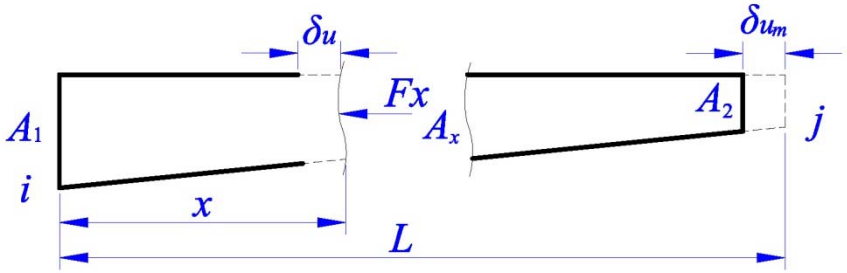

Figure 2-6: Internal axial force and displacement of the non-prismatic member

$$\delta\varepsilon_x = \frac{d(\delta u)}{dx}$$

and

$$\varepsilon_x = \frac{du}{dx}$$

and substituting Eq. 2-14 into Eq. 2-12 will give:

$$\delta W_{\text{int}} = \int_0^L \delta\varepsilon_x EA\varepsilon_x dx = \int_0^L \frac{d(\delta u)}{dx} E\left[A_1(1-\frac{x}{L}) + A_2\frac{x}{L}\right]\frac{du}{dx}dx \qquad (2\text{-}16)$$

Substituting Eq. 2-15 into Eq. 2-16 and performing integration will give:

$$\delta W_{\text{int}} = \frac{\delta u}{L^2} Eu_m\left[A_1(x-\frac{x^2}{2L}) + \frac{x^2}{2L}A_2\right]_0^L$$

$$= \frac{\delta u}{L^2} Eu_m\left(\frac{A_1L + A_2L}{2}\right) = \frac{\delta u}{L}\left(\frac{A_1 + A_2}{2}\right)Eu_m \qquad (2\text{-}17)$$

Substituting Eq. 2-13 into Eq. 2-17 gives:

$$F_x\delta u = \frac{\delta u}{L}\left(\frac{A_1 + A_2}{2}\right)Eu_m$$

or

$$F_x = \frac{E}{2L}(A_1 + A_2)u_m \qquad (2\text{-}18)$$

Since the force-displacement relation is defined through the stiffness of the member, the axial stiffness for the linear non-prismatic member will be:

$$k = \frac{E}{2L}(A_1 + A_2) \qquad (2\text{-}19)$$

Where:

u_m	is the total axial displacement of the member
k	is the stiffness of the member due to the axial force

Applications of force and displacement methods have, in some cases, been applied through the classical procedure known as column analogy and moment distribution. Column analogy can be applied for a plane framed analysis of one closed bend in which the degree of redundancy does not exceed three. This involves a calculation similar to that of stresses in column cross section when is subjected to combined bending moments and axial force. The redundancy is chosen at a point called the elastic centre (Ghali *et al*. 2003). The column analogy principle has been used to derive the stiffness matrix of a linear non-prismatic member. However, the column analogy follows the force method, not stiffness method, and the procedures will end with the formation of a flexibility matrix. To derive a stiffness matrix, a flexible matrix is inevitably inverted.

Fig. 2-7a shows a member of variable cross-section idealised as a straight bar having a varied *EI*. Fig. 2-7b refers to the cross-section of the analogous column. The shape of strip has varying width = 1/*EI* and length = *L*, the same as that of the member; where $EI \equiv EI(x)$ is the flexural rigidity at any point at a distance *x* from *O*, the centroid of the analogous column (the elastic centre).

Fig. 2-7a shows a non-prismatic member with varied depth along the length of the member. Fig. 2-7b depicts the way of using the force method to calculate the flexibility of the member when the far end (*j*) is assumed fixed. Using virtual work, the moment at distance *x* from *O* due to a unit load and unit moment are:

$$M_{u1} = -(L_1 + x)$$
$$M_{u2} = 1 \qquad (2\text{-}20)$$

Since the actual load for deriving the flexibility matrix is considered as unity, the vertical displacement will be:

$$v_y = \left(\int \frac{M_{u1}^2 dx}{EI}\right) F_y + \left(\int \frac{M_{u1} M_{u2} dx}{EI}\right) M_z \qquad (2\text{-}21)$$

and similarly for the rotation:

$$\theta_z = \left(\int \frac{M_{u1} M_{u2} dx}{EI}\right) F_y + \left(\int \frac{M_{u2}^2 dx}{EI}\right) M_z \qquad (2\text{-}22)$$

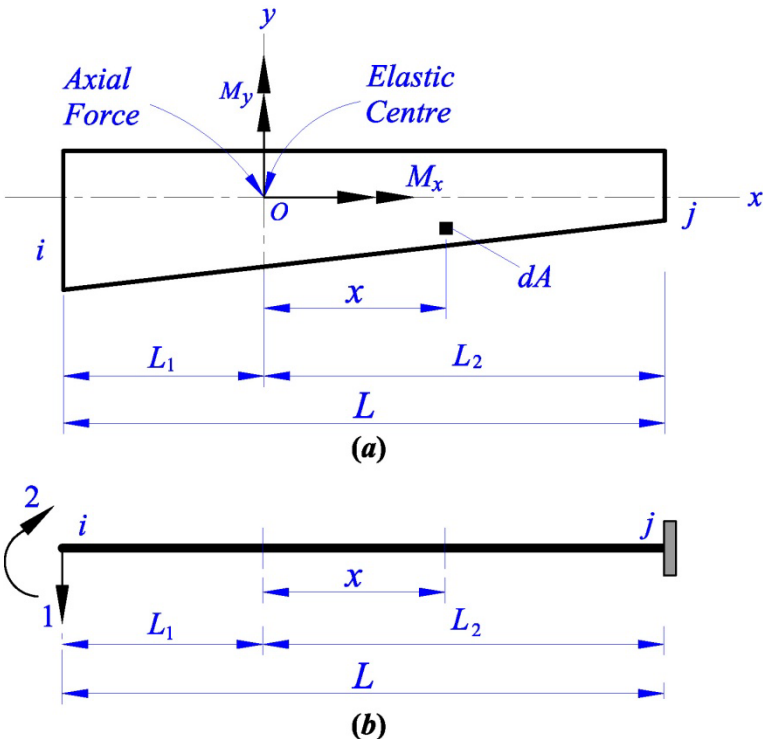

Figure 2-7: (a) Simulation of column analogy on non-prismatic member, (b) application of the unit load method on the non-prismatic member

and therefore the flexibility matrix could be constructed as:

$$[f]=\begin{bmatrix} \int \frac{M_{u1}^2 dx}{EI} & \int \frac{M_{u1}M_{u2}dx}{EI} \\ \int \frac{M_{u1}M_{u2}dx}{EI} & \int \frac{M_{u2}^2 dx}{EI} \end{bmatrix}=\begin{bmatrix} \int \frac{(L_1+x)^2}{EI} & -\int \frac{(L_1+x)}{EI} \\ -\int \frac{(L_1+x)}{EI} & \int \frac{dx}{EI} \end{bmatrix} \qquad (2\text{-}23)$$

As the stiffness is the reciprocal of the flexibility, the flexibility matrix must be inverted to form the stiffness matrix (using one of the methods in Pease, 1965; Friedberg and Insel, 1986; Golub and Van Loan, 1989):

$$[k]=\begin{bmatrix} \frac{1}{\int \frac{x^2}{EI}dx} & \frac{L_1}{\int \frac{x^2}{EI}dx} \\ \frac{L_1}{\int \frac{x^2}{EI}dx} & \frac{1}{\int \frac{1}{EI}dx}+\frac{L_1^2}{\int \frac{x^2}{EI}dx} \end{bmatrix} \qquad (2\text{-}24)$$

and considering the near member end (1) fixed, as shown in Fig. 2-6, and the derived stiffness coefficient for axial displacement (Eq. 2-19), the stiffness matrix for the member could be formed as:

$$[k]=\begin{bmatrix} \frac{E}{2L}(A_1+A_2) & 0 & 0 & -\frac{E}{2L}(A_1+A_2) & 0 & 0 \\ & \frac{1}{\int\frac{x^2}{EI}dx} & \frac{L_1}{\int\frac{x^2}{EI}dx} & 0 & -\frac{1}{\int\frac{x^2}{EI}dx} & \frac{L_2}{\int\frac{x^2}{EI}dx} \\ & & \left(\frac{1}{\int\frac{1}{EI}dx}+\frac{L_1^2}{\int\frac{x^2}{EI}dx}\right) & 0 & -\frac{L_1}{\int\frac{x^2}{EI}dx} & \left(-\frac{1}{\int\frac{1}{EI}dx}+\frac{L_1L_2}{\int\frac{x^2}{EI}dx}\right) \\ & & & \frac{E}{2L}(A_1+A_2) & 0 & 0 \\ & & & & \frac{1}{\int\frac{x^2}{EI}dx} & -\frac{L_2}{\int\frac{x^2}{EI}dx} \\ & & \textit{Synmetry} & & & \left(\frac{1}{\int\frac{1}{EI}dx}+\frac{L_2^2}{\int\frac{x^2}{EI}dx}\right) \end{bmatrix}$$

(2-25)

In the special case, when *EI* is constant, $L_1 = L_2$ and $A_1 = A_2$ then the stiffness matrix becomes that of the prismatic members.

2.4 Regression analysis

The derived stiffness matrix which is applicable to that of general members' geometries, prismatic and non-prismatic, does not seem to be practical. This is because the matrix is constructed by relatively complicated integration parts which make it, to some extent, difficult to solve manually. To overcome this problem, it was decided to conduct large regression analysis of the developed stiffness matrix and consequently to form a practical stiffness matrix so that there is no need to evaluate the integration of the matrix coefficients defined in Eq. 2-25. In statistics, regression analysis is concerned with techniques for modelling and analysis of numerical data consisting of values of dependent and independent variables. In other word, it is a technique to make a function with some constant coefficients (also known as parameters) and variables from a set of available data.

Generally, regression analysis is categorised into linear and non-linear regressions. In linear regression, the linearity refers to the dependent variables and it is not necessary that all the independent variables are linear, i.e. there may be some non-linear independent variables involved in this particular analysis. A simple linear regression may have the following form

$$y_i = a_0 + a_1 x_i + e_i \tag{2-26}$$

In multiple linear regression, there are several independent variables or functions of independent variables. For example, adding a term in x_i^2 to the preceding regression gives:

$$y_i = a_0 + a_1 x_i + a_2 x_i^2 + e_i \tag{2-27}$$

Whereas non-linear regression is a form of analysis by which the observed data are represented by dependent variables and parameters in a non-linear form. A non-linear regression equation may have the following form:

$$y_i = f(x,\alpha) = \frac{\alpha_1 x_i}{\alpha_2 + x_i} \tag{2-28}$$

where:

a_0, a_1, a_2	are constants
x_i	is the independent variable
y_i	is the dependent variable
e_i	is a constant value

The most common method in regression analysis is least squares which can be drawn linearly or in quadratic form (Fig 2-8). Least squares itself is a sort of optimisation technique which attempts to minimise the separation between the proposed graph or line and scattered points adopted from available data. After drawing the best-fit line to the scattered points that represent the data, the coefficient and parameters that can best describe the line are obtained. The accuracy of the line depends on how spread out the data are and on the degree of their scattering.

In order to conduct the regression analysis, the ‘Mathematica’ was employed which is a computational software used in scientific, engineering, and mathematical fields. It is able to solve many complicated mathematical problems in a convenient way. The main advantage ‘Mathematica’ possess is that it works with a large collection of data in a consistent framework and can assess and deal with them instantly.

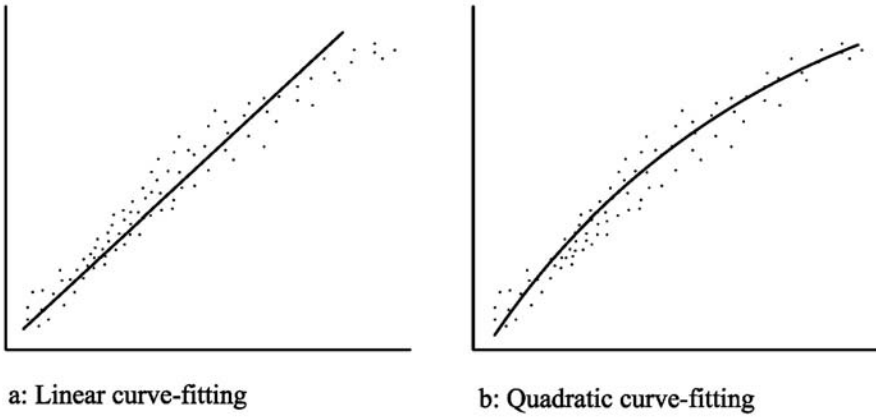

Figure 2-8: Linear and quadratic least squares

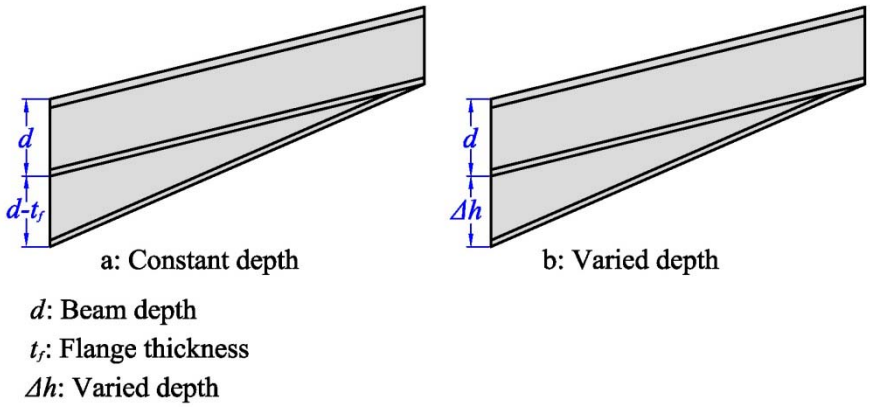

Figure 2-9: A prismatic member with the varied and constant depths

To have more effective curve fitting results, all existing eighty universal beam sections in the categories of standard steel are employed. Their cross-sectional areas and moments of inertia are involved in the developed stiffness matrix. It is assumed a member with a certain length which has a linearly varied depth along its length. Basically, the collection of data relies on two major assumptions; first, when the depth of one member's end is varied, and second, when the depth of one member's end is constant and is approximately twice the other member's end (Fig. 2-9). The depth varies between 10mm and 1280mm which in increments of 10mm. As a result, there will be 128x80 items of data. For the second set of data, the depth does not vary in a given range and is approximately twice the depth of the member section which consequently gives 80 items of data to collect.

The process begins with a programmed stiffness matrix written in Visual Basic 6.0 code. The program is so coded that the values of matrix elements are divided by the sum of the areas of the ends of member for the axial effect part of the matrix, and the

sum of the second moment of areas of the ends of member for the shear and moment effects part of the matrix. Since the length of each member is constant, it is exempted in calculation of each cross-section's stiffness matrix. The data obtained are collected in a 'text' file and then is transmitted to an 'excel' file. They are eventually imported into Mathematica, for linear regression analysis.

The regression analysis was conducted separately for each of two groups of the independent variables; the first group used independent variables with the highest degree of '1'. The second group used independent variables with the highest degree of '2' in the linear regression analysis. However, the second group displayed a better curve than the first one. Once the test was finished, the closest fitting curve was illustrated by Mathematica with the associated equations that include both coefficients and variables. The results reveal that the value of R-squared is 0.998 which indicates high accuracy of the curve fit to the scattered points (Figs. 2-10 to 2-13).

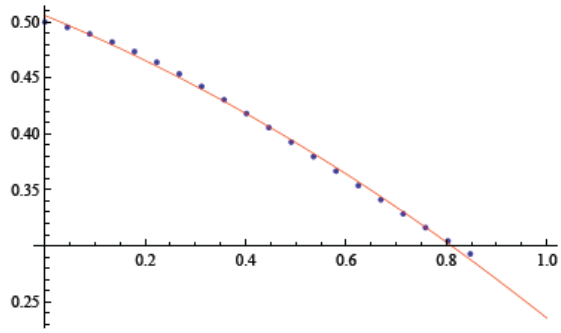


```
In[69]:= << LinearRegression`

Regress[Partition[Riffle[a, Map[Part[#, 9] &, sm3a]], 2], {1, x, x^2}, x]
```

		Estimate	SE	TStat	PValue
ParameterTable →	1	0.505886	0.00189583	266.841	0.
	x	-0.184259	0.010365	-17.777	2.03373×10^{-12},
	x^2	-0.086305	0.0118018	-7.31284	1.21238×10^{-6}

RSquared → 0.998136, AdjustedRSquared → 0.997917, EstimatedVariance → 9.6936×10^{-6},

Figure 2-10: Part of the regression analysis by 'Mathematica'

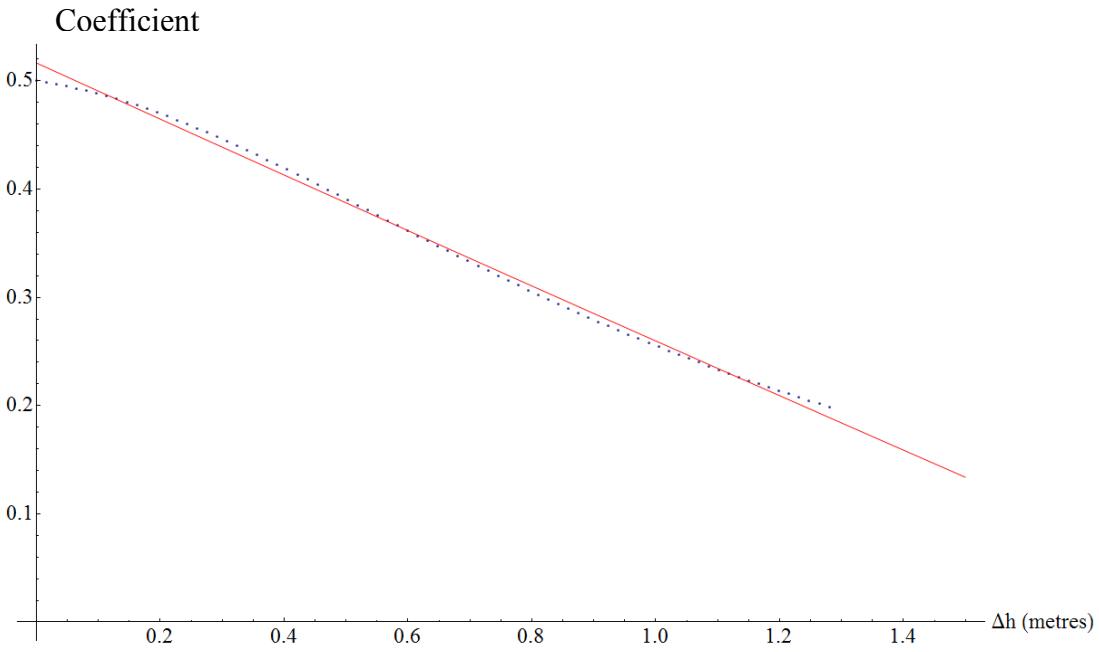

Figure 2-11: Linear curve fitting (least square) conducted by 'Mathematica'

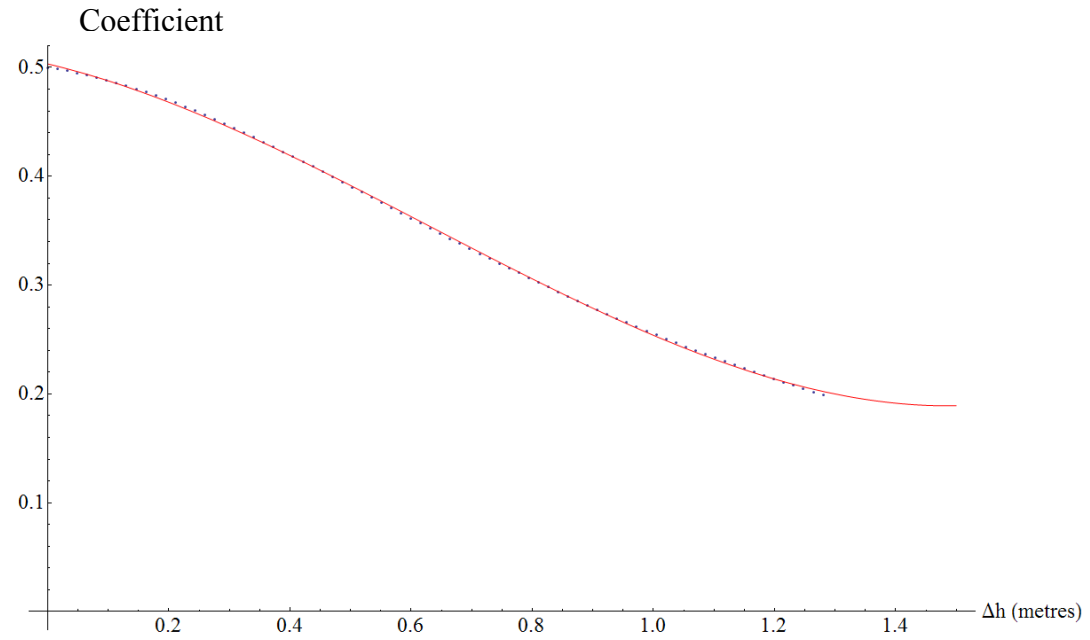

Figure 2-12: Quadratic curve fitting (least square) conducted by 'Mathematica'

The procedure mentioned above, made it possible to develop new practical stiffness matrices which are relatively easy for the engineer to apply. There is no element of integration. This saves the computation time for both hand calculation and computer operation. The developed stiffness matrix, generated by regression analysis, which has a different depth at one end of the member, has the form below:

If $A_1 \geq A_2$:

$$[K] = \frac{E}{L^2}\begin{bmatrix} a(A'L) & 0 & 0 & -a(A'L) & 0 & 0 \\ & b(12I'/L) & c(6I') & 0 & -b(12I'/L) & d(6I') \\ & & e(4I'L) & 0 & -c(6I') & f(2I'L) \\ & & & a(A'L) & 0 & 0 \\ & Symmetry & & & b(12I'/L) & -d(6I') \\ & & & & & g(4I'L) \end{bmatrix} \quad (2\text{-}29)$$

If $A_1 < A_2$:

$$[K] = \frac{E}{L^2}\begin{bmatrix} a(A'L) & 0 & 0 & -a(A'L) & 0 & 0 \\ & b(12I'/L) & d(6I') & 0 & -b(12I'/L) & c(6I') \\ & & g(4I'L) & 0 & -d(6I') & f(2I'L) \\ & & & a(A'L) & 0 & 0 \\ & Symmetry & & & b(12I'/L) & -c(6I') \\ & & & & & e(4I'L) \end{bmatrix} \quad (2\text{-}30)$$

Where:

$A' = A_1 + A_2$

$I' = I_1 + I_2$

$a = 0.50$

$b = 0.50 - 0.53\Delta d + 0.17(\Delta d)^2$

$c = 0.50 - 0.59\Delta d + 0.21(\Delta d)^2$

$d = 0.50 - 0.47\Delta d + 0.13(\Delta d)^2$

$e = 0.50 - 0.56\Delta d + 0.21(\Delta d)^2$

$f = 0.50 - 0.64\Delta d + 0.23(\Delta d)^2$

$g = 0.50 - 0.39\Delta d + 0.08(\Delta d)^2$

A_1 and A_2 are the areas of the member's ends

I_1 and I_2 are the moments of inertia of the member's ends

Δd is the difference between the depths of member's ends

When $A_1 = A_2$ then $\Delta d = 0$, the stiffness matrix defined in the Eqs. 2-29 and 2-30 reverts to the stiffness matrix for prismatic members.

In the case when the depth of one end does not vary and is assumed as approximately twice the depth of the other end, the stiffness matrix has a simpler form:

If $A_1 > A_2$:

$$[K] = \frac{E}{L^2}\begin{bmatrix} 0.50A'L & 0 & 0 & -0.50A'L & 0 & 0 \\ & 0.32(12I'/L) & 0.36(6I') & 0 & -0.32(12I'/L) & 0.29(6I') \\ & & 0.39(4I'L) & 0 & -0.36(6I') & 0.28(2I'L) \\ & & & 0.50(A'L) & 0 & 0 \\ & \textit{Symmetry} & & & 0.32(12I'/L) & -0.29(6I') \\ & & & & & 0.29(4I'L) \end{bmatrix}$$

(2-31)

If $A_1 < A_2$:

$$[K] = \frac{E}{L^2}\begin{bmatrix} 0.50A'L & 0 & 0 & -0.50A'L & 0 & 0 \\ & 0.32(12I'/L) & 0.29(6I') & 0 & -0.32(12I'/L) & 0.36(6I') \\ & & 0.29(4I'L) & 0 & -0.29(6I') & 0.28(2I'L) \\ & & & 0.50(A'L) & 0 & 0 \\ & \textit{Symmetry} & & & 0.32(12I'/L) & -0.36(6I') \\ & & & & & 0.39(4I'L) \end{bmatrix}$$

(2-32)

2.5 Case study

A case study is carried out to investigate the suitability of the developed stiffness matrix in measuring the response of the structure to the applied load. Structural analysis is conducted on a pitched-roof haunched-rafter SPF (given in Fig. 2-13) using direct stiffness method to examine the suitability of the developed matrix. The SPF is assumed to experience a gravity load of 14kN generated by purlins spaced horizontally at 3m centre to centre. A horizontal load of 0.7kN is assumed to act on the frame to portray the sway behaviour. The universal beam sections of 762×267×134 and 686×254×170 are used for the columns and rafters successively and the depth of the haunch is assumed to be equal to the depth of the section of the rafter minus the thickness of the flange (Fig. 2-9).

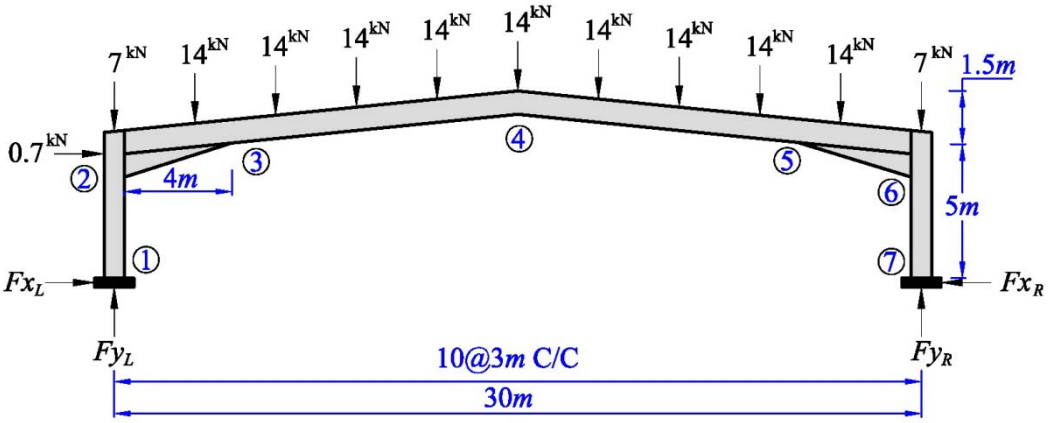

Figure 2-13: The steel portal frames used as case study

Table 2-1: Results of structural analysis on the case study

Component	Case 1	Case 2	Difference (%)
Fx_L, kN	60.11	60.67	0.1
Fx_R, kN	60.81	61.37	0.1
Fy_L, kN	69.88	69.88	0
Fy_R, kN	70.12	70.12	0

The steel frame is analysed twice and named as case 1 and case 2. In case 1 the developed stiffness matrices (Eq. 2-31 and Eq. 2-32) are used to set up a global stiffness matrix. Whereas in case 2 the haunched part of the rafter is subdivided into eight smaller prismatic elements. The outputs of both cases is compared and tabulated in Table 2-1. After analysis of the structural response, it was found that using the idea of subdividing the non-prismatic member into prismatic elements of small lengths to form a global stiffness matrix uses three times more computation time than when Eq. 2-31 and Eq. 2-32 are used.

Where:

Fx_L and Fx_R are the horizontal reaction of the left and right hand side supports respectively

F_{YL} and F_{YR} are the vertical reaction of the left and right hand side supports respectively

In the design optimisation, particularly in GA, there are as many iterations used to measure the response of the structure as the size of population in each generation.

The optimum solution may be achieved after processing for a considerable number of generations. Consequently, the process takes a long time and any saving in time will lead to a quicker time of convergence. The developed stiffness matrix is useful in reducing the computation time since it can save a 200% time in computation of the stiffness matrix for each iteration of optimisation process. This is the main reason for conducting the regression analysis, otherwise the original stiffness matrix can be computed in a very short time by writing a computer program if the aim is only to perform structural analysis of a particular frame, and the regression analysis will not be meaningful.

2.6 Summary

In this chapter, the ways of deriving stiffness matrices for prismatic and non-prismatic members were shown. The equations for the slope deflection method were used to form a stiffness matrix for prismatic members. A column analogy and a virtual work method were implemented to form a stiffness matrix for non-prismatic members. Since elements of the matrix for non-prismatic member possess a number of integration elements, a regression analysis was conducted to form a stiffness matrix for non-prismatic members eliminating all the integration parts from the non-prismatic stiffness matrix. A case study was conducted to validate the appropriateness of the developed stiffness matrix.

Chapter 3: Connections in Steel Structures

3.1 Introduction

In the previous chapter, the stiffness matrices of prismatic and non-prismatic members were discussed. The discussions were made while the connections were assumed to have rigid ends. However, the connections do not behave as rigid in practice and a different stiffness matrix and loads vector should be constructed for the members. In this chapter, the real behaviour and characteristics of connections are addressed. The different types of connections are shown and the models used to illustrate the moment-rotation relationships are discussed.

3.2 Semi-rigid connections

A connection acts as medium through which forces are transferred from one structure member to another. The structural response of a steel frame is closely related to the behaviour of beam-to-column connections (Lorenz *et al*., 1993; Ivany and Baniotopoulos, 2000; de Lima *et al*, 2002; Castro *et al.*, 2007) as they are the main points that transfer the applied loads to the substructures. One of the forces that is transferred through the connection is the bending moment resulting in the rotational deformation (Dhillon and O'Malley III, 1999) which plays an influential role in analysis and design of steel frames.

Generally, there are two types of connections used in the practice by designers, due to their simplicity in design; pinned (flexible) and fixed (rigid) ones. The fully rigid assumption implies that full slope continuity exists between adjoining members where no relative rotation occurs between the connected members, which transmit substantially not only significant amount of bending moment, but also shear and axial forces, between the contiguous members of the structure. In contrast, the pinned joint assumption implies that the beam behaves as if simply supported and prevents any moment transmission between the elements of the structure. However, investigations have shown that the behaviour of a beam-column connection lies

somewhere between the two aforementioned extremes, as shown in Fig. 3-1, known as semi-rigid connection (Jones *et al*., 1980; Bjorhovde *et al*. 1990; Barakat and Chen, 1991; Goto and Miyashita 1998; Kameshki and Saka, 2001; Filho *et al*. 2004; Castro et al. 2007). The semi-rigid joint is one that has the capability to transmit the bending moment intermediate between that of the rigid and the fixed ones. Under load, the interconnected elements of a semi-rigid joints present relative rotation and are able to transmit part of active moment (Filho *et al*. 2004).

The flexibility of connectors is modelled by a spring and used to predict the semi-rigid behaviour of the connection. The behaviour of springs represents, separately, the moment-rotation and force-deformation curves for moment, for axial and shear forces. As a result, no interaction can be found between the springs, and the interaction between the bending moments and forces may be considered, implicitly, as either force-deformation or moment-rotation relationships (Chan *et al*, 2005). To involve such these connections in measuring the response of a structure, an 'initial stiffness' is formulated which represents the spring behaviour. The quality of the overall joints depends on how well the assumed spring stiffness reflects the real load transfer effects between columns and beams (Kattner and Crisinel 2000). In preliminary design, it is difficult to assess the stiffness of semi-rigid joints as there is no unified equation to formulate the initial stiffness of the joint (Jaspart, 2000). Depending on the geometry of the connection, elastic properties of the materials, and the material yielding, the initial stiffness of the moment-rotation curve can be

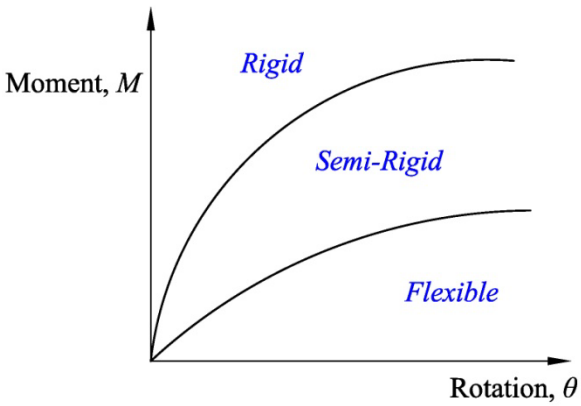

Figure 3-1: Classification of connection in steel frames according to the moment-rotation relationship

obtained (Aggarwal and Coates, 1986; Bahaari and Sherbourne, 1994; Cabrero and Bayo, 2005; Al-khatab and Bouchaïr, 2007).

Some classification systems of connection have been proposed in a number of references independently; among them are Bjorhovde *et al.* (1990), and EC3 CEN, 2005). The classification system proposed by Bjorhovde *et al.* (Fig. 3-2) appears not to consider the overall behaviour of the member, since prior knowledge of the member's details are not available. In contrast, the classification system proposed by the EC3 (Fig. 3-3) is based on the overall behaviour of the member and is more rational if layout and member's details in the structural systems are known in advance. However, the EC3 proposal does not address the ductility demand of the connection, contrary to the Bjorhovde *et al.* one, which considers the ductility in the classification system.

Since analysis and design of semi-rigid frames need the moment-rotation relationship of the connections, several mathematical models of this relationship have been developed. Among these are the Fry and Morris (1975) polynomial model, Kishi and Chen power model (Kishi and Chen, 1990), and EC3's model. These models try to determine the value of initial stiffness of the connection as well as to specify the region of connection, either pinned, semi-rigid, or rigid.

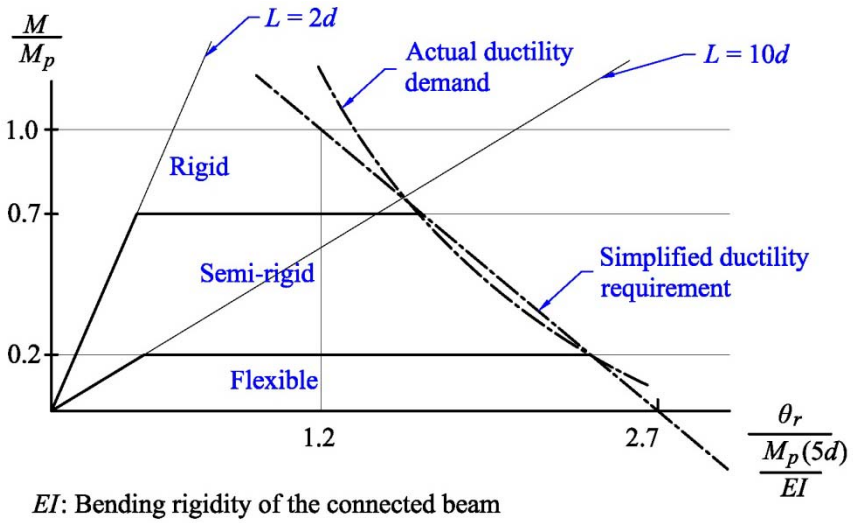

EI: Bending rigidity of the connected beam

d: Depth of beam

M_p: Plastic moment capacity of the connected beam

θ_r: Rotation of the connection

Figure 3-2: Connections classification system according to Bjorhovde *et al.* (1990)

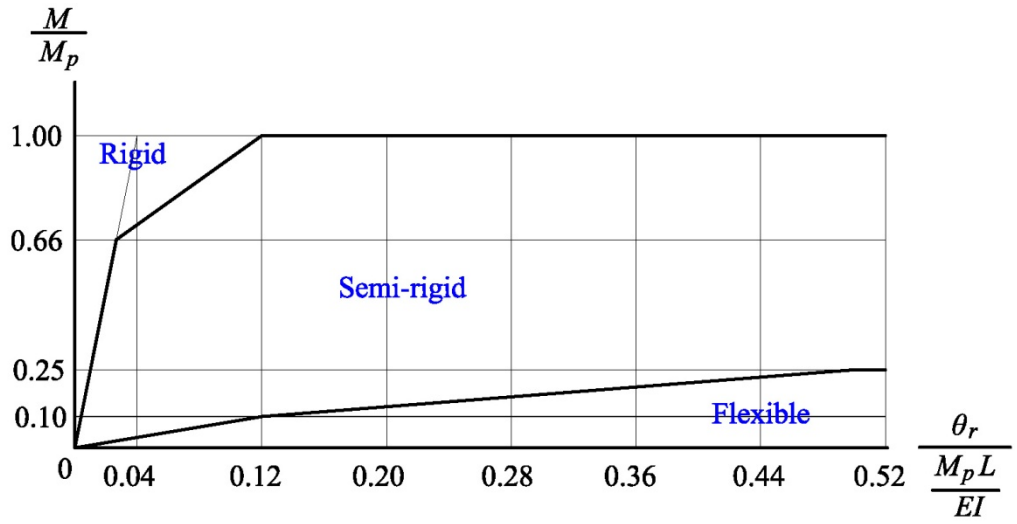

a: Unbraced frame

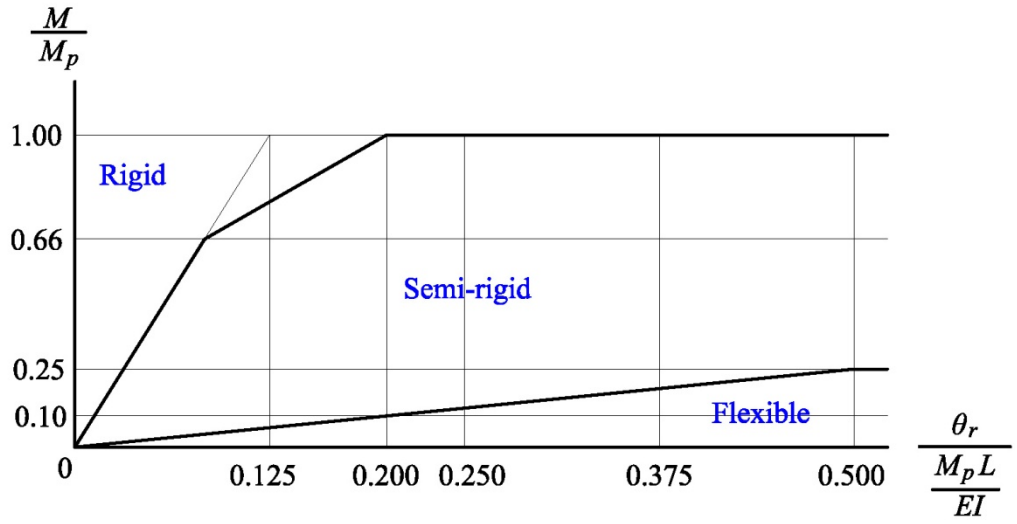

b: Braced frame

EI: Bending rigidity of the connected beam

L: Beam length

M_p: Plastic moment capacity of the connected beam

θ_r: Rotation of the connection

Figure 3-3: Connection classification system according to EC3

3.3 Types of connections

A connection can be defined as a set of the physical components which mechanically fasten the connected elements. Selection of the type of connection depends on the nature and type of the steel frame used in construction. Generally, there are nine types of steel connection commonly used in steel structures; single web angle, double

web angle, single plate, header plate, top and seat angles, top and seat angles with double web angle, extended end plate on the tension side, extended end plate on both tension and compression sides, flush end plate, and T-stub. Fig. 3-4 depicts the moment-rotation relationship of different connections.

A single web angle connection (Fig 3-5) consists of an angle either welded or bolted to both beam and column and is only fastened to the column on one side of the beam. A double web angle connection (Fig 3-6) has two angles that are fastened to the column on both sides of the beam. A single plate connection (Fig 3-7) uses the plate instead of an angle. Since a simple plate is used for the connection, a single plate connection will result in less material used in the connection. In addition, as one side of the plate is fully welded to the column flange, it can have higher rigidity than a single web-angle connection has. A header plate connection (Fig 3-8), by contrast, consists of an end plate, whose length is less than the depth of beam and is welded to the beam and bolted to the column. A top and seat angle connection (Fig 3-9) is a combination of a top angle which provides lateral support of the compression flange of the beam and a seat angle which has the responsibility to transfer the vertical reaction of the beam to the column. The seat does not give a significant restraining moment on the end of the beam. However, experimental observations have shown that the seat does not only transfer the vertical load, but also some end moment of the beam, to the column (Chen *et al*., 1996). As it appears from its name, a top and seat angle with double web angle has double angles which connect the beam and column in addition to top and seat angles (Fig 3-10). The web angles are to transfer the shear forces and improve the restraint characteristics of the connection, whereas the top and seat angle provide some moment resistance. This type of connection can better illustrate semi-rigid behaviour of a connection.

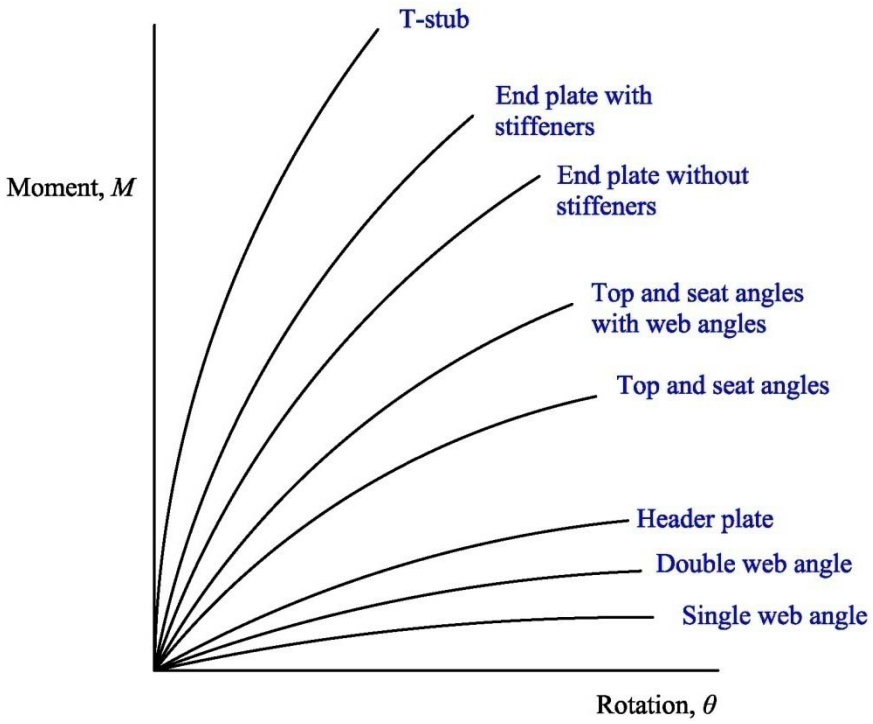

Figure 3-4: Moment-rotation curves of different types of connections (After: Chen *et al*., 1996)

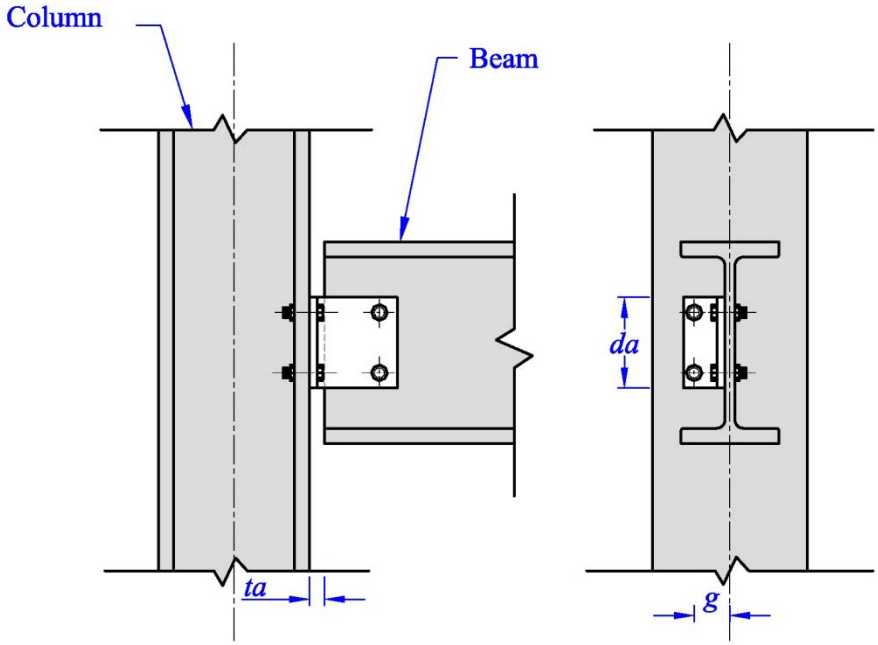

Figure 3-5: A single web angle connection

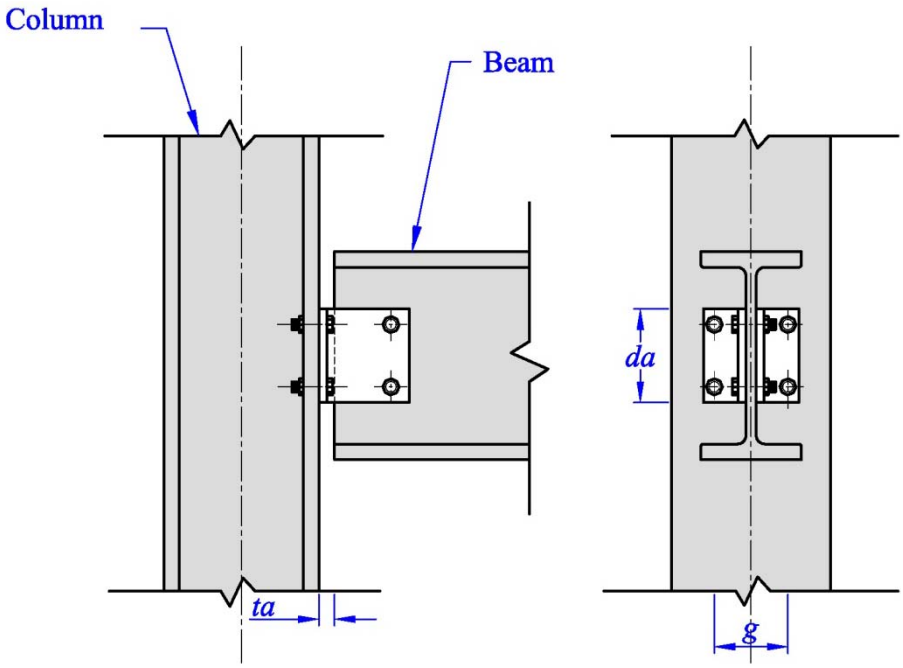

Figure 3-6: A double web angle connection

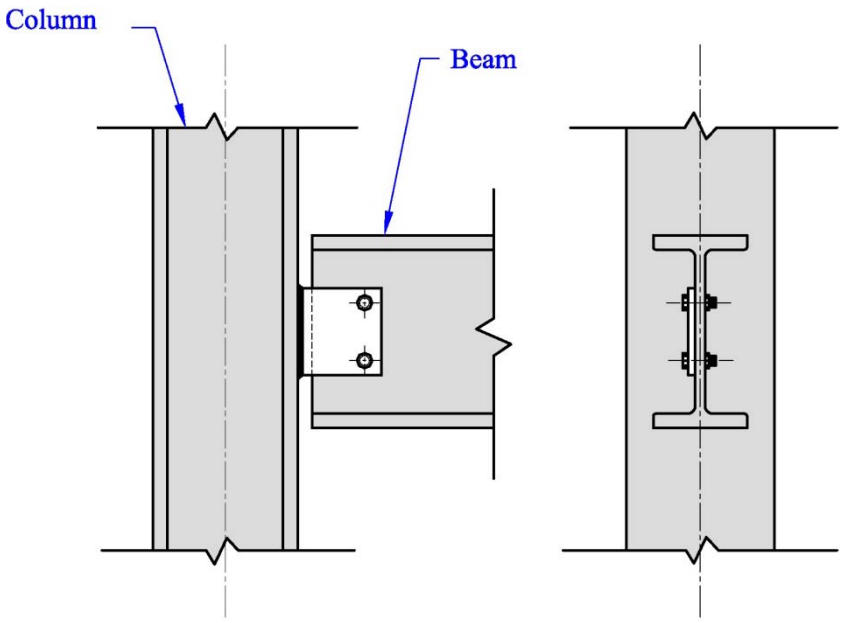

Figure 3-7: A single plate connection

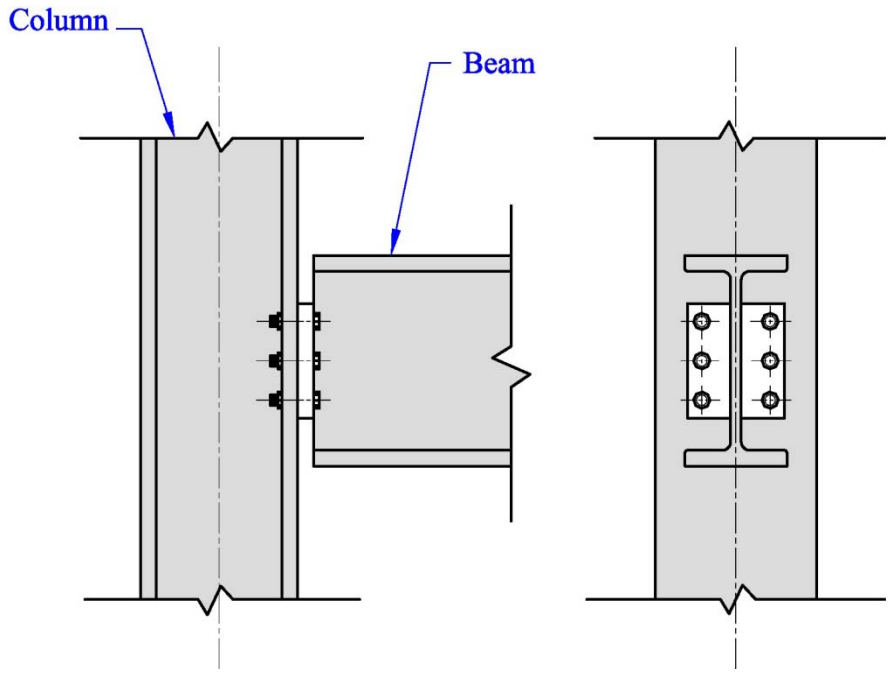

Figure 3-8: A header plate connection

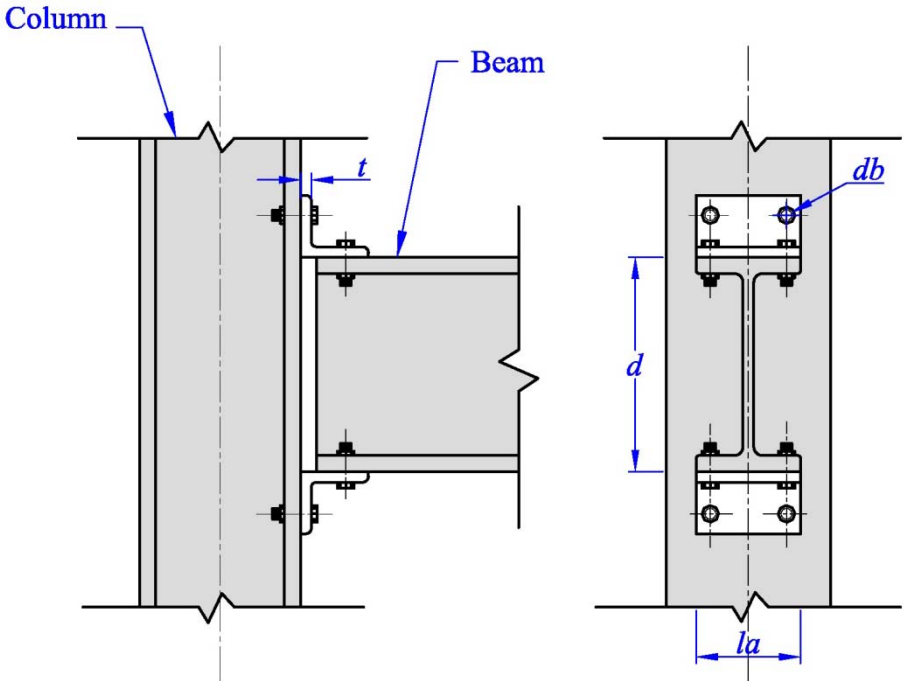

Figure 3-9: A top and seat angle connection

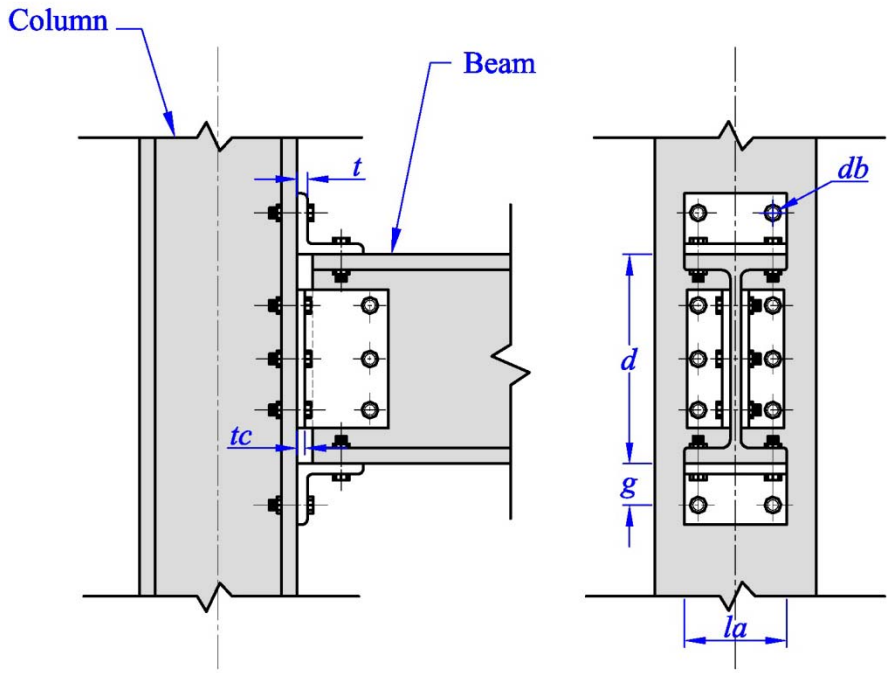

Figure 3-10: A top and seat angle with web angles connection

Bolted connections, especially the end plate type, have increased their popularity as less supervision in construction is required and are shorter assembled than welded joints. In general, end plate connections include a plate which is fully welded to the beam on entire area of both flange and web in the fabrication workshop and the beam is bolted in-situ to the column. These types of connection are accounted as fully rigid connections with a high stiffness. There are two types of extended end plate connections; an extended end plate on the tension side only (Fig 3-11) that will improve the connection to withstand a heavy negative moment and an extended plate on both compression and tension sides (Fig 3-12) which is capable of responding well to the reversal moment like what occurs due to seismic forces. A comparison of moment-rotation curves has shown that the extend of plate on the compression side has limited influence on the behaviour and strength of the connections (Bahaari and Sherbourne 1994). In some cases, stiffeners are used for the column with end plate connections due to large axial forces from the steel beam (Fig 3-13). Bolted flush end-plates (Fig. 3-14) are the most popular type of connections that are used in the multi-storey building to assemble the structural elements of the steel works (Mohamadi-shooreh and Mofid 2008). The plate is rectangular with depth and width slightly larger than those in the beam and the plate is fully welded to the beam end. Bolted flush end-plates are attached to the face of a column or another beam near to

the tension and compression zones of the beam by means of one or two pairs of high strength bolts. This type of steel connection is frequently used in SPFs. A T-stub connection (Fig 3-15) consists of two double web angles which are either welded or bolted at the top and bottom of the beam and connected to the column. A T-stub connection has substantial moment restraint, and transfers shear force and end bending moments to the column. This type of connection possesses all the characteristics of a highly rigid connection.

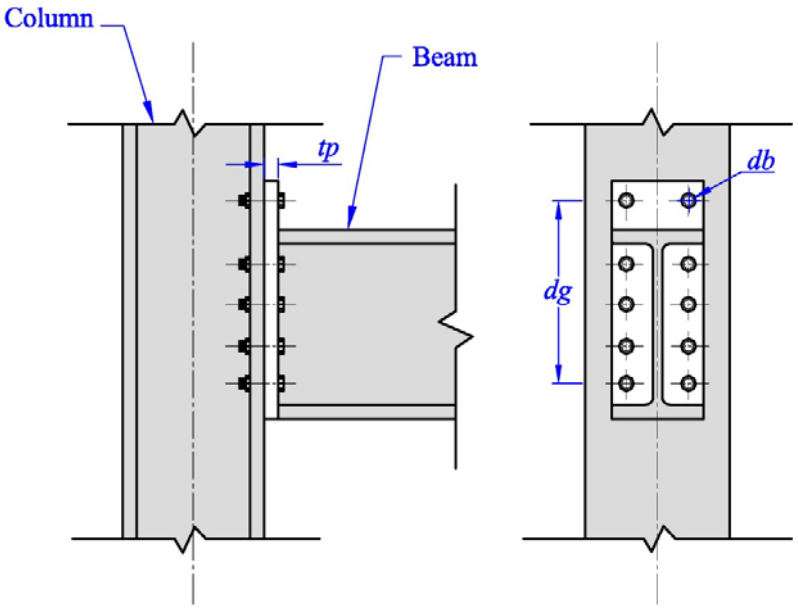

Figure 3-11: An extended end plate on tension side

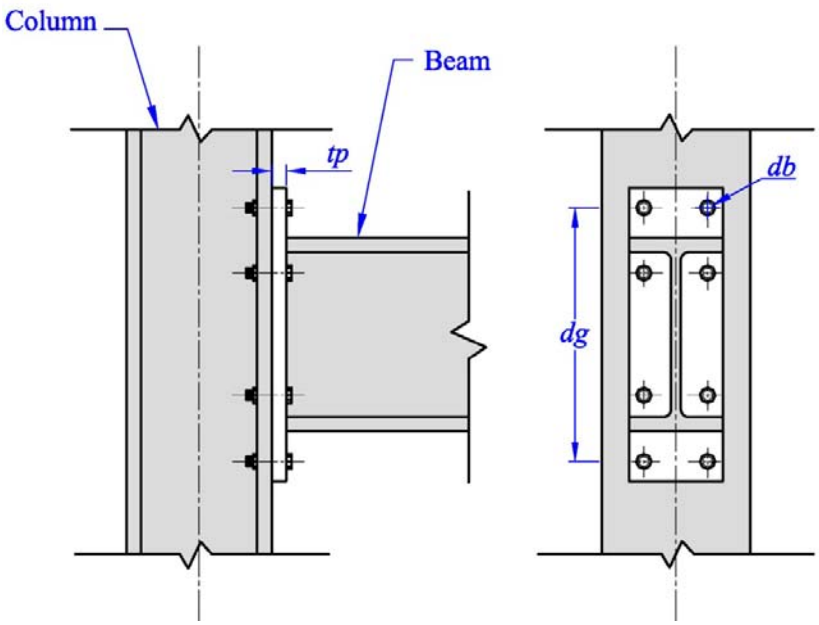

Figure 3-12: An extended end plate on both tension and compression sides

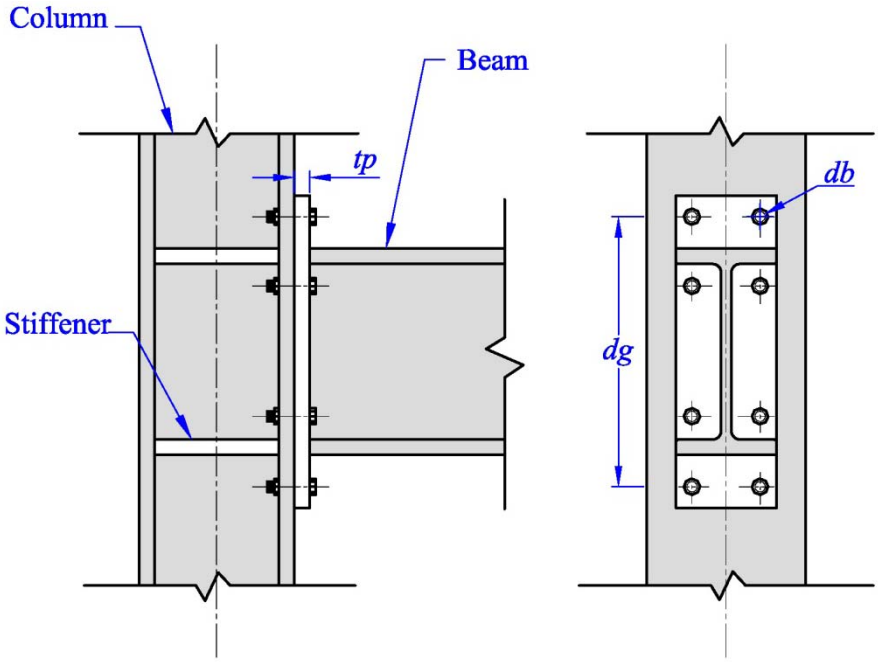

Figure 3-13: An extended end plate with column stiffeners

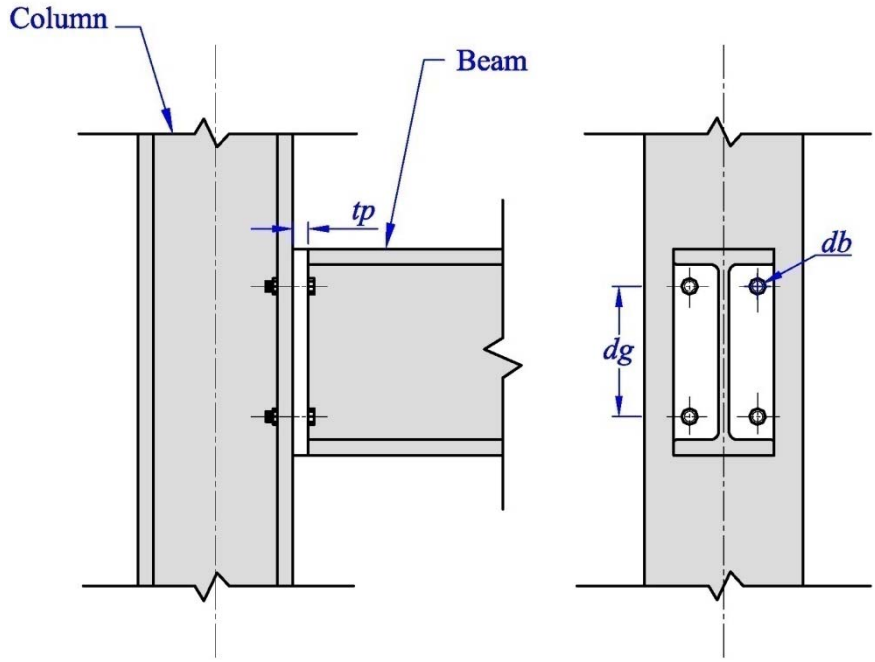

Figure 3-14: A flush end connection

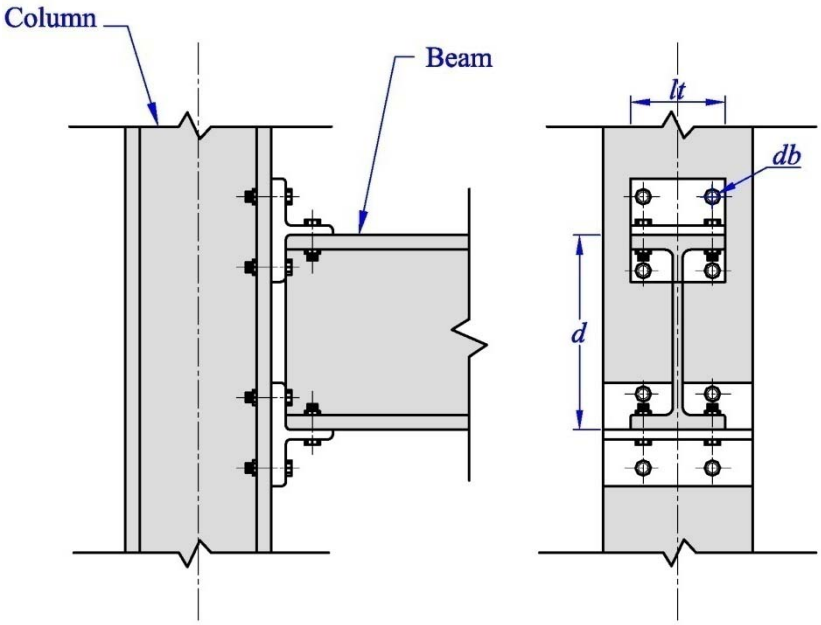

Figure 3-15: A T-stub connection

3.4 Analysis of semi-rigid members

The derivation of a stiffness matrix for a member with semi-rigid ends can be carried out by modifying the slope deflection equations. For the beam, as shown in Fig. 3-16, the relative rotational spring of both ends are related to the spring stiffness, known as initial stiffness. This can be found as:

$$\theta_{ri} = \frac{M_i}{R_{ki}} \tag{3-1a}$$

and

$$\theta_{rj} = \frac{M_j}{R_{kj}} \tag{3-1b}$$

Where:

M_i and M_j are bending moment at ends i and j respectively
R_{ki} and R_{kj} are initial stiffness at the member's ends
θ_{ri} and θ_{rj} are the rotations at the member's ends

The slope deflection equation has the following general form for members with rigid connections:

$$M_{AB} = \frac{EI}{L}\left[4\theta_A + 2\theta_B - 6\frac{\Delta}{L}\right] \quad \text{(3-2a)}$$

$$M_{BA} = \frac{EI}{L}\left[2\theta_A + 4\theta_B - 6\frac{\Delta}{L}\right] \quad \text{(3-2b)}$$

Where:

Δ is the relative lateral displacements of ends A and B

θ_A is the slope angle of member end A

θ_B is the slope angle of member end B

The absence of the cross-sectional area of the member in these equations implies that the slope deflection method neglects the effect of shear and axial deformations.

The modified slope deflection can be re-written as:

$$M_i = \frac{EI}{L}\left[4(\theta_i - \theta_{ri}) + 2(\theta_j - \theta_{rj})\right] \quad \text{(3-3a)}$$

$$M_j = \frac{EI}{L}\left[2(\theta_i - \theta_{ri}) + 4(\theta_j - \theta_{rj})\right] \quad \text{(3-3b)}$$

Substituting Eq. 3-1 into Eq. 3-3 gives:

$$M_i = \frac{EI}{L}\left[4\left(\theta_i - \frac{M_i}{R_{ki}}\right) + 2\left(\theta_j - \frac{M_j}{R_{kj}}\right)\right] \quad \text{(3-4a)}$$

$$M_j = \frac{EI}{L}\left[2\left(\theta_i - \frac{M_i}{R_{ki}}\right) + 4\left(\theta_j - \frac{M_j}{R_{kj}}\right)\right] \quad \text{(3-4b)}$$

Solving the simultaneous Eq. (3-4a) and Eq. (3-4b), M_i and M_j are formed to be (Chen and Lui, 1991):

$$M_i = \frac{EI}{L}\left(S_{ii}\theta_i + S_{ij}\theta_j\right) \quad \text{(3-5a)}$$

$$M_j = \frac{EI}{L}\left(S_{ij}\theta_i + S_{jj}\theta_j\right) \quad \text{(3-5b)}$$

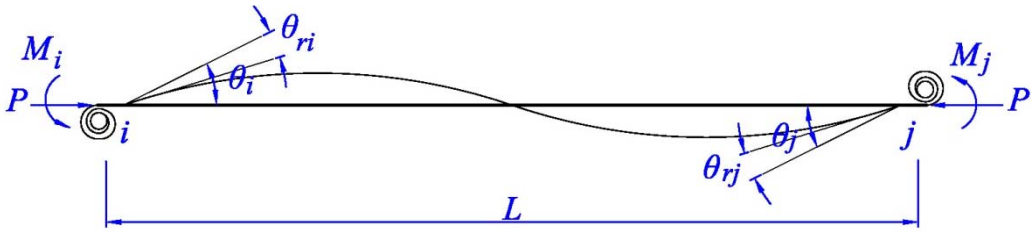

Figure 3-16: A beam element with rotational spring

where

$$S_{ii} = \frac{1}{R^*}\left(4 + \frac{12EI}{LR_{kj}}\right) \tag{3-6a}$$

$$S_{jj} = \frac{1}{R^*}\left(4 + \frac{12EI}{LR_{ki}}\right) \tag{3-6b}$$

$$S_{ij} = \frac{2}{R^*} \tag{3-6c}$$

$$R^* = \left(1 - \frac{4EI}{LR_{ki}}\right)\left(1 + \frac{4EI}{LR_{kj}}\right) - \left(\frac{EI}{L}\right)^2\left(\frac{4}{R_{ki}R_{kj}}\right) \tag{3-7}$$

Transferring Eq. 3-6a and Eq. 3-6b into a matrix relationship of a member stiffnesses with six degrees of freedom, including the axial stiffness coefficient, the following stiffness matrix for a plane-frame member with semi-rigid ends can be obtained:

$$k = \frac{EI}{L}\begin{bmatrix} \frac{A}{I} & 0 & 0 & -\frac{A}{I} & 0 & 0 \\ & \frac{(S_{ii}+2S_{ij}+S_{jj})}{L^2} & \frac{(S_{ii}+S_{ij})}{L} & 0 & \frac{-(S_{ii}+2S_{ij}+S_{jj})}{L^2} & \frac{(S_{ij}+S_{ij})}{L} \\ & & Sii & 0 & \frac{-(S_{ii}+S_{ij})}{L} & S_{ij} \\ & & & \frac{A}{I} & 0 & 0 \\ & Symmetry & & & \frac{(S_{ii}+2S_{ij}+S_{jj})}{L^2} & \frac{-(S_{ij}+S_{ij})}{L} \\ & & & & & Sjj \end{bmatrix} \tag{3-8}$$

In case that only one of the member's ends is semi-rigid and the other one is rigid, the initial stiffness value of the rigid ends approaches infinity. For example, if the member end *i* is semi-rigid and the end *j* is rigid, then the following modification must be accounted:

$$S_{ii} = \frac{4}{R^*} \tag{3-9}$$

$$R^* = 1 - \frac{4EI}{LR_{ki}} \tag{3-10}$$

Considering both member's ends as hinged will yield zero values for S_{ii}, S_{ij}, and S_{jj} which will consequently form the stiffness matrix of members that are subjected to axial forces only (truss members).

Dhillon and O'Malley III (1999) derived end moments for the semi-rigid connections, based on the slope deflection method and superposition of loads. Fig. 3-17 depicts the beam element that they used to derive end moments.

According to Dhillon and O'Malley III (1999), consider the beam *ij* with rotational springs of stiffness R_{ki} and R_{kj} at ends *i* and *j* subject to concentrated load:

$$M_i = R_{ki}\theta_{ri} \tag{3-11a}$$

$$M_j = R_{kj}\theta_{rj} \tag{3-11b}$$

They replaced the beam-with-spring model by a simply supported beam which is subjected to three loads; concentrated load, and moments at the ends as shown in Fig. 3-17. Then, they applied superposition and derived the two semi-rigid member ends bending moments to be:

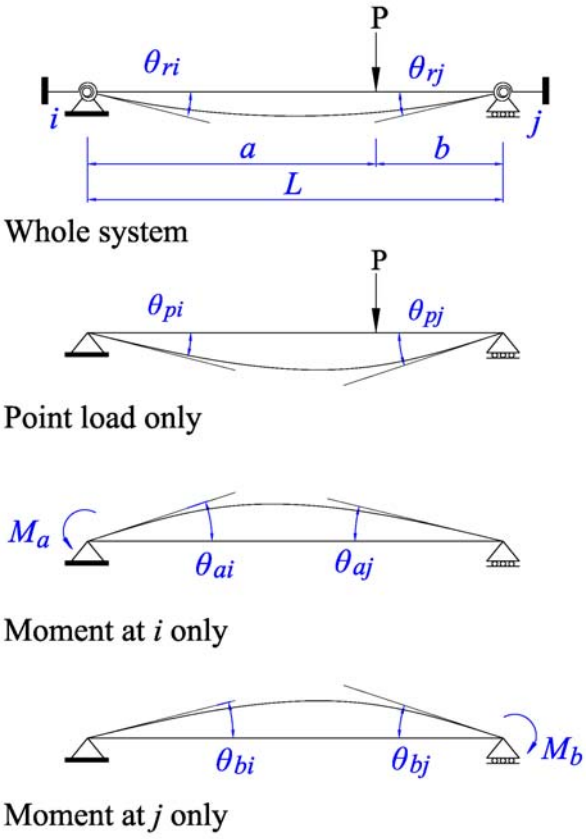

Figure 3-17: A beam element with semi-rigid ends

$$M_{SF} = \frac{M_{Fi} + 6\alpha_B M_{Fj}}{1 + 4\alpha_A + 4\alpha_B + 12\alpha_A\alpha_B} \tag{3-12a}$$

$$M_{SF} = \frac{M_{Fj} + 6\alpha_A M_{Fi}}{1 + 4\alpha_A + 4\alpha_B + 12\alpha_A\alpha_B} \tag{3-12b}$$

where:

$$\alpha_A = \frac{EI}{LR_{ki}} \tag{3-13a}$$

$$\alpha_B = \frac{EI}{LR_{kj}} \tag{3-13b}$$

E	is the modulus of elasticity
I	is second moment of area of the member's cross-section
M_{SRi} and M_{SRj}	are the semi-fixed end moments
M_{Fi} and M_{Fj}	are the fixed end moments

When the both member's ends are considered as rigid ones, the value of α_A and α_B will be zero then Eq. 3-13 yields fixed end moments for rigid ends.

3.5 Modelling of connections

The preliminary requirement of measuring the responses of structures is to determine the initial stiffness of the connection. This must be found before starting any analysis process. As mentioned earlier, there are three popular models which are used to find the initial stiffness of the connection. These models are the Frye-Morris polynomial model, Kishi-Chen power model, and EC3 proposed model. In addition to these models, a number of models such as the linear model, B-spline model, and exponential model are presented by Chen and Lui (1991). Also, some studies have been conducted to obtain the initial stiffness of connection using the finite element method. Mohamadi-shooreh and Mofid (2008) recently developed an equation for the initial stiffness of connection after a large regression analysis. They implemented the method on the flush end plate connection with high strength bolts.

3.5.1 Frye-Morris polynomial model

The most popular model adopted in structural analysis of steel frames with semi-rigid connection is the Frye-Morris polynomial model. Frye and Morris (1975) used the method of least squares to find the relationship between moment and rotation by employing different types of connections. The model they developed has the general form of:

$$\theta_r = C_1(KM)^1 + C_2(KM)^3 + C_3(KM)^5 \qquad (3\text{-}14)$$

Where:

K	is a standardization parameter depending upon the connection and its geometry
C_1, C_2, and C_3	are parameters obtained by curve fitting

The polynomial form demonstrates the M-θ_r behaviour reasonably well. The main drawback of the model is that a polynomial essentially has a peak and a trough within a certain range (Chen and Lui, 1991). It is, however, easy to apply in practice.

By taking the first derivative for Eq. 3-14, the initial stiffness of the connection can be found:

$$(d\theta_r) = C_1 KM(dM) + 3C_2(KM)^2(dM) + 4C_3(KM)^4(dM)$$

or

$$d\theta_r = [C_1 KM + 3C_2(KM)^2 + 4C_3(KM)^4]dM$$

therefore:

$$R_k = \frac{dM}{d\theta_r} = \frac{1}{C_1 KM + 3C_2(KM)^2 + 5C_3(KM)^4} \qquad (3\text{-}15)$$

Where:

R_k is the slope of the M-θ_r curve called as initial stiffness

The standardization parameter, K, and the curve-fitting constants, C_1, C_2, and C_3, are to be found from Table 3-1:

Table 3-1: Curve fitting and standardization constants developed by Frye and Morris (1975)

Connection type	Curve-fitting constants	Standardization constants
Single web angle connection	$C_1 = 4.28\times10^{-3}$ $C_2 = 1.45\times10^{-9}$ $C_3 = 1.51\times10^{-16}$	$K = d_a^{-2.4} t_a^{-1.81} g^{0.15}$
Double web angle connection	$C_1 = 3.66\times10^{-4}$ $C_2 = 1.15\times10^{-6}$ $C_3 = 4.57\times10^{-8}$	$K = d_a^{-2.4} t_a^{-1.81} g^{0.15}$
Header plate connection	$C_1 = 5.10\times10^{-5}$ $C_2 = 6.20\times10^{-10}$ $C_3 = 2.40\times10^{-13}$	$K = t_p^{-1.6} g^{1.6} t_w^{-0.5} d_p^{-2..3}$
Top and seat angles with double web angles connection	$C_1 = 2.23\times10^{-5}$ $C_2 = 1.85\times10^{-8}$ $C_3 = 3.19\times10^{-12}$	$K = d^{-1.287} t^{-1.128} t_c^{-0.415} l_a^{-0.694} g^{1.35}$

Connection type	Curve-fitting constants	Standardization constants
End plate connection without column stiffeners	$C_1 = 1.83\times10^{-3}$ $C_2 = -1.04\times10^{-4}$ $C_3 = 6.38\times10^{-6}$	$K = d_g^{-2.4} t_p^{-0.4} d_b^{-1.5}$
End plate connection with column stiffeners	$C_1 = 1.79\times10^{-3}$ $C_2 = -1.76\times10^{-4}$ $C_3 = 2.04\times10^{-4}$	$K = d_g^{-2.4} t_p^{-0.6}$
T-stub connection	$C_1 = 2.1\times10^{-4}$ $C_2 = 6.2\times10^{-6}$ $C_3 = -7.6\times10^{-9}$	$K = d^{-1.5} t^{-0.5} l_t^{-0.7} d_b^{-1.1}$

All the required parameters for standardization constants have been depicted in Fig. 3-5 to Fig. 3-15, where:

d is the depth of beam section
d_a is the height of the single end plate
d_b is the diameter of the bolt
d_g is the distance between the far tension and compression bolts
dp is the depth of plate in the header plate connections
g is the distance between the centre of bolts in the same row
l_a is the width of the end plate
t is the thickness of the top seat angle section
t_a is the gap between the beam end and the face of the column
t_c is the thickness of the web angle
t_p is the thickness of the end-plate
t_w is the web thickness of the beam

3.5.2 Kishi and Chen power model

The Kishi and Chen (1990) power model is virtually a semi-empirical connection model which is based on three parameters; the initial connection stiffness, R_k, the ultimate moment capacity, M_u, and the shape parameter, n. The proposed power model has the form of:

$$\theta_r = \frac{M}{R_k \left[1 - \left(\frac{M}{M_u} \right)^n \right]^{\frac{1}{n}}} \tag{3-16}$$

Where:

M_u is the ultimate bending moment capacity of the connection

M is the applied bending moment

n is the shape parameter

3.5.3 EC3 proposed equation

Although EC3 considers the ultimate strength in classification of the connections, it does not take into account the behaviour of the serviceability limit state. In addition, EC3 adopts an approximate formula to evaluate the load carrying capacity of the frame. The model is also too simple to reflect, generally, the effect of geometry and member's details of the frame, on the connection behaviour. As a result, the existing classification systems are still very approximate in nature (Goto and Miyashita 1998).

EC3 proposes finding the initial connection stiffness by determining the connection rotation. In the determination of connection rotation, it suggests attributing the deformation of components in the compression zone, tension zone, and shear zone of the member. For the bolted end plate connection, the deformation of the tension zone comes from the deformation of the end plate and the elongation of the bolt. The model suggested by EC3 is limited to the members which experience an axial force not greater than 5% of the allowable axial stress. This indicates that this kind of connection cannot be reasonably used for the SPFs since the axial force is one of the major load applied to the member. This applies particularly to rafters. Provided that the axial force does not exceed 5% of the allowable axial stress, the formula suggested by EC3 for the initial connection stiffness has the following form:

$$R_k = \frac{Ez^2}{\sum_i \frac{1}{k_i}} \tag{3-17}$$

Where:

z is the vertical distance between the centre of tension bolts and centre line of the compression flange

k_i is the stiffness coefficient of the basic joint component i

The stiffness coefficient of joint component, k_i, depends upon the connection type and the bolt row in tension. The main components of the stiffness coefficient can be specified from Fig. 6-11 in part 1.8 of the EC3.

3.5.4 Modelling by finite element

There are a number of studies so far that have used the finite element method to model the moment-rotation relationships to obtain the initial stiffness of connections. Mohamadi-shooreh and Mofid (2008) have recently developed formulae to calculate initial stiffness of a connection. They conducted the study on the bolted flush end-plate connection. After performing the finite element analysis, they carried out regression analysis to set up a number of equations to represent the initial stiffness of certain connections. The advantages of the developed equations are that thay have involved as many geometric parameters as possible and they can provide a reasonable accuracy for the value of the initial stiffness of the connection. The proposed formulae by Mohamadi-shooreh and Mofid are as follows:

$$R_{k1} = \frac{Ez^2}{\dfrac{m^3}{0.9 l_{eff} t_p^3} + \dfrac{L_{bolt}}{1.6 A_s}} d_b^{\alpha_0} \times b^{\alpha_1} \times m^{\alpha_2} \times b_p^{\alpha_3} \times t_p^{\alpha_4} \times t_{fb}^{\alpha_5} \times t_{wb}^{\alpha_6} \times d_{bo}^{\alpha_7} \qquad (3\text{-}18a)$$

$$R_{k2} = \frac{1}{\dfrac{1}{K_{eq-endplate}} + \dfrac{1}{K_{eq-bollt}}} \qquad (3\text{-}18b)$$

$$R_{k3} = \frac{0.0473 \dfrac{b}{d_{bolt}} - 0.291 \left(\dfrac{b}{d_{bolt}} \right)^2 + 1.429}{\dfrac{1}{K_{eq-endplate}} + \dfrac{1}{K_{eq-bollt}}} \qquad (3\text{-}18c)$$

where:

$$K_{eq-bollt} = \frac{Ez^2 L_b}{A_s} d_b^{\alpha_0} \times b^{\alpha_1} \times m^{\alpha_2} \times b_p^{\alpha_3} \times t_p^{\alpha_4} \times t_{fb}^{\alpha_5} \times t_{wb}^{\alpha_6} \times d_{bolt}^{\alpha_7} \times e^{\alpha_8} \quad (3\text{-}19a)$$

$$K_{eq-endplate} = \frac{Ez^2 m^2}{t_p^3} d_b^{\alpha_0} \times b^{\alpha_1} \times m^{\alpha_2} \times b_p^{\alpha_3} \times t_p^{\alpha_4} \times t_{fb}^{\alpha_5} \times t_{wb}^{\alpha_6} \times d_{bolt}^{\alpha_7} \times e^{\alpha_8} \quad (3\text{-}19b)$$

A_s is the bolt net area

b is the vertical distance between the centre of tension bolts and the centre-line of the beam tension flange

b_{fb} is the flange width of the beam

b_p is the width of the end-plate

d_b is depth of the beam

d_{bolt} is the nominal bolt diameter

E is the modulus of elasticity

h_b is the beam section height

h_{wb} is the web height of the beam

$K_{eq\text{-}plate}$ is the bolt equivalent initial stiffness in bending

$K_{eq\text{-}endplate}$ is the end-plate equivalent initial stiffness in bending

L_{bolt} is the length of the bolt

m is the horizontal distance between the centre of the tension bolt and beam web-effective fillet weld

t_{fb} is the flange thickness of the beam

t_p is the thickness of the end-plate

t_{wb} is the web thickness of the beam

z is the vertical distance between the centre of tension bolts and the centre-line of the compression flange

$\alpha_1, \alpha_2, \ldots, \alpha_8$ are dimensionless coefficients defined in Table 5 of Mohamadi-shooreh and Mofid (2008)

The defined parameters are presented in Fig. 3-18.

Since the majority of the connections used in SPFs are flush end plate connection, they are found suitable for this research. However, this method is too complicated to use in practice and a program needs to be set up to measure the response of steel frames against the applied loads.

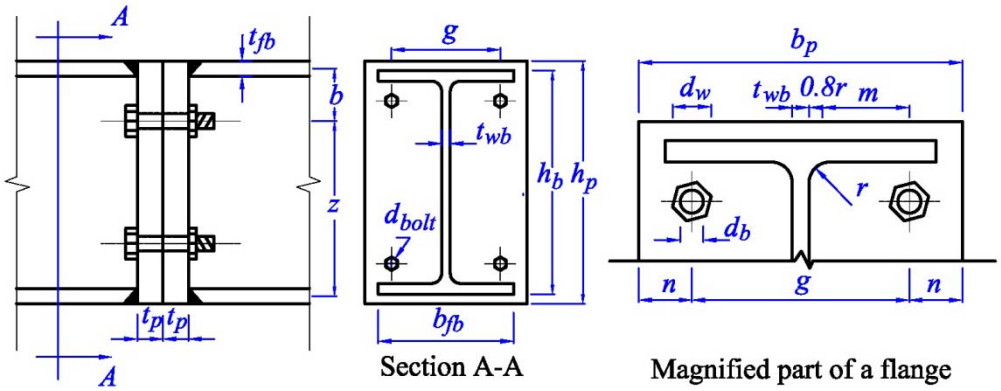

Figure 3-18: Details of flush end plate connection used in the study by Mohammadi-shooreh and Mofid (2008)

A higher joint capacity will be achieved with larger sections and with higher grade or diameter of the bolt, for bolted flush end-plate connections. It is essential that the screw be positioned as close as possible to the flange of member to prevent local buckling of the web due to compressive stress. This is because the joint relies on transferring bending moments carried through the member flange by means of the shear capacity of the screws positioned in the web (Mills and LaBoube, 2004).

3.6 Summary

The real characteristics and behaviour of the connection was discussed. A number of proposed classification systems of connection, including the one proposed by Bjorhovde et al. (1990) and the one proposed by EC3, were addressed with their positive and negative attributes. A number of connections that are commonly used in a real-life steel structure were portrayed, highlighting their essential characteristics and behaviours. The methods of deriving the stiffness matrix and semi-fixed moment of the member with semi-rigid ends were shown. Then four models of connection, proposed by different authors, were presented and discussed thoroughly. It was decided to use a Frye-Morris polynomial model for finding the initial stiffness required for structural analysis of frames with semi-rigid connections. On the other hand, it was also decided to use the model developed by finite elements (Mohammadi-shooreh and Mofid, 2008) as the majority of connections in SPFs are flush end plate connections. A comparison will be made between the results of these two models and will be presented in chapter 7.

Chapter 4: Design Procedures According to BS 5950 and EC3

4.1 Introduction

Structural design can be defined as a nomenclature of an operation for some projects which involves the expert and knowledge of hundreds of researchers (Yourdan and Constantine, 1979). The code of practice can be regarded as a consensus of what is acceptable which incorporates and balances recent research findings and accepted practical experiences (Majid, 1974). The code of practice is regarded as an aid to design which includes allowable stress levels, member capacities, design formulae and recommendations for good practice rather than as a manual or textbook on design.

Once a decision is taken to construct a structure, the structural design must be conducted by selecting a suitable structural system. A structural system includes selection of a structural form for the design stage so that it should be robust in relation to likely hazards. The way of resisting applied loads must also be assessed and then, after the critical load pattern has been defined it must be used to design a suitable structure. There are essentially two stages in the design process for a building. First, analysis to measure the response of the structure to applied loads so that the equilibrium can be maintained. Second, checking the capacity of the member sections to resist the applied loads and achieve continuity of member connections.

4.2 Loading

Assessment of the design loads for a particular structure includes identification of the loads which the structure must accept, and then assigning a suitable value to them. After that, several different ways of imposing loads, either single, or in combination, must be considered. For buildings, the usual forms of the loads are dead load, live load and wind load. In addition, loads due dynamic and seismic forces have to be considered in areas where earthquakes frequently happen. Depending on the

environmental conditions, induced loads by temperature variation, or subsidence might also be considered (Mahfouz, 1999).

4.2.1 Dead Load

Determination of the dead load requires finding the weight of bare steel work as well as the weight of the non-structural parts of the building like the floor slabs, partition walls, ceiling, plaster finishes and services such as pipes and air conditioning ducts. For SPF, the estimated dead load might be practically between 0.25kN/m^2 and 1.0kN/m^2.

4.2.2 Live Load

Live loads in buildings are assigned to those loads which are moveable. Live loads cover items such as occupancy by people, office floor loading, and moveable equipment within the building. The effect of snow sits normally within the live load category.

4.2.3 Wind Load

The effect of the wind load on the structure normally has a dynamic nature. In practice, however, it is customary for most types of structures to treat this as an equivalent static load. Wind dynamic pressure can be determined by identifying the basic wind speed for the geographical location of the building and correcting the pressure by infering the effect of topography, ground roughness and length of exposure to the wind. Depending on building shape, the pressure is then converted into applied load and acts on structural members. BS 6399 Part 2 is dedicated for the wind load estimation on building.

4.3 Design of steel structure to BS 5950

The BS 5950 design procedure is based on limit state theory and includes principles from elastic and plastic theories by incorporating other relevant factors. The design relies on the actual behaviour of the material. The limiting conditions are grouped into two main categories; ultimate limit state and serviceability limit state. The ultimate limit state is the ultimate capability before any increase in load, whereas the

serviceability limit state checks the need for action to prevent utility loss (Mahfouz, 1999). The ultimate limit state is concerned with checking the strength (including general yielding, rupture and buckling), stability against overturning, fracture due to fatigue and brittle fracture. Serviceability limit state checks the deflection, repairable damage due to fatigue and corrosion, vibration, and durability. In the elastic design approach, the design stress is achieved by scaling down the material strength of the member using a factor of safety, whereas the loads are taken as service loads (unfactored).

4.3.1 Load Combination

All the possible load combinations that act on the structure should be taken into consideration. The critical load case is then chosen for the design load. Table 5-1 gives the load factor used for load combinations according to BS 5950: Part 1.

Table 4-1: Load factor of safety and combination (Ref: BS 5950, Table 2)

Loading	**Factor γ_f**
Dead Load	1.4
Dead Load restraining uplift or overturning	1.0
Dead Load acting with *Wind* and *Imposed loads* combined	1.2
Imposed Loads	1.6
Imposed Load acting with *Wind Load*	1.2
Wind Load	1.4
Wind Load acting with *Imposed* or *Crane Load*	1.2
Forces due to temperature effects	1.2
Vertical Crane Load	1.6
Vertical Crane Load acting with Horizontal Crane Loads (crabbing or surge)	1.4
Horizontal Crane Load	1.6
Horizontal Crane Load acting with Vertical	1.4
Crane acting with *Wind Load*	1.2

The load combination for design is selected according the requirements and function of the structure. The majority of the load combination is associated with gravity

loads (combined dead and live loads). However, in some areas which are predicted to be exposed to remarkable wind pressure, the combination of loads includes gravity and wind loads.

In the ultimate limit state, the applied load is multiplied by a factor, γ_f, which is given in Table 4-1. The factored load should act in the most unfavourable but realistic combination for the part of the structure under consideration. The load carrying capacity of the members or joints should be such that they can resist the factored load without failure. Generally three load combinations are taken into consideration in BS 5950:

Load combination 1: Dead load and imposed load (gravity loads);
Load combination 2: Dead load and wind load;
Load combination 3: Dead load, imposed load and wind load.

4.3.2 Notional Horizontal Force

Notional horizontal force is assumed to allow for the effect of practical imperfection of the steel frame. This makes the structure experience an extra horizontal load. BS 5950 has specified a 5% of the gravity load (load combination 1) to be the notional the horizontal force. The horizontal force should be assumed to act simultaneously with the gravity load only on one side of the frame.

4.3.3 Design Strength

Before starting the design, a steel grade has to be adopted. After that a section is assigned to the structural members from the steel table. By considering the minimum thickness of the selected steel, design strength can be specified. Table 9 in BS 5950: Part 1 gives an indication of the value of the design strength, p_y. The given value in the table has been assigned for common steel grade and steel section from the product standards specified in BS 5950: Part 2. In addition, for the elastic properties of the steel, the following values as given in BS 5950: Part 1 should be used:

Modulus of elasticity: $E = 205\ 000\ N/mm^2$
Poisson's ratio: $\nu = 0.30$

Table 4-2: Design strength value (Ref: BS 5950: Part 2, Table 9)

Steel grade	**Thickness less than or equal to, *mm***	**Design strength p_y, N/mm^2**
S 275	16	275
	40	265
	63	255
	80	245
	100	235
	150	225
S 355	16	355
	40	345
	63	335
	80	325
	100	315
	150	295
S 460	16	460
	40	440
	63	430
	80	410
	100	400

4.3.4 Classification of the Cross-Sections

The next step for design is to classify the cross sections that are assumed for the structural members. BS 5950: Part 1 has classified the sections into four classes to determine whether local buckling influences their capacity without calculating their local buckling resistance. This kind of classification is based on the section's width-to-thickness ratio when they are subject to compression stress due to either bending moment or axial forces. The following classes should be applied according to BS 5950: Part 2:

Class 1, Plastic Cross-section: cross section which has the capacity of the plastic hinge rotation

Class 2, Compact Cross-section: cross section which has a capacity of plastic moment

Class 3, Semi-compact Cross-section: cross section which does not have a plastic moment capacity but a compression stress at the extreme compression fibre reach the design strength capacity

Class 4, Slender Cross-section: cross section where the occurrence of local buckling is allowed

To meet the limitations requirement given in Table 11 of BS 5950: Part 1 for rolled I-shaped cross section, the class of the selected steel cross section is specified from the table.

4.3.5 Shear Capacity

Shear capacity of a selected section for structural members must be greater than the applied shear force. The check is done according to:

$$P_v = 0.6 p_y A_v \geq F_v \tag{4-1}$$

In BS 5950: Part 1, the shear area of the cross section A_v is determined as follows:

For rolled I, H and channel sections:

$$A_v = tD \tag{4-2}$$

And for built up sections:

$$A_v = td \tag{4-3}$$

where:

t is the thickness of the web

d is the depth of the web

D is the total depth of the section

Fig. 4-1 shows the shear area which is used to check the shear capacity.

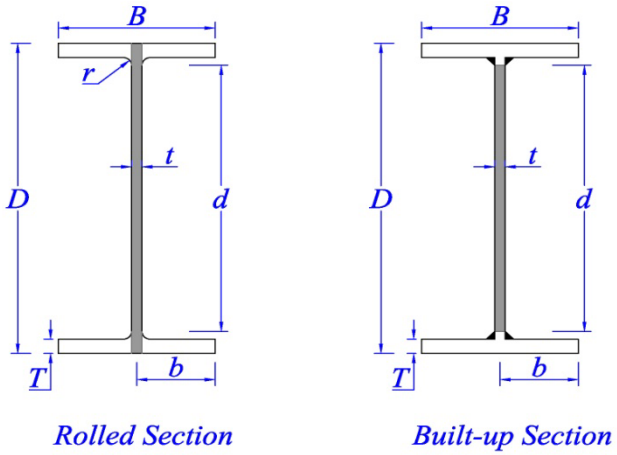

Figure 4-1: Shear area of the UB-section used for SPF

For a rolled section when the depth-to-thickness ratio of a web becomes

$$\frac{d}{t} \geq 63\varepsilon \tag{4-4}$$

the section should be checked for shear buckling using

$$\frac{F_v}{V_{cr}} \leq 1 \tag{4-5}$$

where:

V_{cr} is the shear resistance and can be determined using

$$V_{cr} = q_{cr} dt \tag{4-6}$$

q_{cr} is the critical shear strength which can be obtained from Tables 21(a) to (d) of BS 5950: Part1.

4.3.6 Moment Capacity

The moment capacity of a section, according to BS 5950, depends on the amount of shear in the section. If the shear force at the section of the maximum moment does not exceed 60% of the shear capacity, i.e.:

$$\frac{F_v}{0.6P_v} \leq 1 \tag{4-7}$$

then the moment capacity will be:

$$M_c = \begin{cases} p_y S_x & \text{for class 1 plastic or class 2 compact cross-sections} \\ p_y Z_x & \text{for class 3 semi-compact cross-sections} \\ p_y S_{x,eff} & \text{or alternatively (class 3 semi-compact cross-sections)} \\ p_y Z_{x,eff} & \text{for class 4 slender cross-sections} \end{cases} \quad (4\text{-}8)$$

If the applied shear force exceeds 60% of the shear capacity, i.e.

$$\frac{F_v}{0.6P_v} > 1 \quad (4\text{-}9)$$

then the moment capacity should be taken as:

$$M_c = \begin{cases} p_y (S_x - \rho S_v) & \text{for class 1 plastic or class 2 compact cross-sections} \\ p_y (Z_x - \rho \frac{S_v}{1.5}) & \text{for class 3 semi-compact cross-sections} \\ p_y (S_{x,eff} - \rho S_v) & \text{or alternatively (class 3 semi-compact cross-sections)} \\ p_y (Z_{x,eff} - \rho \frac{S_v}{1.5}) & \text{for class 4 slender cross-sections} \end{cases} \quad (4\text{-}10)$$

where:

S_v is the plastic modulus of shear area, A_v

ρ is a factor which is given as

$$\rho = \left(\frac{2F_v}{P_v} - 1 \right)^2 \quad (4\text{-}11)$$

4.3.7 Lateral torsional buckling

One of the major failures that may take place in any steel frame member, particularly with a high moment value, is lateral torsional buckling. Lateral torsional buckling will not occur if the member slenderness is low or the member bends about the minor axis. Since it is clear that the occurrence of lateral torsional buckling reduces the maximum load carrying capacity of the member, it is an important design criterion for steel members (Chen and Lui, 1991). In each length between lateral restraints for equal flanged rolled sections, the equivalent uniform moment, M_{equ}, should not exceed the buckling resistance moment, M_b, i.e.:

$$\frac{M_{equ}}{M_b} \leq 1 \tag{4-12}$$

The buckling resistance moment can be determined according to the following equation:

$$M_b = \begin{cases} p_b S_x & \text{for class 1 plastic or class 2 compact cross-sections} \\ p_b Z_x & \text{for class 3 semi-compact cross-sections} \\ p_b S_{x,eff} & \text{or alternatively (class 3 semi-compact cross-sections)} \\ p_b Z_{x,eff} & \text{for class 4 slender cross-sections} \end{cases} \tag{4-13}$$

Having the values of the design strength, p_y and the value of the equivalent slenderness, λ_{LT}, the bending strength, p_b can be determined from Table 16 of BS 5950. For equal flange rolled I-section, p_b can be found from Table 20 of BS 5950.

The equivalent slenderness, λ_{LT}, is evaluated as follows:

$$\lambda_{LT} = nuv\lambda \tag{4-14}$$

The slenderness factor, v can be determined from Table 19 of BS 5950 depending on the value of λ and the torsional index of the section. The minor axis slenderness is evaluated as follows:

$$\lambda = \frac{L_E}{r_y} \tag{4-15}$$

where:

L_E is the effective length of the member between two restraints

r_y is the radius of gyration about the minor axis of the member's cross-section

The equivalent uniform moment can be evaluated according to the equation below:

$$M_{equ} = m_{LT} M_x \tag{4-16}$$

where:

M_x is the maximum major axis moment in the segment

m_{LT} is an equivalent uniform factor which can be determined either by Table 18 of BS 5950: Part 1 or using the following equation:

$$m_{LT} = 0.57 + 0.33\beta + 0.10\beta^2 \geq 0.43 \tag{4-17}$$

4.3.8 Local Capacity Check

One of the essential capacity checks, according to BS 5950, is to measure the resistance of the cross-section against the interaction of applied axial force and bending moment. The checking procedures are different for the member that is subjected to axial tensile force, than the member that is subjected to axial compressive force.

4.3.8.1 Tension Members

The greatest axial load and bending moment usually occur at the middle or the ends of the member. For checking the local capacity, therefore, both loads are taken into consideration as given in BS 5950: Part 1:

$$\frac{F_t}{p_y A_e} + \frac{M_x}{M_{cx}} \leq 1 \tag{4-18}$$

The effective area can be obtained using the formulae below:

$$A_e = \begin{cases} K_e A_n & \text{if} \quad K_e A_n \leq A_g \\ A_g & \text{if} \quad K_e A_n > A_g \end{cases} \tag{4-19}$$

where

A_e is the effective area of the section

A_g is the gross area taken from relevant standard table given in BS 5950

A_n is the net area determined according to the following equation:

$$A_n = A_g - \sum_{i=1}^{n\varphi} A_i \tag{4-20}$$

K_e is a factor and depends on the grade of the steel used for the member

$n\varphi$ is the total of number of holes in the cross-section

4.3.8.2 Compression Members

Compression members should be checked for local capacity at the points with the maximum bending moment and axial force. This capacity may be limited either by yielding or local buckling depending on the section properties.

$$\begin{cases} \dfrac{F_c}{p_y A_g} + \dfrac{M_x}{M_{cx}} \le 1 & \text{generally, except for class 4 slender cross-sections} \\ \dfrac{F_c}{p_y A_{eff}} + \dfrac{M_x}{M_{cx}} \le 1 & \text{For class 4 slender cross-sections} \end{cases} \quad (4\text{-}21)$$

The member which is exposed to both axial compression and the bending stresses must be checked for the overal buckling resistance as follows:

$$\begin{cases} \dfrac{F_c}{P_c} + \dfrac{m_x M_x}{p_y Z_x} \le 1 \\ \dfrac{F_c}{P_{cy}} + \dfrac{m_{LT} M_{LT}}{M_b} \le 1 \end{cases} \quad (4\text{-}22)$$

where

P_c is the compression resistance of the member's cross-section that has the smaller value of P_{cx} or P_{cy} and is found according to equations below:

$$P_c = \begin{cases} A_g p_c & \text{generally, except for class 4 slender cross-section} \\ A_{eff} p_{cs} & \text{for class 4 slender cross-section} \end{cases} \quad (4\text{-}23)$$

where

p_{cs} is the value of p_c for a reduced slenderness of $\lambda(A_{eff} / A_g)^{0.5}$ and is calculated from section 5.7.5 of BS 5950.

4.3.9 Web Buckling Resistance

BS 5950 has limited the ratio of the member web d/t to a value of 70ε for rolled and 62ε for welded sections. If the value exceeds from limitation then the requirements for shear buckling resistance must be checked. The shear buckling resistance with or without an intermediate transverse stiffener can be determined according to the following equations:

$$V_b = V_w = dtq_w \quad (4\text{-}24)$$

where

q_w is the shear buckling strength and can be obtained from Table 21 of BS 5950 depending on the values d/t and a/d, where a is the stiffener spacing.

4.3.10 Deflection Limits

The deflection and displacement experienced by the steel frame members should neither impair the strength of the frame nor affect plaster and finishing. For this purpose, BS5950 has specified some limitations depending on the nature of structure member. The realistic value of the applied load (service load) is taken into account for deflection calculation. Table 4-3 presents some of the limitations given by Table 8 of BS 5950.

Table 4-3: Deflection limits (Ref: BS 5950, Table 8)

Vertical deflection of beam due to imposed load	***Limits***
Beam carrying plaster or other brittle finish	Span/360
Other beams (except purlin and sheeting rails)	Span/200
Horizontal deflection of the columns due to imposed and wind loads	
Columns in portal frame building, not supporting crane runways	To suit cladding

As all the members of steel portal frames behave like a beam-column, a limitation of Span/360 may be considered for the deflection limits check for all the existing joints.

4.3.11 Steel Portal Frame

All the aforementioned strength and serviceability limit states have to be checked for steel portal frames. The limitations are generally used for all types of structures. The point which apparently distinguishes the steel portal frame from other types of structure concerns some additional limitations which must be taken into account when the design is conducted. In-plane stability is the primary requirement of the

SPF which has to be considered before any decision is taken for design. The following limitation should be checked for symmetrical SPFs, as per BS 5950.

$$\frac{L}{h} \leq 5.0 \tag{4-25}$$

and:

$$\frac{h_r}{L} \leq 0.25 \tag{4-26}$$

Where

L is the span of the steel portal frame

h is the clear height of the column

h_r is the height of the apex above the tops of the columns

Furthermore, at any section of the tapered member which represents haunch in steel portal frame, the following equation must be satisfied:

$$\frac{F}{A_x} + \frac{M}{S_x} \leq p_b \tag{4-27}$$

where:

F is the applied axial force

M is the applied bending moment

A_x is the cross-sectional area at the section considered

S_x is the plastic modulus at the section considered.

As a result, although the appearance of steel portal frames is simple, more limitations are considered and should be taken into account when the design is set.

Fig. 4-2 demonstrates the procedures of design checking all the requirements of steel frames according to BS 5950.

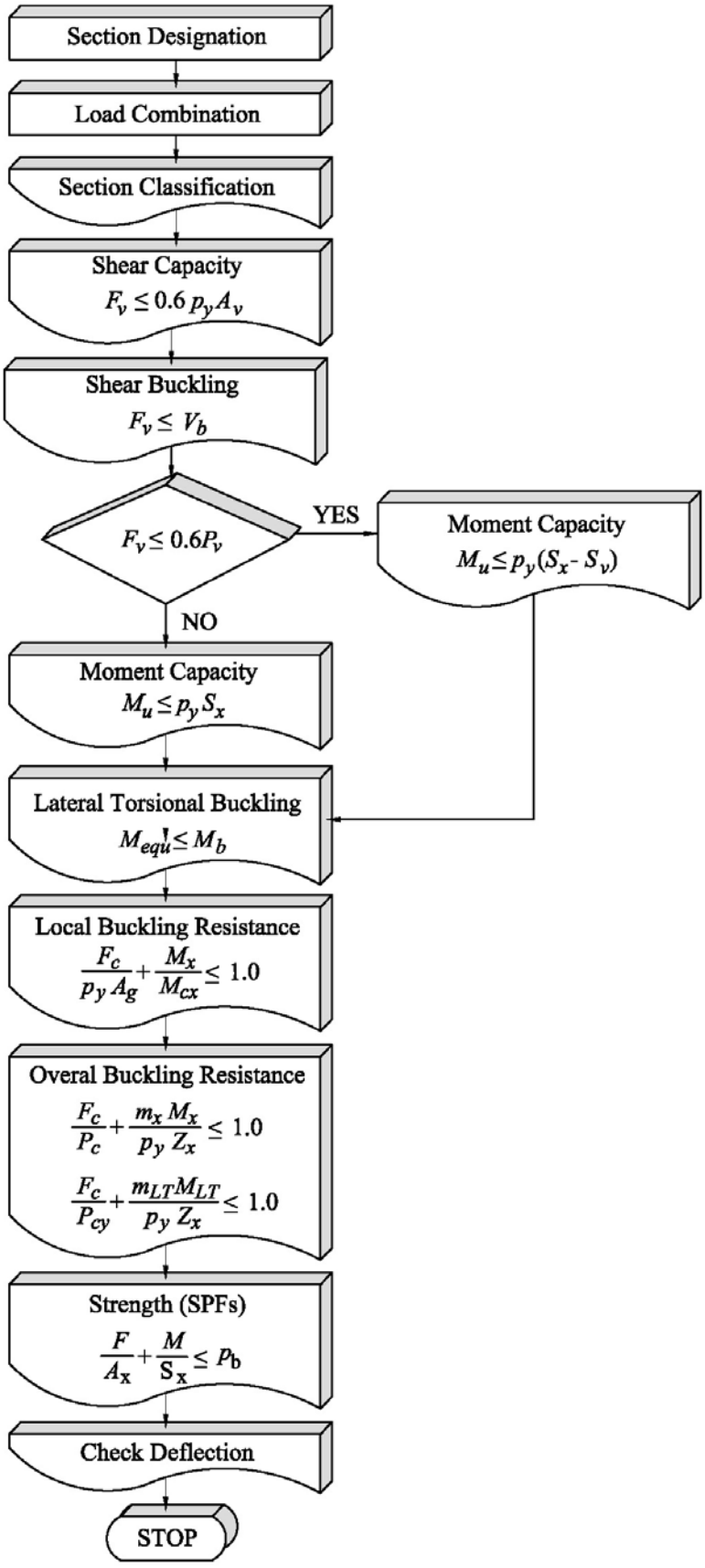

Figure 4-2: The flowchart for the design of steel structures according to BS 5950

4.4 Design of steel structure to EC3

Eurocode 3 (EC3), like BS 5950, applies limit state theory for the design of the elements of steel structure. One of the basic differences between EC3 and BS 5950 is the way it treats with single storey buildings. EC3 considers the structure up to two storeys as single storey buildings whereas BS 5950 takes into account one-storey structures as single storey ones (Taylor *et al*. 1999). Another difference which is worthwhile stating is the use of principal axes for steel cross-sections. Fig. 4-3 depicts clearly the differences in using the axes with respect to parts of the section for both EC3 and BS 5950.

4.4.1 Steel grade

EC3 covers three nominal grades of steel with the addition of two more by Annex D. Those added have yield strength of 235 N/mm^2 and 420 N/mm^2. These are not used in the UK (Taylor *et al*. 1999). Generally three grades of steel which are used for design in the UK are S 275, S 355, and S 460. BS 5950 reduces the design strength of the steel at 16mm, 40mm, 63mm, and 100mm thickness. However, the nominal value of yield strength, f_y, is reduced at 40mm and 80mm in EC3. The nominal values of yield strength, f_y, should be found in Table 3.1 of EC3 and are collected in Table 4-4.

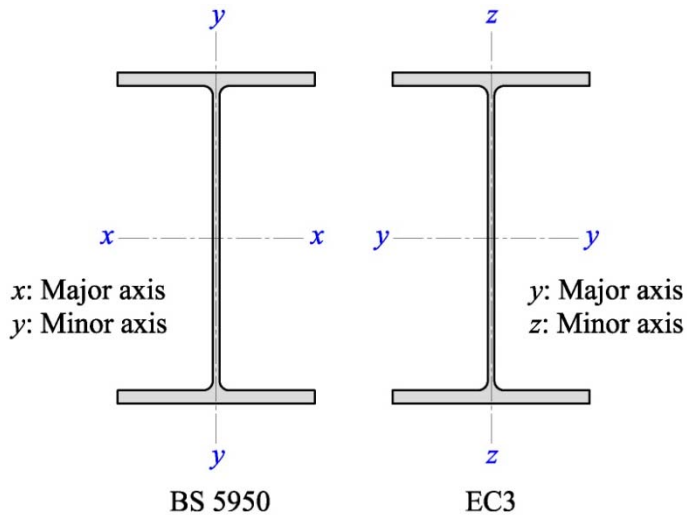

Figure 4-3: Major and minor axes in BS 5950 and EC3

Table 4-4: Nominal values of yield strength f_y and ultimate tensile strength f_u for hot rolled structural steel (Ref: EC3, Table 3.1)

Standard	**Steel grade**	**Nominal thickness of the element t**			
		t ≤ 40 mm		**40 < t ≤ 800 mm**	
		f_y **N/mm²**	f_u **N/mm²**	f_y **N/mm²**	f_u **N/mm²**
EN 10025 - 2	S 235	235	360	215	360
	S 275	275	430	255	410
	S 355	355	510	335	470
	S 450	440	550	410	550
EN 10025 - 3	S 275 N/NL	275	390	255	370
	S 355 N/NL	355	490	335	470
	S 420 N/NL	420	520	390	520
	S 460 N/NL	460	540	430	540
EN 10025 - 4	S 275 M/ML	275	370	255	360
	S 355 M/ML	355	470	335	450
	S 420 M/ML	420	520	390	500
	S 460 M/ML	460	540	430	530
EN 10025 - 5	S 235 w	235	360	215	340
	S 355 W	355	510	335	490

Where:

f_y yield stress

f_u ultimate tensile stress

EC3 uses a value of 210 000N/mm^2 for the modulus of elasticity of steel (E) and a value of 81 000N/mm^2 for the shear modulus (G). Furthermore, it uses a value of 0.3 for Poisson's ratio (υ) in the elastic stage and the coefficient of linear thermal expansion (α) is 12×10^{-6} per Kelvin.

4.4.2 Load combination

A term of 'action' is used to describe a load or imposed deformation in Eurocodes. The basis of design where the load combination is addressed has been embedded in Eurocode 0 (EC0). In Eurocodes, the dead load is called "permanent action" and the imposed load is "variable action". The actions that simultaneously occur are combined before the design of the steel structure. For each load cases, the critical actions are considered as the design load of the structure. There are three different combinations of actions in EC0 depending on the design situations. The general format of effect of actions when they are combined for persistent or transient design situations (also called fundamental combination) should be as follows (Equation 6.9a, EC0):

$$E_d = \gamma_{Sd} E\{\gamma_{g,j} G_{k,j}; \gamma_p P; \gamma_{q,1} Q_{k,1}; \gamma_{q,i} \psi_{0,i} Q_{k,i}\} j \geq 1; i > 1 \qquad (4\text{-}28)$$

It is noted that, according to the EC0, the combination of the actions considered should be based on both the design value of the leading variables action and the design combination of the values of accompanying variable actions; therefore (Equation 6.9b, EC0):

$$E_d = E\{\gamma_{G,j} G_{k,j}; \gamma_p P; \gamma_{Q,1} Q_{k,1}; \gamma_{Q,i} \psi_{0,i} Q_{k,i}\} j \geq 1; i > 1 \qquad (4\text{-}29)$$

Following the above equation (Eq 4-30), the combination of actions in brackets { } can either be expressed as (Equation 6.10, EC0):

$$\sum_{j \geq 1} \gamma_{G,j} G_{k,j} "+" \gamma_p P "+" \gamma_{Q,1} Q_{k,1} "+" \sum_{i>1} \gamma_{Q,i} \psi_{0,i} Q_{k,i} \qquad (4\text{-}30)$$

Or alternatively the less unfavourable by the two following equations (Equations 6.10a and 6.10b):

$$\sum_{j \geq 1} \gamma_{G,j} G_{k,j} "+" \gamma_p P "+" \gamma_{Q,1} \psi_{0,1} Q_{k,1} "+" \sum_{i>1} \gamma_{Q,i} \psi_{0,i} Q_{k,i} \qquad (4\text{-}31)$$

$$\sum_{j \geq 1} \xi \gamma_{G,j} G_{k,j} "+" \gamma_p P "+" \gamma_{Q,1} Q_{k,1} "+" \sum_{i>1} \gamma_{Q,i} \psi_{0,i} Q_{k,i} \qquad (4\text{-}32)$$

Where:

E is the effect of actions

E_d is the design value of the effect of the actions

$G_{k,j}$ is the characteristic value of permanent action *j*

P is the relevant representative value of a pre-stressing action

$Q_{k,1}$ is the characteristic value of the leading variable action 1

$Q_{k,i}$ is the characteristic value of the accompanying variable action *i*

$\gamma_{G,j}$ is the partial factor for permanent action *j*

γ_P is the partial factor for pre-stressing actions

$\gamma_{Q,1}$ is the partial factor for variable action 1

$\gamma_{Q,i}$ is the partial factor for variable action *i*

ξ is a reduction factor for unfavourable permanent actions G

ψ_0 is the factor for the combination value of a variable action

"+" implies "to be combined with"

$\sum$ implies "the combined effect of"

As Eq. 4-31 and Eq. 4-32 will result in lighter loads than others, they are commonly used as parametric study (Lim *et al.*, 2005).

Employing the recommended values for ξ, ψ_0, γ_G, and γ_Q given in Table A1.1, Table A1.2(A), A1.2(B), and Table A1.2(C) of EC0, the less favourable of the following combination of actions may be considered (Lim *et al.*, 2005):

Action combination 1: 1.15 Permanent + 1.50 Variable + 0.75 Wind + NHL

Action combination 2: 1.15 Permanent + 0.75 Variable + 1.50 Wind + NHL

Action combination 3: 1.35 Permanent + 0.75 Variable + 0.75 Wind + NHL

Action combination 4: 1.15 Permanent + 1.50 Variable + NHL

where:

NHL is the notional horizontal load which is 0.5% of the factored reaction at the base of the column and acts at the top of the column according to EC3.

4.4.3 Classification of Cross-Sections

Like BS 5950 the sections are classified in EC3 to determine their susceptibility for local buckling without calculating their local buckling capacity. The cross-section classifications appears similar to BS 5950 and are grouped as follows:

Class 1 cross-section: those sections that can form plastic hinges and have rotation capacity without reduction of strength.

Class 2 cross section: those sections that have limited rotation capacity due to local buckling and can develop their plastic moment resistance.

Class 3 cross-section: those sections where the stress is distributed elastically at the extreme fibre of the cross section, but local buckling prevents the cross-section from having a plastic moment resistance capacity.

Class 4 cross-section: those sections where the stress is distributed elastically and the local buckling occurs before the attainment of yield stress.

Specifying the cross-section type depends on width-to-thickness ratio of the web and flange of cross-section. Meeting the limitations given in Table 5.2 of EC3 the class of web and flange are specified separately and then the less unfavourable is considered when assigning the class of cross-section. These are summarised into Table 4-5 and the parameters required are found in Figs. 4-4, 4-5 and 4-6.

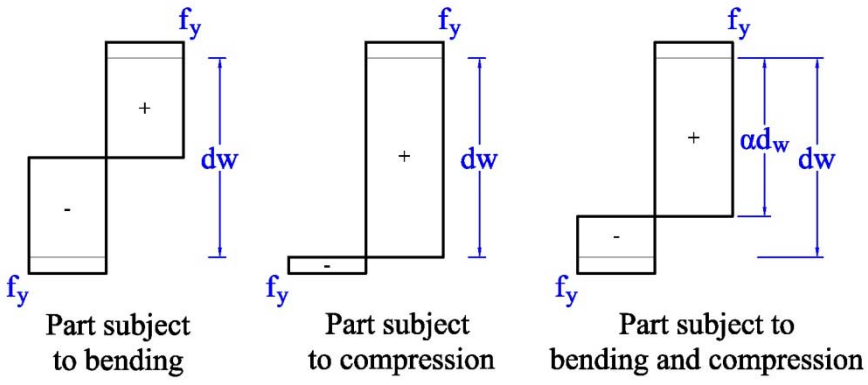

Figure 4-4: Stress distribution for class 1 and 2 cross-sections

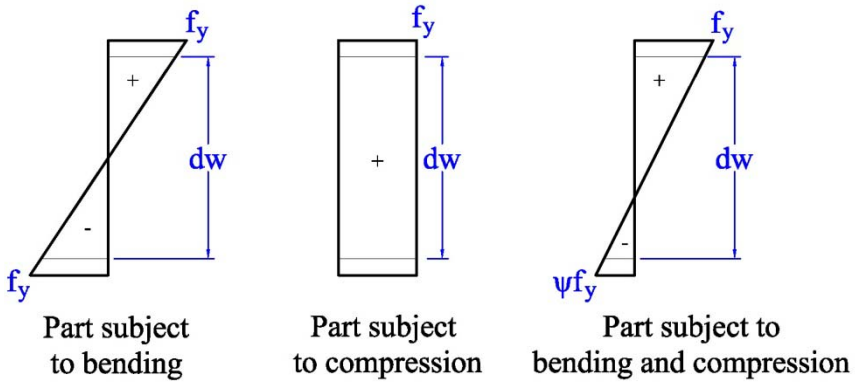

Figure 4-5: Stress distribution for class 3 and 4 cross-sections

Table 4-5: Limitation of height-to-thickness ratio of I-section web for compression parts (Ref: EC3, Table 5.2 Sheet a)

Class	Part subject to bending	Part subject to compression	Part subject to bending and compression
1	$d_w / t_w \le 72\varepsilon$	$d_w / t_w \le 33\varepsilon$	When $\alpha > 0.5$: $d_w / t_w \le \frac{396}{13\alpha - 1}\varepsilon$ When $\alpha \le 0.5$: $d_w / t_w \le \frac{36}{\alpha}\varepsilon$
2	$d_w / t_w \le 83\varepsilon$	$d_w / t_w \le 38\varepsilon$	When $\alpha > 0.5$: $d_w / t_w \le \frac{456}{13\alpha - 1}\varepsilon$ When $\alpha \le 0.5$: $d_w / t_w \le \frac{41.5}{\alpha}\varepsilon$
3	$d_w / t_w \le 124\varepsilon$	$d_w / t_w \le 42\varepsilon$	When $\psi > -1$: $d_w / t_w \le \frac{42}{0.67 + 0.33\psi}\varepsilon$ When $\psi \le -1$: $d_w / t_w \le 62\varepsilon(1-\psi)\sqrt{(-\psi)}$
4	$d_w / t_w > 124\varepsilon$	$d_w / t_w > 42\varepsilon$	When $\psi > -1$: $d_w / t_w > \frac{42}{0.67 + 0.33\psi}\varepsilon$ When $\psi \le -1$: $d_w / t_w > 62\varepsilon(1-\psi)\sqrt{(-\psi)}$

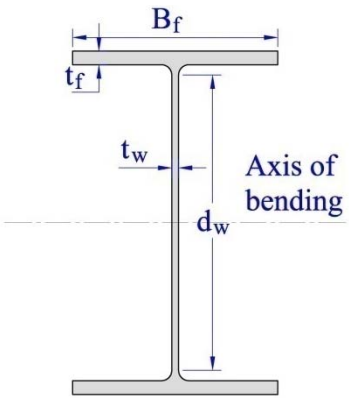

Figure 4-6: Typical I-section cross-section

The limitation of width-to-thickness ratio of I-section flange for compression parts is simpler. As there is no bending stress with respect to the minor axis in 2D (uni-axial bending moment), the flanges are subject to compression and tension only. EC3 has limited the cross-section classes into the following ranges:

$$\begin{aligned} &\text{Class 1:} && B_f / t_f \le 9\varepsilon \\ &\text{Class 2:} && B_f / t_f \le 10\varepsilon \\ &\text{Class 3:} && B_f / t_f \le 14\varepsilon \\ &\text{Class 3:} && B_f / t_f > 14\varepsilon \end{aligned} \qquad (4\text{-}33)$$

Baddoo *et al.* (1993) have suggested using the following formulae for α and ψ depending on the axial compression and tension stresses applied to the cross-section:

For class 1 and class 2 cross-sections:

$$\alpha = 0.5(1 + \gamma_{M0} \frac{\sigma_w}{f_y}) \qquad (4\text{-}34)$$

$$\sigma_w = \frac{N_{Sd}}{d_w t_w} \qquad (4\text{-}35)$$

For class 3 and class 4 cross-sections:

$$\psi = 2\gamma_{M0} \frac{\sigma_a}{f_y} \qquad (4\text{-}36)$$

$$\sigma_a = \frac{N_{Sd}}{A} \tag{4-37}$$

Where:

A is the gross area of the cross-section

B_f is the breadth of the flange

d_w is the depth between the fillets

N_{Sd} is the axial member force

t_f is the thickness of the flange

t_w is the thickness of the web

α is the coefficient measured as the height of the compression area

γ_{M0} is the partial factor and equals 1.0 as given by EC3

ε is $\sqrt{235 / f_y}$

σ_a is the axial stress, it is positive when in compression and negative when in tension.

ψ is the stress ratio of the extreme fibre

4.4.4 Shear capacity

There are two different ways of checking the shear capacity of a cross-section depending upon the class of cross-section. According to EC3, the applied shear force must not exceed the plastic design shear resistance of the section for class 1 and class 2, i.e.:

$$V_{Ed} \le V_{pl,\,Rd} \tag{4-38}$$

where:

V_{Ed} is the design value of the shear force

$V_{pl,Rd}$ is the plastic design shear resistance which can be calculated as:

$$V_{pl,Rd} = \frac{(f_y / \sqrt{3})}{\gamma_{M0}} A_v \tag{4-39}$$

A_v is the shear area (Fig. 4-7) which for rolled I and H sections should be taken as:

$$A - 2\, b_f\, t_f + (t_w + 2r)\, t_f$$

r is the root radius

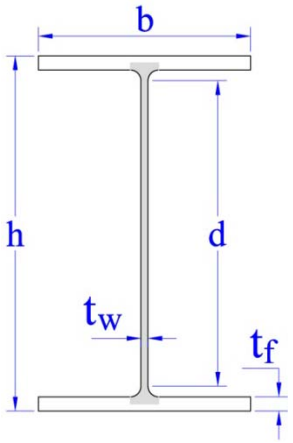

Figure 4-7: Shear area of the section according to EC3

For class 2 and class 3:

$$\tau_{Ed} \le \frac{f_y}{\sqrt{3}\gamma_{M0}} \qquad (4\text{-}40)$$

Where:

τ_{Ed} is obtained from

$$\tau_{Ed} = \frac{V_{Ed} S}{It}$$

I is moment of inertia of the whole cross-section

S is the first moment of area about the centroidal axis of that portion between the boundary of the cross-section and the point at which the shear is required.

t is the thickness at the required point

4.4.5 Shear Buckling

In addition to shear resistance check, EC3 suggests checking the shear buckling resistance for the web without intermediate stiffeners at the point that the maximum shear occurs. EC3 has specified the limitation and proposed following the procedures given in EN 1993–1-5 (EC3, 1-5) to check the shear buckling. If the height-to-

thickness ratio of the web exceeds the following limitation for unstiffened webs, then checking for shear buckling is necessary:

$$\frac{h_w}{t_w} > 72\frac{\varepsilon}{\eta} \tag{4-41}$$

Where:

h_w is the height of web

η is the factor for shear area and can be taken as 1.2 for steel grade up to S460 and 1.0 otherwise. It may be conservatively taken as 1.0

According to EC3-1-5, the applied shear forces must not exceed the value of shear buckling resistance of the section:

$$V_{Ed} \le V_{b,Rd} \tag{4-42}$$

where:

$V_{b,Rd}$ is the buckling shear resistance

The shear resistance of an unstiffened slender section reduces with an increasing of h_w/t_w ratio. Both flange and web contribute to the buckling resistance for shear. According to EC3 (1-5), for both stiffened and unstiffened webs the design shear resistance should be taken as:

$$V_{b,Rd} = V_{bw,Rd} + V_{bf,Rd} \le \eta \frac{f_{yw}/\sqrt{3}}{\gamma_{M1}} h_w t_w \tag{4-43}$$

where:

$V_{bw,Rd}$ is the buckling shear resistance of the web

$V_{bf,Rd}$ is the buckling shear resistance of the flange

The contribution from the web can be defined as:

$$V_{bw,Rd} = \chi_w \frac{f_{yw}/\sqrt{3}}{\gamma_{M1}} h_w t_w \tag{4-44}$$

Where:

χ_w is the factor for the contribution of the web to shear buckling and can be obtained from Table 5-1 or Figure 5.2 of EC3 (1-5).

The value of χ_w can be obtained as:

$$\chi_w = \begin{cases} \eta & \overline{\lambda}_w < 0.83 \\ 0.83/\overline{\lambda}_w & \overline{\lambda}_w \geq 0.83 \end{cases} \quad (4\text{-}45)$$

where:

$\overline{\lambda}_w$ is the modified web plate slenderness, and defined as:

$$\overline{\lambda}_w = 0.76\sqrt{\frac{f_{yw}}{\tau_{cr}}} \quad (4\text{-}46)$$

τ_{cr} is the critical elastic local buckling stress which Trahair *et al.* (2008) have formulated as:

$$\tau_{cr} = \frac{\pi^2 E k_\tau}{12(1-\upsilon^2)(d_w t_w)^2} \quad (4\text{-}47)$$

υ is steel's Poisson's ratio and is taken as 0.30 according to EC3.

k_τ is the bucling coefficient and is approximated as:

$$k_\tau = \begin{cases} 5.34 + 4\left(\frac{d_w}{L}\right)^2 & \text{for } L \geq d_w \\ 4 + 5.34\left(\frac{d_w}{L}\right)^2 & \text{for } L < d_w \end{cases} \quad (4\text{-}48)$$

L is the length of the member

However, for simplicity EC3 (1-5) has the following equation used to determine the slenderness parameter for the members that have transverse stiffness at support:

$$\overline{\lambda}_w = \frac{1}{86.4\varepsilon}\frac{h_w}{t_w} \quad (4\text{-}49)$$

When the bending moment resistance of the flange is greater than the applied bending moment which is not utilised by the flange moment resistance then the contribution of the flange should be considered as follows:

$$V_{bf,Rd} = \frac{f_{yf}}{\gamma_{M1}} \frac{b_f t_f^2}{c} \left[1 - \left(\frac{M_{Ed}}{M_{f,Rd}} \right) \right] \quad (4\text{-}50)$$

Where:

$M_{f,Rd}$ is the bending moment resistance of the flange

f_{yf} is the yield strength of the flange

c is a coefficient defined by

$$c = a \left(0.25 + 1.6 \frac{f_{yf}}{f_{yw}} \frac{b_f}{h_w^2} \frac{t_f^2}{t_w} \right) \quad (4\text{-}51)$$

a is the distance between transverse stiffeners

The contribution of the flange in resisting the shear buckling is so small that it can be neglected in verifying the shear buckling resistance.

4.4.6 Bending moment capacity

The design value of the bending moment at each cross-section must not exceed the design resistance for the bending moment which must satisfy:

$$M_{Ed} \leq M_{c,Rd} \quad (4\text{-}52)$$

where:

M_{Ed} is the design value of the bending moment

$M_{c,Rd}$ is the design resistance for the bending moment about one principal axis of a cross-section

The design resistance for a bending moment, $M_{c,Rd}$, will be determined as follows:

For class 1 and class 2 cross-sections:

$$M_{c,Rd} = M_{pl,Rd} = W_{pl} \frac{f_y}{\gamma_{M0}} \quad (4\text{-}53)$$

For class 3 cross-section:

$$M_{c,Rd} = M_{el,Rd} = W_{el,\min} \frac{f_y}{\gamma_{M0}} \tag{4-54}$$

For class 4 cross-section:

$$M_{c,Rd} = W_{eff,\min} \frac{f_y}{\gamma_{M0}} \tag{4-55}$$

Where:

$M_{pl,Rd}$ is the design plastic resistance bending moment of the cross-section

$M_{cl,Rd}$ is the design elastic resistance bending moment of the cross-section

$W_{pl,\ min}$ is the minimum plastic section modulus of the cross-section

$W_{el,min}$ is the minimum elastic section modulus of the cross-section

In the case of coexisting shear and moment an allowance should be made for the effect of shear on the moment resistance. If the value of the shear force is not greater than half the plastic shear resistance, the effect of shear on moment resistance is neglected. Otherwise, the reduced moment resistance will be expressed as follows:

$$M_{c,Rd} = W_y \frac{(1-\rho) f_y}{\gamma_{M0}} \tag{4-56}$$

where:

W_y is the section modulus and can be defined as:

For class 1 and class 2: $W_y = W_{pl}$

For class 3: $W_y = W_{el,\ min}$

For class 4: $W_y = W_{eff,\ min}$

ρ is the shear effect reduction factor and can be obtained by:

$$\rho = \left(\frac{V_{Ed}}{0.5 V_{pl,Rd}} - 1 \right)^2 \tag{4-57}$$

4.4.7 Compression capacity

Unlike BS 5950, EC3 has directly related the compression capacity to the yield strength of the cross-section. The design value of the compression force should not exceed the design resistance of the cross-section, i.e.:

$$N_{Ed} \leq N_{c\,Rd} \tag{4-58}$$

The design resistance of cross-section is determined for two groups of classes. When the cross-section is classified as either class 1, class 2, or class 3 then the design resistance can be determined as:

$$N_{c,Rd} = \frac{f_y}{\gamma_{M0}} A \tag{4-59}$$

and for class 4 cross-section

$$N_{c,Rd} = \frac{f_y}{\gamma_{M0}} A_{eff} \tag{4-60}$$

Where:

N_{Ed} is the design value of the compression force

$N_{c\,Rd}$ is the design uniform compression resistance of cross-section

A is the gross cross-sectional area

A_{esff} is effective area

EC3-1 refers to the effective area determination in EC3-5 which should be obtained separately for the flange and web of the I-section. The effective area may be obtained from:

$$A_{eff} = \sum A_{c,eff} \tag{4-61}$$

where:

$A_{c,eff}$ is the effective area of a flat compression element comprising the cross-section (web and flange in case of I-section), which can be obtained from its gross cross-sectional area (A_g):

$$A_{c,eff} = \rho\, A_g \qquad (4\text{-}62)$$

ρ is reduction factor and for an internal compression element (web) is given by:

$$\rho = 1.0 \qquad \text{for } \bar{\lambda}_p \le 0.673$$

$$\rho = \frac{\bar{\lambda}_p - 0.055(3+\psi)}{\bar{\lambda}_p^{\,2}} \le 1.0 \qquad \text{for } \bar{\lambda}_p > 0.673$$

And for an outstanding element (flange) is determined by:

$$\rho = 1.0 \qquad \text{for } \bar{\lambda}_p \le 0.748$$

$$\rho = \frac{\bar{\lambda}_p - 0.188}{\bar{\lambda}_p^{\,2}} \le 1.0 \qquad \text{for } \bar{\lambda}_p > 0.748$$

$\bar{\lambda}_p$ is the stress ratio factor and may be determined by:

$$\bar{\lambda}_p = \frac{\bar{b}/t}{28.4\varepsilon\sqrt{k_\sigma}}$$

$\bar{b}$ is the appropriate width depending on the cross-section element. It is the outstanding part of the flange or the depth between fillets for web in I-section.

t is the thickness of the web or flange

k_σ is the buckling factor corresponding to ψ and to the boundary conditions. It has a value of 4.0 for internal compression elements and a value of 0.43 for the outstanding compression elements in case of uniform compression as given in Table 4.1 and Table 4.2 of EC3, Part 1-5.

4.4.8 Bending moment with axial compression effect

In order to check the capacity of the cross-section to withstand compressive stress, it is necessary to consider the compressive stress generated simultaneously by bending moments and axial forces. In this case, allowance should be made for the effect of axial force on the moment resistance of the cross-section. EC3 states that the allowance is not needed for the effect of axial force on the moment resistance about the major axis if the following criteria are satisfied:

$$\frac{N_{Ed}}{N_{pl,Rd}} \le 0.25 \qquad (4\text{-}63)$$

and

$$N_{Ed} \le \frac{h_w t_w f_y}{2\gamma_{M0}} \tag{4-64}$$

Otherwise, for a doubly symmetric *I* or *H* section categorised as class 1 or class 2 cross-sections, the following equation allows the effect of axial force on the plastic moment resistance about the major axis:

$$\frac{M_{Ed}}{M_{N,Rd}} \le 1 \tag{4-65}$$

where:

$$M_{N,Rd} = M_{pl,Rd} \frac{1-n}{1-0.5a} \le M_{pl,Rd} \tag{4-66}$$

$$n = \frac{M_{Ed}}{N_{pl,Rd}} \tag{4-67}$$

$$a = \frac{A - 2b_f}{A} \le 0.5 \tag{4-68}$$

For class 3 and class 4 the following condition should be satisfied:

$$\frac{N_{Ed}}{A_y f_y / \gamma_{M0}} + \frac{M_{Ed} + N_{Ed} e_{Ny}}{W_y f_y / \gamma_{M0}} \le 1 \tag{4-69}$$

where:

A_y is the effective area for class 4 cross-section; is the gross area for class 3 cross-section

e_{Ny} is the distance between the neutral axis of gross cross-section and the neutral axis of effective cross-section. Its value is zero for the class 3 cross-section as there is no reduction in gross cross-sectional area.

W_y is the section modulus and can be defined as:

$$W_y = \begin{cases} W_{el,y} & \text{For a Class 3 cross-section} \\ W_{eff,y} & \text{For a Class 4 cross-section} \end{cases}$$

W_{el} is the elastic section modulus

$W_{eff,y}$ is the effective section modulus

4.4.9 Overall buckling resistance

A compression member must be able to withstand overall buckling. Depending on slenderness and stiffness of the member, a compression member should be checked for overall buckling. According to EC3, the general verification for a compression member against buckling is as follows:

$$N_{Ed} \le N_{b,Rd} \tag{4-70}$$

Where:

$N_{b,Rd}$ is the design buckling resistance of the compression member, which is given by:

For class 1, class 2, and class 3 cross sections:

$$N_{b,Rd} = \chi \frac{Af_y}{\gamma_{M1}} \tag{4-71}$$

For class 4 cross sections:

$$N_{b,Rd} = \chi \frac{A_{eff} f_y}{\gamma_{M1}} \tag{4-72}$$

χ is the reduction factor due to the relevant buckling mode and is determined depending on the appropriate non-dimensional slenderness, $\bar{\lambda}$ and relevant buckling curve:

$$\chi = \frac{1}{\Phi + \sqrt{\Phi^2 - \bar{\lambda}^2}} \le 1.0$$

$$\Phi = 0.5\left[1 + \alpha(\bar{\lambda} - 0.2) + \bar{\lambda}^2\right]$$

Where:

$\bar{\lambda}$ is non-dimensional slenderness and can be determined as follows:

Class 1, class 2, and class 3: $\bar{\lambda} = \sqrt{\frac{Af_y}{N_{cr}}} = \frac{L_{eff}}{i}\frac{1}{\lambda_1}$

Class 4: $\bar{\lambda} = \sqrt{\frac{A_{eff} f_y}{N_{cr}}} = \frac{L_{eff}}{i}\frac{\sqrt{A_{eff}/A}}{\lambda_1}$

A is the gross cross-sectional area

A_{eff} is the effective cross-sectional area

N_{cr} is the elastic critical buckling force due to Euler's formula

L_{eff} is the segment length between two restraints (buckling length) in the buckling plane considered

i is the radius of gyration about the axis where the buckling plane is located

λ_1 slenderness value to determine the relative slenderness, $\overline{\lambda}$. It can be obtained by using the following equation according to EC3:

$$\lambda_1 = \sqrt{\frac{\pi^2 E}{f_y}} = 93.3\varepsilon$$

α is an imperfection factor and depends on the buckling curve

Table 4-6 specifies how to select the buckling curve for a rolled section with a double symmetric shape.

Table 4-6: Selection of buckling curve for rolled section cross-sections (Ref: EC3, Table 6.2)

Limits		Buckling about axis	Buckling curve	
			S 235 S 275 S 355	S 460
$h/B_f \leq 1.20$	$t_f \leq 100$ mm	Major	a	a
		Minor	c	a
	$t_f > 100$ mm	Major	d	c
		Minor	d	c
$h/B_f > 1.20$	$t_f \leq 40$ mm	Major	a	a_0
		Minor	b	a_0
	40 mm $< t_f \leq 100$ mm	Major	b	a
		Minor	c	a

The imperfection factor, α, for the appropriate buckling curve should be obtained from Table 4-7:

Table 4-7: Imperfection factor for buckling curve (Ref: EC3, Table 6.1)

Buckling curve	a_0	a	b	c	d
Imperfection factor, α	0.13	0.21	0.34	0.49	0.76

4.4.10 Lateral torsional-flexural buckling

In steel structural elements, particularly in beams, failure may be caused by lateral buckling which is originated from the flexural compression stress. A laterally unrestrained member should be checked for lateral torsional buckling. According to EC3, the following equation should be checked to make sure that the member has sufficient resistance against lateral torsional buckling:

$$M_{Ed} \le M_{b,Rd} \tag{4-73}$$

where:

$M_{b,Rd}$ is the design buckling resistance moment and can be obtained from:
For class 1 and class 2 cross-sections:

$$M_{b,Rd} = \chi_{LT} \frac{W_{pl} f_y}{\gamma_{M0}} \tag{4-74}$$

For class 3 cross-section:

$$M_{c,Rd} = \chi_{LT} \frac{W_{el,\min} f_y}{\gamma_{M0}} \tag{4-75}$$

For class 4 cross-section:

$$M_{b,Rd} = \chi_{LT} \frac{W_{eff,\min} f_y}{\gamma_{M0}} \tag{4-76}$$

χ_{LT} is the reduction factor due to torsional-flexural buckling

EC3 has introduced two methods to determine the value of the reduction factor, χ_{LT}. One is simple but conservative and is used as a general case. It is used for bending members of constant cross-section and is formulated as:

$$\chi_{LT} = \frac{1}{\phi_{LT} + \sqrt{\phi_{LT}^2 - \overline{\lambda}_{LT}^2}} \le 1.0 \tag{4-77}$$

where:

$$\phi_{LT} = \frac{1}{2}\left[1 + \alpha_{LT}(\bar{\lambda}_{LT} - 0.2) + \bar{\lambda}_{LT}^2\right]$$

α_{LT} is the imperfection factor which can be specified in Table 6.3 and 6.4 of EC3.

$$\bar{\lambda}_{LT} = \sqrt{W_y \frac{f_y}{M_{cr}}}$$

λ_{LT} is the slenderness ratio for lateral torsional buckling

M_{cr} is the elastic critical moment for lateral torsional buckling

The latest available draft of EC3 does not mention the procedures to find the value of elastic critical moment for lateral torsional buckling, M_{cr}. However, this value can be adopted from different sources such as AISC LRFD or other codes of practice. For a double symmetry I-rolled section where the shear centre is at the centroid of the section, the value of elastic critical moment, M_{cr}, can be obtained as follows (Serna *et al.* 2006):

$$M_{cr} = C_1 \frac{\pi^2 EI_z}{(kL)^2}\left\{\sqrt{\left(\frac{k}{k_w}\right)^2 \frac{I_w}{I_z} + \frac{(kL)^2 GI_t}{\pi^2 EI_z}}\right\} \qquad (4\text{-}78)$$

where:

E is the modulus of elasticity and equals 2100000 N/mm^2

G is the shear modulus and equals 81000 N/mm^2

L is the distance between lateral supports

k is the lateral bending coefficient which has a value of 1.0 for simply supported beams and a value of 0.5 in case of fixed supports where the prevention will occur for both lateral bending and warping

k_w is the warping coefficient which has a value of 1.0 for simply supported beams and a value 0.5 in case of fixed support

I_w is the warping constant

I_z is the second moment of inertia about the minor axis

C_1 is the coefficient which takes into account the moment gradient along the beam. It is the inverse of the equivalent factor for lateral torsional buckling, m_{LT} introduced in BS5950.

$$C_1 = \frac{M_{\max}}{0.2M_{\max} + 0.15M_A + 0.5M_B + 0.15M_C} \leq 2.273$$

M_A, M_B & M_C are bending moments at L/4, L/2 and 3L/4 of the steel members respectively, taken as absolute values.

The other method of determining the reduction factor for lateral torsional buckling, χ_{LT}, is less conservative than the previous one and is specifically used for rolled or equivalent welded steel cross-sections. The appropriate non-dimensional slenderness may be obtained as:

$$\chi_{LT} = \frac{1}{\phi_{LT} + \sqrt{\phi_{LT}^2 - \beta\bar{\lambda}_{LT}^2}} \leq \frac{1}{\bar{\lambda}_{LT}^2} \qquad (4\text{-}79)$$

where:

$$\phi_{LT} = \frac{1}{2}\left[1 + \alpha_{LT}(\bar{\lambda}_{LT} - \bar{\lambda}_{LT,0}) + \beta\bar{\lambda}_{LT}^2\right]$$

For rolled sections, the following values are recommended for the parameters $\bar{\lambda}_{LT,0}$ and β, according to EC3:

$$\bar{\lambda}_{LT,0} = 0.4$$

$$B = 0.75$$

However, for taking into account the moment distribution between the lateral restraints of members, EC3 recommends that the reduction factor χ_{LT} be modified as follows:

$$\chi_{LT,\mathrm{mod}} = \frac{1}{f}\chi_{LT} \qquad (4\text{-}80)$$

where:

f is a value which is recommended by the following minimum value

$$f = 1 - 0.5(1 - k_c)\left[1 - 2(\overline{\lambda}_{LT} - 0.8)^2\right]$$

k_c is a correction factor that depends on the bending moment and can be determined according to Table 6.6 of EC3 or can be calculated from the following equation (Traihair *et al.* 2008)

$$k_c = \sqrt{\frac{\sqrt{M_2^2 + M_3^2 + M_4^2}}{1.75 M_m}} \geq 0.632$$

M_m is the maximum moment of the segment between two lateral restraints

M_2 is the value of the moment at the one-quarter point of the segment

M_3 is the value of moment at the mid-point of the segment

M_4 is the value of moment at the three-quarter point of the segment

4.4.11 Interaction of axial force and bending moment

EC3 considers the geometry of the cross-section to evaluate the limitation of the combined axial compressive and bending stresses. If the section is not double symmetric, or its effective area, rather than the gross area, is considered for the calculation (Class 4), then the eccentricity of centroidal axes of gross and effective areas must be brought into the calculations. Members that are subjected to combined axial and bending compression should satisfy the following limitations:

For class 1 and 2:

$$\frac{N_{Ed}}{\chi_y \frac{f_y A}{\gamma_{M1}}} + k_{yy} \frac{M_{y,Ed}}{\chi_{LT} \frac{W_{pl,y} f_y}{\gamma_{M1}}} \leq 1.0 \qquad \text{(4-81a)}$$

$$\frac{N_{Ed}}{\chi_z \frac{f_y A}{\gamma_{M1}}} + k_{zy} \frac{M_{y,Ed}}{\chi_{LT} \frac{W_{pl,y} f_y}{\gamma_{M1}}} \leq 1.0 \qquad \text{(4-81b)}$$

For class 3:

$$\frac{N_{Ed}}{\chi_y \frac{f_y A}{\gamma_{M1}}} + k_{yy} \frac{M_{y,Ed}}{\chi_{LT} \frac{W_{el,y} f_y}{\gamma_{M1}}} \le 1.0 \qquad (4\text{-}82a)$$

$$\frac{N_{Ed}}{\chi_z \frac{f_y A}{\gamma_{M1}}} + k_{zy} \frac{M_{y,Ed}}{\chi_{LT} \frac{W_{el,y} f_y}{\gamma_{M1}}} \le 1.0 \qquad (4\text{-}82b)$$

For class 4:

$$\frac{N_{Ed}}{\chi_y \frac{f_y A}{\gamma_{M1}}} + k_{yy} \frac{M_{y,Ed} + e_{N,y} N_{Ed}}{\chi_{LT} \frac{W_{eff,y} f_y}{\gamma_{M1}}} \le 1.0 \qquad (4\text{-}83a)$$

$$\frac{N_{Ed}}{\chi_z \frac{f_y A}{\gamma_{M1}}} + k_{zy} \frac{M_{y,Ed} + e_{N,y} N_{Ed}}{\chi_{LT} \frac{W_{eff,y} f_y}{\gamma_{M1}}} \le 1.0 \qquad (4\text{-}83b)$$

Where:

χ_y are the reduction factors due to flexural buckling about the major axis and are found from Figure 6.4 of EC3

χ_z are the reduction factors due to flexural buckling about the minor axis and are found from Figure 6.4 of EC3

k_{yy} and k_{zy} are the interaction factors that are calculated from Table A.1 and Table B.1 of EC3.

A flowchart for design checking all the requirements of steel frames according to EC3 is shown in Fig. 4-8.

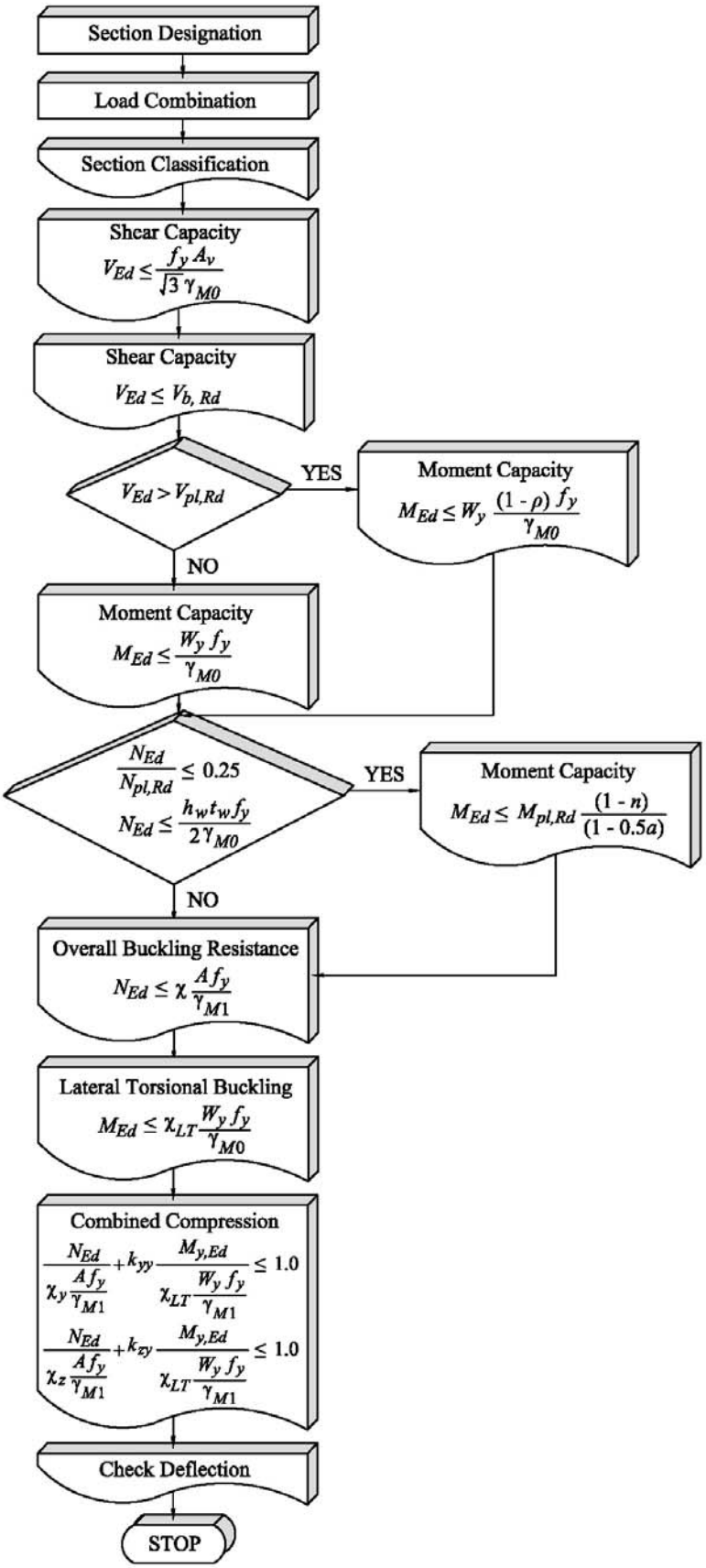

Figure 4-8: The flowchart of design to EC3 for steel structures

4.5 Summary

An objective function and a set of constraints must be defined in order to conduct the optimisation process. In structural engineering the set of constraint includes the limitations imposed by codes of practice. Since this study aims to use BS 5950 and EC3 as the codes of practice, all limitations required for a design according to these two codes of practice have been presented and discussed thoroughly. Some of the limitations were clarified by extracting knowledge from different sources.

Chapter 5: Distributed Genetic Algorithms

5.1 Introduction

Every structural engineer attempts to design a safe and economical structure. Achieving safe design is helped by using the limitations given as a set of design rules in the codes of practice like BS 5950 and EC3. A systematic way of achieving economical design is to formulate the design problem and solve it by one of the optimisation techniques. Owing to a large degree of redundancy existing in the steel structures, formulating a design problem and solving it by intuition and experience is nearly impossible. Therefore, implementing an optimisation technique to solve the design problem is a desirable goal.

In this chapter, the fundamental aspects of the optimisation are addressed and the key characteristics are highlighted. An optimisation technique known as a genetic algorithm (GA) is selected for this study. The GA will be thoroughly explained and its attributes will be critically discussed. Since a simple GA has very slow operation, some essential modifications are carried out to improve the algorithm and speed up its operation. Aspects of the modifications are critically discussed and their main contributions to knowledge are highlighted. Amongst the contributions is a new stiffness matrix, derived from regression analysis. In addition to the developed stiffness matrix and its use in structural design, other contributions include a number of new GA mutation schemes, along with the twin analogy idea and reproduction, a new penalty function, and implementation of another optimisation solution called displacement maximisation.

The resulting program, called DO-DGA, which is coded in Visual Basic 6.0, is introduced and its main characteristics are explained. The capability and objectives of the program are addressed and the benefits of the program to design optimisation are discussed.

5.2 Optimisation problems

In simple terms, optimisation is a way to seek the minimum or maximum point of a certain mathematical function. In structural engineering, it implies implementation of optimisation technique to minimise or maximise elements of a design so as to result in a cost-effective structure. For example, the design problem could be about maximisation of the load capacity for a given structure. However, increasing the load capacity necessitates having a bigger and heavier section which might increase costs in many aspects including finishing. Optimisation method finds ways of reducing such cost while maximising the load capacity. In addition, this idea can work when the designer is not limited in certain areas and can play with the dimensions to work out the ideal shape of the frame to design.

Another design optimisation problem which has been approached by a majority of researchers is to minimise the weight of structure. Nonetheless, the question arises whether minimisation of structural weight necessarily leads to a cost-effective design. Reinforced concrete structures are affected by a number of factors which influence the cost function. A reduction in weight may cause a remarkable increase in formwork and consequently an increase in cost. A pre-cast reinforced concrete structure, in contrast, may give a cheaper frame than the in-situ cast one. On the other hand, the scenario is different with steel structures as they are already prefabricated. Essentially, the cost of a structure can be outlined as the follows:

1) Material: this includes weight of steel members.
2) Construction: this includes the cost of steel fabrication, cladding.
3) Transportation: the cost of transportation is highly affected by the weight of the materials.
4) Utility services: comprises the mechanical and electrical services
5) Finishing: the last stage of building construction to have a portion of the total structure cost.

Assuming a fixed area for a structure, utility services depend on the client demands and cannot be a function of optimisation set by a structural engineer. The cost of finishing relies on the exposed external and internal areas and these are fixed

according to architects' plans. The cost of the fabrication mostly depends on the weight of the utilised material, i.e. steel for members and piles, clay for the bricks, and reinforced concrete for the foundation. Since the cost of transportation varies with the weight of loadings, a reduction in weight of the materials can result in a decrease in the cost of transportation. In addition, a decrease in the weight of the structure can lead to a decrease in applied loads on the foundation and consequently fewer materials are required for the foundation. As a structural engineering task in this context, weight minimisation is found to be the best option for optimisation problems as it can give a reasonable cost-effective steel structure to clients. In some special structures such as trusses, weight minimisation can yield a heavier structure as some members have a null axial force, and different sections should be given for them. This kind of structure can better respond when a topology optimisation (Rajeev and Krishnamoorthy, 1992; Ghasemi *et al.*,1999; Akin and Arjona-Baez, 2001; Balling *et al.*, 2006) is conducted, by which the shape of the optimum truss is defined. On the other hand, a steel frame, particularly a SPF, can give better response to the weight minimisation since they are not complicated in shape and the weight forms the main part of the total cost. In the light of this hypothesis, much research is found to approach the design weight minimisation of steel structures, among them are Adeli and Kumar (1995); Camp *et al*. (1998); Pezeshk et al. (2000); Gutkowski *et al.* (2000); Kameshki and Saka (2001); Toropov and Mahfouz (2001); Wang and Arora (2006); Saka (2008); Krajnc and Beg (2009).

5.3 Design variables

Design variables are those quantities that define and describe a structural system and are varied by the design modification procedure (Atrek *et al*., 1984). Implicitly, any optimisation problem relies on the design variables and these variables specify the direction toward the optimum solution. A design variable vector has a number of variables, x, and can be expressed in vector form, i.e.:

$$x = \{x_1, x_2, x_3, ..., x_n\} \tag{5-1}$$

Generally, design variables in structural optimisation are the cross sectional area or the dimensions making the cross-section. However, they can be defined as the nodes

of the joints which are frequently used in shape and topology optimisation, or as the second moment of area which are used to maximise the stiffness of the structure. There are, essentially, two types of design variable: continuous and discrete. Any value can be given to a continuous design variable in a certain range of variation. On the other hand, a discrete design variable deals with a whole number which is isolated and can be any number assigned to the existing items in the a list.

Since standard steel rolled sections are picked from the available steel category with fixed dimensions, in structural optimisation the variables are discrete. Nonetheless, if the design problem aims at using built-up sections, continuous design variables could be potentially used so that the solution, to some extent, can reach the upper limits of the constraints. Although the design problem with discrete design variables seems to be easier to solve, it is actually more difficult since the discrete design space is disjoint and non-convex (Arora *et al.*, 1994). Even if continuous design variables are used instead of discrete variables in a particular structural optimisation problem, they should be discretised at the end to obtain a reasonable solution. However, discretising the design variables is susceptible to error.

5.4 Objective function

Optimisation process necessitates creating a function and improving it so that it can give minimum and maximum values to a solution. An objective function is an aggregation of several individual criteria that is formed systematically to achieve a certain goal. An objective function can be aimed at weight or cost minimisation, displacement maximisation, and stiffness or load capacity maximisation. As a result, the objective function can be a measure of the effectiveness of the design, since it includes design variables and provides a basis for choice between the alternative acceptable designs. The objective function may be expressed as linear or non-linear functions depending on the nature of design variables. In general, an objective function may be defined by the following vector:

$$F(x) = \{f_1(x), f_2(x), f_3(x), ..., f_n(x)\} \tag{5-2}$$

In some cases of structural optimisation, the problem may have simultaneously two or more conflicting objectives. This kind of optimisation problem is called multi-

objective or multi-criteria design optimisation. In structural optimisation, it can be any combination of weight, rigidity (stiffness), cost, load capacity, or so on.

5.5 Constraints

In structural optimisation, constraints are the limitations imposed by one of the accredited codes of practice and function of the building structure. Essentially, they can be categorised into displacement, stress, size, and side constraints. The displacement constraints make sure that the design optimisation proceeds within the range of serviceability and the stress constraints limit frame failure due to lack of strength against applied loads. With some construction limitations, there might be size constraints to be taken into consideration during the optimisation process, such as the upper limit of the width of beam which should not be greater than the width of column in connections. Depending on the function of building, the side constraints are defined as the limitation in span, height, and space. Constraints may generally have the following form:

$$g_i(x) \leq \overline{g}_i(x) \qquad i = 1, 2, 3, \ldots, m \qquad (5\text{-}3)$$

Where:

$g_i(x)$ is the calculated value of the i^{th} constraints

$\overline{g}_i(x)$ is the limited value of the i^{th} constraints

m is the number of existing constraints

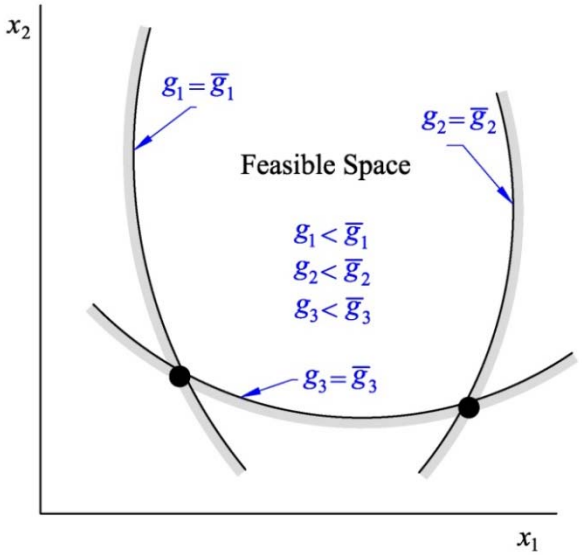

Figure 5-1: A feasible design space encompassed by constraints

5.6 Genetic Algorithms

The literature survey addressed approaches to heuristic search techniques, and the benefits of these techniques were discussed. In general, heuristic search techniques offer practical solutions which are rarely optimal, but which indicate the direction of the optimum solution within the feasible design space. Heuristic operators perform modification in a logical manner, and have a potential power of searching the fittest individuals (Lee *at al.*, 2008). Although they have the great advantage of finding the optimal or near-optimal solutions, they suffer from the problem of excessive computation time required to find such a solution in most cases.

Among heuristic search techniques is the GA which has been implemented in many structural optimisation problems with varying degrees of success. They are inspired by the evolution mechanism of genes and are based on the principle of Darwinian theory of evolution through natural selection. GA theory was developed by John Holland, his colleagues, and students at the University of Michigan in the US in the 1960s. They were not developed to solve a particular problem, but rather to formally study the phenomenon of adaptation as it occurs in nature and to investigate the possible and feasible ways to import the mechanism of natural adaptation into computer systems (Mitchell, 1999).

GA are developed by applying the principle of natural evolution to a numerical search method. GA differ from traditional optimisation methods in the following aspects (Goldberg, 1989):

1) Unlike traditional methods, GA work with an *encoded* set of variables.
2) They start the operation with a population of points rather than a single point of traditional techniques.
3) GA do not use the gradient of the objective and/or constraints functions.
4) GA use a transition scheme which is probabilistic, whereas traditional methods use a deterministic gradient.

GA are used as function optimisers particularly when the variables have discrete values. They achieve this by first selecting an initial population where each individual is constructed by bringing together the total number of variables respectively in a binary or other code form. These individuals are called artificial chromosomes and they have a finite string length (Kameshki and Saka, 2001). Each string is made up of a series of characters (typically binary numbers), representing the values of combined design variables for a single solution. The fitness of each string is the measurement of the design variables' performance which is formulated into an objective function. The binary code for such design variables represents the sequence number of this variable in the discrete set. The initial population is replaced by a new population and the steps are repeated until a certain individual dominates the population or until a pre-selected number of generations is reached. The fittest individual of all the generations represents the best (optimal) solution. GA consist basically of three main parts (Camp *et al*., 1998):

1) Coding and decoding the variables into strings
2) Evaluating the fitness values of the combined design variables
3) Applying the genetic operators to produce the new design variables for the next generation.

GA are capable of solving complicated problems which are difficult to solve using other optimisation techniques. The key feature of the GA is that it can reach many points of the design space simultaneously and therefore can avoid becoming entrapped into a local optimum (Joghataie and Asbmarz, 2008).

A flowchart of the GA procedure is shown in Fig. 5-2.

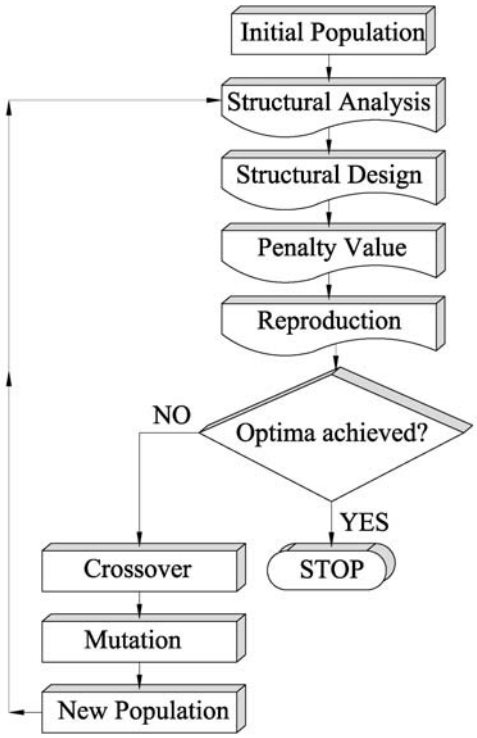

Figure 5-2: A flowchart of conventional GA

5.6.1 Encoding and decoding

The first step in the algorithm is to encode the design variables. The real numbers that represent the design variables are converted into binary at the beginning of the generation. Then the entire variables of a design are concatenated to form an artificial chromosome called a string. Assume that a problem has three design variables (steel cross-section) which have values of 36, 43, and 06 to identify their positions in a steel catalogue. If the length of each string is fixed to be six digits, the values will be represented in binary as '100011', '101010', and '000101' respectively (see Table 5-1). They are then concatenated to form a whole string: '100011101010000101' which comprises of the positions of the three design variables in the steel category. The process of conversion to the binary system is conducted to make the process easier when the string undergoes genetic operations. At the end of each generation the surviving binary strings are converted back into real numbers to deal with the cross-section properties given in the steel category.

This process is called decoding. The aforementioned processes are applied to as many numbers of strings as there numbers of design variables.

Table 5-1: Encoding the universal beams in steel catalogue

Position in catalogue	**Section encode**	**Section designation**	**Weight, kg**	**Other properties**
1	0000000	1016x305x487 UB	486.6	.....
2	0000001	1016x305x437 UB	436.9	.....
.....	.....	.....	.....	.....
28	0011011	610x305x149 UB	149.1	.....
29	0011100	610x229x140 UB	139.9	.....
.....	.....	.....	.....	.....
79	1001110	152x89x16 UB	16	.....
80	1001111	127x76x13 UB	13	.....

The process of encoding occurs just before the genetic operations are implemented on the design variables (obviously after the analysis and design process), whereas the decoding process must be done before the analysis and design process, as finding the cross-section in steel category requires working with real numbers.

5.6.2 Evaluation: Fitness values and the penalty function

In GA, the fitness value is the value of a formulated objective function. The fitness of an individual is an indicator of how well it is suited to its current environment or problem. As there is no explicit relationship between the objective function and the constraints in GA, this relation is defined by a penalty function. The value of the penalty is included in the fitness value. The nature of GA is to maximise the objective function, and if the minimisation is the aim to be accomplished, there should be some modification in the body of the fitness function. The fitness value of an individual among the population can be determined according to the following equation:

$$F_i = (1 + C)F_j \tag{5-4}$$

where:

F_i is the fitness value

F_j is the value of the objective function

C is the penalty value

The penalty value, C, is the summation of any constraint violation that is committed by the individual. In fact, this value is the bridge between the objective function and constraints. To obtain the penalty value, first all of the constraints should be expressed in ratio form and then the inequality must be rearranged in order that the opposite side becomes zero, i.e. Eq. 5-3 can be rearranged as:

$$\left|\frac{g_i(x)}{\bar{g}_i(x)}\right| - 1 \le 0 \qquad i = 1, 2, 3, \ldots, m \tag{5-5}$$

Then the penalty value is formed as:

$$C = C_p \sum_{i=1}^{m} \left(\left|\frac{g_i(x)}{\bar{g}_i(x)}\right| - 1 \right) \tag{5-6}$$

where:

C_p is the penalty coefficient

There are number of ways to deal with the penalty coefficient in the fitness function. Adeli and Cheng (1993) believe that when a small value is used for the penalty-function coefficient the solution usually converges to infeasible design space because the contribution of the penalty function to reduce the fitness value will be small. On the other hand, when a large value of the penalty coefficient is used the solution will oscillate undesirably. As the fitness value is sensitive to the minimisation of the penalty function, it is important to choose an appropriate value for the penalty function coefficient.

Camp *et al*. (1998) used two different penalty functions in their study: multiple segment penalty function and quadratic penalty function. For the multiple segment penalty function, they implemented the following function:

$$\Phi_i = \begin{cases} 1 & \text{if} \quad \left|\dfrac{p_i}{p_{\max}}\right| \le 1.0 \\ k_1 \left|\dfrac{p_i}{p_{\max}}\right| & \text{if} \quad 1 < \left|\dfrac{p_i}{p_{\max}}\right| \le c_1 \\ k_2 \left|\dfrac{p_i}{p_{\max}}\right| & \text{if} \quad \left|\dfrac{p_i}{p_{\max}}\right| > c_1 \end{cases} \tag{5-7}$$

where:

Φ_i is the penalty value for constraint i

p_i is the structural parameter or response (deflection, stress, etc)

$p_{\max}$ is the maximum allowable value of each p_i

k_1 and k_2 are the violation rates

c_1 is limiting percentage for constraint violation

The quadratic penalty function takes the form:

$$\Phi_i = 1 + k_3 (q_i - 1)^2 \tag{5-8}$$

where:

k_3 is the quadratic penalty rate

q_i is defined as:

$$q_i = \begin{cases} 1 & \text{if} \quad \dfrac{|p_i|}{p_{\max}} \le 1 \\ \dfrac{|p_i|}{p_{\max}} & \text{if} \quad \dfrac{|p_i|}{p_{\max}} > 1 \end{cases}$$

Pezeshk *et al*. (2000) divided the penalty value into three parts so that the penalty could be squared for bigger violation of the constraints. The penalty function they used was:

$$C = \begin{cases} 0 & \text{if} \quad \alpha \le 0 \\ \alpha & \text{if} \quad 0 < \alpha \le 1.0 \\ \alpha^2 & \text{if} \quad \alpha > 1.0 \end{cases} \tag{5-9}$$

where α is formulated as below,

$$\alpha = \sum_{i=1}^{m} \left(\frac{|p_i|}{p_{\max}} - 1 \right)$$

$$F = W(1 + C) \tag{5-10}$$

where:

C is constraint violation value.

Using this form of penalty function allows the penalty quantity to be a percentage of the total weight of the structure. In the other words, the larger the violation, the heavier the steel frame.

Foley and Schinler (2003) used the following penalty function:

$$p_j = 1.0 + k_j (q_j - 1)^{n_j} \tag{5-11}$$

where:

k_j is the penalty scaling multiplier

n is the penalty scaling exponent

p_i is the scaled constraint violation

q_j is scaling parameter and can be calculated as below:

$$q_j = \begin{cases} 1.0 & \text{if } \Phi_j \le 1.0 \\ \Phi_j & \text{if } \Phi_j > 1.0 \end{cases}$$

Φ is the penalty multiplier

Saka (2003) used a violation coefficient to penalise the objective function as follows:

$$F = W(1 + C \sum_{i=1}^{m} v_i) \tag{5-12}$$

where

v_i is the violation coefficient computed as:

$v_i = g_i$ if $g_i > 0$

$v_i = 0$ if $g_i \le 0$

$$g_i = \frac{|p_i|}{p_{\max}} - 1$$

p_i the structural parameter or response

$p_{\max}$ the maximum allowable value of p_i.

Following the aforementioned rules to define the relation between constraints and objective functions, the constraints imposed by codes of practice are transformed according to the following procedures:

- Displacement and deflection

$$\frac{\delta_i}{\delta_{iu}} - 1 \le 0 \qquad i=1, 2, 3, \ldots, nj \qquad (5\text{-}13)$$

$$\frac{\Delta_j}{\Delta_{ju}} - 1 \le 0 \qquad j=1, 2, 3, \ldots, nm \qquad (5\text{-}14)$$

- Dimensions

$$\frac{B_{fbk}}{B_{fck}} - 1 \le 0 \qquad k=1, 2, 3, \ldots, nbc \qquad (5\text{-}15)$$

- Strength

BS 5950

$$\frac{M_{xj}}{M_{cxj}} - 1 \le 0 \qquad j=1, 2, 3, \ldots, nm \qquad (5\text{-}16)$$

$$\frac{F_j}{A_{gj} p_y} + \frac{M_{xj}}{M_{cxj}} - 1 \le 0 \qquad j=1, 2, 3, \ldots, nm \qquad (5\text{-}17)$$

$$\frac{F_j}{A_{gj} p_{cj}} + \frac{m_j M_{xj}}{p_y Z_j} - 1 \le 0 \qquad j=1, 2, 3, \ldots, nm \qquad (5\text{-}18)$$

$$\frac{F_j}{A_{gj} p_{cyj}} + \frac{m_{LT\,j} M_{LTj}}{M_{bj}} - 1 \le 0 \qquad j=1, \ldots, nm \qquad (5\text{-}19)$$

$$\frac{F_i}{A_i p_b} + \frac{M_i}{S_{xi} p_b} - 1 \le 0 \qquad i=1, 2, \ldots, nh \qquad (5\text{-}20)$$

EC3

$$\frac{M_{xj}}{M_{cxj}} - 1 \le 0 \qquad j=1,2, \ldots, nm \qquad (5\text{-}21)$$

$$\frac{P_j}{P_{bxj}} + k_{xx} \frac{M_{xj}}{M_{cxj}} - 1 \le 0 \qquad j=1, \ldots, nm \qquad (5\text{-}22)$$

$$\frac{P_j}{P_{bxj}} + k_{xx} \frac{M_{xj}}{M_{bj}} - 1 \le 0 \qquad j=1, \ldots, nm \qquad (5\text{-}23)$$

$$\frac{P_j}{P_{byj}} + k_{yx} \frac{M_{xj}}{M_{bj}} - 1 \le 0 \qquad j=1, \ldots, nm \qquad (5\text{-}24)$$

Where:

A_{gj}	the gross section area of member j
B_{fbk} & B_{fck}	width of the beam and column at the intersection joint
F_j	axial member force of member j
k_{xx} & k_{yx}	interaction factors depend on equivalent moment factor
M_{bj}	lateral torsional buckling resistance moment
M_{cxj}	bending moment capacity of member j
m_j	the equivalent moment factor for member j
M_{LTj}	the maximum bending moment in the segment j
m_{LTj}	the equivalent moment factor for segment j
M_{xj}	maximum bending moment about major axis
nbc	number of beam-column connections
ng	number of member groups
nj	total number of joints
nm	number of members in a group
P_{bxj} & P_{byj}	buckling capacity of member j about major and minor axes
p_{cj}	the compressive strength of member j
p_{cyj}	the compressive strength about the minor axis
P_j	axial member force of member j
p_y	design strength

V_j volume of member j

W total weight if frame

Z_j the section modulus of the member j

Δ_j maximum deflection of member j

Δ_{ju} maximum allowable deflection

∂ total lateral displacements of joints

δ_i horizontal or vertical displacements of joint i

δ_{iu} upper limit of displacements

γ_m unit weigh of the member group

5.6.3 Genetic operator 1: Reproduction

The reproduction of GA starts with assessing the fitness value of each string. The assessment can be achieved by selecting a systematic statistics operation implemented so that it can give a higher survival probability to the fittest individuals. There are number of reproduction schemes that have been applied by researchers, such as Camp *et al*., (1998) who introduced three reproduction schemes: inverse scheme, partitioning strategy, and generation-dependent distribution.

The inverse scheme comes from a simple logical deduction: inverting a large number gives a small value. The effect of the inverse scheme is to give the fittest design variable a high probability of survival while the less fit variables are adjusted to approach zero probability. The fitness values they use are scaled as follows:

$$F_i' = \frac{F_{\max} - (F_{\min} / \alpha)}{F_i - (F_{\min} / \alpha)} \tag{5-25}$$

where:

F_i is the original fitness value of string i in the current generation

$F_{\max}$ is the maximum value of the fitness in the current generation

F_{main} is the minimum value of the fitness in the current generation

F_i' is the scaled fitness value of string i

α is a constant slightly larger than 1 (typically 1.01).

The value of α prevents numerical problems when evaluating the inverse of $F_{\min}$.

The selection probability of each solution string is obtained as follows:

$$P_i = \frac{F_i^{'}}{\sum_{j=1}^{np} F_j^{'}} \tag{5-26}$$

where:

P_i selection probability for string i

np population size

The partitioning strategy (shown in Fig. 5-3) divides the population into two groups. A smaller proportion of the population, for instance 20%, which have better fitness value, are collected into one group with a certain probability of selection and the rest form the second group. The discrepancy among the populations in each group is overlooked whereas the discrepancy among two groups is emphasized. Then the better individuals are selected to drop into a mating pool with a higher probability value. However, some of the less fit individuals are selected as well with smaller probability values of selection.

The generation-dependent distribution scheme (Fig. 5-4) employs a set of generation-dependent distributions instead of using a single selection probability. During the earlier generations, a uniform selection probability is applied to explore more design space, but after a certain number of generations the selection probability is shifted to the fitter portion of the population, increasing the probability that the fittest individuals are selected for reproduction. After this period, the selection scheme becomes more elitist, focusing on an explorative local search.

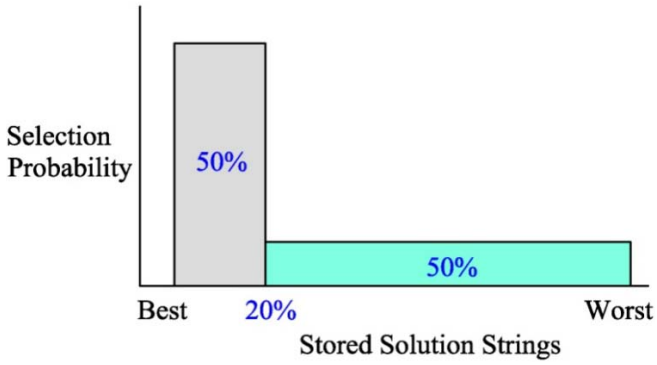

Figure 5-3: Idealization of partitioning reproduction scheme (Camp *et al.*, 1998)

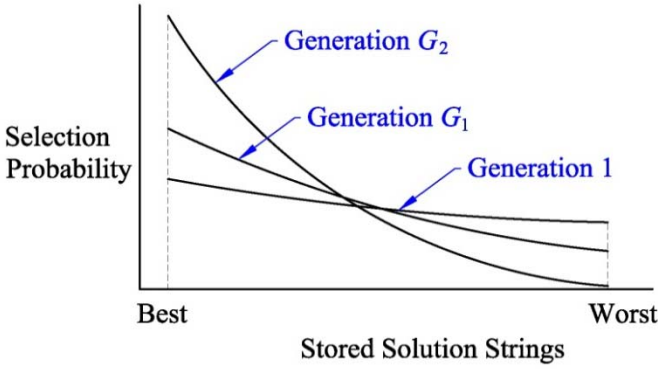

Figure 5-4: Idealization of general-dependent reproduction scheme

In addition to the above schemes, a scheme was introduced by Toropov and Mahfouz (2001). If the problem is minimisation, the fitness function should be so modified that it can form the equation suitable for the minimisation process, i.e. the smallest value will become the largest one among the population:

$$F_i^{New} = F_{\max} + F_{\min} - F_i \tag{5-27}$$

where:

F_i^{New}	the new fitness value of the individual i
$F_{\max}$	the maximum fitness value among the population
$F_{\min}$	the minimum fitness value among the population

After calculating the new fitness values for the population, they all undergo some statistical operations. First the average of the fitness value is found, then any individual that has a fitness value below the average is killed off and the rest are prepared to be selected for the following genetic operations. The selection occurs using any one of the schemes mentioned above.

There are generally two types of traditional reproduction schemes: ranking selection and tournament selection (Goldberg, 1989; Man and Kwang, 1999; Coley, 2005). In ranking selection, the individuals are sorted from the best to worst and the probability of the selection is fixed during the whole process. Then one of two rules – either roulette wheel sampling or stochastic universal sampling – is applied to sample individuals in the population and to drop them into a mating pool. In the roulette wheel method, each individual is assigned a slice of a circular roulette wheel

whose size depends on the proportionality of the fitness value, and the number of slices equals the size of the population. The wheel is spun as many times as the size of population and the individuals are passed through the slices to the mating pool to become parents of the next generation. In contrast, stochastic universal sampling spins the wheel once and all the required individuals are selected depending on the proportionality of their fitness value. The advantage of the ranking method is that there is no premature convergence and no need to specify every fitness value. Nevertheless, this method requires sorting the individuals' fitness values that should be carried out before implementing the procedure.

Tournament selection is a competitive method in which two individuals are compared to each other and the better one is selected for the mating pool. The competition step is repeated once for every member of the population. The comparison will most likely increase the number of fittest individuals that are dropped into the mating pool. The main advantages of this method are that it does not require explicit fitness and it prevents premature convergence. In contrast to the ranking method, there is no global sorting among the population before the selection process.

5.6.4 Genetic operator 2: Crossover

The next essential step of genetic operation is the crossover. This is the procedure wherein the string of the parent is broken down into two or more segments which are swapped with corresponding segments of another parent string through a random process. Two main strategies that crossover techniques use to locate the optimum are exploration and exploitation (Hasançebi and Erbatur, 2000). Exploration is a search technique through which a crossover should be capable of doing a thorough search of the design space. The exploitation strategy is when a technique that works from a previous point and searches for a more optimal one.

Basically, there are three types of crossover scheme: single-point crossover, two-point crossover, and uniform crossover. In addition to these, there are a number of crossover schemes that have been developed to improve the quality of the GA (these were addressed in the literature survey). In the single-point crossover, a fixed number

is randomly chosen as the crossover point and the part of parents' string is swapped, resulting in production of offspring. Fig. 5-5 depicts the single-point crossover.

In the two-point crossover, two points are randomly selected and the genes of the parents' strings between these two points are swapped, producing two offspring (Fig. 5-6). The same procedure is repeated for the case of three-point crossover where three points are randomly selected and the swap takes place at one or two parts of the parents' strings.

The uniform crossover is a character-based mating scheme in which a binary string is produced that equals the length of the parents' strings. The binary string is called a 'mask' and is generated randomly. 20 to 40% of the mask's genes are set to '0' and

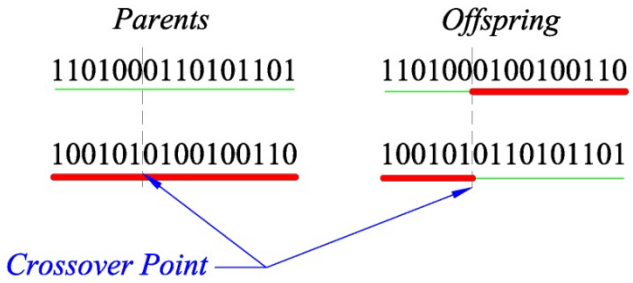

Figure 5-5: Single-point crossover and swap process

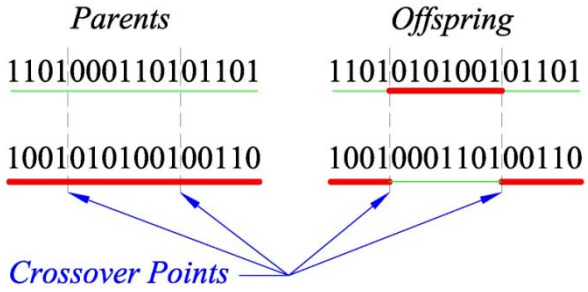

Figure 5-6: Two-point crossover and swap process

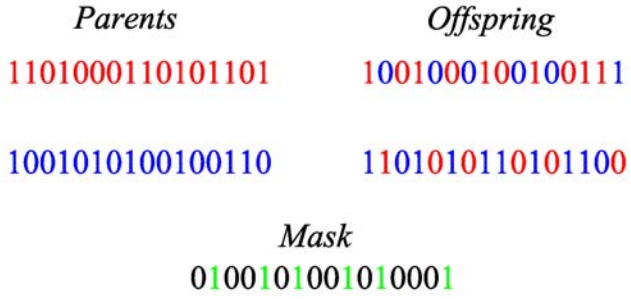

Figure 5-7: Uniform crossover and swap process

the rest to '1'. Then at the position '1' of the gene, the swap occurs between two parents, and the offspring are produced. Swaps only take place at positions where a mask has a '1' gene. Fig. 5-7 depicts this process.

In order to have the crossover, a number is randomly generated and compared to the predetermined crossover probability. If the number is less than the probability then the crossover occurs, otherwise it is overlooked.

5.6.5 Genetic operator 3: Mutation

Mutation is a secondary operation and is also a character-based operator. After crossover, a probability is assigned to each gene of the offspring to undergo a mutation operation. The mutation occurs such that a probability (normally very small) is assigned and compared to a randomly-generated number. If the number is less than the mutation probability, the gene is flipped from '0' to '1' or vice versa, otherwise the gene will remain intact. Although mutation is a secondary operator, it nevertheless plays a substantial role in exploring the feasible design space making possible to explore the region where the algorithm has never experienced. Mutation will change dramatically the characteristics of the chromosome (string) and produce different offspring that do not possess the complete characteristics of parents. Fig. 5-8 demonstrates the mutation process.

5.6.6 Elitist strategy

Since the genetic operations are conducted stochastically, it has been observed that the best individuals of the population are unlikely to produce good offspring for the next generation due to genetic operators. To make up for this deficiency, the elitist strategy is adopted, which fixes this potential source of loss of information by copying the best individuals into the succeeding generation. After ranking the individuals from best to the worst, the best individuals are selected logically and they

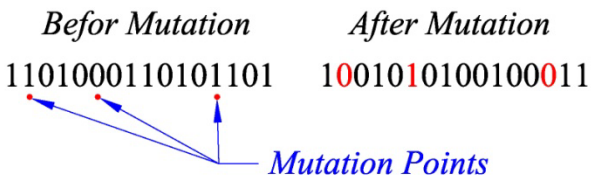

Figure 5-8: Occurrence of mutation in the offspring's genes

are removed from further genetic operations, being secured for the next generation without changing their genetic characteristics. The strategy improves the algorithm's convergence to the optimum solution and speed up domination by the fittest individual.

5.7 Distributed genetic algorithms (DGA)

In a distributed genetic algorithm (DGA), the performance of a conventional GA is improved by minor modifications to its main algorithm whereby a population is divided into a certain number of subpopulations. Then a GA is executed on each subpopulation separately, which leads to quicker convergence and higher searching capability compared to conventional GA (Starkweather *et al*. 1990; Mühlenbein *et al*. 1991).

Researchers have recently tried to increases the speed of the algorithm using parallel or distributed population groups. GA are naturally suited to the parallel process. There are two approaches of parallel GA known as the *inland* model and the *diffusion* model. In the inland model the population is subdivided into subpopulations and migration among the subpopulations occurs periodically during the searching process. In the diffusion model, each individual is restricted to a small area and the population is considered as a system that interacts only with contiguous population areas (Garai and Chaudhuri, 2007).

In the simple GA, there is a possibility that the algorithm search could be confined to the local optimum after a only few iterations. This may happen due to a lack of diversity among the individuals of the population for which the search cannot explore the design spaces as uniformly as possible. This nature of problem may be either due to the deviation of the algorithm, or due to the inefficiency of the approach to the location of a global optimum solution. The problem can be eliminated by making a uniform search as far as possible over the feasible design space by dividing the population into smaller subpopulations. The DGA operation is illustrated in Figure 5-9.

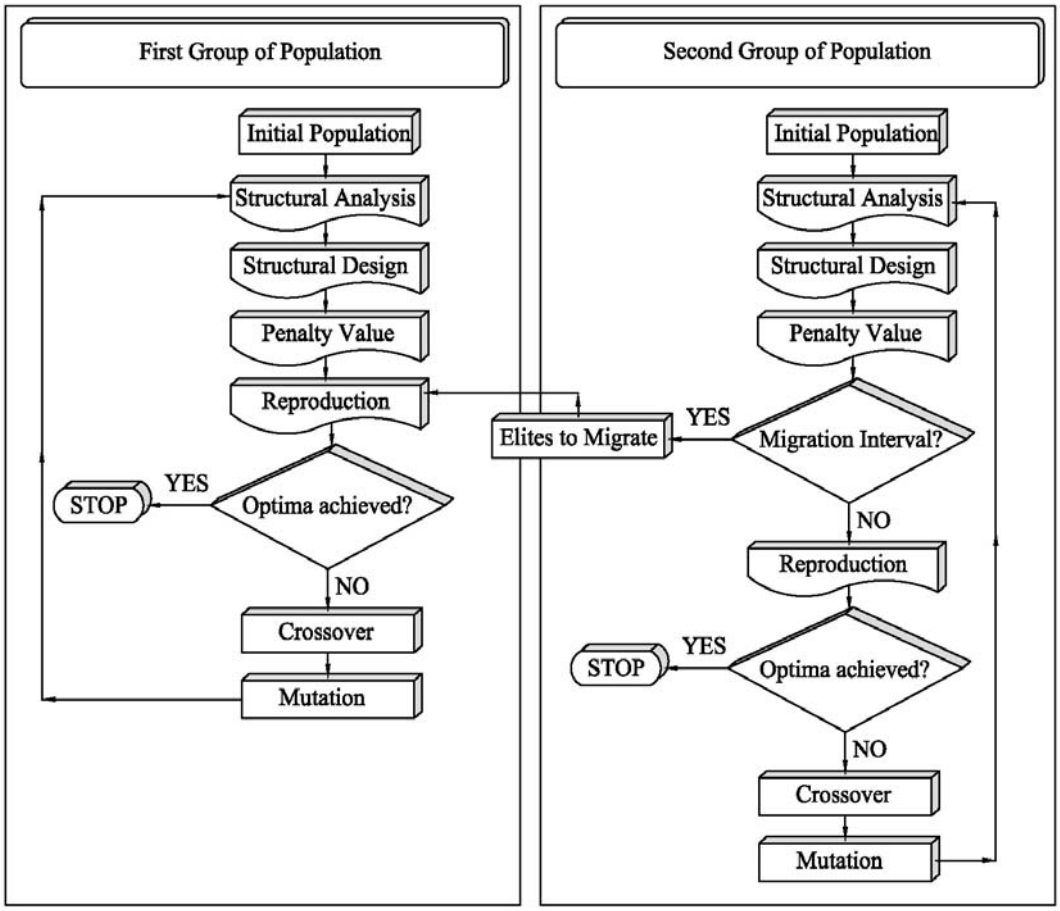

Figure 5-9: A flowchart of optimum design by DGA

5.7.1 Migration

DGA involves the concept of migrating elite individuals to improve a population. This idea has been adopted into DGA by allowing some elite individuals to migrate to other subpopulation groups, assisting the algorithm to improve its quality in convergence to the optimum solution. This is the main aspect which distinguishes DGA from GA.

Migration makes DGA effectively a parallel process, by simultaneously investigating multiple regions of the search space with each iteration. Within various alternative strategies, migration is governed and modelled by two main parameters: migration interval and migration rate. A probability is assigned to select a certain number of elite individuals that are allowed to migrate in a pre-selected generation interval.

5.8 DGA modification

From the literature survey, it was learned that some shortcomings of DGA can be fixed by modifying the algorithm. These modifications are the essence of the contributions to knowledge in this study. Attempts have been made to improve schemes of the main algorithm and enhance the quality and performance of the DGA. These aspects are vital factors to prevent the algorithm as much as possible from getting stuck in a local optimum solution, and simultaneously boost the capacity of the algorithm to approach global optimum solutions. The main objective of the modification is to accelerate convergence of the design problem to the optimum solution. These modifications should encourage structural engineers to use these structural optimisation techniques in practice. In addition, the improvements to the algorithm are also of benefit to general DGA optimisation problems, and are not just limited to the field of structural engineering. The DGA developed in this project thus has the potential for application beyond the scope of the current study. The objectives of the modification can be outlined as follows:

1) The algorithm must be able to deal with real-life design optimisation problems.
2) The algorithm should manage convergence to global optimum with reasonable time consumption.
3) While using the discrete design variables, the algorithm should be linked to the databases of steel catalogues to get instant access to the information of steel cross-sections.
4) The algorithm will deal with as many number of design variables as required.
5) The algorithm will handle different optimisation problems based on the behaviour of structural frames.
6) The algorithm will contribute to optimisation problems in different scientific fields.

In light of the above aims, all aspects of the modifications are discussed in the following sections.

5.8.1 Fitness value

As the algorithm approaches the end of its process, diversity among the population decreases. This is because one fittest individual (i.e. the optimum solution) usually comes to dominate the population. To obtain a penalty value, it is necessary to conduct structural design and analysis, but this process will take much computation time. To overcome this problem, the algorithm does not pass similar individuals through the structural analysis and design process. Only one of them is passed and its penalty value is assigned to the rest of the similar individuals. The preliminary tests' results show that structural analysis and constraint-checking consumes 71% of the computation time if all the individuals undergo the process. The idea of excluding similar individuals from the process reduces the computation time by 18% according to the preliminary results of tests conducted in this study.

5.8.2 Reproduction and the twin analogy

Neither the ranking method nor the tournament method is used to select the individuals for the mating pool. Instead, an 'accumulation' method is used to assist the algorithm to converge to the optimum solution more quickly. After the fitness values of all individuals are found, they are accumulated. Once again the fitness values of the elite individuals are accumulated to the new value, and these elite individuals are allowed to reproduce twice. After that a number between 0 and 1 is randomly generated and multiplied by the summation of the fitness values. Then any individual that has an accumulative number right above the randomly generated one is dropped into the mating pool. The idea can be better justified when the fitness values of elite individuals are added at the end of the accumulation process. Since it is most likely that a high random number is generated, the elite individuals are in a better position to be selected as they have a high accumulative value. However, this can lead the algorithm to a premature convergence, and this can be fixed by modification of other operators like mutation. According to tests, involving the elite individual twice in the reproduction process, while they are already secured for the next generation, can give up to 3% reduction in the time of convergence.

The modified DGA uses the idea of twinning to produce more offspring. Since the best parents in the population will likely give better offspring, a probability is assigned to the fittest parents that allowing them to breed twins. This makes it possible to further increase the number of fitter individuals among the population.

5.8.3 Crossover

In addition to the number of schemes addressed by the literature, the developed algorithm includes four-point and five-point crossovers. Overall, there are six mutation schemes that are simultaneously implemented in the algorithm. Before choosing one of them, a number is randomly generated to specify which crossover scheme should be applied. Number 1 is assigned to one-point crossover, 2 to two-point crossover, 3 to three-point crossover, 4 to four-point crossover, 5 to five-point crossover, and 6 to uniform crossover. Depending on the crossover point after specifying the scheme, numbers are randomly generated to specify the position of the crossover point in the individuals' strings. For a uniform crossover, it is decided to have 40% of zeros in the string of the mask.

5.8.4 Mutation

The core modification of DGA occurs with the creation of mutation schemes. In contrast to the studies that have used a constant value for mutation probability, the modified DGA uses a number of mutation schemes. It is believed that mutation has an influential role in diversifying the population and exploring more feasible design space, so the aim is to have a high value of mutation probability at the earlier stages of the operation. This produces greater diversity among the population and consequently more feasible design spaces can be explored. Diversity in genetic algorithms is usually high, particularly in earlier generations, due to the implementation of a population of variables, but this does not imply that the individuals will experience more feasible design space. The crossover operator attempts to exploit the space whilst mutation attempts to generate more points to get the optimum solution. If the mutation probability is low, premature convergence is more likely. In contrast, a high mutation probability will prevent the algorithm from converging to the optimum solution. This is because a high mutation probability

drastically changes the characteristics of the genes and will prevent domination of a particular individual in a population. In the light of this behaviour, the decision is made to formulate the mutation probability value. The result is that at the earlier stages, more feasible design space can be explored due to high mutation probability. Also, as long as the elitism strategy exists, the best individuals are secured for subsequent generations after reproduction, crossover and mutation, and consequently the risk of losing fitter individuals is reduced. Although the mutation probability is reduced as the generation proceeds, this value is still high in the first 20 to 30 generations. It is believed that this period will be enough to explore more feasible design space and find more elite individuals. The later stages allow the algorithm to creep into an optimum solution, which will not take place unless the mutation probability is reduced. Because more feasible design space has been explored and the elite individuals have been specified, the chance of finding the optimum solutions increases.

In the developed algorithm, three mutation schemes are examined to appraise the role of mutation in computation speed and convergence to the global optimum. The schemes are expressed in linear, quadratic, and exponential forms of equation, which give a varied mutation probability for each generation along the optimisation process.

Linear mutation probability

$$P_m^{G_C} = P_m^{\max} - \frac{G_C - 1}{N_G - 1}(P_m^{\max} - P_m^{\min}) \tag{5-28}$$

Quadratic mutation probability

$$P_m^{G_C} = P_m^{\max} - \frac{G_C{}^2 - 1}{N_G{}^2 - 1}(P_m^{\max} - P_m^{\min}) \tag{5-29}$$

Exponential mutation probability

$$P_m^{G_C} = P_m^{\max} - \frac{e^{-1/20} - e^{-G_C/20}}{e^{-1/20} - e^{-N_G/20}}(P_m^{\max} - P_m^{\min}) \tag{5-30}$$

where:

G_C	is the number of current generation
N_G	is the number of predetermined generations.
P_m^{Gc}	is the mutation probability of the current generation
P_m^{max}	is the maximum mutation probabilities
P_m^{min}	is the minimum mutation probabilities

Fig. 5-10 depicts the three aforementioned formulated equations when the maximum mutation probability is set to be 0.2 and the minimum is 0.0005 for 100 generations. The figure shows that in earlier generations the mutation value is high, and that over time it will decreases.

The quadratic mutation starts with a high mutation probability value which decreases slowly at first, and more quickly at the end. The exponential mutation has the opposite effect, decreasing most quickly at the beginning. The linear mutation scheme lies between the other two schemes, with a constant rate of probability reduction. These three probability functions are examined to investigate their effect on the performance of the DGA.

5.8.5 Displacement maximisation

Genetic algorithms can deal with optimisation problems other than weight minimisation, but weight optimisation in the design is relatively well-documented. However, in some special structures there might be revision of the design problem.

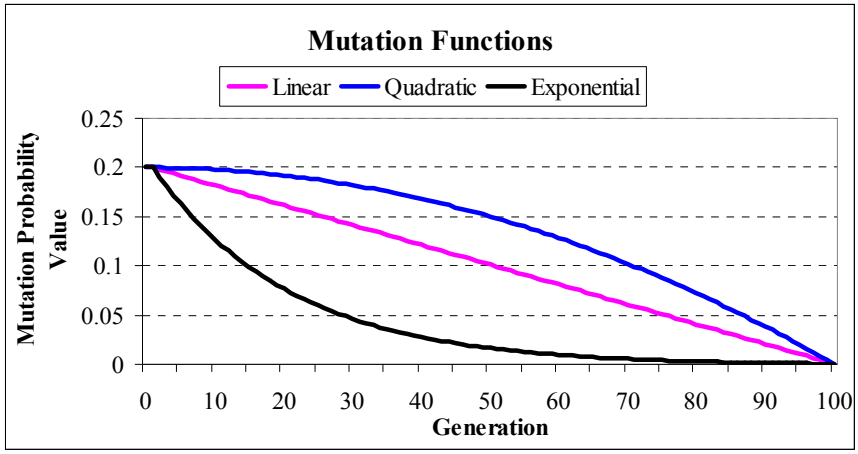

Figure 5-10: Diagram of three mutation probabilities

SPFs are very much affected by displacement. If they are subjected to gravity loads, vertical displacement is the most significant factor in the design constraints. On the other hand, if a large lateral load is applied to a SPF, excessive lateral sway is expected, and therefore the design is controlled by lateral (horizontal) displacement. With this is mind, the candidate has decided to maximise the lateral and vertical displacement in the case of gravity load and large lateral load applications respectively. Nevertheless, displacement maximisation seems to be uncommon for structural engineers as they avoid failure due to deflection and displacement. From the literature review, the drawn conclusion is that displacement maximisation is an under-researched area of study. The current project hopes to address the need for research in this area.

Formulating a design optimisation problem with displacement maximisation is not an easy task, as many criteria must be taken into consideration. In weight minimisation, the individuals that violate the constraints are not discarded as it is believed they may be capable of producing better offspring during the crossover and mutation operations. This is true since the only variable in the objective function is the cross-section area. In contrast, to formulate an objective function for displacement maximisation, the function relies on the area *and* the second moment of area of the steel cross-sections. It cannot be found any one-to-one relation between area and the second moment of area for rolled steel sections available in the catalogue. This means that the increase in area does not necessarily result in an increase in the second moment of area, and vice versa, or if increased, the ratio of increase is not compatible. However, this can be rectified by using built-up sections and arranging the problem so that an increase in area brings an increase in the second moment of area. As a result, the individuals that violate any constraint must be discarded to obtain better result. Excluding the committed individuals requires initiating the algorithm with a larger population size, with the result of increasing computation time.

5.8.6 Penalty function

The penalty function is the link between the objective function and constraints, therefore it is essential to formulate a penalty function in a way that contributes to the

performance of the algorithm. The modified DGA uses two different penalty functions: one for weight minimisation and one for the displacement maximisation. The developed penalty function is based on the severity of the violation. If the violation is low, then a small penalty is imposed, and the larger the violation, the larger the penalty. The penalty function for weight minimisation has the following form:

Defining

$$g_p = \sum_{j=1}^{nc} \left(\left| \frac{g_j(x)}{\bar{g}_j(x)} \right| - 1 \right) \qquad i = 1, 2, 3, ..., m \tag{5-31}$$

the penalty function, C_i, will be:

$$C_i = \begin{cases} 0 & \text{if } g_p \le 0 \\ g_p & \text{if } 0 < g_p \le 1.0 \\ 2g_p & \text{if } 1.0 < g_p \le 2.0 \\ 2g_p^2 & g_p > 2.0 \end{cases} \tag{5-32}$$

And the fitness function involves the penalty value by:

$$\text{Minimise } F_i = (1 + C_i)W_i \qquad i = 1, 2, 3, ..., np \tag{5-33}$$

where:

C_i the penalty value accrued on the individual i

g_p the summation of the violation

np the total number of population

W_i the weight of the frame represented by individual i

The penalty function for the displacement maximisation has a different form. As mentioned earlier, the individuals that violate the constraints are discarded:

$$C_i = \begin{cases} 1 & \text{if } g_p \le 0 \\ 0 & \text{if } g_p > 0 \end{cases} \tag{5-34}$$

The fitness function has the following form:

$$\text{Maximise } F_i = C_i D_j(u,v) \tag{5-35}$$

where:

$$D_j(u) = \sum_{j=1}^{nj} u_j$$

or

$$D_j(v) = \sum_{j=1}^{nj} v_j$$

nj total number of joints in frame

u_j horizontal displacement of the joint j

v_j vertical displacement of joint j

5.9 DO-DGA

All the mentioned modifications on the DGA are brought into a program called design optimisation using distributed genetic algorithm (DO-DGA). The program is written in Visual Basic 6.0 (Schneider, 2004), which can handle all aspects of the modification. Attempts are made to develop a program as user-friendly as possible. The attributes of developed DO-DGA can be outlined as:

1) The program is able to conduct design optimisation on different types of the plane steel framework in real-life situations.
2) It can measure structural response while considering both rigid and semi-rigid connection.
3) It is able to deal with the two major codes of practice for steel structures, namely BS 5950 and EC3.
4) It operates like the user friendly software that deals flexibly with inputting the data necessary for the optimisation process.
5) The program has potential capability to save computation time by applying the necessary modification in the developed algorithm and the structural analysis process.

6) Most importantly, DO-DGA is a complete program that does not need to be linked with any available finite element analysis software in the market, which would add to costs.

The DO-DGA is developed in two stages: structural analysis and design, and the modified DGA, which are explained in details in the following sections.

5.9.1 Input data

Input data is an important part of a program, therefore making it possible for a user to input data easily is vital. DO-DGA has two stages of data input: geometry data and loading data, which are explained in the following sections. The program starts by asking for the load system and measurement units and creating a new file. It comprises of a main menu, which is a platform to call for different windows required for inputting the data and to analyse them.

5.9.1.1 Geometry data

This type of data includes coordinate of joints, member assignments, members' characteristics, support specifications, and connections data. In the coordinates of joints and member assignments, the user inputs the coordinates of all structural frame joints and the name of each member is assigned (Fig. 5-11). The characteristics of members are specified in the section parameters form (Fig. 5-12), including: frame shape (prismatic or non-prismatic), member ends (pinned, rigid, semi-rigid, or combination of all), member cross-section (standard steel sections, rectangular section, or I-shaped section), and the type of material to specify the modulus of elasticity. In assigning the member cross-section with the available standard steel sections, the program is linked to a developed data base including all required properties of the universal beams and columns sections. After assigning the member with one of the standard steel section, the program reads the properties from the data base and assigns to the member including weight, area, second moment of area, root radius, section modulus, torsional constant, warping constant, and so on.

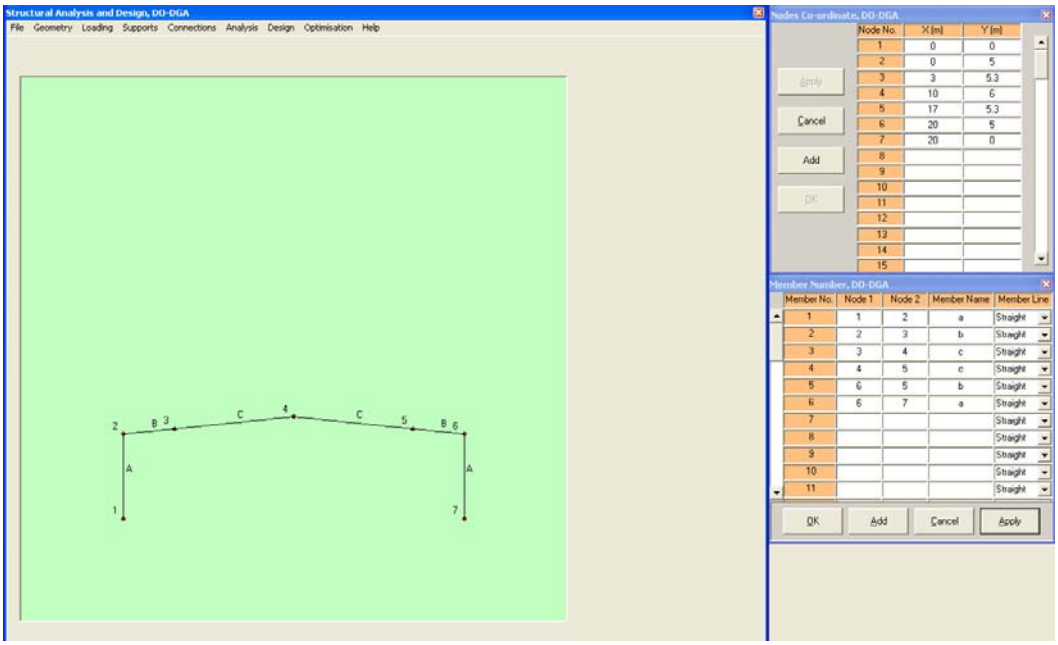

Figure 5-11: DO-DGA form for inputting the joints coordinate and members' assignments

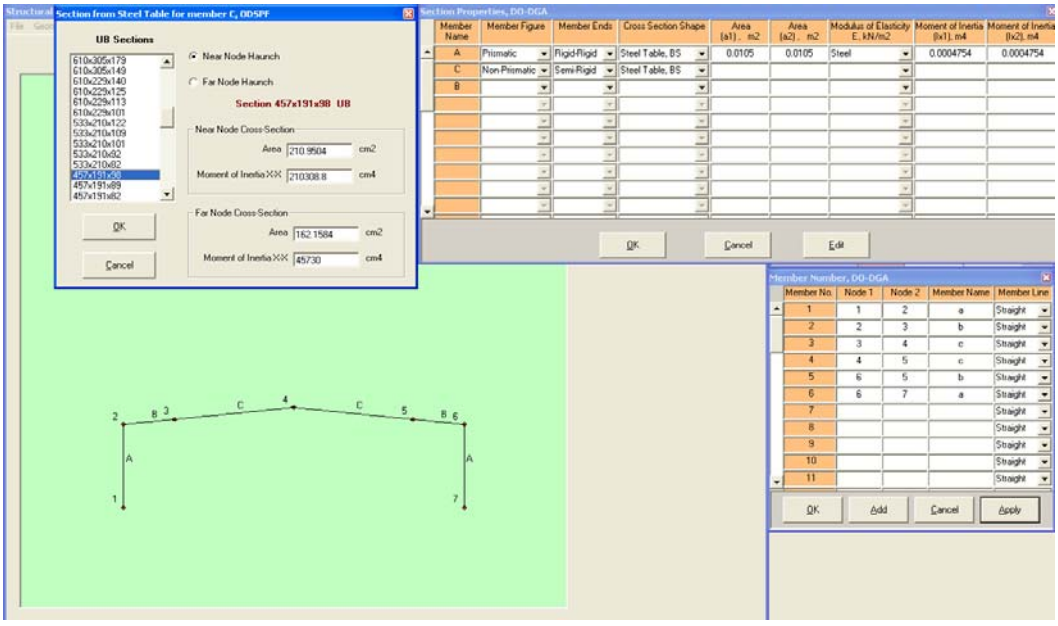

Figure 5-12: DO-DGA form for inputting the cross-sections properties

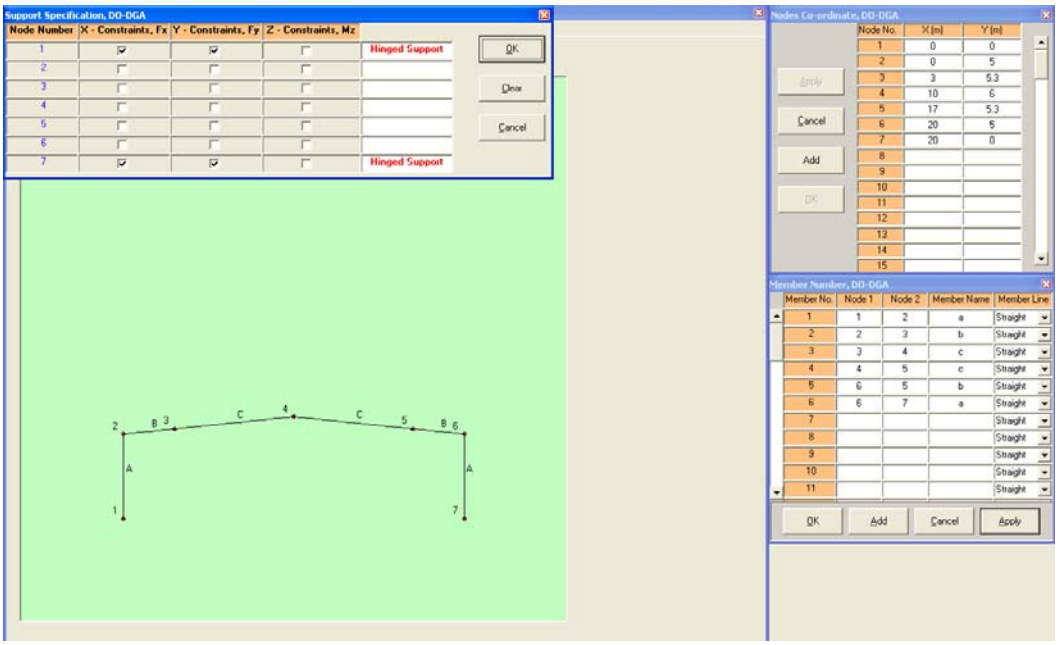

Figure 5-13: DO-DGA form for inputting the support specifications

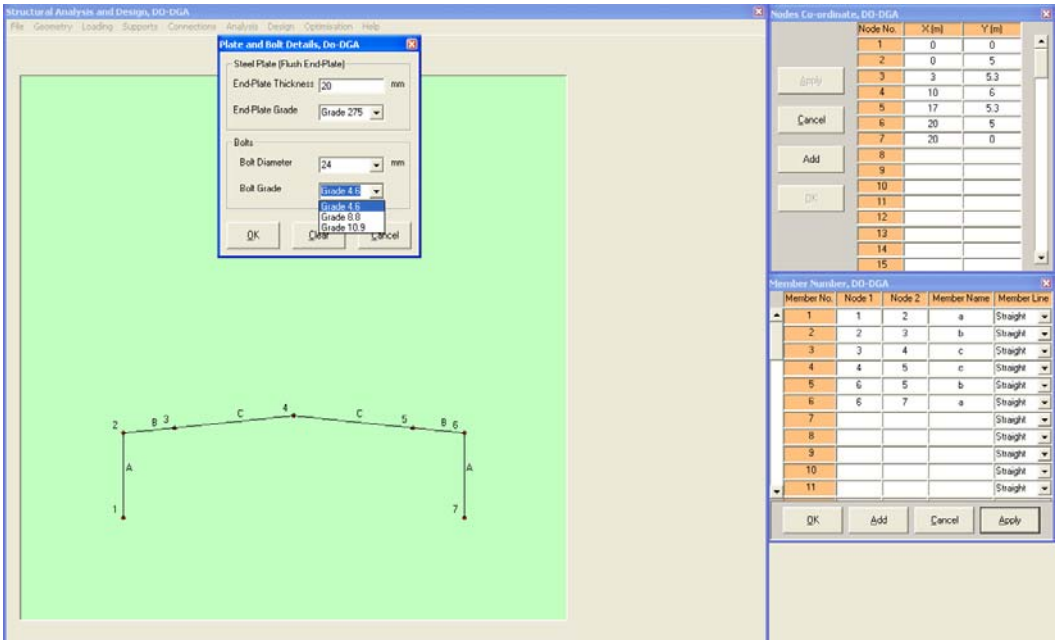

Figure 5-14: DO-DGA form for inputting the details of the connection

The types of frame supports are specified in the support specification form, as shown in Fig. 5-13. Also, it is possible to input the amount of settlement in the support in the supports sub menu.

Since some information about the plate thickness, bolt diameter and grades are needed for connections, the DO-DGA has provided the user with a form called plate

and bolt details. In this form, a user can easily input the end plate and bolt grades, end plate thickness, and bolt diameter as shown in Fig. 5-14.

The DO-DGA computes the height and breadth of the end plate depending on the assigned section and requirements of codes. It also correlates the bolt diameter with the end plate thickness if the input bolt diameter is not enough to match the codes requirements.

5.9.1.2 Loadings data

The applied loads to a structure are specified depending on the type of structure, location, and functions. Using DO-DGA, a user can deal with different types of loads existing in the nature and combined them in the ways that are required for the structures. The DO-DGA involves the load combinations according to BS 5950 and EC3 and a user will decide to have either of them for the analysis and design process. Fig. 5-15 and Fig. 5-16 show how to input the loading data in the load cases form.

All types of loads can be input in the load cases form including uniformly distributed loads, point loads, nodal loads, and self weight in different directions. The dead loads, live loads, and wind loads or combinations of all are taken into consideration as the loading inputs. There is the possibility to input 50 point loads acting on a member. It should be mentioned that all the load are working loads and then are magnified using load factors according to the specified codes of practice.

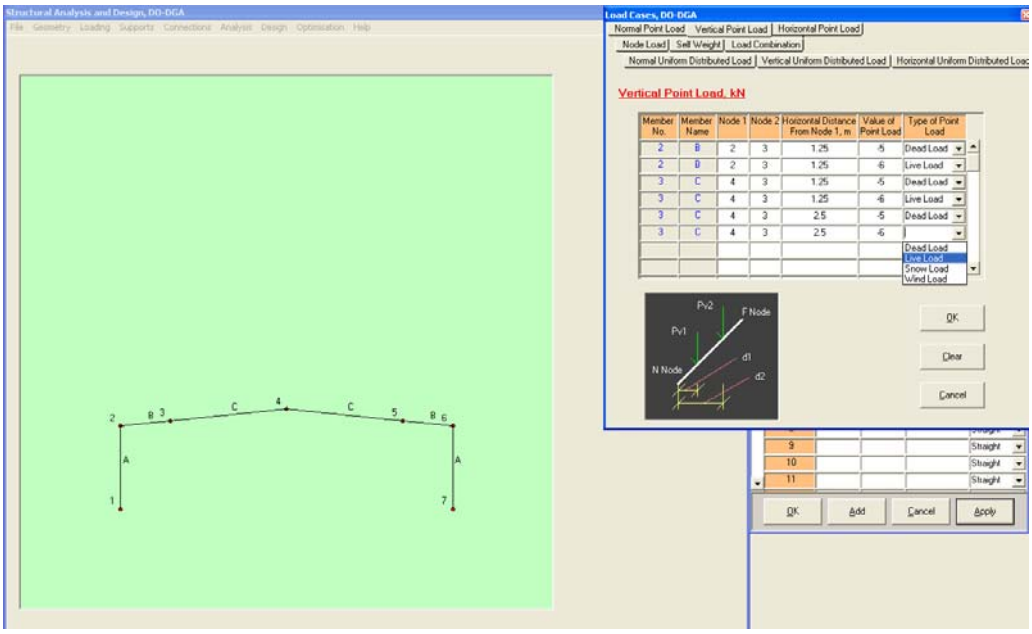

Figure 5-15: DO-DGA form for inputting the point loads for the frame

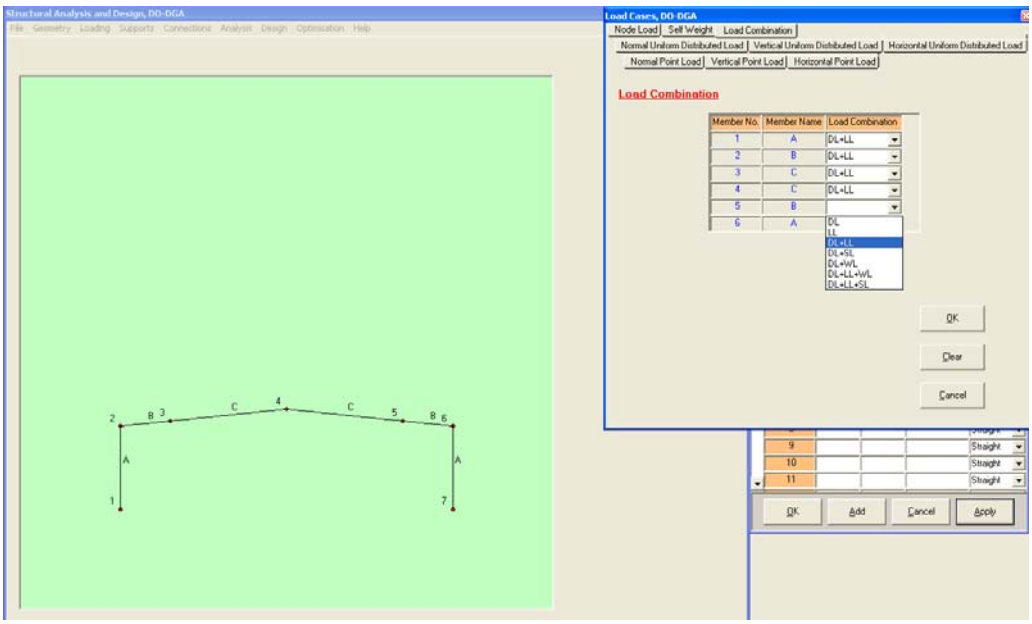

Figure 5-16: DO-DGA form for specifying the load combinations

5.9.2 Analysis

Once all required data are input, the DO-DGA performs the structural analysis process. It uses a direct stiffness method, which is a part of the finite element method, to measure the response of the structure against the applied loads. For this purpose, all the developed and defined stiffness matrices for prismatic and non-prismatic members are involved in the program. Also, DO-DGA can handle with the

stiffness matrix for the member with different ends, whether rigid-to-rigid, semi-rigid-to-semi-rigid, or rigid-to-semi-rigid joints. After the analysis, information such as the support reactions, the member forces, and joint displacements are saved as a text file. This process is shown in Fig. 5-17 and Fig. 5-18.

5.9.3 Design

In the design part of the program, the constraints imposed by both BS 5950 or EC3 are checked for the frame. If any member of the frame violates any constraints, then an alternative and appropriate section is assigned to member so that can check all constraints. The process starts by specifying a code of practice by user in the main menu of program as shown in Fig. 5-19. Then the steel grade and number of lateral restraints for columns and beams are input.

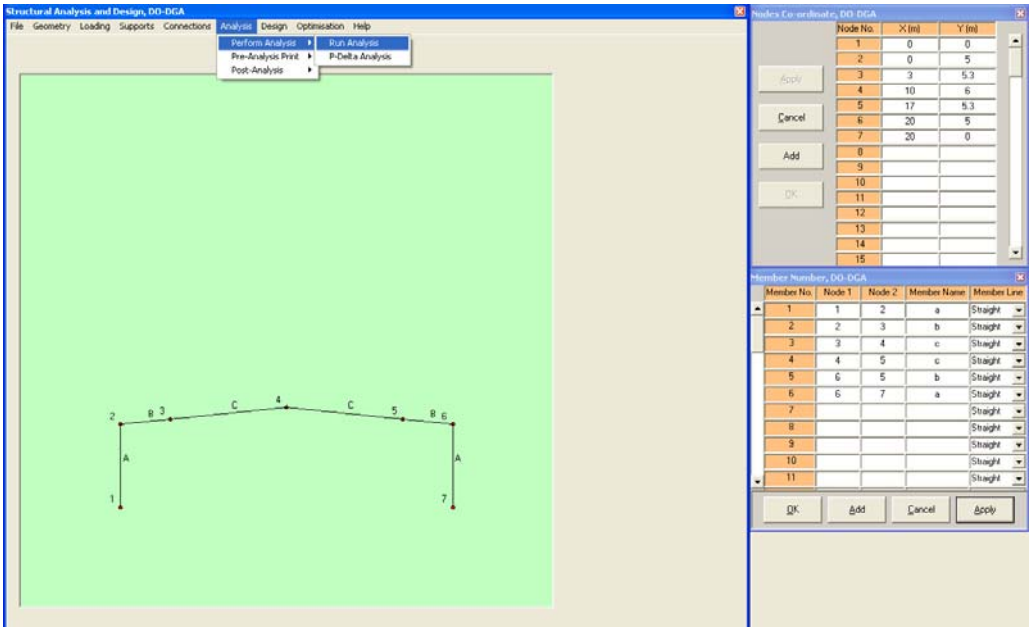

Figure 5-17: DO-DGA form for process of running analysis

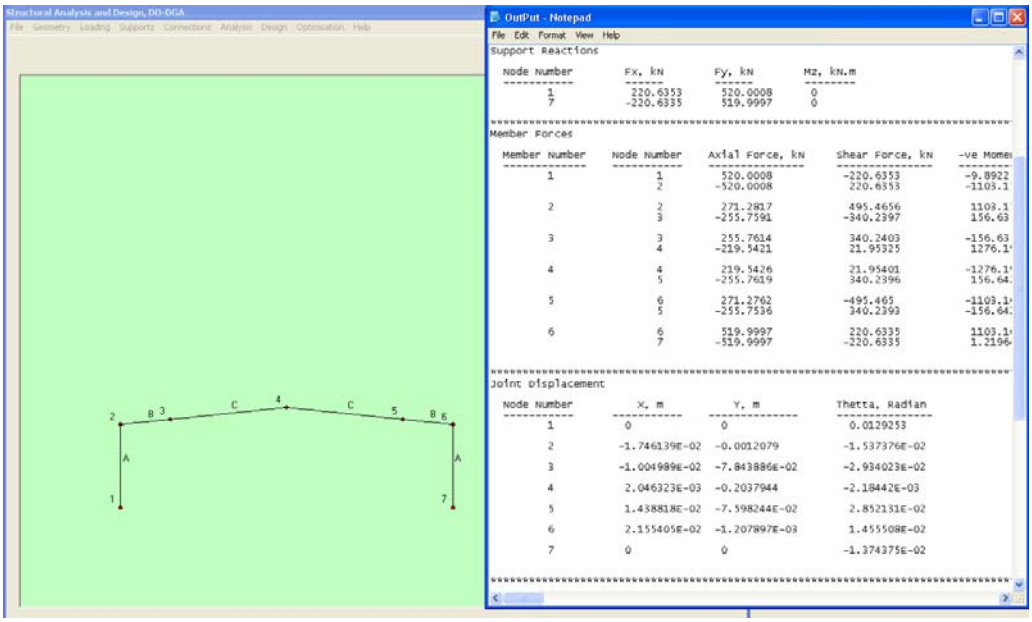

Figure 5-18: DO-DGA form for output of running the analysis

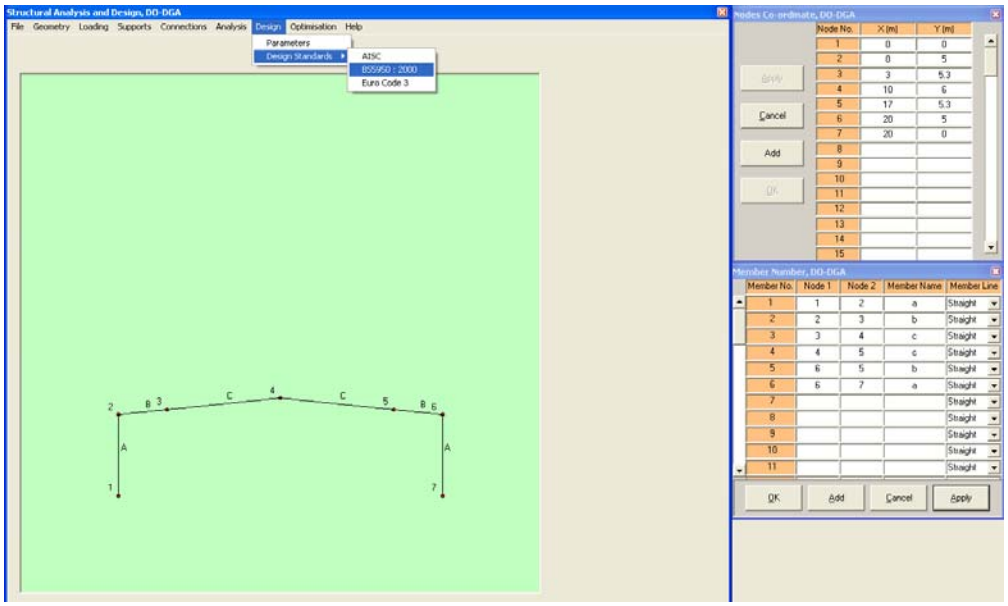

Figure 5-19: DO-DGA form for specifying a code of practice for design process

5.9.4 Optimisation

The structural optimisation part is a core characteristic of DO-DGA. A modified DGA has been embedded into the program, independent from the analysis and conventional design that are performed in other parts of DO-DGA. The developed algorithm is a combination of all processes such as the joint coordinates, member assignments, analysis, and constraint checks. Initially, all required genetic parameters

are input in a form which is shown in Fig. 5-20. The involved parameters are: size of population, number of generations, number of genes, twin breeding probability, crossover and mutation probabilities, elitism rate, migration rate, and migration interval. On this form, there are some optional choices that relate to the nature of optimisation problem. A user can choose either multi-storey frame, pitched-roof SPF, or curved rafter SPF. The user is given the decision to choose either weight minimisation or displacement maximisation as the objective function of design problem. For the SPF, the user can decide whether to deal with varied or constant haunch depth. Once all data are input, the optimisation process begins and usually lasts a few minutes depending on the number of design variable and the scale of the decided frame. After the design optimisation, the solution is printed in a text file and appears on the screen as shown in Fig. 5-21. This file includes all procedures of the genetic operations, analysis process and constraint checks. It also indicates how the design is controlled. In addition to the results output, the weights, displacements, initial stiffness of connections, the mutated genes, and some necessary results are recorded in different files and imported into a numerical spreadsheet file for statistical analysis.

Each step of the structural analysis part of DO-DGA is compared with the finite element analysis software available on the market, and its analysis matches the accredited software. After ensuring correctness in analysis and design process, the developed algorithm is embedded into DO-DGA. The algorithm was then examined by using a simple quadratic mathematical function for minimisation and maximisation. The correctness of the algorithm is proved as it yielded the exact minimum and maximum point of the proposed mathematical function. It is highly hoped that the developed DO-DGA can contribute to the campaign of bringing the design optimisation into daily office used by structural engineers.

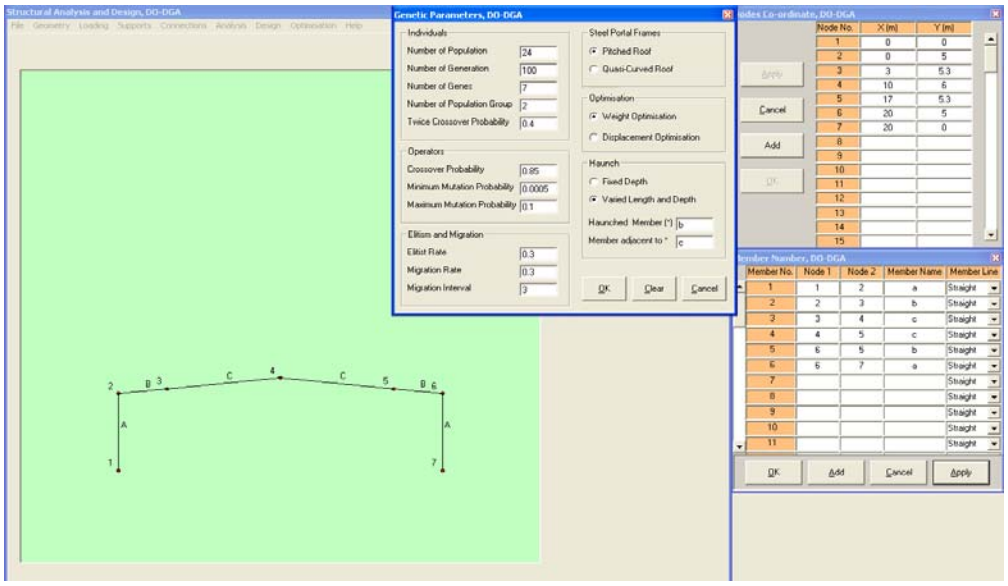

Figure 5-20: DO-DGA form for inputting the genetic parameters

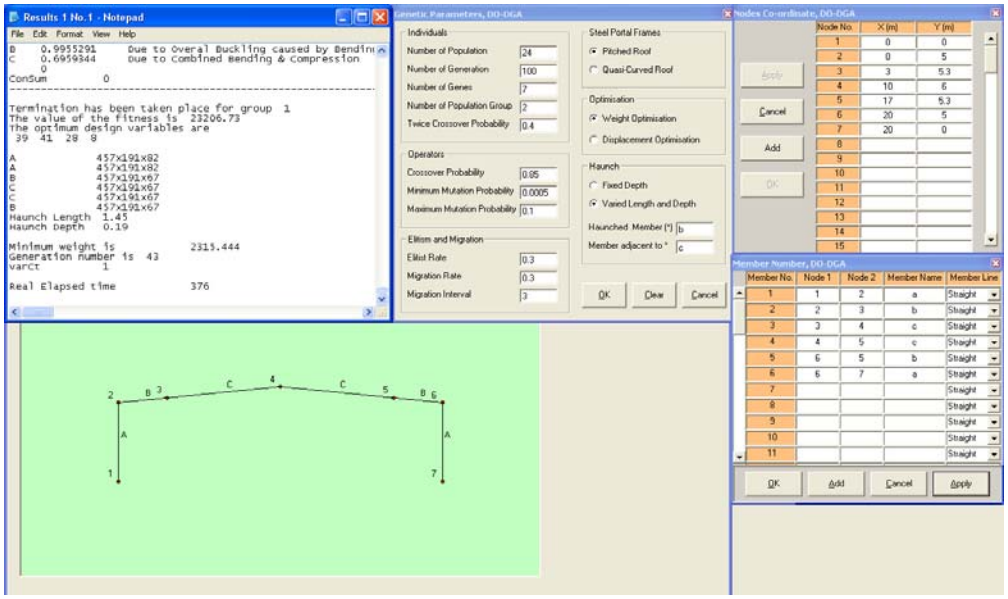

Figure 5-21: DO-DGA form for output of the design solution of a SPF obtained by running DO-DGA

5.10 Summary

The reasons necessary for the weight minimisation of steel frames were highlighted. The concepts of optimisation components such as design variable, objective function and constraints were discussed. The procedure which shows how GA work was explained. Then the new aspects that distinguish DGA from GA were addressed. All aspects of modifications designed to improve the performance and quality of DGA

were discussed in details. This was where the contribution to the knowledge was made. A new objective function called displacement maximisation was introduced. Since the modified DGA has been embedded into a computer program called DO-DGA, all features and attributes of this program were presented. In the following chapters the program is validated and implemented for further investigation of SPFs.

Chapter 6: Evaluation of Modified DGA

6.1 Introduction

A modified DGA is developed using mutation schemes and adding new procedures to the algorithm. To examine the appropriateness and validity of the modified DGA, a number of tests are conducted. These tests are grouped into two categories: evaluation and assessment. In the evaluation section attempts are made to maximise a mathematical function and to investigate the effects of the new schemes on the performance of the developed algorithm. As genetic operators are quite sensitive in terms of their probability values, the focus will be on assigning the probability values of genetic operators in the way that the developed DGA can give a better performance.

By applying different trials to assign the best probabilities to the genetic operators, as well as obtaining a suitable size of population, the modified DGA is validated using previously published steel frame designs. As a part of the validation, the results of the DO-DGA run are compared to those conducted with MP and heuristic search techniques. Since the majority of design optimisations in the contemporary literature minimise weight, the DO-DGA performs weight minimisation problems according to BS 5950 and EC3 codes of practice.

6.2 Algorithm evaluation

In the previous chapter, the DO-DGA is introduced and its highlighted its new modifications to the standard DGA. To assess the effects of the newly added schemes and the other operators of the modified DGA, the algorithm is used to maximise a simple third degree equation. Then, the appropriateness and effectiveness of the schemes and the genetic operators are investigated. In each assessment, attempts are made to run the DO-DGA three times for each ratio, and the average of generations and optimum values are recorded.

The equation to be maximised has the following form:

$$\text{Maximise } f(x) = x^3 + 2x^2 + 3x \qquad (6\text{-}1)$$

$$\text{Provided that, } 0 \le x \le 31$$

It can be easily proved mathematically that the function $f(x)$ has a maximum value of 31806 when $x = 31$ as shown in Fig. 6-1.

6.2.1 Twin analogy

A range of values between 0.0 and 1.0 are assigned to the twin probability ratio to maximise the given equation (Eq. 6-1). Fig. 6-2 shows the relationships of the twin probability with the convergence generation and the function value.

The function has a consistent maximum value of 31806 for all the twin probabilities. Fig. 6-1 indicates that increasing twin probability results in convergence of the equation problem to the optimum solution at an earlier stage. This indeed proves the effectiveness of the twin analogy in improving the quality of the algorithm by rapid convergence to the optimum solution, consequently saving computation time.

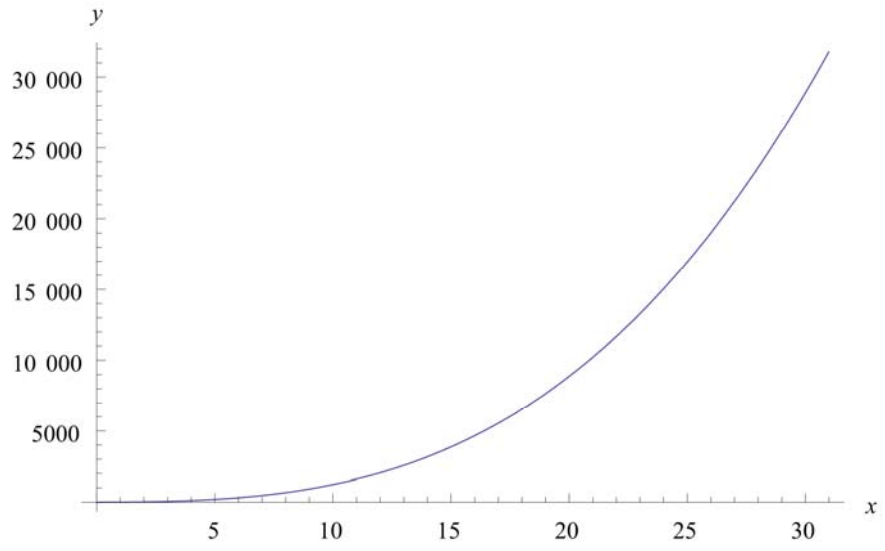

Figure 6-1: Graph of the function $x^3 + 2x^2 + 3x$

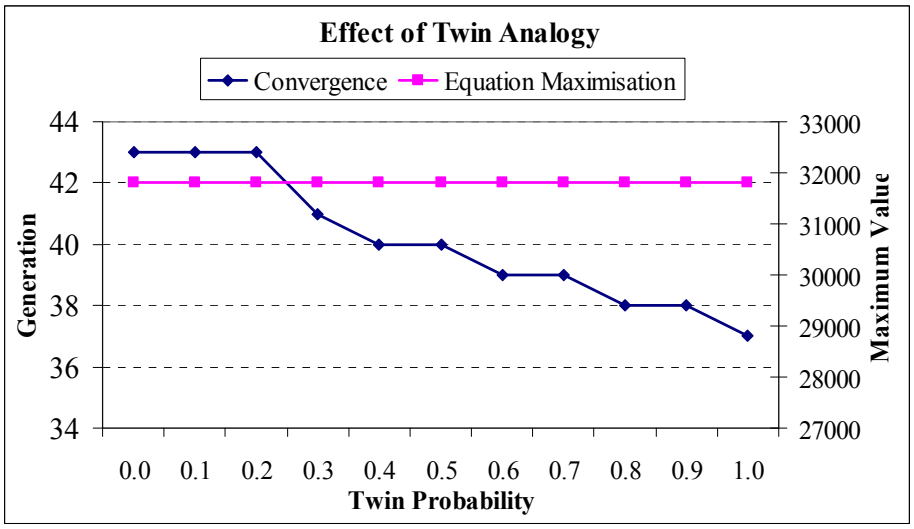

Figure 6-2: The relations between twin probability, convergence generation, and maximum value

6.2.2 Migration rate

One of the main aspects of the DGA is the use of migration to allow the elite individuals of a group to switch into different groups of populations. This is believed to enhance the quality of the algorithm in convergence to the optimum solution. For each migration rate ranging between 0.0 and 1.0, the DO-DGA is run three times and the average of generations and maximum values are recorded. During this test, all other parameters required for the DO-DGA to run are kept unchanged. Fig. 6-3 demonstrates the relationships of the migration ratio with the generation and the maximum.

It is found that as the migration rate increases, the number of generations decreases, i.e. a quicker convergence takes place.

6.2.3 Migration interval

The migration of elite individuals should take place in a predetermined migration interval. A range of 1 to 10 generations is used here to demonstrate the effect of the migration interval on the convergence of the equation problem and the optimum solution. The relation of the migration interval to the average generation and maximum value are presented in Fig. 6-4.

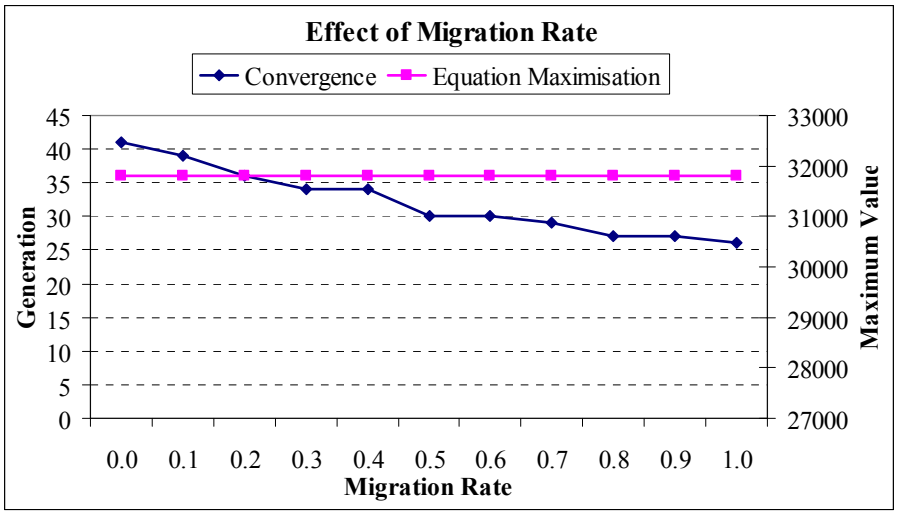

Figure 6-3: The relations between migration rate, convergence generation, and maximum value

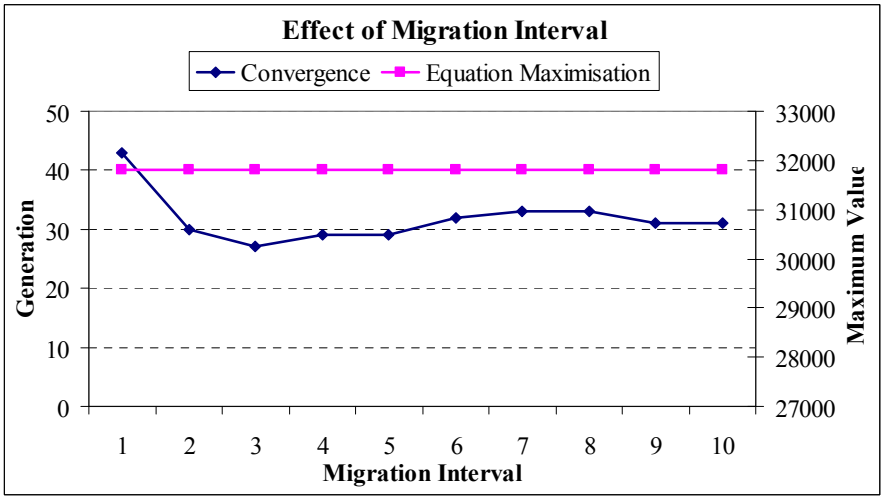

Figure 6-4: The relations between migration interval, convergence generation, and maximum value

As can be seen from Fig. 6-4, the migration interval does not have a noticeable effect on the convergence to the optimum solution. The migration interval of 1 gives the slowest convergence to the optimum solution, whereas the quickest convergence occurred with the migration interval of 3. Despite having a consistent maximum value for the function, there is some fluctuation in the average generation as the migration interval changes.

6.2.4 Population size

To find the effect of population size on the convergence of the problem, a set of population sizes ranging between 10 and 50, in increments of 10, are selected for the test. Fig. 6-5 shows that an increase in the population size increases the maximum value of the function. However, the increase in population size also results in an increase in computation time since the number of generations required to converge to the optimum solution is increased.

6.2.5 Population group

Another aspect of DGA assessment is the possession of more than one population group. In this stage of testing, a set of population groups are chosen to investigate the influence of the number of population group on the quality of the algorithm. For this purpose, a range between 1 and 5 is chosen as the population group and the convergence to the optimum solution as well as the maximum value of the function are computed for each group. After that, the relations of the population group with the average of generations and the function value are constructed (Fig. 6-6).

The results show that an increase in the number of population groups leads to a more rapid convergence to the optimum solution. On the other hand, it decreases the number of generations which makes for a quicker convergence.

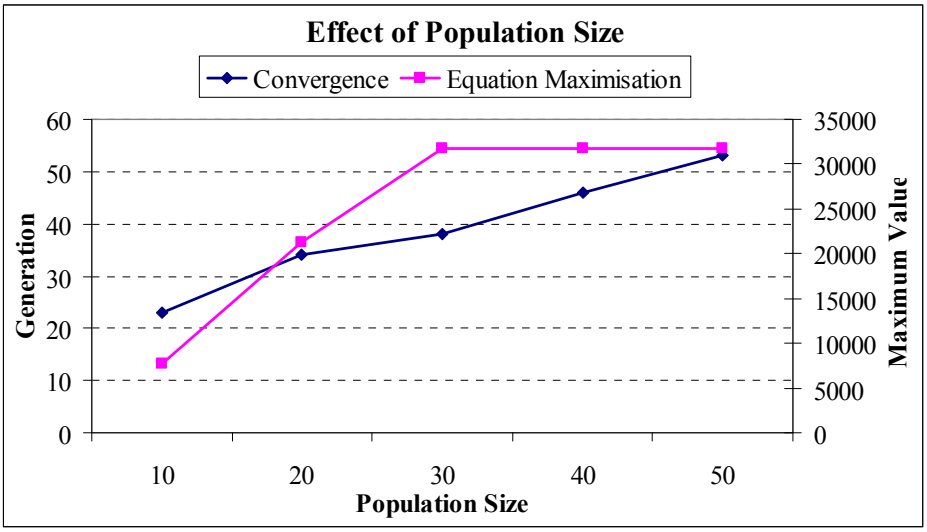

Figure 6-5: The relations between population size, convergence generation, and maximum value

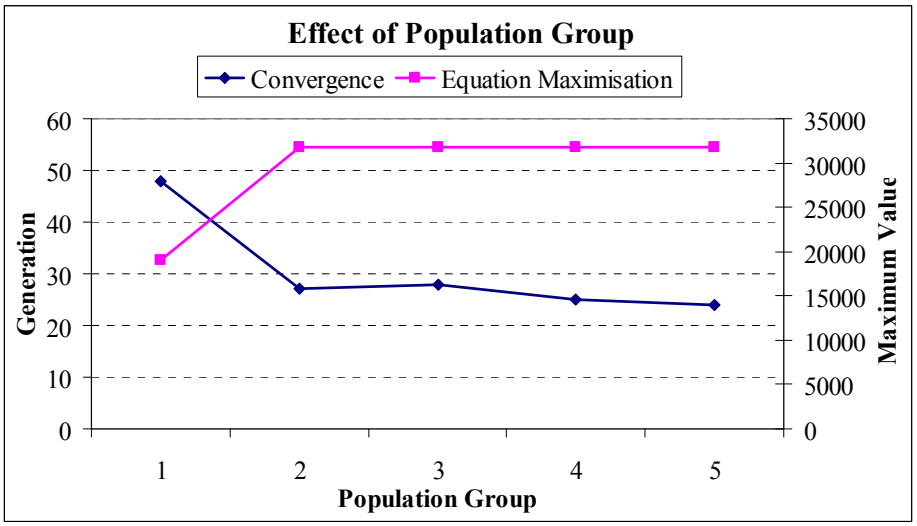

Figure 6-6: Relations between population group, convergence generation, and maximum value

6.2.6 Elitism

Theoretically, the potential effect of the elitism strategy in GA is considerable. It assures keeping the best individuals, in spite of the fact that the genetic operators are likely to change the characteristics of all individuals. In order to investigate the effects of elitism on convergence to the optimum solution, a set of elitism rates are chosen ranging between 0.1 and 1.0 by an increment of 0.1. Then the relations of the elite rate with the average generation and the maximum values are plotted (Fig. 6-7).

It can be seen that elitism does not have a huge impact on the convergence of the design problem to the optimum solution, but it keeps the design solution consistent for all runs of DO-DGA. Although the highest elite rate presents a quicker convergence to the optimum solution, there is no indication that an increase in the elite rate results in faster convergence. However, elitism demonstrates its ability to preserve the best individuals and secure their existence in the following generations.

6.2.7 Crossover

Crossover is the main operator in GA which should necessarily be implemented in the algorithm. It is decided to implement a set of crossover probabilities between the range of 0.1 and 1.0. After each operation, the average values are calculated, and

relations of the crossover probability with the generation and the maximum value are presented in Fig. 6-8.

The results indicate that the crossover probability does not have much impact on convergence speed, nor does it keep the solution consistent, as there is a fluctuation in the function value over the various crossover probabilities.

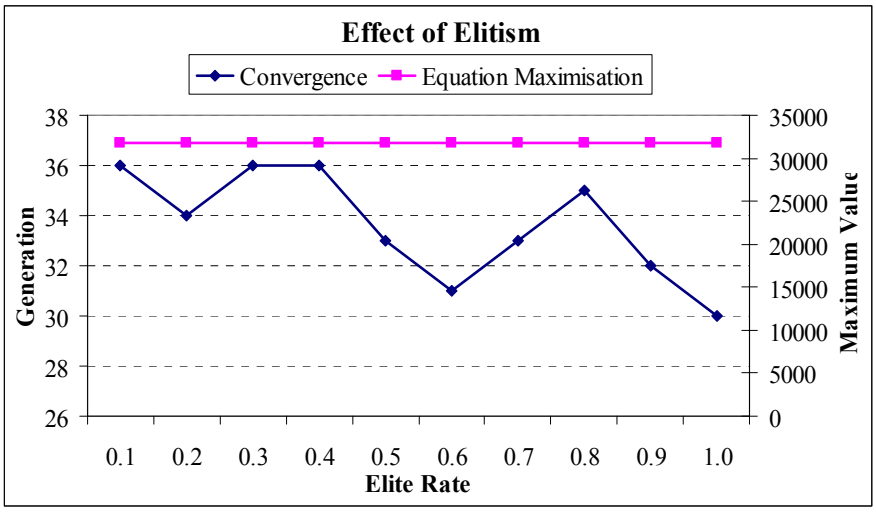

Figure 6-7: The relations between elite rate, convergence generation, and maximum value

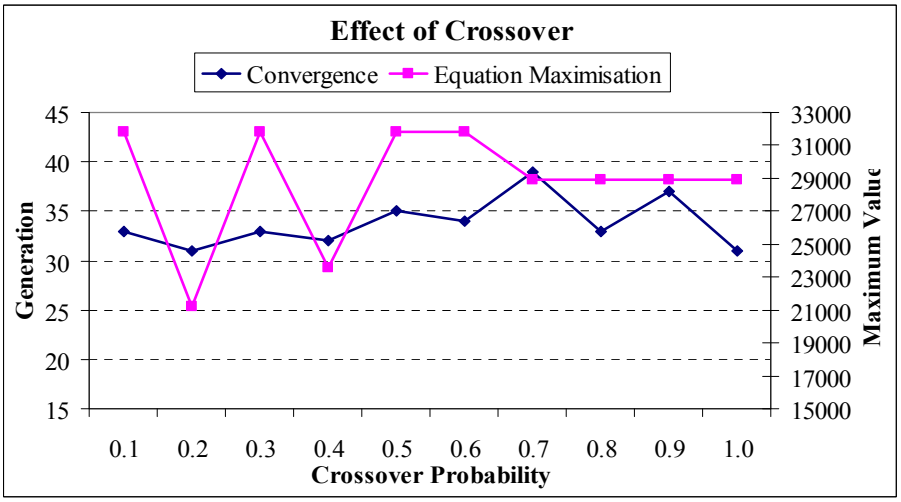

Figure 6-8: The relations between crossover probability, convergence generation, and maximum value

6.2.8 Mutation

Fig. 6-9 demonstrates the effect of the developed mutation schemes on the convergence to the optimum solution. In the test with the linear mutation scheme, the DO-DGA is run ten times, whilst the maximum mutation probability is set to 0.1 and the minimum to 0.0005. The linear mutation makes it possible to reach the equation problem to optimum solution consistently for all the ten runs. In the worst case convergence takes place after 38 generations.

In the test with the quadratic mutation scheme, convergence to the optimum solution occurs after 48 generations in the worst case. The obtained optimum solutions are consistent for all the ten runs of the algorithm.

The exponential mutation scheme yields consistent values for the objective function among all ten runs of the algorithm. In the worst case, it allows the problem to converge to the optimum solution after 27 generations.

Making a comparison between the three mutation schemes, it can be concluded that the exponential mutation scheme reaches the optimum solution quicker than the other two schemes. In this sense, the linear mutation outperforms the quadratic mutation. Having said that, all of them are approximately equally powerful tools for keeping the design solution consistent for as many runs as DO-DGA performs.

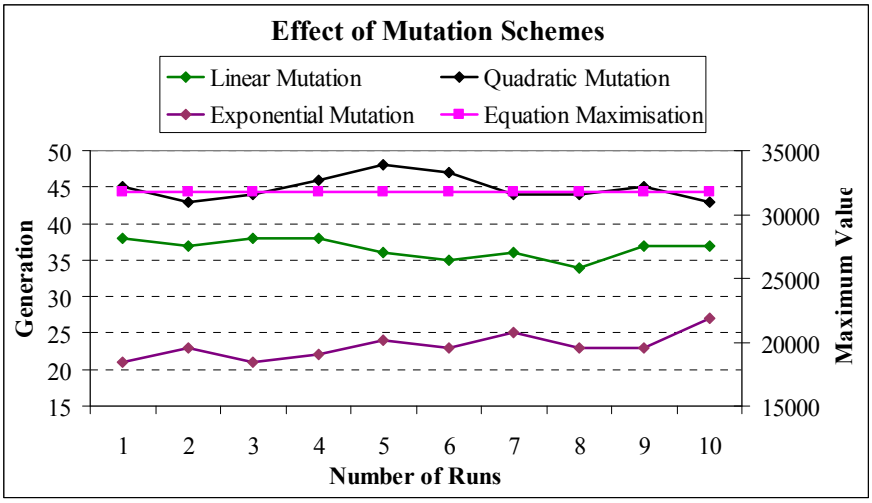

Figure 6-9: The relations between mutation probabilities, convergence generation, and maximum value

6.3 DGA validation

In this section, the developed algorithm is examined by comparing typical examples with the results obtained in the published literature. In the selection of literature, different steel frameworks are included as well as different methods of optimisation.

Preliminary results show that the exponential mutation scheme exhibits quicker convergence to the optimum solution while gaining the same results as the other schemes. Therefore, in validating the algorithms, the modified DGA will adopt the exponential mutation scheme.

6.3.1 Single-bay single-storey portal frame

Gutkowski *et al.* (2000) investigated the design optimisation of a simple SPF according to EC3. The objective function was weight minimisation, and the relevant parameters are as follows: The frame was subjected to a sum of working permanent and variable loads of 12.5kN/m on the beam and a working wind load of 12kN applied at the left top of the frame. The frame had a span of 7.5m and a height of 4.5m (Fig. 6-10). The maximum lateral displacement is 20mm and vertical displacement was 30mm whereas DO-DGA considers maximum lateral and vertical displacements as 15mm (h/300) and 21 mm (l/360). The steel grade is S275 and the beam flange is considered as fully restrained on one test, and free to rotate on the other test; the beam is partially restrained only at supports only. Gutkowski *et al* used HEB European sections for both columns and beam groups.

Initially the trials are made to specify the best value of genetic parameters with running the algorithm only, and the following parameters seemed to give the best convergence to optimum solution:

Number of population = 26
Maximum number of generations = 100
Number of population groups = 2
Probability of twin breeding = 0.40
Crossover probability = 0.85
Minimum mutation probability = 0.0005

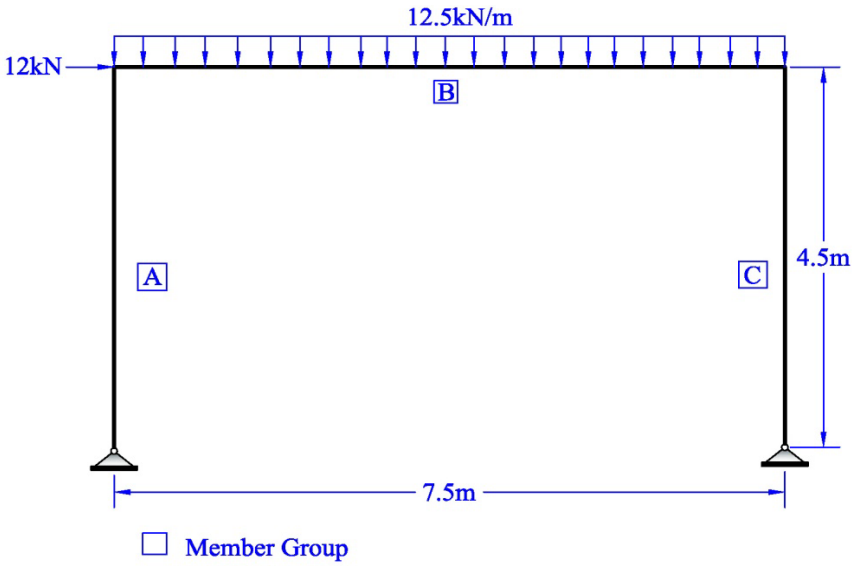

Figure 6-10: Single-bay single-storey steel frame designed by Gutkowski et al. (2000)

Maximum mutation probability = 0.40

Percentage of elite = 0.30

Migration rate = 0.30

Migration interval = 3 Generations

The cross-section of each frame member is considered as a design variable, which results in the optimisation problem having a total of three design variables. The optimum design is controlled by the lateral displacement due to the lateral applied wind load to the frame. In the case of fully restrained beam, the displacement ratio reached the absolute upper limit, which is 1.00. The design of left hand side column is controlled by the combined axial and bending compression, whereas the right hand side is controlled by the lateral torsional buckling due to a large moment produced by the lateral applied load. Since the beam was fully restrained, the design control is the bending moment with axial force effect (according to EC3).

The lateral displacement ratio of the frame reached to a value of 0.95 due to the assumption that the beam was restrained at supports only. The design solution converged after 44 generations for the full restrained beam and 39 for the restrained at supports. Table 6-2 and 6-3 shows more details of results.

Comparing the results to the ones obtained by Gutkowski *et al.* (2000), it indicates that DO-DGA yields a remarkable 27% reduction in weight of the steel frame in the case of a fully-restrained beam, and a reduction of 19% with a restrained beam at its ends. In each case, displacement reached the upper limit. Thus the fully restrained beam yields smaller section than the partially restrained one. The statistical analysis shows that the calculated mean value is quite close to the minimum weight of the frame for both fully- and partially-restrained steel frames. Also, the frequency of the minimum weight is higher than the frequency of the other obtained weight, which is expressed as the mode value.

Table 6-1: The optimum solution obtained by DO-DGA and Gutkowski et al. (2000)

Beam Status	**Column 1, UC**	**Column 2 , UC**	**Beam, UB**	**Weight , kg**	**Weight by Gutkowski *et al.* (2000)**
Fully restrained	203x203x60	254x254x73	406x140x46	943.9	1285.1 kg
Partially restrained	203x203x46	254x254x73	457x191x67	1039.7	

Table 6-2: Statistical analysis of the results

Case	**Mean**	**Mode**	**Variance**	**Standard Deviation**
Fully Restrained	950.33	943.95	51.35	7.17
Partially Restrained	1050.27	1039.65	187.97	13.71

6.3.2 Single-bay single-storey steel frame

Saka (2009) implemented Harmony Search Algorithm (HSA) to investigate the optimum design of a simple steel portal frame with a span of 5m and height of 4m. The frame experienced a factored uniform gravity load of 50kN/m and a factored concentrated load of 100kN which acts at the top of the frame, as shown in Fig. 6-11. The frame's members were grouped into two different design variables: one for both

columns (A) and one for the beam (B). The constraints are set to follow the limitations of the BS 5950.

With the same design variables, dimensions, and the loading system the frame is redesigned by DO-DGA according to both BS 5950 and EC3 cods of practice. The steel grade is consistently used as S275. Once again, a number of trials are carried out to find the best suited values of the genetic parameters for the design problems, and the decision is made to use the following values:

Number of population = 20
Maximum number of generations = 100
Number of population groups = 2
Probability of twin breeding = 0.40
Crossover probability = 0.85
Minimum mutation probability = 0.0005
Maximum mutation probability = 0.80
Percentage of elite = 0.30
Migration rate = 0.30
Migration interval = 3 Generations

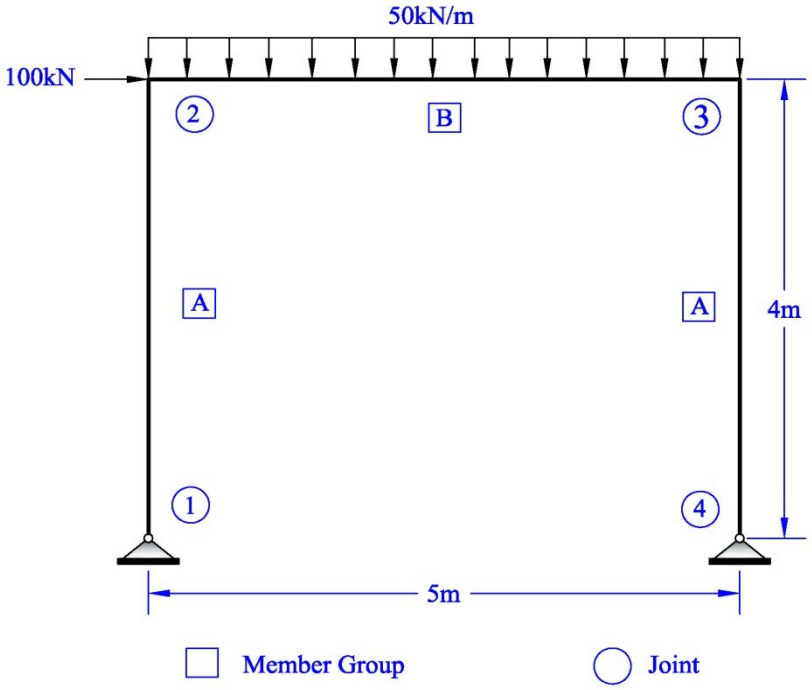

Figure 6-11: Single-bay single-storey steel frame designed by Saka (2009)

Table 6-3 proves the suitability of using DO-DGA while considering the limitations imposed by BS 5950.

Table 6-3: The optimum solutions obtained by DO-DGA and Saka (2009)

Literatures	**Columns A**	**Beam B**	**Weight, kg**
DO-DGA, BS 5950	254x254x73 UC	457x191x67 UB	920.30
DO-DGA, EC3	254x254x73 UC	457x191x67 UB	920.30
Saka (2008)	254x254x89 UC	406x140x46 UB	941.20

The strength ratio of the right hand side column nearly reached its maximum value, which is 0.98. The maximum strength ratio of the beam reached a value of 0.63, which is due to the interaction of the axial force and bending moment. As the beam is assumed to be fully restrained, there is no failure due to lateral torsional buckling. Lateral displacement reached to its upper limit, with a displacement ratio of 1.00. Neither vertical displacement nor vertical deflection reached to their upper limit.

The frame is redesigned by DO-DGA, this time considering the limitations given by EC3. The same genetic parameters and the steel grade as the previous design optimisation are used. The results show that the design considering EC3 limitation does not exhibit different results than the BS 5950 limitations, and yields the same weight. This owes to the control of displacement over design since displacement calculation needs to consider the working loads.

6.3.3 Pitched roof steel portal frame

Implementing the GA, Saka (2003) conducted the design optimisation on steel portal frames considering the limitations imposed by BS 5950. The frame he used had a span of 20m with a column height of 5m, and apex height of 6.5m. A number of 10kN concentrated loads were applied on the rafter, generating from purlins which were laid at a horizontal distance of 1.25m centre to centre (Fig. 6-12). The columns were provided with three lateral bracings to make smaller effective length against buckling. Saka (2003) considered four design variables which were the cross-sections of column and rafter, length of the haunch, and depth of haunch. The depth of the haunch was selected from a set that varied from 100mm to 740mm with an

increment of 20mm. The haunch length was assumed to vary from 500mm to 5000mm in increments of 250mm. Saka considered only 64 out of 80 cross-sections available in the steel catalogue. This is to be rounded to a binary order of 2^6 (=64). He subdivided the frame member elements into a number of smaller elements to deal easier with the applied point loads. Nevertheless, this significantly increases the total degree of freedom to be solved, hence much more computation time would be required. Saka used the stiffness matrix developed by Matheson *et al*. (1959; cited in Saka, 2003) to form the stiffness matrix for the haunched part of the rafter (non-prismatic member).

In this work, the frame is designed by DO-DGA according to both BS 5950 and EC3. Furthermore, the frame is not subdivided into smaller element as it was by Saka (2003). Instead, there will be only six elements for the structural analysis and constraints check: two for columns, two for haunched rafter; and two for the rest of rafters. All eighty universal beam cross-sections available in the steel catalogue are involved in the design optimisation. Furthermore, the developed stiffness matrix is used to form the stiffness matrix of the haunched element (Eq. 2-29 and Eq. 2-30). The steel grade is S275.

The following genetic parameters are used due to their suitability for this particular problem:

Number of population = 36
Maximum number of generations = 100
Number of population groups = 2
Probability of twin breeding = 0.40
Crossover probability = 0.85
Minimum mutation probability = 0.001
Maximum mutation probability = 0.15
Percentage of elite = 0.30
Migration rate = 0.30
Migration interval = 3 Generations

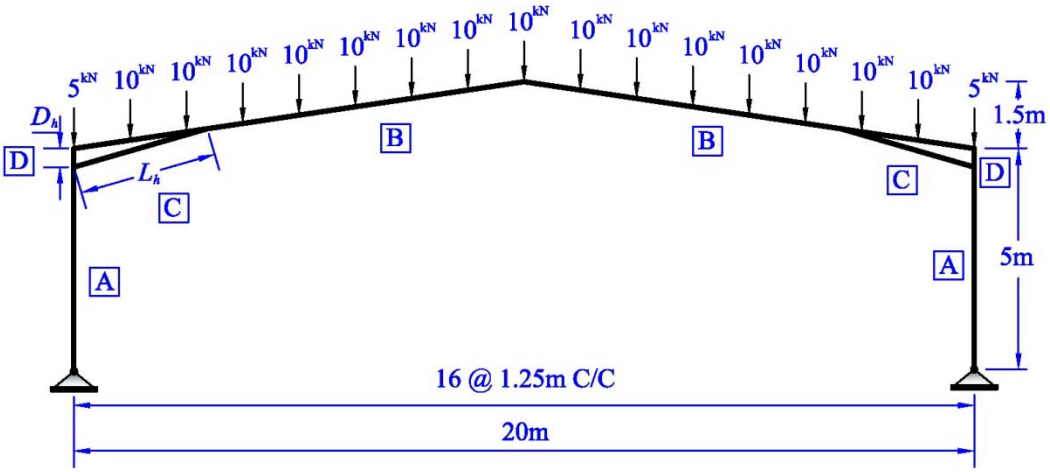

Figure 6-12: The pitched-roof steel portal frame used by Saka (2003)

Table 6-4: Optimum solutions obtained by DO-DGA and Saka (2003)

Literature	Column, UB	Rafter, UB	Haunch length	Haunch depth	Weight, kg
Saka (2003)	6103x229x101	356x127x33	1.50m	0.42m	2260.0
DO-DGA, BS5950	533x210x82	457x152x60	1.75m	0.47m	2138.0
DO-DGA, EC3	533x210x82	457x152x52	1.95m	0.85m	2028.2

Looking at the results (Table 6-4), it can be seen that the optimum design obtained by DO-DGA is lighter than that of Saka (2003) by 5% (which done according to BS 5950), and by 10% (which done according to EC3). Both displacement and strength reached their absolute upper limits, with ratios of 1.00. Due to the large moment, particularly at the connections of column and rafter, the strength is controlled by the combined axial and bending compression, whilst the displacement is controlled by the vertical displacement of the apex. The design optimisation according to EC3 results in longer and deeper haunches. The convergence happened after 37 and 40 generations to the optimum solution for design optimisation to BS 5950 and EC3 respectively.

6.3.4 Two-bay three-storey frame

Using GA, Pezeshk *et al.* (2000) studied the weight optimisation of two-bay three-storey frame according to American codes of practice known as AISC-LRFD. All the

loadings and dimension details of the frame are shown in Fig. 6-13. The frame was previously designed by Hall *et al.* (1989).

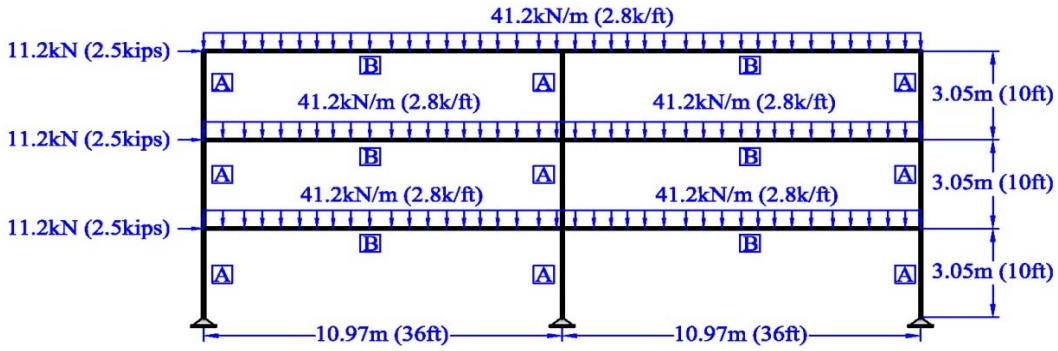

Figure 6-13: Two-bay two-storey steel frame designed by Pezeshk et al. (2000)

According to Pezeshk *et al.* (2000), the frame has two groups of design variables: all columns are assigned as group A and beams as group B. The columns do not have lateral bracing and the beams are only restrained at the connection to columns. To redesign the frame, DO-DGA keeps the same design variables. Initially the trials were made to specify the suitable values for the genetic parameters by running only the developed algorithm. After a number of trials, the following parameters seemed to give the best convergence to optimum solution:

Number of population = 30
Maximum number of generation = 100
Number of population groups = 2
Probability of twin breeding = 0.40
Crossover probability = 0.85
Minimum mutation probability = 0.0005
Maximum mutation probability = 0.30
Percentage of elite = 0.30
Migration rate = 0.30
Migration interval = 3 Generations

The frame is redesigned according to the EC3 limitations with the steel grade of S275, and the results are shown in Table 6-5. The DO-DGA is run ten times and all the runs yielded the same results. The frame is controlled by the strength while the displacement ratio is 0.60. The beams were controlled by the lateral torsional

buckling as they are only restrained at the ends and there are no intermediate restraints. Whereas the columns are controlled by the combined axial compressive and bending stresses, and reached to a ratio of 0.89. The strength ratio of beams was 0.94.

Table 6-5: The optimum design obtained by DO-DGA and the literature

Literature	**Columns A**	**Beams B**	**Weight, kg**	**Weight Saving**
DO-DGA	254x254x73 UC	610x229x101 UB	8345.2	-
Pezeshk *et al.* (2000)	W10×60	W24×62	8523.9	2.1%
Hall *et al.* (1989)	W10×60	W24×62	8523.9	2.1%

The consistency of the ten runs by the DO-DGA is remarkable. All runs give the same solution for the design problem. An outstanding convergence takes place with DO-DGA as the optimum solution was obtained after only 25 generations. The results obtained by Pezeshk *et al*. (2000) reveal that the weight has an average value of 10004.4kg among 30 runs of the algorithm. In addition, the weight with the highest frequency (13/30 or 43%) is 9111.8kg. On the other hand, the minimum weight had only 6 frequencies which constitute 20% of the runs. The minimum obtained weight by DO-DGA is consistent and has a 100% frequency among runs. The variance and standard deviation of results obtained by Pezeshk *et al*. (2000) are 33931589 and 5825.083 respectively, whereas in the test results obtained by DO-DGA these values are zero.

6.3.5 Two-bay three-storey frame

Foley & Schinler (2003) used a conventional GA to study the design optimisation of a steel frame with semi-rigid connections. The structure is a two-bay three-storey plane frame with equal bays spanning 6.10m and storey height of 3.66m (Fig. 6-14). The framed was designed according to the AISC-LRFD. The first and second floor beams were subjected to a uniform factored dead load of 17.52kN/m and uniform factored live load of 20.44kN/m, whereas a uniform factored dead load of 10.51kN/m and a uniform factored live load of 20.44kN/m were applied to the top

floor beams. The frame experienced a uniform lateral factored wind load of 9.84kN/m along the total height of the frame at the left hand side.

The frame is redesigned implementing the modified DGA. The well known Frye-Morris model is adopted to compute the initial stiffness of the semi-rigid connection.

Overall, there are seven design variables assigned A to G as shown in Fig. 6-13. The initial trials found the following genetic parameters suitable for this particular steel frame:

Number of population = 34
Maximum number of generations = 100
Number of population groups = 2
Probability of twin breeding = 0.40
Crossover probability = 0.85
Minimum mutation probability = 0.001
Maximum mutation probability = 0.40
Percentage of elite = 0.30
Migration rate = 0.30
Migration interval = 3 Generations

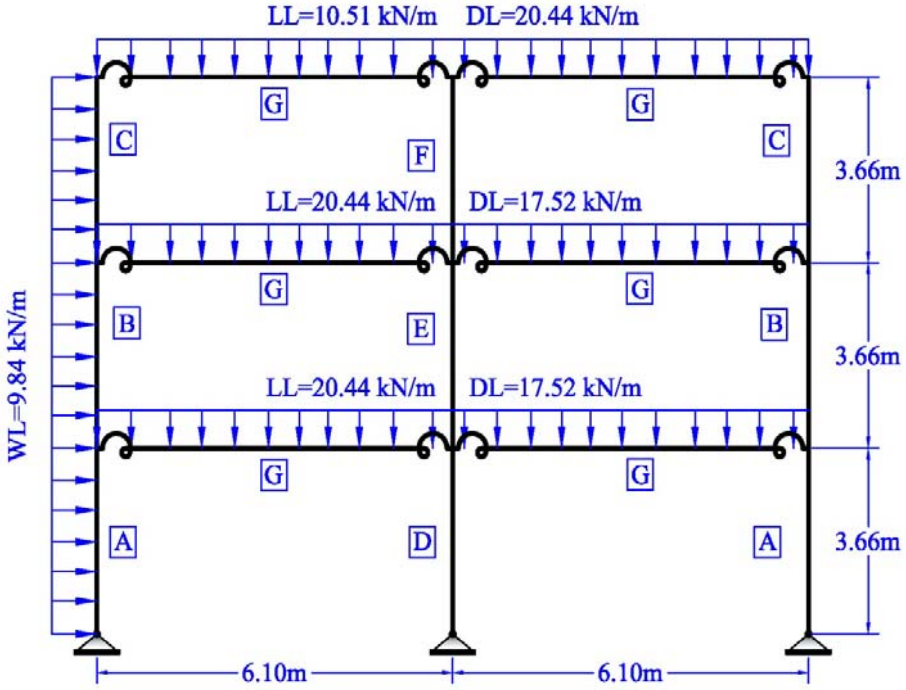

Figure 6-14: Two-bay three-storey steel frame designed by Foley & Schinler (2003)

The results are shown in Table 6-6 making comparison between the literature and DO-DGA results.

The optimum solution is the same as obtained by Foley and Schinler (2003). Despite of the lateral applied force, the design is hardly affected by the lateral displacement, and rather is controlled by the stress limitation. The maximum strength ratio is 0.96 in columns C and D. The strength ratio for beams is 0.94. Except for column F which is controlled by the lateral torsional buckling, the frame members were controlled by combined axial compressive and bending stresses. The maximum lateral displacement occurred at the third floor. The optimum solution was achieved after 70 generations, which was mainly due to the large number of variables.

Table 6-6: Optimum solutions by DO-DGA and Foley & Schinler (2003)

	DO-DGA	**Foley and Schinler (2003)**
Column A	203x203x46 UC	W310x60
Column B	203x203x46 UC	W250x58
Column C	152x152x23 UC	W250x58
Column D	254x254x73 UC	W360x64
Column E	254x254x73 UC	W250x58
Column F	152x152x23 UC	W200x52
Beam G	356x127x39 UB	W410x46
Weight, kg	2891.9	2930.7

6.3.6 One-bay ten-storey frame

Camp *et al.* (2005) applied the ant colony method to minimise the weight of a one-bay ten-storey frame. The span of the frame is 9.14m (30ft) and the first storey has a height of 4.57m (15ft) with a 3.66m (12ft) height for the rest of the storeys. As shown in Fig. 6-15, the frame beams experience factored uniform loads of 88.2kN/m (6k/ft) while factored concentrated loads of 44.8kN (10kips) act on top of each storey. Using the available AISC W-shapes steel section in the catalogue, the frame was designed to AISC-LRFD.

Camp *et al.* (2005) grouped the frame into nine design variables, A to I as shown in Fig. 6-14. In this study, the same groups of members as design variables are used for the purpose of weight minimisation. A number of trials are carried out to assign the genetic operators and the following values are found suitable to this particular problem:

Number of population = 50
Maximum number of generations = 150
Number of population groups = 2
Probability of twin breeding = 0.40
Crossover probability = 0.85
Minimum mutation probability = 0.0005
Maximum mutation probability = 0.65
Percentage of elite = 0.30
Migration rate = 0.30
Migration interval = 3 Generations

To redesign the frame with DO-DGA, a steel grade of S275 is used and the design is conducted according to the BS 5950 limitations. The compression flanges of the beams are assumed fully restrained against lateral torsional buckling. The results of the optimum design are compared with that of Camp *et al*. (2005). Table 6-7 shows the details of the optimum design.

The DO-DGA saves 12% of weight compared to the design using ant colony optimization. This is because the obtained results by DO-DGA nearly fully-stressed all members, and the displacements reached their upper limit. All the strength ratios were above the 0.93 except beam G which was 0.82. The maximum strength ratio is 0.97 for column A and beam H. In addition, beam H was controlled by the bending moment limitation, whereas the rest of members were controlled by the combined axial and bending stresses. The maximum lateral displacement took place at third storey with a ratio of 0.76. The convergence to the optimum solution occurred after 100 generations.

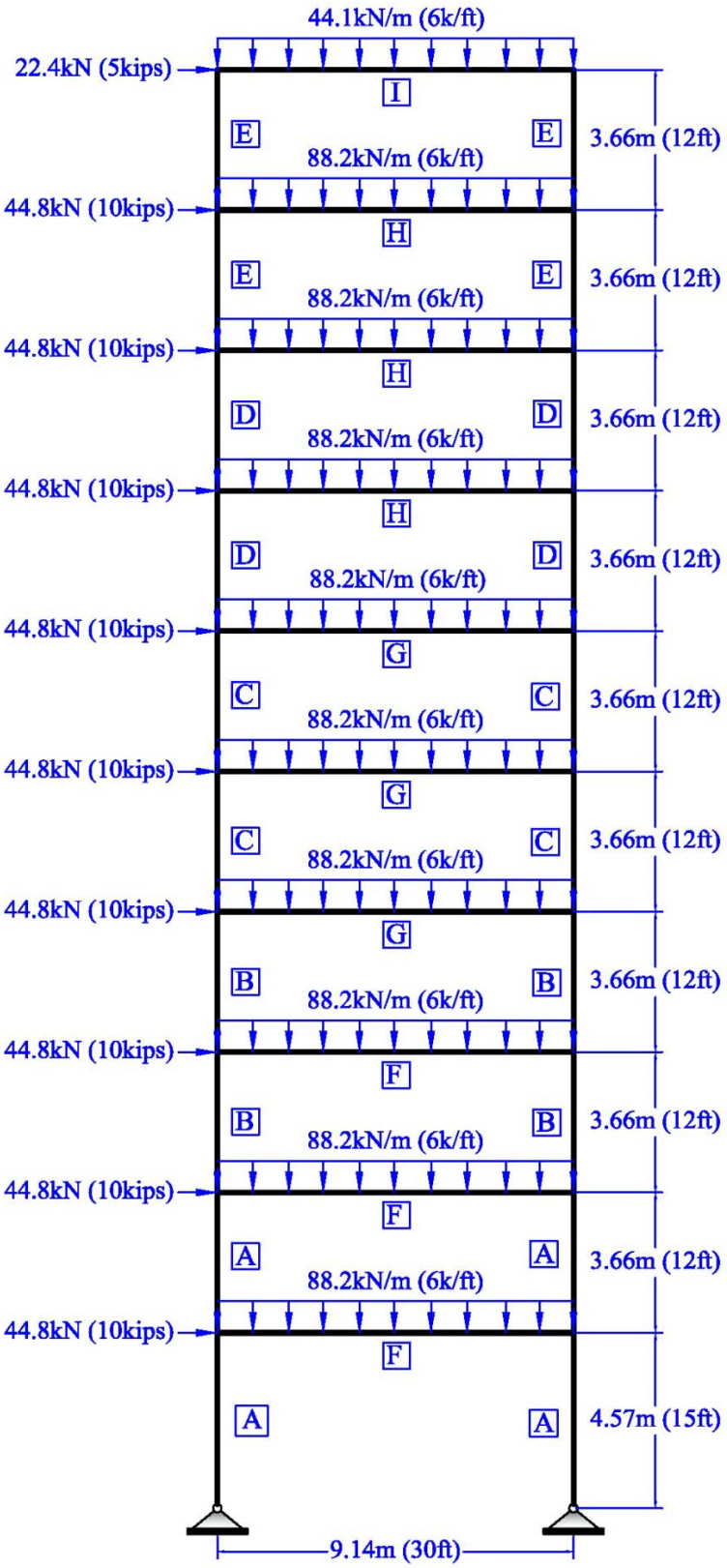

Figure 6-15: One-bay ten-storey frame designed by Camp *et al*. (2005)

Table 6-7: The optimum solutions obtained by DO-DGA and Camp *et al*. (2005)

Element group	**DO-DGA**	**Camp *et al*. (2005)**
Column A	356x406x287 UC	W14x233
Column B	356x406x235 UC	W14x176
Column C	356x368x177 UC	W14x145
Column D	356x368x129 UC	W14x99
Column E	254x254x107 UC	W12x65
Beam F	762x267x134 UB	W30x108
Beam G	762x267x134 UB	W30x90
Beam H	610x229x101 UB	W27x84
Beam I	457x191x74 UB	W21x44
Weight, kg	24928.5	28399.4

6.3.7 Two-bay six-storey frame

Saka (2007) investigated the application of the HSA method to minimise the weight of a two-bay six-storey frame. The dimensions and length of steel frame's members are shown in Fig. 6-16. Saka (2007) categorised the structural elements into six groups of steel cross-sections from A to F.

The beams of the frame were loaded by a factored gravity load of 50kN/m while the whole frame experienced a number of horizontal concentrated loads with the value of 25kN that acted at the top of each storey representing the equivalent static seismic forces. He imposed the limitations according to BS 5950 to accomplish the weight minimisation design of the frame.

The frame is redesigned by DO-DGA with the same number of design variables. The steel grade applied is S275 and the design imitated the limitation imposed by BS 5950. The results of the design solution are presented in Table 6-8. After several trials, DO-DGA uses the following genetic parameters to redesign the steel frame:

Number of population = 50
Maximum number of generations = 150
Number of population groups = 2

Probability of twin breeding = 0.40

Crossover probability = 0.85

Minimum mutation probability = 0.0005

Maximum mutation probability = 0.40

Percentage of elite = 0.30

Migration rate = 0.30

Migration interval = 3 Generations

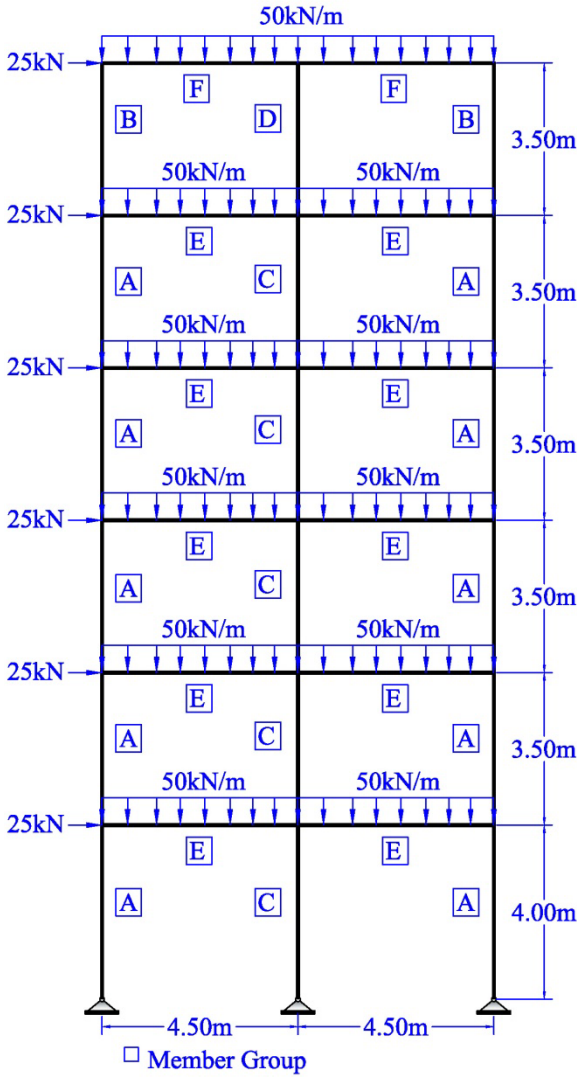

Figure 6-16: Two-bay six-storey steel frame designed by Saka (2007)

Table 6-8: The optimum solutions obtained by DO-DGA and Saka (2007)

Element Group	**DO-DGA**	**Saka (2007) GA**	**Saka (2007) HSA**
Column A, UC	305x305x97	203x203x71	203x203x60
Column B, UC	152x152x23	203x203x46	152x152x30
Column C, UC	305x305x97	356x368x129	356x368x129
Column D, UC	152x152x23	203x203x46	152x152x30
Beam E, UB	457x152x52	457x152x52	457x191x67
Beam F, UB	305x102x33	356x171x45	305x102x33
Weight, kg	8122	8121	8112

The results show that the optimum design obtained by DO-DGA is heavier by 1% than that of Saka (2007) using HAS. However, the optimum solution is the same as that found by GA. Convergence took place after 76 generations. Overall, the design was controlled by the lateral displacement as the displacement ratio reached to its absolute value which is 1.00. The intermediate column and the right bay beam of the first floor had almost the largest strength ratios. Due to the fully restrained beams, the strength of the steel frame was not controlled by lateral torsional buckling. Instead, a combined compressive axial and bending stresses dominated over the solution. The right hand side columns and left hand side beams had the larger values of the strength limits. The maximum strength ratios among the columns and the beam reached 0.96 and 0.93 respectively.

On the other hand, if the group of columns are so rearranged that the first three stories have side columns A, intermediate columns C and the beams E, and the second three stories have side columns B, intermediate columns D, and the beams F, then there will be a remarkable saving in weight of the steel frame, as shown in Table 6-9.

Table 6-9: The optimum solution by rearranging the member's groups of two-bay six-storey steel frame designed by Saka (2007)

Element Group	**DO-DGA**
Column A, UC	203x203x52
Column B, UC	152x152x30
Column C, UC	356x368x153
Column D, UC	203x203x46
Beam E, UB	457x152x60
Beam F, UB	356x127x33
Weight, kg	6448

Rearranging the members of groups results in a saving of 21% weight of the steel frame.

6.4 Summary

The results of weight minimisation generated from the developed program, DO-DGA, were compared to ones obtained from other work published in the literature. An attempt was made to use different types of frames with different characteristics and behaviour as well as different optimisation techniques. A comparison was also made considering the semi-rigid connections for steel frames. The results obtained reveal that DO-DGA can handle all types of plane steel frame; this produced promising results. In all cases, comparing different optimisation techniques, DO-DGA yields a substantial saving in steel material. It also obtains the optimum solution within an acceptable time because of the essential modification to the genetic operators. This gives the promise of using DO-DGA in the design office. The DO-DGA can now be used to investigate the behaviour of SPFs confidentially.

Chapter 7: Statistical and Parametric Analyses

7.1 Introduction

This chapter illustrates the effect of the modified DGA on convergence to the optima for different types of SPFs, using statistical and parametric analyses. Three benchmark examples (BEs) are studied in detail, with different applied load cases, to investigate the optimum solutions of SPFs. The focus is on the use of two types of steel portal frames with different objective functions. Frames are examined with both rigid and semi-rigid connections, and comparison is made between these two types of connections in terms of reducing the weight of steel portal frames. Each frame undergoes a design optimisation according to the limitations given by both BS 5950 and EC3. The tests are grouped into: weight minimisation for rigid and semi-rigid connections, displacement maximisation, constant depth for both haunch ends with varied length, and weight minimisation of the curved rafter. Comparisons are made for all types of objective functions, and there are some parametric studies of SPFs for optimum solutions with different spans and pitch angles.

The steel grade is assumed to be S275 for all the benchmark examples. As the response of the structure against the applied loads shows, a large bending moment acts at the joint which connects the rafter to the column. It is therefore manipulated using the universal beams as steel cross-sections for columns due to a large moment applied on them. In order to involve all existing eighty cross-sections of the universal beams in the steel catalogue, a string length of seven genes is used for each design variable. This makes a range of variation equal to 2^7, i.e. 128, which runs from '0000000' to '1111111' in binary. If any value obtained for the next generation exceeds 80, then a random steel section will be selected from 1 to 80, because there are not more than 80 steel sections available in steel category. The haunch length varies between 50mm and 6400mm with an increment of 50mm, whereas the depth of the haunch varies from 10mm to 1280mm in increments of 10mm.

The frame members are not subdivided into smaller elements and the frame has only six member elements: two columns, two haunched parts of the rafter and two other rafter parts. Due to the variation in haunch length, the positions of the concentrated loads are changed. This will likely introduce movements of the point loads from the haunched part of the rafter to the adjacent part, and vice versa. DO-DGA handles this problem by defining a subroutine for the load transfer depending on the haunch length (Fig. 7-1).

The genetic parameters for all the benchmark examples are consistent as they depend very much on the size of population and design variables. The genetic parameters are assigned so that the optimum solution may be consistently obtained among a number of runs performed by DO-DGA. This is aided by assuming a higher mutation probability in the earlier stages. The following genetic parameters are used for all the benchmark examples:

Size of population = 30
Maximum number of generation = 100
Number of genes = 7
Groups of population = 2
Probability twin breeding = 0.4
Crossover probability = 0.85
Maximum mutation probability = 0.2
Minimum mutation probability = 0.001
Elite ratio = 30%
Migrated individual ratio = 30%
Migration interval = 3 generations

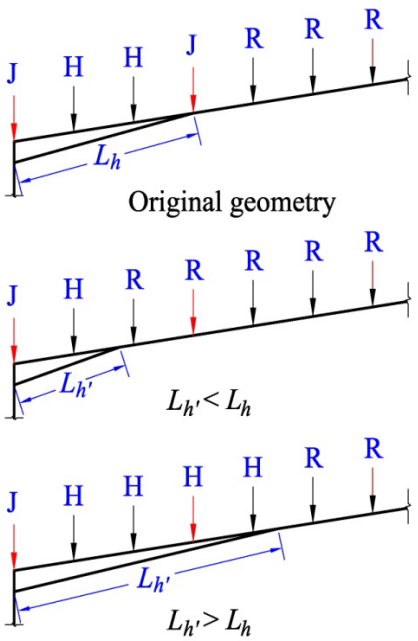

Figure 7-1: Load transfer from the haunched member to the rafter and vice versa

7.2 BE1: Pitched-roof SPF with gravity loads

The first benchmark example is a pitched-roof haunched-rafter SPF (Fig. 7-2). It has a span of 21m with the column height of 5m and a central height of 6.5m (apex). Each column of the frame is assumed to have three lateral bracings, making the column four elements of effective length against the buckling. The purlins span a 6m bay, and they are laid at equal horizontal distances of 1.05m centre to centre.

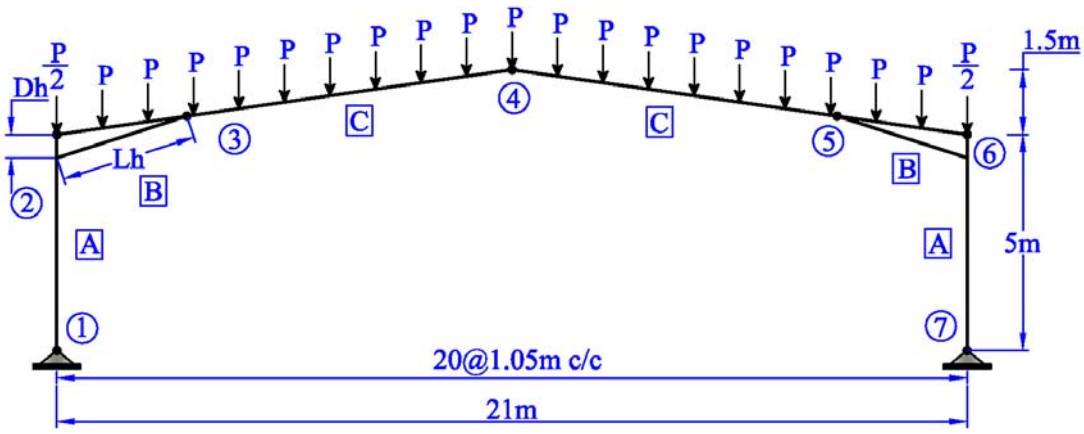

Figure 7-2: Pitched-roof SPF with gravity loads of BE1

The frame experiences a gravity load P, as shown in Fig. 7-2, generated by purlin reactions. The concentrated load, P, has been calculated to have a working dead load of 2.6kN and a working imposed load of 6.6kN. There are an overall of twenty concentrated loads acting on the frame. Four possible design variables are assumed to form the objective functions which are column cross-section, rafter cross-section, haunch length, and haunch depth. The maximum allowable lateral displacement is 16.67mm (H/300) and the maximum allowable vertical displacement is 58.33mm (L/360).

7.2.1 Weight minimisation (WM) with rigid connections for BE1

The first group of tests are conducted for the purpose of minimising the weight of the pitched-roof haunched-rafter SPF. In this group of tests, all the introduced mutation schemes are set and while considering the rigid connections, and the design is checked against BS5950 imposed limitations. The DO-DGA ran ten times for each scheme and the obtained results are collected in Table 7-1 and shown in Figs. 7-3 to 7-8 for all mutation schemes.

The three new mutation schemes are compared to constant and reverse mutation probabilities. A constant mutation value of 0.01 is adopted for all subsequent generations. A reverse mutation scheme is examined to evaluate the idea of using a varied mutation. The scheme is the reverse of the linear mutation, so that at the earlier stage the value is low and as the generations proceed its value rises.

The maximum displacement ratio is 0.89 which occurred at the apex. The maximum strength ratio reaches to its absolute upper limit of 1.00, and that is controlled by overall buckling due to the combined axial and bending stresses at the haunch. The maximum strength ratio for the column reached 0.94 due to the combined axial and bending stresses.

Fig. 7-3 and Table 7-1 indicate that using the exponential mutation makes the design problem converge on the optimum solution more quickly than the other mutation schemes. The slowest convergence takes place with quadratic mutation. Fig. 7-4 depicts that the linear mutation is efficient in obtaining more similar optimum solution among ten runs of DO-DGA. Figs. 7-5 and 7-6 show that the exponential mutation reveals best results in terms of the average weight and the standard

deviation of weights among the ten runs of DO-DGA. The reverse mutation totally fails to present the optimum solution.

Table 7-1: Weight minimisation according to BS 5950 for BE1

Mutation Schemes	**Column UB**	**Rafter UB**	**L_h, m**	**D_h, m**	**Generation**	**Weight, kg**
Linear	533x210x82	457x191x67	1.40	0.11	85	2305.49
Quadratic	533x210x82	457x191x67	1.40	0.11	91	2305.49
Exponential	533x210x82	457x191x67	1.40	0.11	45	2305.49
Constant	533x210x82	457x191x67	1.40	0.11	76	2305.49
Reverse	533x210x82	457x152x67	1.75	0.11	100	2322.66

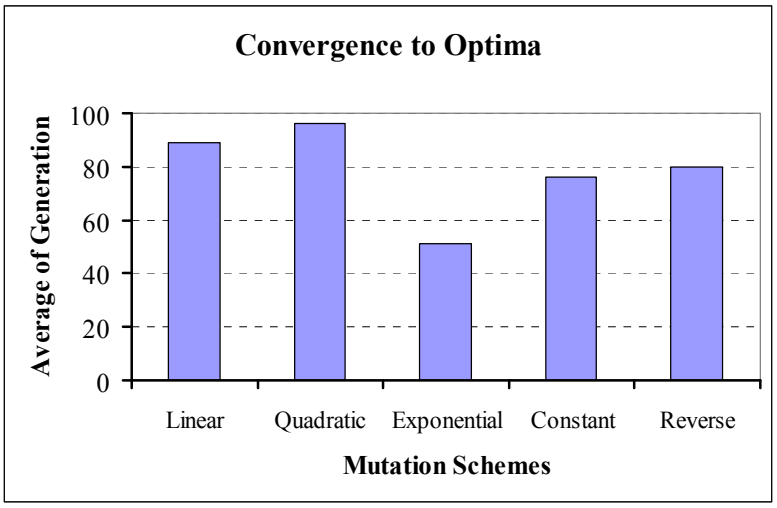

Figure 7-3: Convergence to optima of WM according to BS 5950 for BE1

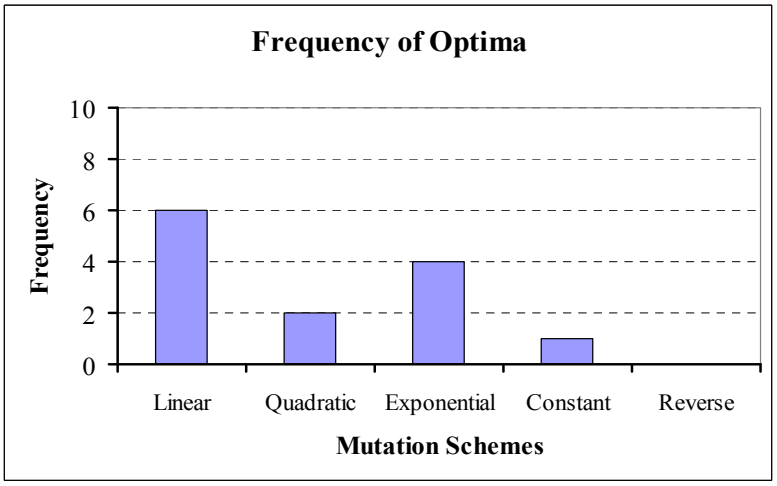

Figure 7-4: Frequency of optima of WM according to BS 5950 for BE1

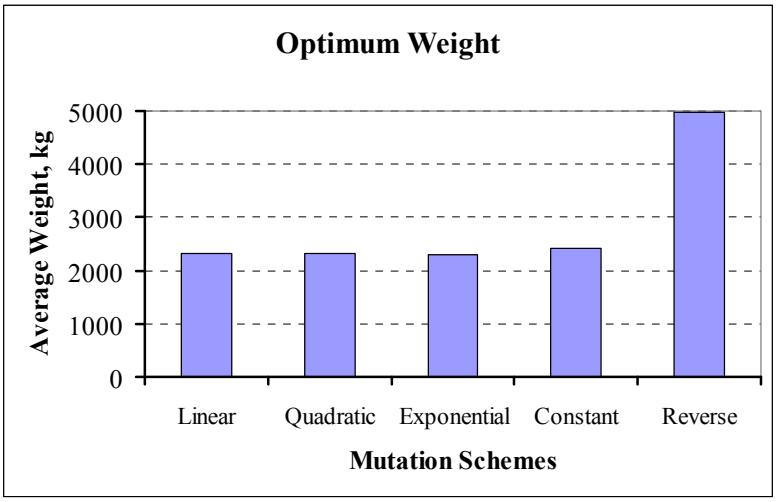

Figure 7-5: Average weight of WM according to BS 5950 for BE1

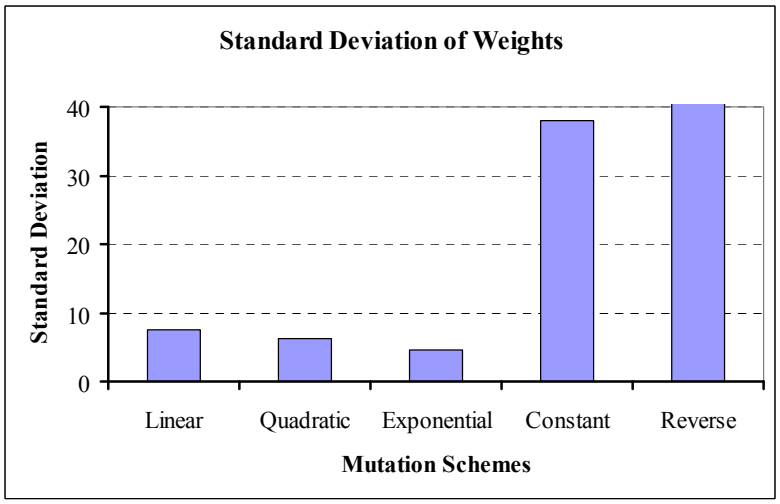

Figure 7-6: Standard deviation of weights of WM according to BS 5950 for BE1

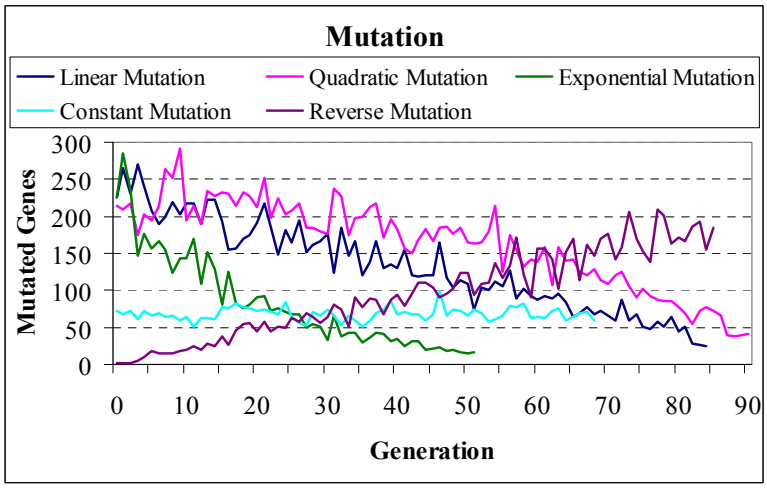

Figure 7-7: Genes mutation of WM according to BS 5950 for BE1

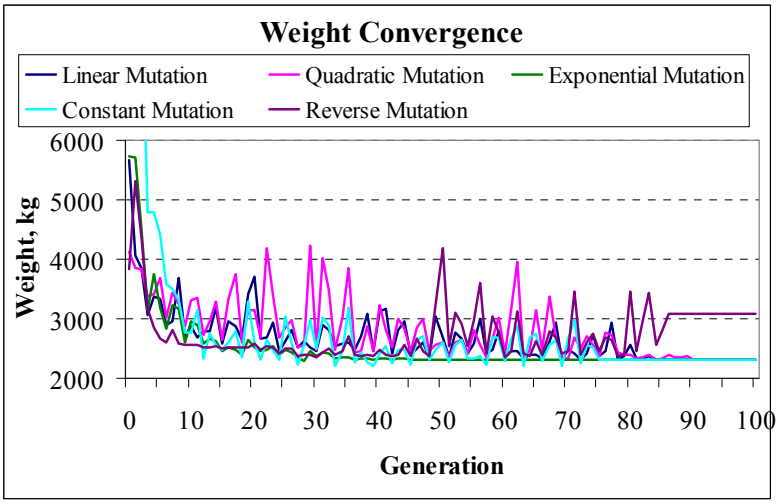

Figure 7-8: Weight convergence of WM according to BS 5950 for BE1

The same frame (BE1) undergoes design optimisation according to EC3 to minimise the weight while using different mutation schemes. The results are presented in Table 7-2 and Figs. 7-9 to 7-14.

The optimum design is controlled by the vertical displacement of the apex as it reached its upper limits and gives a strength ratio of 1.00. The highest strength ratio of the optimum solution reached 0.88, which is due to the interaction of the axial compressive force and bending moment for the haunch. The average strength ratio for the optima is 0.82, which was the highest average amongst the other optimum solutions. The heaviest frame has the highest strength ratio of 0.94 for the column, but a small strength ratio for the rafter.

Table 7-2 indicates that the solution obtained from the WM applying the exponential mutation has the least weight among the other mutation schemes. Nevertheless, it only happened once (Fig. 7-10) among the ten runs of DO-DGA. Fig. 7-9 shows that the exponential mutation enables the design problem to converge to the optimum solution faster than the other schemes. Except the reverse scheme, all other mutation schemes have almost the same average weight as shown in Fig. 7-11. The quadratic mutation has the lowest value of standard deviation of weight, as shown in Fig. 7-12, which implies that the all ten obtained results have the weight value close to each other. Once again, the reverse mutation failed to obtain the optimum solution.

Table 7-2: Weight minimisation according to EC3 for created mutation schemes

Mutation Schemes	Column UB	Rafter UB	L_h, m	D_h, m	Generation	Weight, kg
Linear	533x210x82	457x152x52	1.65	0.60	85	2032.51
Quadratic	533x210x82	457x152x52	1.65	0.60	99	2032.51
Exponential	533x210x82	457x152x52	1.60	0.58	49	2027.53
Constant	533x210x82	457x152x52	1.65	0.60	74	2032.51
Reverse	457x191x74	457x152x52	2.35	1.24	97	2086.14

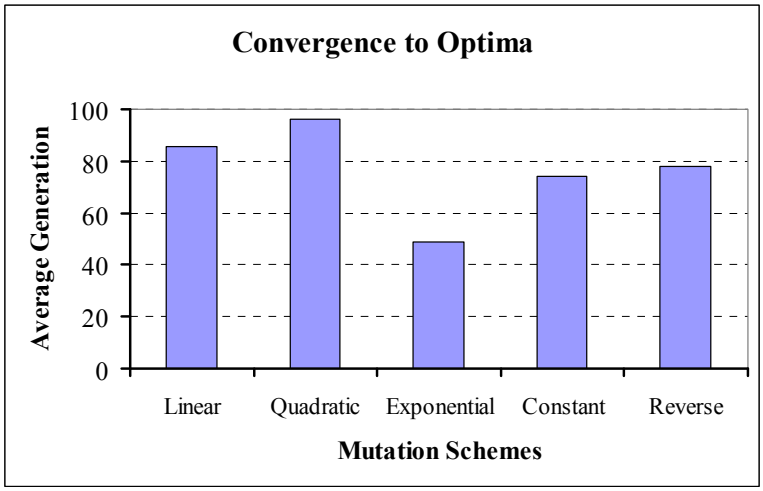

Figure 7-9: Convergence to optima of WM according to EC3 for BE1

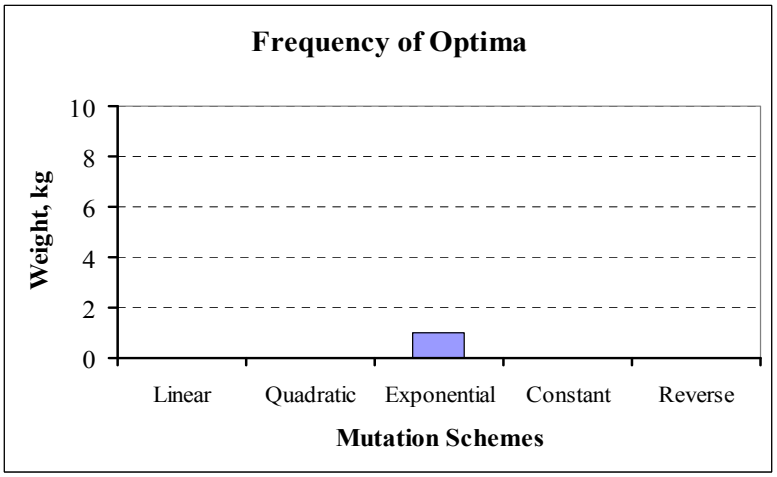

Figure 7-10: Frequency of optima of WM according to EC3 for BE1

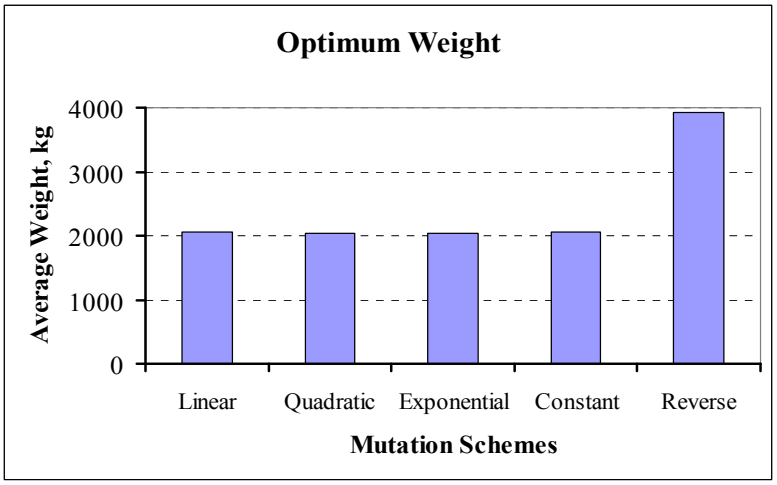

Figure 7-11: Average weight of WM according to EC3 for BE1

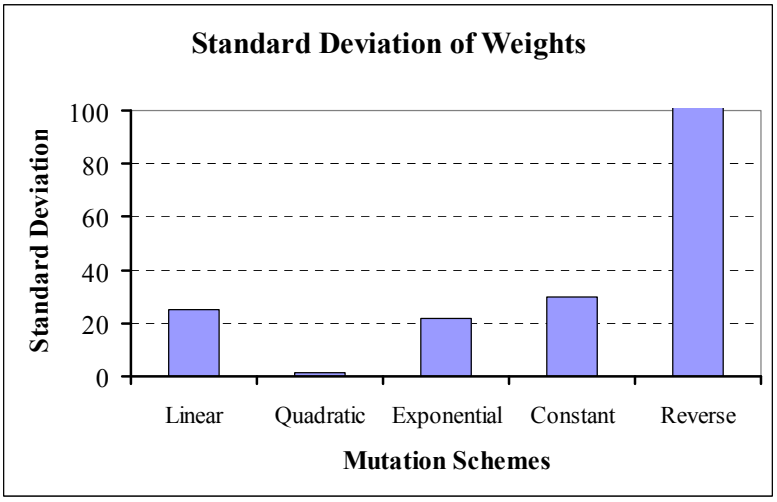

Figure 7-12: Standard deviation of weights of WM according to EC3 for BE1

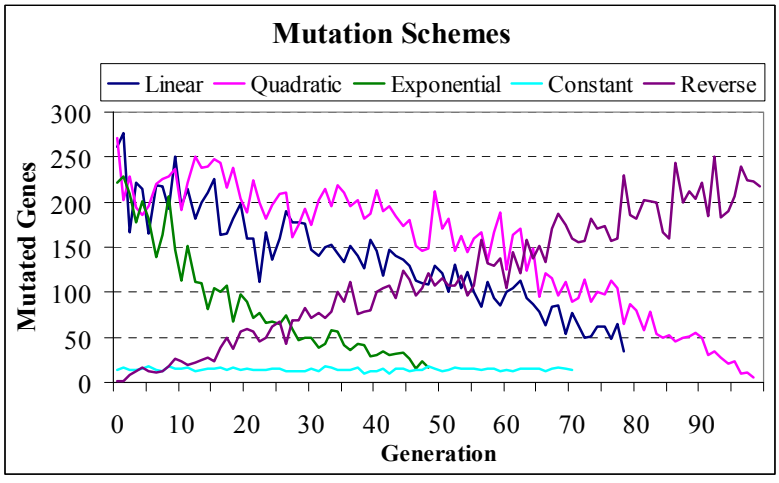

Figure 7-13: Genes mutation of WM according to EC3 for BE1

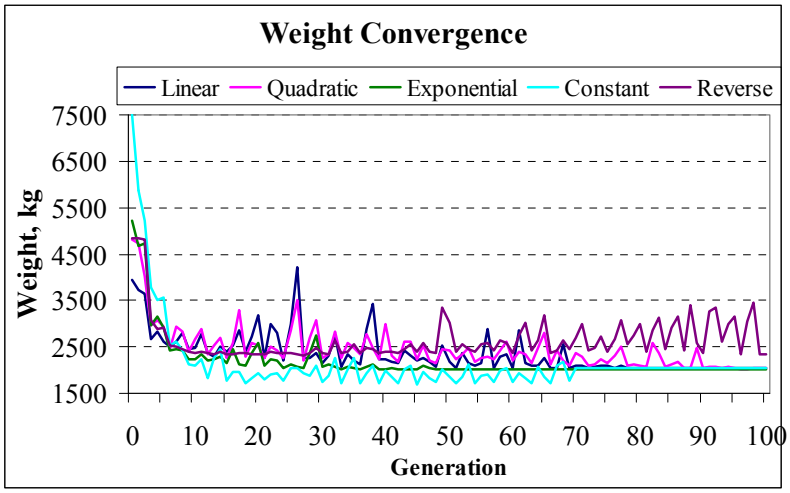

Figure 7-14: Weight convergence of WM according to EC3 for BE1

7.2.2 WM with semi-rigid connections for BE1

These tests are grouped into two tests of WM according to BS 5950 and two according to EC3. The main focus of tests will be on the effect of semi-rigid connections on the design optimisation of SPFs. Two methods of calculating the initial stiffness are presented which include the finite element method developed by Mohamadi-shooreh and Mofid (2008) and the well-known method of Frye-Morris. Assuming the semi-rigid connections, the bolted flush end plate connection is assumed to make the eaves and the apex. Initial results show that the axial force in the rafter sometimes exceeds 5% of the compression strength. As a result, the use of initial stiffness proposed by EC3 is not taken into consideration in the analysis. As the exponential mutation presented better results than the other schemes in terms of the optimum weight and faster convergence, the decision is made to apply exponential mutation in all design optimisation.

Table 7-3 collects the results of the WM considering semi-rigid connections. Results show that there is little difference between the solutions obtained according to BS 5950 and EC3 since they are all controlled by displacement. Implementing the Frye-Morris model yields lighter frame than Mohammadi-Mofid model, as shown in Fig. 7-15. As expected, the design was controlled by the displacement, and this is due to the fact that the semi-rigid connections make the frame more flexible, hence having larger vertical and lateral displacements. The displacement ratio reached its highest possible value, whereas the best strength ratio of the optimum solution reached only 75%. The strength constraints were mostly controlled by the columns where the

highest strength ratio was achieved. This value is due to the combined axial compressive and bending stresses applied to the columns.

Table 7-3: Weight minimisation assuming semi-rigid connections for BE1

Model	Code	Column UB	Rafter UB	L_h, m	D_h, m	Weight, kg
Mohamadi-Mofid	BS 5950	533x210x82	533x210x82	3.05	0.84	2886.86
	EC3	533x210x82	533x210x82	3.05	0.63	2838.72
Frye-Morris	BS 5950	457x152x60	457x152x60	2.15	0.98	2067.29
	EC3	457x152x60	457x152x60	2.20	0.98	2071.96

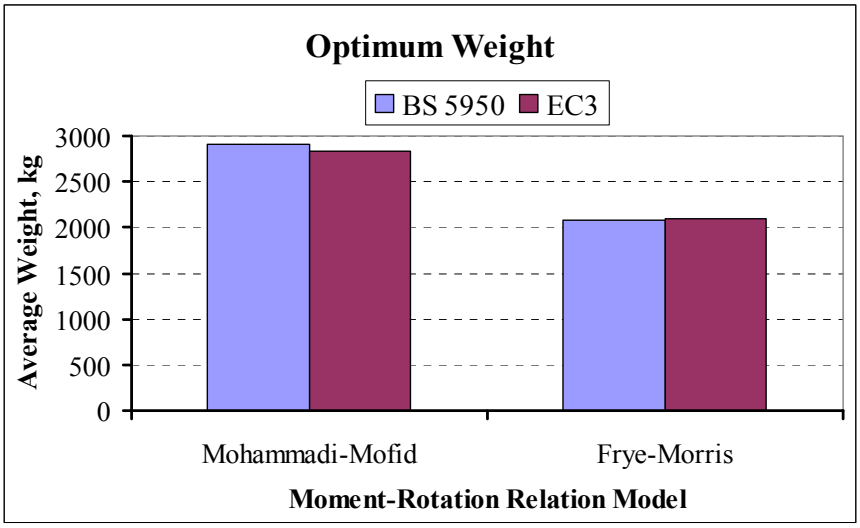

Figure 7-15: Average weight assuming semi-rigid connections for BE1

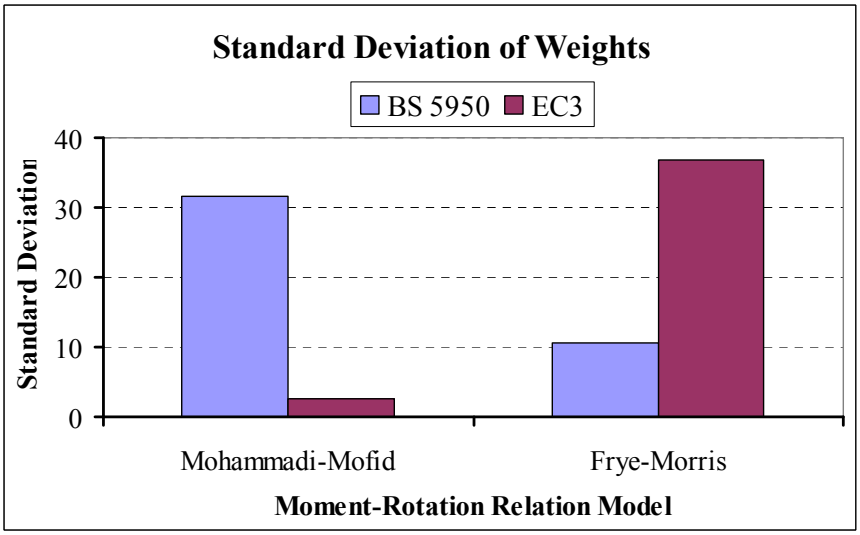

Figure 7-16: Standard deviation of weights assuming semi-rigid connections for BE1

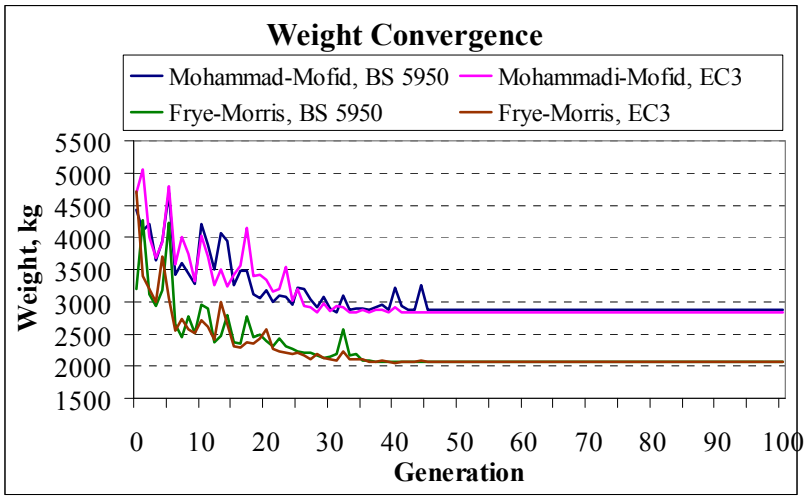

Figure 7-17: Weight convergence assuming semi-rigid connections for BE1

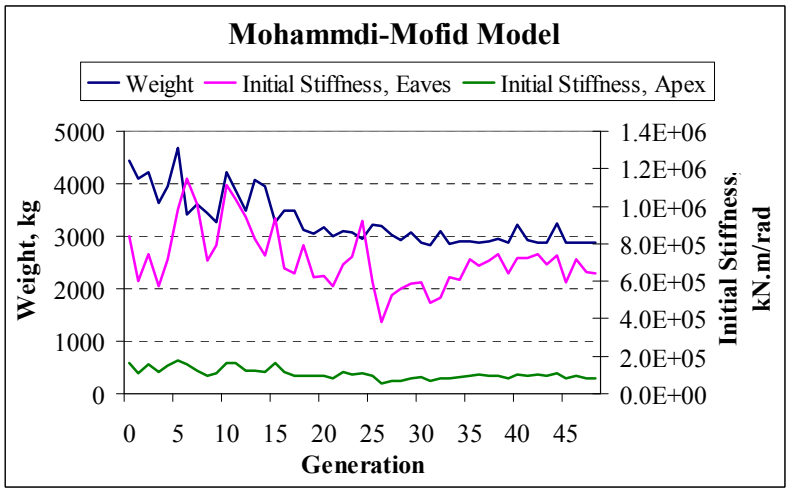

Figure 7-18: Initial stiffness versus weight using Mohammdi-Mofid model for BE1

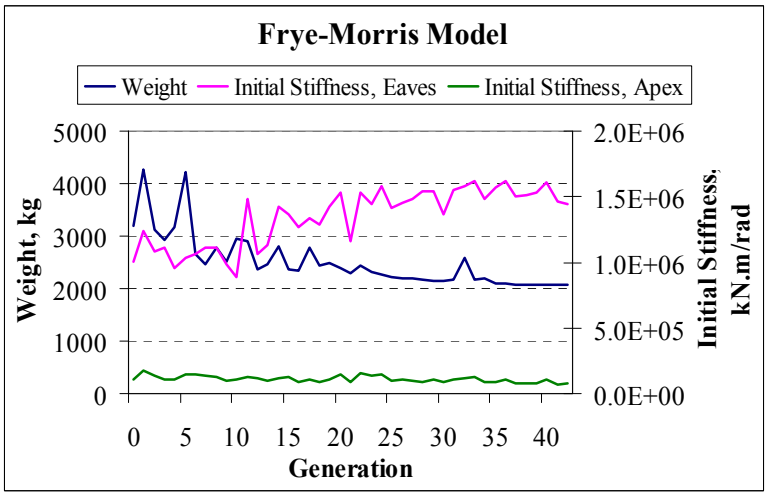

Figure 7-19: Initial stiffness versus weight using Frye-Morris model for BE1

Fig. 7-16 depicts that the WM according to EC3 while implementing the Mohammadi-Mofid model to compute the initial stiffness of semi-rigid connections gives better standard deviation than others. It can be clearly seen from Fig. 7-17 that applying the Frye-Morris model gives faster convergence and a lighter frame than the Mohammadi-Mofid model. Figs. 7-18 and 7-19 show that there is no considerable change in the value of the initial stiffness at apex, whereas this value increases at the eaves as the design optimisation proceeds. This is because by approaching the design problem to the end of optimisation process and controlling displacement over the solution, the depth of eaves increases, hence increasing the initial stiffness.

A notable result is that the average strength ratio and the average displacement ratio of the optimum solution do not have the highest values among the obtained optimum solution, and that these values are found in the heaviest frame.

7.2.3 Displacement maximisation for BE1

This group of tests comprises design optimisation to maximise the displacement of frame BE1 joints. As previously discussed, a different penalty coefficient is used than the one for weight minimisation, and the individuals that violate any constraints are discarded. All the frame's connections are considered to be rigid. The constraints are checked against limitations imposed by both BS 5950 and EC3 codes of practice. In the previous optimisation processes, the design was controlled by the vertical displacement, hence, the attempt is made to maximise lateral displacement of the frame.

The results of displacement maximisation of BE1 are collected in Table 7-4. They show that the best solution of the design optimisation according to EC3 yields higher average lateral displacement and lighter weight than BS 5950.

The maximum lateral displacement ratio was 0.48 for the top of the columns, whereas it reached 0.99 for the vertical displacement of the apex. The maximum strength ratio reached to 0.99 due to the overall buckling by the combined axial and bending stresses. The strength ratio of column is 0.92 due to the combined axial and bending stresses. The optimum solution does not have the minimum weight among the other solutions. The maximum average total displacement and largest value of the

strength ratio belong to the frame with the lightest weight. Figs. 7-20 and 7-21 show the convergence of displacement and weight for the best optimum solutions. Although the aim is displacement maximisation, it should be noted that the weight is well converged while the displacement convergence has high fluctuations.

Table 7-4: Displacement maximisation for BE1

Codes	**Column UB**	**Rafter UB**	**L_h, m**	**D_h, m**	**Weight, kg**	**Average Lateral Displacement**
BS 5950	457x191x82	457x191x74	0.25	0.15	2409.37	0.382
EC3	457x191x74	457x191x74	0.15	0.41	2329.84	0.384

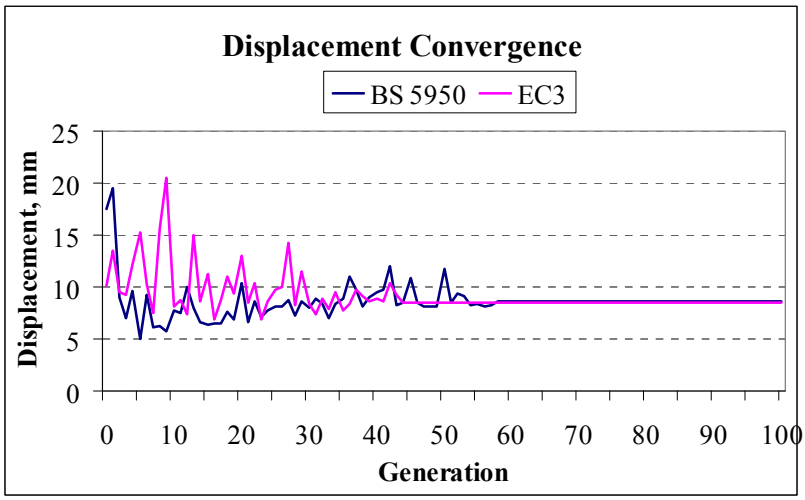

Figure 7-20: Displacement convergence of displacement maximisation for BE1

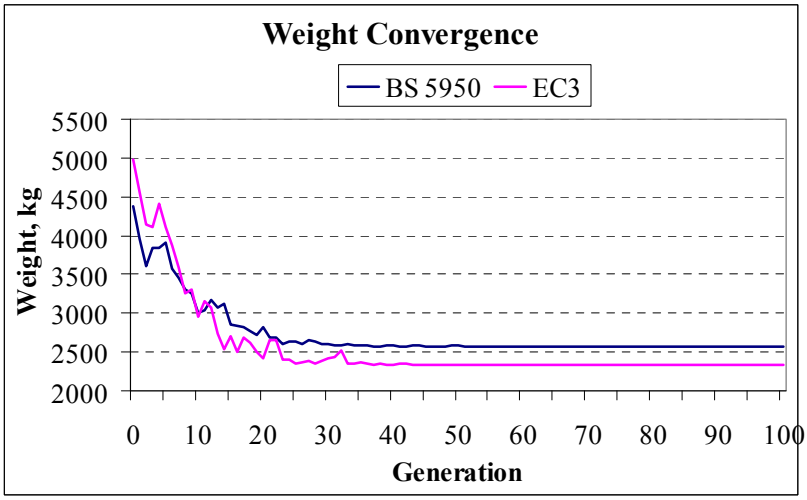

Figure 7-21: Weight convergence of displacement maximisation for BE1

7.2.4 WM with fixed haunch ends depth for BE1

The varied haunch depth will likely increase the cost of the manufacturing, since a built-up section should be provided and welded to the required part of the rafter. In this group of tests, the same frame is redesigned while considering a fixed depth and varied length. For this reason, the tests are devoted to the frames in which haunch depth equals depth of the section minus the flange thickness. This will halve the standard steel rolled section longitudinally, having the length equal the length of the haunch, and does not require building up a section by welding. Then the halved section is welded to the end part of the rafter making a non-prismatic member with three flanges. As a result, there are only three variables in the design optimisation: column cross-section, rafter cross-section, and haunch length.

The WM according to BS 5950 is controlled by strength whereas the WM according to EC3 is controlled by displacement. Table 7-5 and Fig. 7-22 indicate that the WM according to EC3 yields a lighter frame than BS 5950. This refers to the smaller

Table 7-5: WM with fixed haunch ends depths for BE1

Codes	Column UB	Rafter UB	L_h, m	Weight, kg
BS 5950	457x191x82	457x191x67	1.60	2349.654
EC3	533x210x82	457x152x52	2.10	2039.881

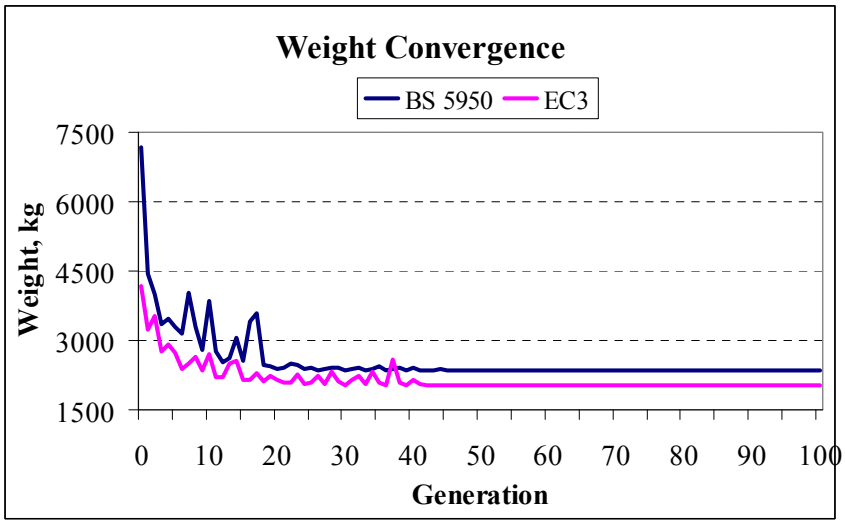

Figure 7-22: The weight convergence of WM with fixed haunch ends depths for BE1

factored load that the design according to EC3 applies and allows the displacement to control over design. The maximum strength ratio of the WM according to BS 5950 and EC3 reached to 1.00 and 0.94 respectively. These values for the displacement ratio reached 0.96 and 1.00 for the WM according to BS 5950 and EC3 respectively. The results among ten solutions obtained by DO-DGA indicate that the best solution does not have the highest average strength and displacement ratios.

7.2.5 WM of curved rafter SPF for BE1

In this group of tests, the shape of the frame is altered to a curved rafter. A curved rafter SPF with the same span, height, and the loading system undergoes the same design optimisation process. The curve of the rafter is subdivided into eight equal elements and the design optimisation is conducted considering both varied and fixed haunch depths. The haunch length is set to be constant and equals to one of the subdivided elements of rafter. The curved rafter SPF is designed according to both BS 5950 and EC3 codes of practice. Fig. 7-23 depicts the details of the curved rafter SPF of this test group.

The design optimisation is conducted twice. First it was considered the depth of one haunch end as variable and the other as constant. Secondly, it is considered both depths of member ends as fixed. In the former case, the total number of design variables reached 3, whereas the latter one is 2. The columns and rafter cross-sections are the other two design variables. The results for both cases are collected in Table 5-26.

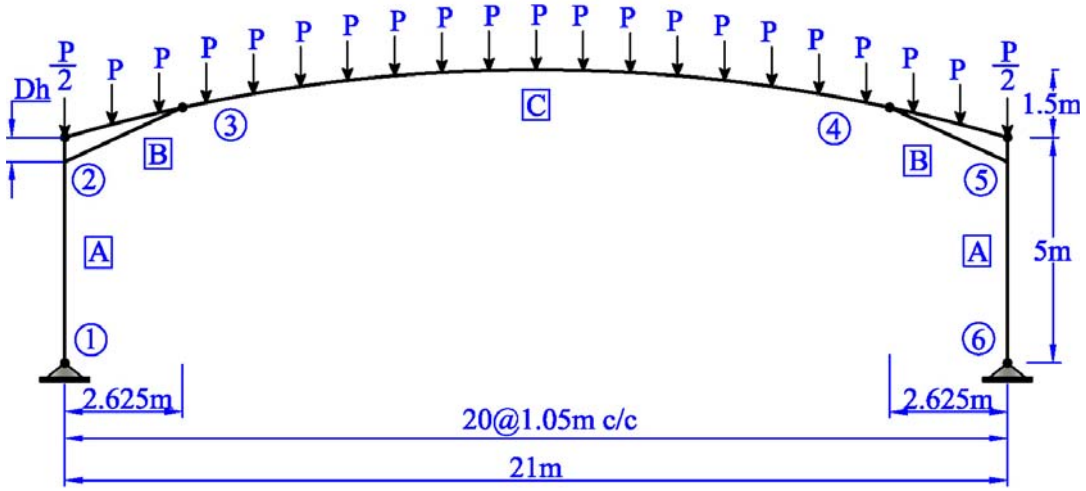

Figure 7-23: A curved rafter SPF for BE1

Table 7-6 shows that the WM according to EC3 while fixed haunch ends depths yields the lightest frame. A small value has been obtained for the haunch depth in the design according to BS 5950. The reason for this small value is that the solution is controlled by strength rather than displacement. Since the WM according to EC3 was controlled by displacement, the value of the haunch depth is reasonably large. Due to the geometry of the rafter, the strength was controlled by columns. This is because the curved shape transfers the stresses to the abutments. Since the curved shape of rafter gives a longer length and also having a fixed length for the haunch, the overall weight of a curved rafter SPF is heaver than the pitched-roof SPF. A pitched-roof SPF can save nearly 2% and 11% saving of steel material for WM according to BS 5950 and EC3 respectively.

Table 7-6: The WM of the curved rafter for BE1

Codes	**Depth**	**Column UB**	**Rafter UB**	***D_h, m***	**Weight, kg**
BS 5950	Varied	533x210x82	457x152x67	0.11	2368.27
	Fixed	457x191x82	457x191x67	---	2427.69
EC3	Varied	533x210x82	457x152x52	0.66	2110.48
	Fixed	533x210x82	457x152x52	---	2074.75

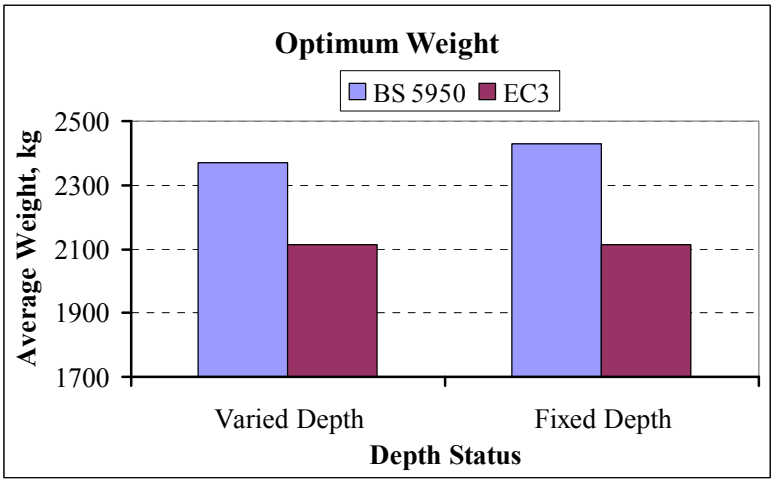

Figure 7-24: The average weight of WM of the curved rafter SPF for BE1

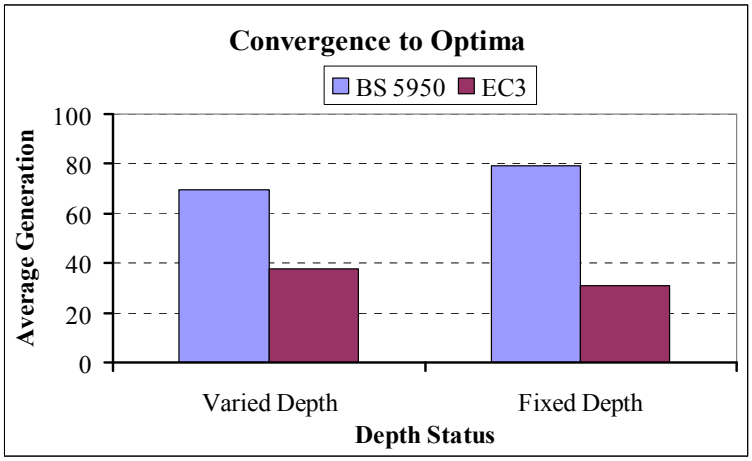

Figure 7-25: Convergence to optima for the WM of curved rafter SPF for BE1

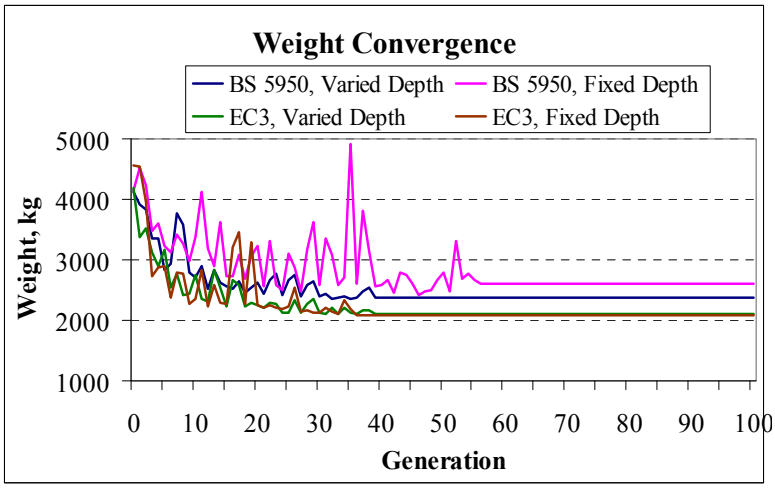

Figure 7-26: Weight convergence of curved rafter SPF for BE1

7.3 BE2: Pitched-roof SPF with uniform lateral loads

In this BE, a pitched-roof SPF with a span of 25m undergoes design optimisation. The column height is 5.5m and the distance from the top of the apex to the top of the columns is 1.5m (Fig. 7-27). A number of gravity concentrated loads, P, are applied to the rafter at an equal distance of 1.25m centre to centre generated from the purlin reactions. The gravity load, P, includes a working dead load with a value of 2.50kN, and a working imposed load with a value of 6.25kN. The left column is subjected to a working uniform wind load, w, with a value of 2.20kN/m. The columns are assumed to have three lateral bracings to exhibit sufficient resistance against lateral torsional buckling. The maximum allowable lateral displacement is 18.33mm (H/300) and the maximum allowable vertical displacement is 69.44mm (L/360).

A part of the rafter adjacent to the eaves, joint number 2 (Fig. 7-27), is haunched with the varied length and depth. Like the previous frame, there are four design variables for the optimisation problems which include: column cross-section, rafter cross-section, haunch length (L_h), and haunch depth (D_h). The design optimisation is conducted according to both BS 5950 and EC3 codes of practice.

7.3.1 WM for BE2

In this group of tests, different created mutation schemes are examined. Since the constant and reverse mutations have not proved their efficiency in the previous experiments, they are not included in this group of tests.

Table 7-7 shows that the exponential mutation scheme made the design problem converge to the optimum solution quicker than the other mutation schemes. It also shows that the WM according to EC3 yields a 10% lighter frame than BS 5950.

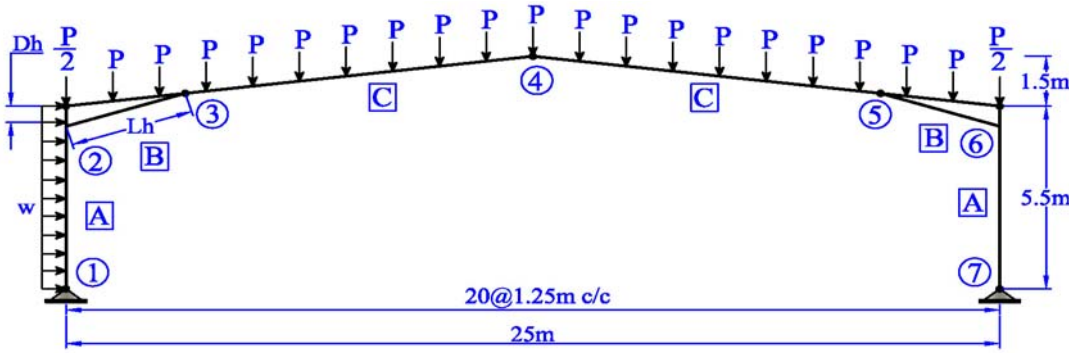

Figure 7-27: The pitched-roof SPF with the gravity and lateral wind loads as BE2

Table 7-7: The WM according to BS 5950 and EC3 for BE2

Codes	Mutation Scheme	Column UB	Rafter UB	L_h, m	D_h, m	Gene-ration	Weight, kg
BS 5950	Linear	533x210x82	533x210x82	0.05	0.22	82	2976.87
	Quadratic	533x210x82	533x210x82	0.05	0.22	97	2976.87
	Exponential	533x210x82	533x210x82	0.05	0.22	40	2976.87
EC3	Linear	610x229x101	457x152x52	3.60	0.74	85	2680.65
	Quadratic	610x229x101	457x152x52	3.60	0.74	97	2680.65
	Exponential	610x229x101	457x152x52	3.60	0.74	46	2680.65

The WM according to BS 5950 is controlled by the strength since the strength ratio of the haunch and column reach to 1.00 and 0.97 respectively due to the combined axial and bending stresses. On the other hand, the values of haunch's length and depth are so small that they can be neglected. There is an increase in lateral displacement due to the lateral applied load. However, the lateral displacement can only reach 69% of the upper limits. In contrast, the WM according to EC3 is controlled by the vertical displacement of the apex which reaches to the 100% of upper limit. The maximum strength ratio of column and rafter for the best solution reaches to 0.69 and 0.94 respectively. The maximum lateral displacement of the frame reaches to 74% of the upper limit. This occurs at the top of the right hand side column (node 6) of the frame for BE2 (Fig. 7-27). The best solution does not have the highest value of average weight ratio, but it does have the highest average displacement ratio. This raises the question whether the fully stressed frame implies that the optimum solution has been reached.

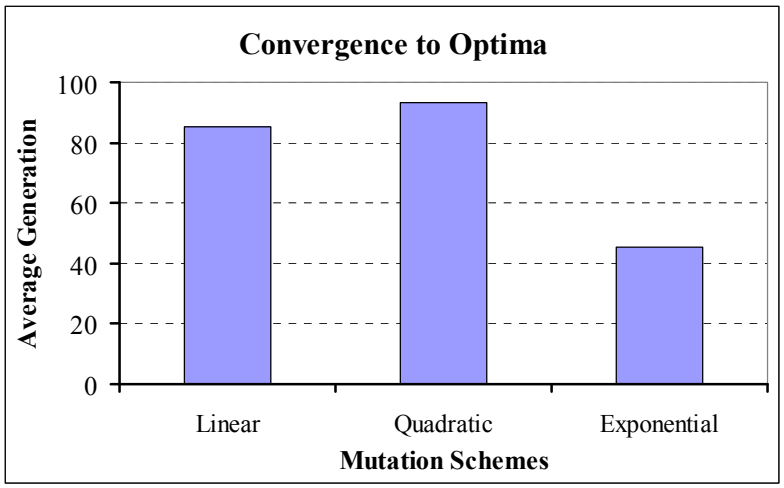

Figure 7-28: Convergence to optima of WM according to BS EC3 for BE2

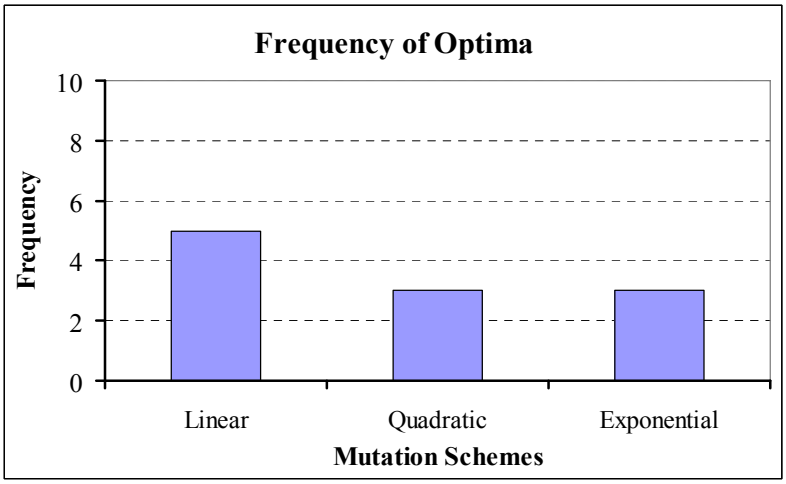

Figure 7-29: Frequency of optima of WM according to EC3 for BE2

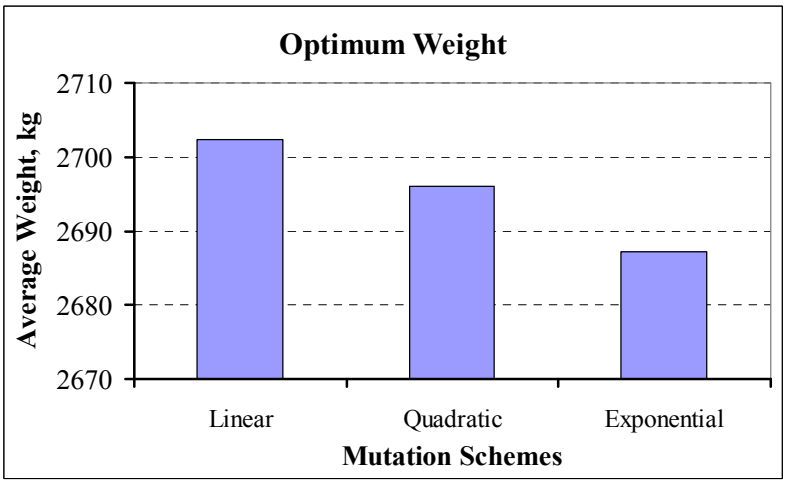

Figure 7-30: Average weight of WM according to EC3 for BE2

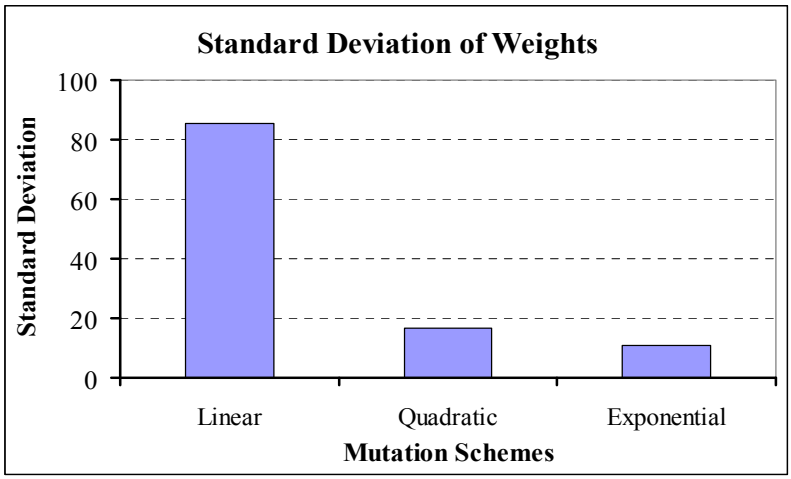

Figure 7-31: Standard deviation of weights of WM according to EC3 for BE2

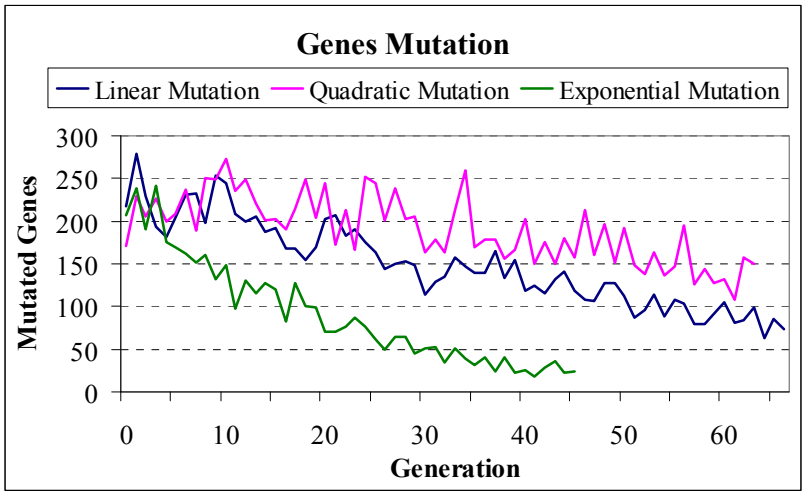

Figure 7-32: Genes mutation of WM according to EC3 for BE2

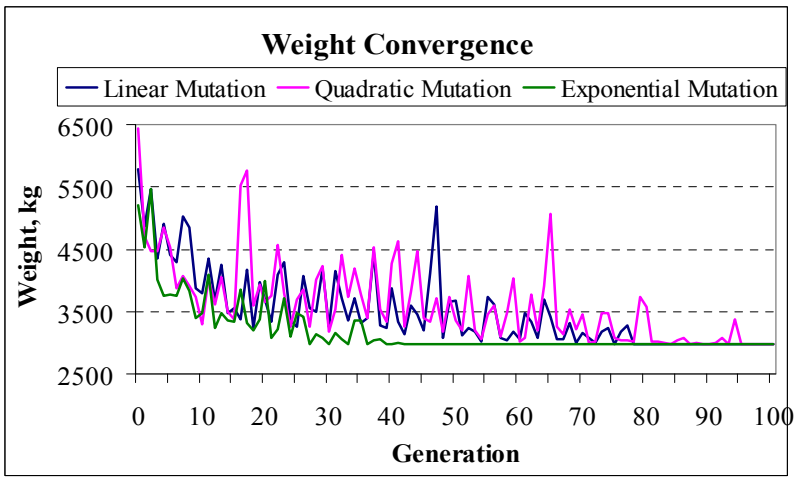

Figure 7-33: Average weight of WM according to BS 5950 for BE2

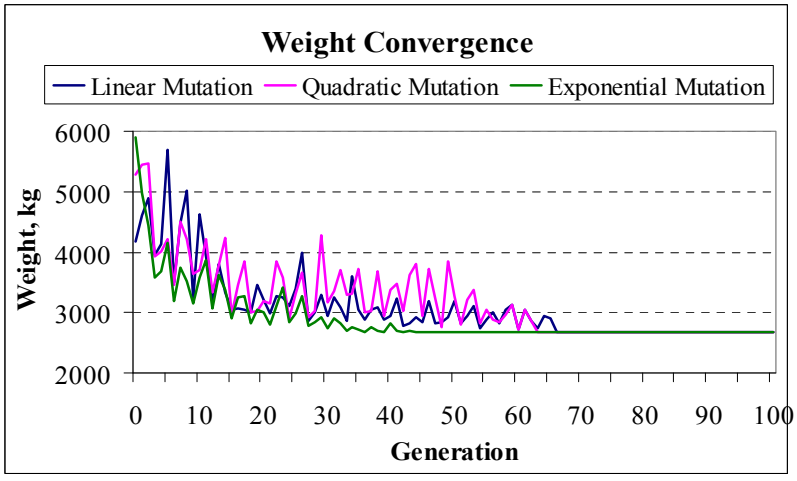

Figure 7-34: Average weight of WM according to EC3 for BE2

Fig. 7-28 shows that the convergence to the optimum solution takes place quicker for the WM applying exponential mutation schemes than the other two schemes. The efficiency of the exponential mutation in obtaining the lightest average weight and lowest standard deviation of weights are portrayed in Figs. 7-30 and 7-31. The linear mutation scheme has the capacity of obtaining the highest number of best solutions among the ten runs of DO-DGA, as shown in Fig. 7-29. As depicted in Fig. 7-32, genes are mutated depending on the scheme that is applied in the optimisation process. Figs. 7-33 and 7-34 clearly show how WM problems converged to the optimum solution. In both cases, efficiency of the exponential mutation is observed.

7.3.2 WM assuming semi-rigid connections for BE2

The results of the WM assuming the semi-rigid connection at the eaves (node 2 and 6) and apex (node 6) of BE2 are shown in Table 7-8. WM is conducted according to BS 5950 and EC3 while applying Mohammdi-Mofid and Frye-Morris models.

Table 7-8: The WM assuming semi-rigid connections for BE2

Model	**Code**	**Column UB**	**Rafter UB**	L_h, **m**	D_h, **m**	**Weight, kg**
Mohamadi-Mofid	BS5950	610x229x101	533x210x82	4.45	1.37	3828.74
	EC3	610x229x101	533x210x82	4.25	1.17	3735.83
Frye-Morris	BS5950	533x210x82	533x210x82	3.60	0.98	3390.86
	EC3	533x210x82	533x210x82	3.45	0.90	3352.75

As expected, the optimum solution according to both BS 5950 and EC3 are controlled by displacement, which reach 100% of the upper limit. Due to excessive displacement the strength ratios of column and rafter are small and at best they reach 0.64 and 0.70 respectively. Control of the design solution by displacement made the haunch depth and length relatively large.

Using the Frye-Morris model to compute the initial stiffness of semi-rigid connections yields relatively the same weight for the WM according to both BS 5950 and EC3. It also gives lighter frame by 11% than the Mohammadi-Mofid model. Initial investigation shows that the Frye-Morris model dramatically reduces the displacement of joints compared to the developed model by finite element. Nevertheless, it increases slightly the rotations of joints. In general, the WM

assuming semi-rigid connections gives a heavier frame than rigid connections. Applying Mohammadi-Mofid models leads to a heavier frame by 28% and 39% for the WM according to BS 5950 and EC3 respectively, whereas applying Frye-Morris model gives 12% and 20% heavier frame than rigid connections for WM according to BS 5950 and EC3 respectively.

Fig. 7-35 depicts the convergence of the design problem to the optimum solution. Figs. 7-36 and 7-37 show that as the generation precedes the value of the initial stiffness at eaves increases while this value decreases slightly at apex. This is due to increasing in haunch depth as the problem converges to the optimum solution.

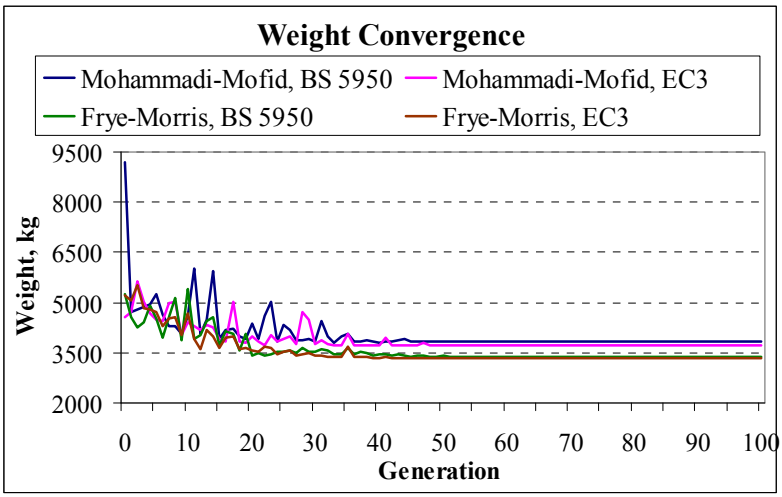

Figure 7-35: Weight convergence assuming semi-rigid connections for BE2

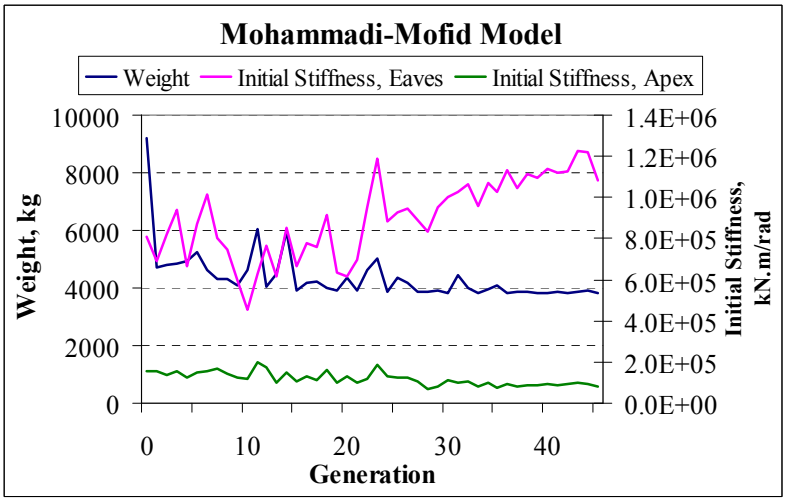

Figure 7-36: Initial stiffness versus weight using Mohammadi-Mofid model for BE2

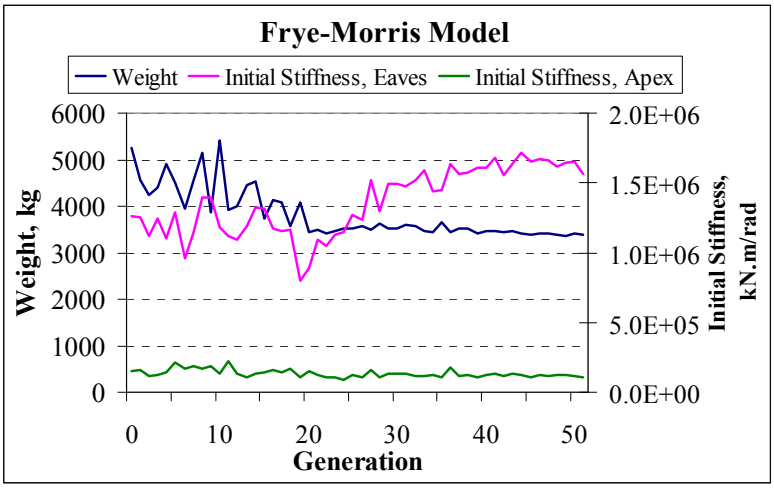

Figure 7-37: Initial stiffness versus weight using Frye-Morris model for BE2

7.3.3 Displacement maximisation for BE2

Table 7-9 collects the results of displacement maximisation. It shows that the maximum average lateral displacement is the same for the design according to BS 5950 and EC3. However, the displacement maximisation according to EC3 yields a frame heavier than BS 5950 by 8%. Displacement maximisation reduces the average strength ratio by 3% and 6% for the design according to BS 5950 and EC3 respectively. The displacement maximisation according to BS 5950 yields 19% heavier frame than the WM, whereas the design to EC3 gives 43% heavier frame.

The optimum solution is controlled by strength in displacement maximisation according to BS 5950. Because the increase in lateral displacement has prevented the vertical displacement extending, the strength ratio is allowed to rise and hence controls the solution. This makes the haunch length and depth so small that they can be neglected. The displacement maximisation according to EC3 is controlled by vertical displacement of the apex. It is notable in the results that the frame that has the maximum average lateral displacement is not the lightest frame among the ten solutions obtained by DO-DGA.

Fig. 7-38 depicts that the stress and vertical displacement limitations does not allow the lateral displacement to increase as the optimisation process proceeds to end. Fig. 7-39 shows the convergence of weight in displacement maximisation.

Table 7-9: Displacement maximisation considering BS 5950

Code	Column UB	Rafter UB	L_h, m	D_h, m	Gen	Weight, kg	Average Lateral displacement Ratio
BS 5950	457x191x98	457x191x98	0.10	0.68	39	3568.29	0.413
EC3	838x292x176	406x178x74	1.00	0.15	44	3858.30	0.412

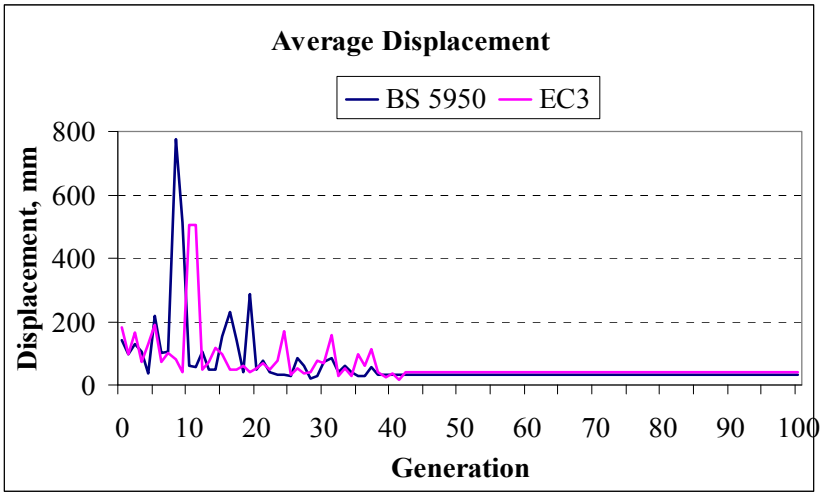

Figure 7-38: Displacement convergence of displacement maximisation for BE2

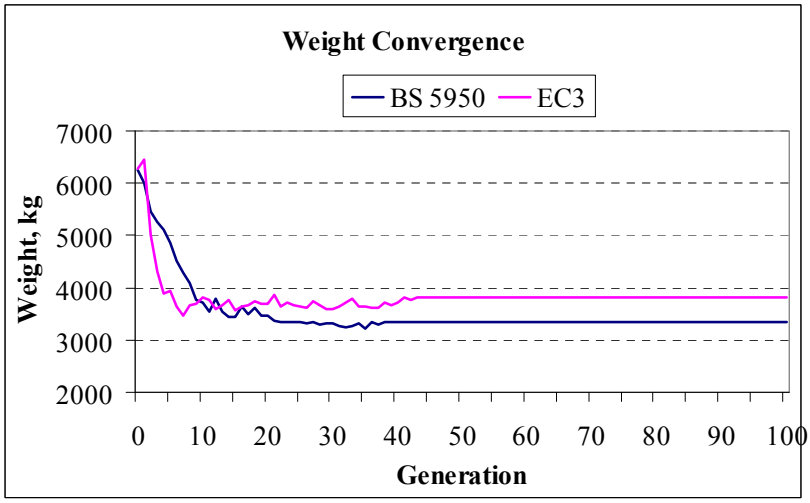

Figure 7-39: Weight convergence of displacement maximisation for BE2

7.3.4 Weight minimisation with fixed haunch depth

Table 7-10 shows that the WM according to EC3 yields 6% lighter frame than BS 5950. In addition, the WM according to EC3 for fixed haunch ends depths yields 11% heavier frame than one varied haunch end depth. There is no significant difference between considering fixed and varied haunch ends depths for WM according to BS 5950.

The optimum solution for the WM according to BS 5950 is controlled by strength. The value of the haunch length is so small that it can be neglected. The vertical displacement of the apex controls the optimum solution for WM according to EC3. Fig. 7-40 depicts the weight convergence of WM considering fixed haunch ends depths. Since there is no need to construct a built-up inverted T-beam section for the SPF with fixed haunch ends depths, the WM may make a cost-effective frame.

Table 7-10: WM with fixed haunch ends depths for BE2

Code	Column UB	Rafter UB	L_h, m	Weight, kg
BS 5950	533x210x82	533x210x82	0.05	2977.98
EC3	610x229x101	457x152x60	3.00	2796.30

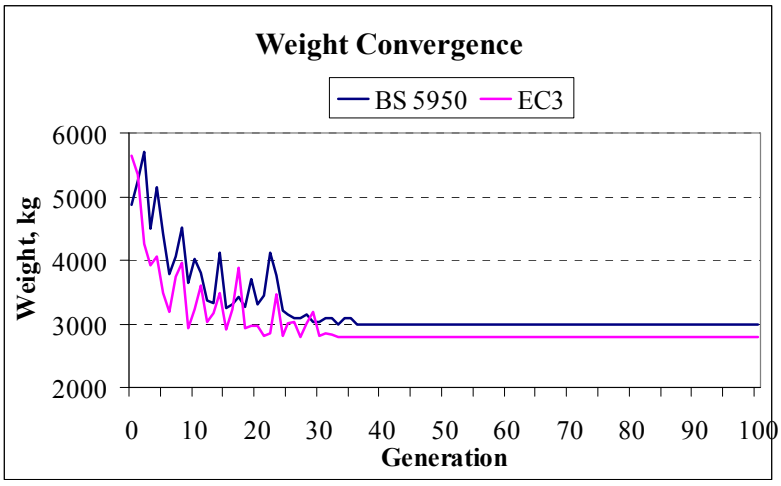

Figure 7-40: Weight convergence of WM with fixed haunch ends depths for BE2

7.3.5 WM of curved rafter SPF for BE2

Fig. 7-41 illustrates the same loading cases and dimension of SPF given as BE2, but with curved rafter. The haunch length is assumed fixed and is equal to 3125mm (span/8).

The results collected in Table 7-11 reveal that the WM according to EC3 gives a lighter frame than BS 5950. The optimum solution is controlled by strength for the WM according to BS 5950. In contrast, the WM according to EC3 is controlled by displacement. Since the haunch depth in WM according to BS 5950 is small, it can be concluded that the haunch may be effective in controlling the displacement rather than stresses induced due applied loads. Due to fixed haunch length, neither maximum strength ratio nor displacement ratio has reached its maximum possible value.

Fig. 7-42 depicts how the WM problem converges to optimum solutions.

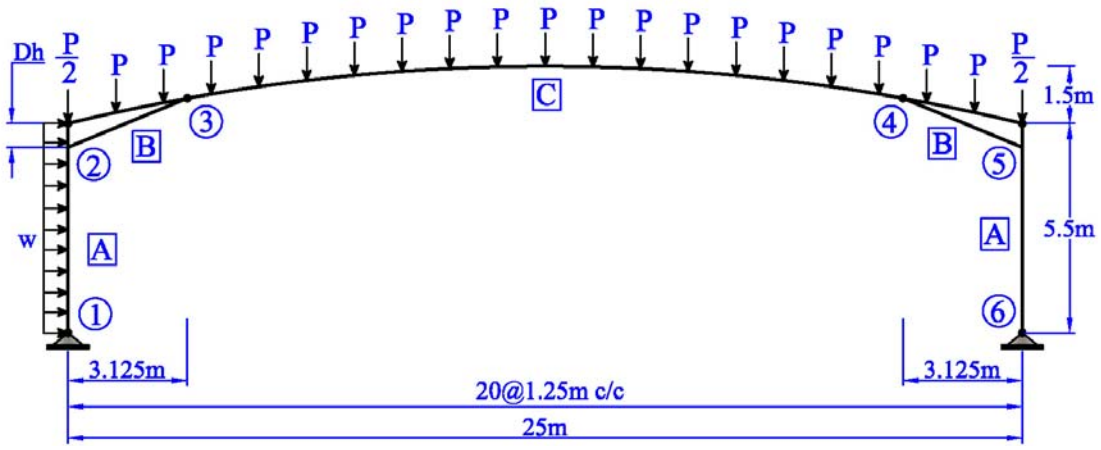

Figure 7-41: The curved rafter SPF for BE2

Table 7-11: The WM of curved rafter SPF for BE2

Code	Depth	Column UB	Rafter UB	D_h	Weight, kg
BS 5950	Varied	533x210x82	533x210x82	0.11	3139.64
	Fixed	533x210x82	533x210x82	---	3236.89
EC3	Varied	610x229x101	457x152x60	0.75	2873.82
	Fixed	610x229x101	457x191x67	---	3018.62

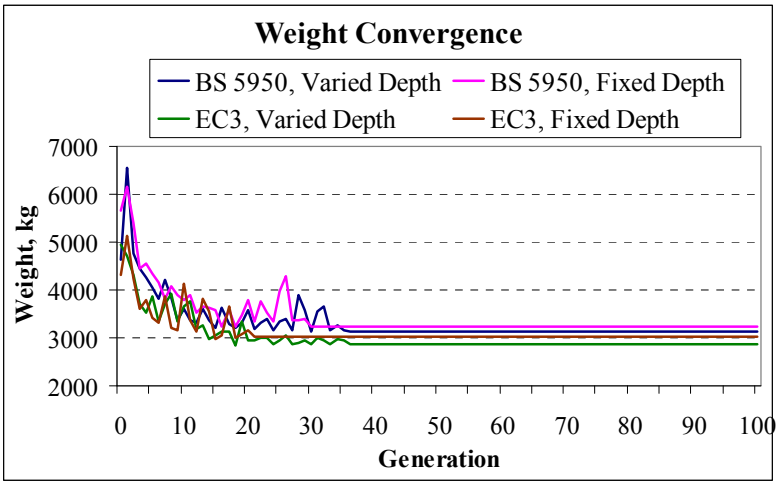

Figure 7-42: Weight convergence of curved rafter SPF for BE2

7.4 BE3: Pitched-roof SPF with lateral point loads

A pitched roof steel portal frame (Fig. 7-43) has been selected as the last BE to undergo the design optimisation considering rigid and semi-rigid connections.

As shown in Fig. 7-43, the pitched-roof FPF has a span of 15.40m with a column height of 5m and an apex height of 6m. The columns are assumed to have three lateral bracing out of plane to control the excessive buckling. The purlins are laid at the equal horizontal distance of 1.10m centre to centre.

The frame experiences two types of loads, which are gravity and lateral horizontal loads. The gravity concentrated load, P, comprises the working dead load of 2.65kN, and working live load of 6.60kN generated from the purling and acting on the position of the purlin-to-rafter joints. There are a total of 14 concentrated loads that

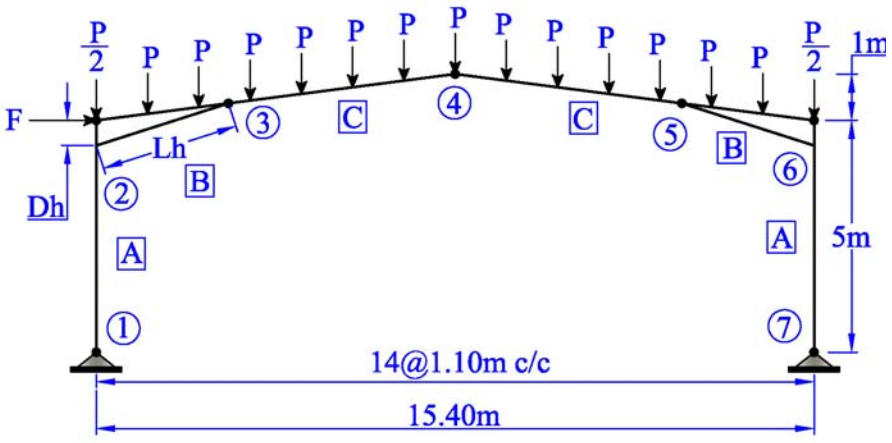

Figure 7-43: The pitched-roof SPF with gravity and lateral point loads

act on the rafter of the SPF. A working static concentrated load, F, which might be treated as an equivalent static load generated from the seismic forces is imposed at the top of the left hand column, joint 2 (Fig. 7-43), with the value of 35kN. The design variables include the column and rafter cross-sections, and the haunch length and depth. The maximum allowable lateral displacement is 16.67mm (*H*/300) and the maximum allowable vertical displacement is 42.77mm (*L*/360).

7.4.1 WM with rigid connections for BE3

The results of the best solutions for WM according to BS 5950 and EC3 while applying different mutation schemes are collected in Table 7-12. The results reveal no significant difference between weights obtained by WM according to BS 5950 and the WM according to EC3. In both cases the optimum solutions are controlled by lateral displacement due to remarkable sway caused by large applied lateral concentrated load. This makes the haunch dimensions increase in order to have a stiff frame against excessive sway.

Table 7-12: The WM applying created mutation schemes for BE3

Code	**Mutation Scheme**	**Column UB**	**Rafter UB**	L_h, **m**	D_h, **m**	**Gene-ration**	**Weight, kg**
BS 5950	Linear	610x229x101	533x210x82	2.65	0.83	88	2565.54
	Quadratic	610x229x101	533x210x82	2.65	0.83	96	2565.54
	Exponential	610x229x101	533x210x82	2.65	0.83	52	2565.54
EC3	Linear	610x229x113	457x191x67	4.45	0.74	91	2556.36
	Quadratic	610x229x113	457x191x67	4.45	0.74	97	2556.36
	Exponential	610x229x113	457x191x67	4.45	0.74	49	2556.36

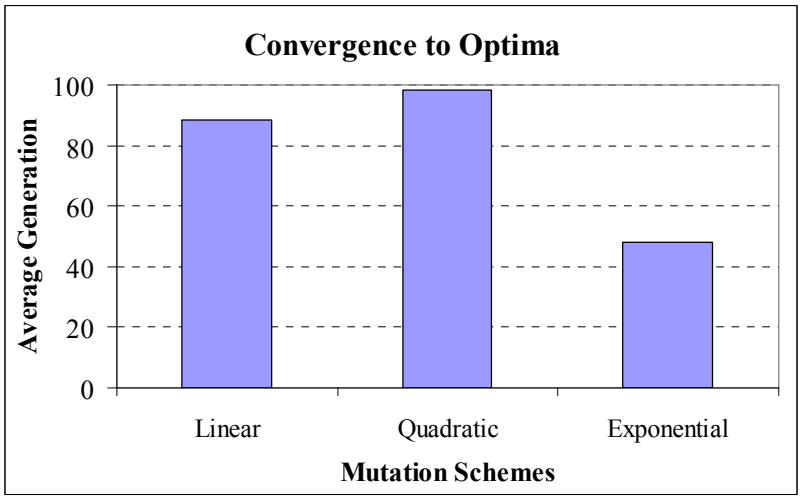

Figure 7-44: Convergence to optima for WM of BE3

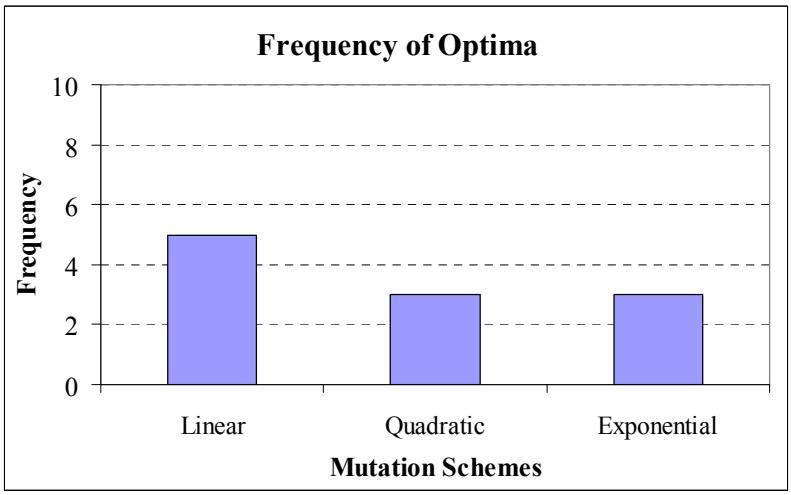

Figure 7-45: Frequency of optima for WM of BE3

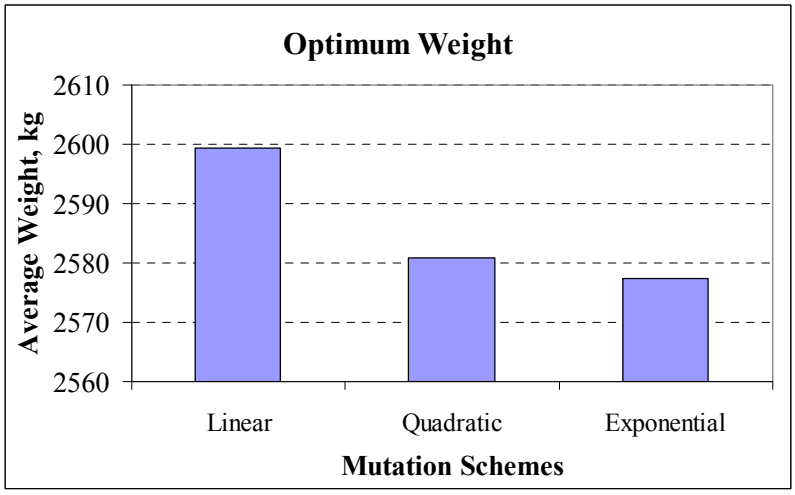

Figure 7-46: Average weight of WM for BE3

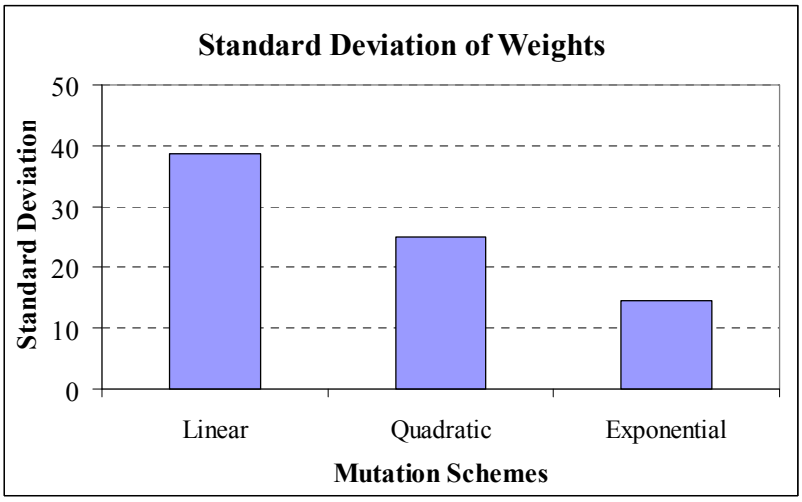

Figure 7-47: Standard deviation of weight in WM for BE3

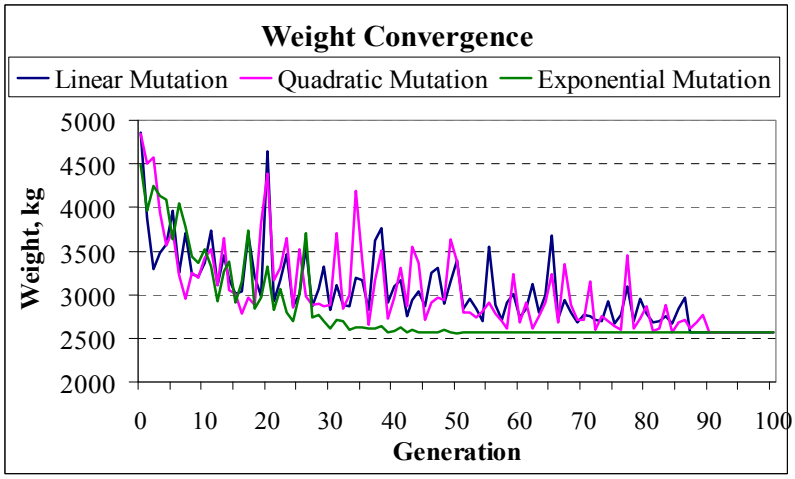

Figure 7-48: Weight convergence WM according to BS 5950 for BE3

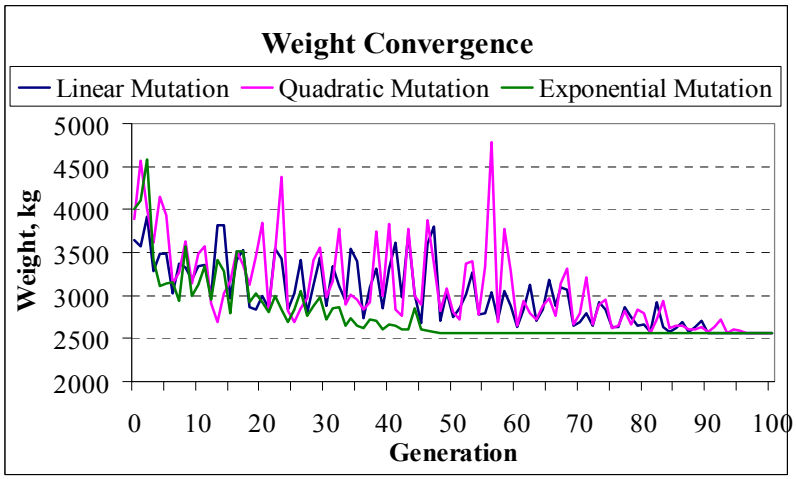

Figure 7-49: Weight convergence WM according to EC3 for BE3

Fig. 7-44 shows that the exponential mutation exhibits the quicker convergence to optimum solution than the other two mutation schemes. It also makes the lightest average of weights among ten solutions obtained by ten runs of DO-DGA, as shown in Fig. 7-46. The linear mutation is efficient in obtaining the larger numbers of best solution among ten runs of DO-DGA (Fig. 7-45). The values of standard deviation of weights (Fig. 7-47) indicate that there are no significant differences between weights of optimum solutions obtained by ten runs of DO-DGA for the WM applying exponential mutation scheme. Figs. 7-48 and 7-49 show the weight convergence of WM applying three created mutation schemes.

7.4.2 WM assuming semi-rigid connections for BE3

The Frye-Morris model used to compute initial stiffness exhibits better results than Mohammadi-Mofid model. In this test, the attempt is made to calibrate the Mohammadi-Mofid model so that it can yield the same results as the well known Frye-Morris model. The calibration is made by increasing 80% of the initial stiffness obtained by Mohammadi-Mofid model.

Table 7-13 collects the results of tests and it reveals that the optimum solutions are the same for all connection models and codes of practice. However, they are 12% heavier frame than WM assuming rigid connections. The optimum solutions are controlled by lateral displacement, and the haunch lengths obtained are small enough to be neglected. This does not imply that the haunch is not effective in control of displacement since there are 20% and 13% increases in depths of column and rafter respectively compared with the WM assuming rigid connections. The larger rafter depth has minimised the role of the haunch in displacement control. The strength ratios of frame members fail to reach 0.5.

Table 7-13: The WM assuming semi-rigid connections for BE3

Model	**Code**	**Column UB**	**Rafter UB**	L_h, **m**	D_h, **m**	**Weight, kg**
Mohammadi-Mofid	BS 5950	762x267x134	610x229x101	0.05	0.98	2917.18
	EC3	762x267x134	610x229x101	0.05	0.98	2917.18
Frye-Morris	BS 5950	762x267x134	610x229x101	0.05	0.98	2917.18
	EC3	762x267x134	610x229x101	0.05	0.98	2917.18

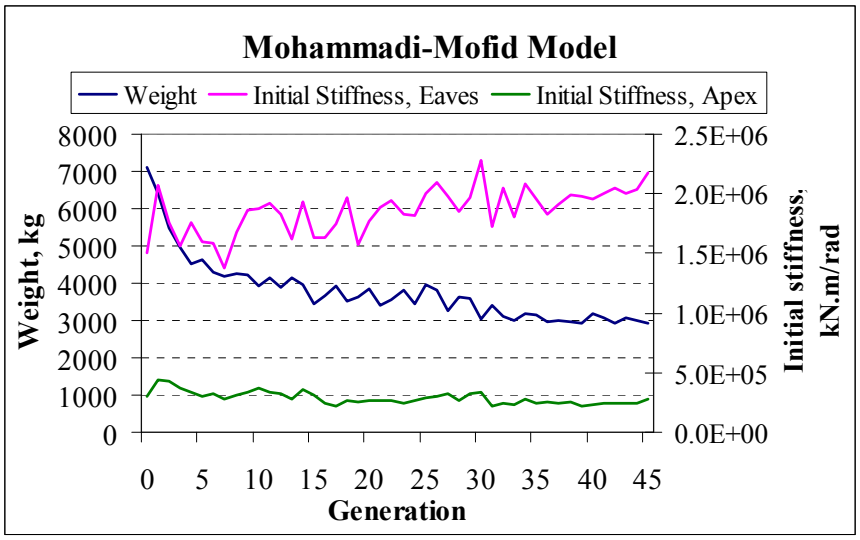

Figure 7-50: Initial stiffness versus weight using Mohammadi-Mofid model for BE3

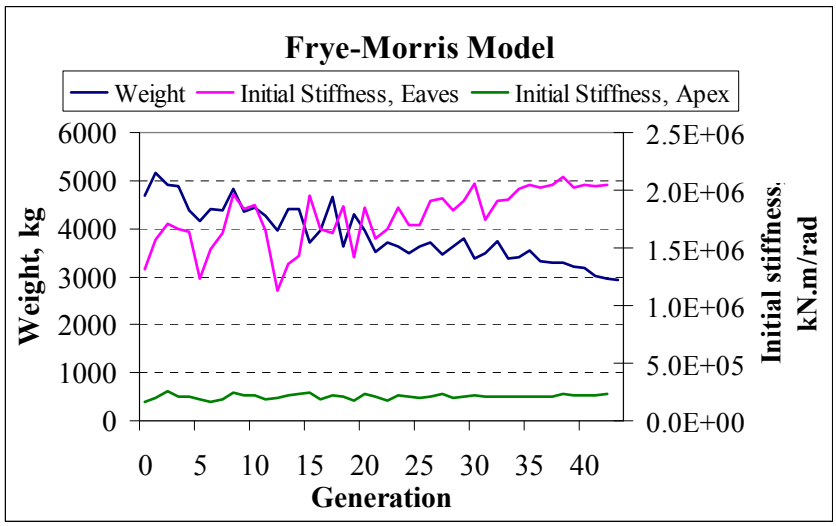

Figure 7-51: Initial stiffness versus weight using Frye-Morris model for BE3

Figs. 7-50 and 7-51 depict the values of initial stiffness for eaves and apex increase as the generation proceeds due to increasing in height of rafter section.

7.5 Parametric studies

The research has identified a further way in which the design process can be made simpler and quicker for structural engineers. From the results of structural optimisation by DO-DGA, graphs and tables can be developed to eliminate complicated structural analysis of SPFs.

In this section, the relationships between structural parameters of SPF, such as span length, haunch length, loads, and member forces, are illustrated. Extracting the

optimum solutions of BEs, the role of haunch is appraised in control of excessive displacement and induced stresses. A SPF with varied span, angle of pitched-roof, and applied loads is employed to conduct the other parametric studies such as the load-weight relationships and coefficients of bending moments, shear forces, and axial forces. As shown in Fig. 7-52, the frame is assumed to experience a uniform factored load, *w*. The reason for the parametric study is to have an insight for the structural engineers to calculate bending moments, shear forces, and axial forces induced in SPFs' members as well as the selection of appropriate standard steel sections at the initial stage of design.

7.5.1 Role of haunch

A number of optimum solutions with similar column and rafter cross-sections were selected to investigate the effect of haunch on the lateral displacement and the average strength ratio of SPFs. The surface area of haunch that is taken into account involves only the depth and the length of haunch. Fig. 7-53 shows that there is a direct relationship between the surface area of haunch and the average displacement ratio, i.e. the optimum solution with smaller average displacement ratio has smaller haunch length and depth and vice versa. In contrast, there is an inverse relationship between the surface area of haunch and the average strength ratio as shown in Fig. 7-54, i.e. the optimum solution that possesses higher strength ratio has smaller haunch length and depth. This demonstrates the influential role of the haunch in controlling the displacement rather than strength. This implies that the construction of the haunch depends much more on displacement rather than the large bending moment.

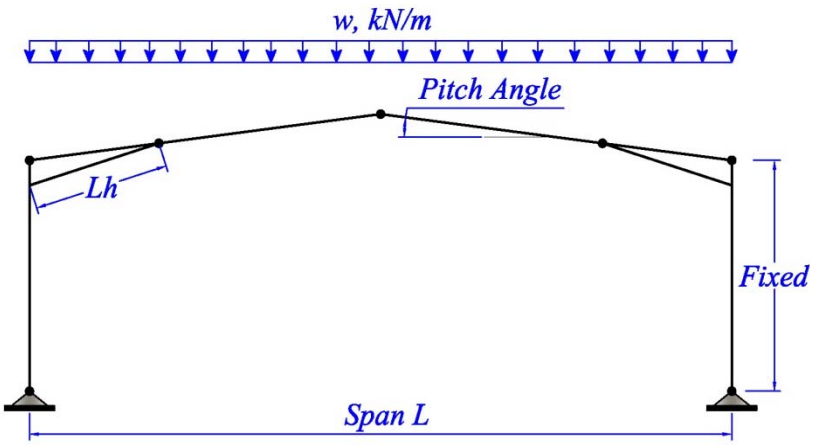

Figure 7-52: The SPF for the parametric studies

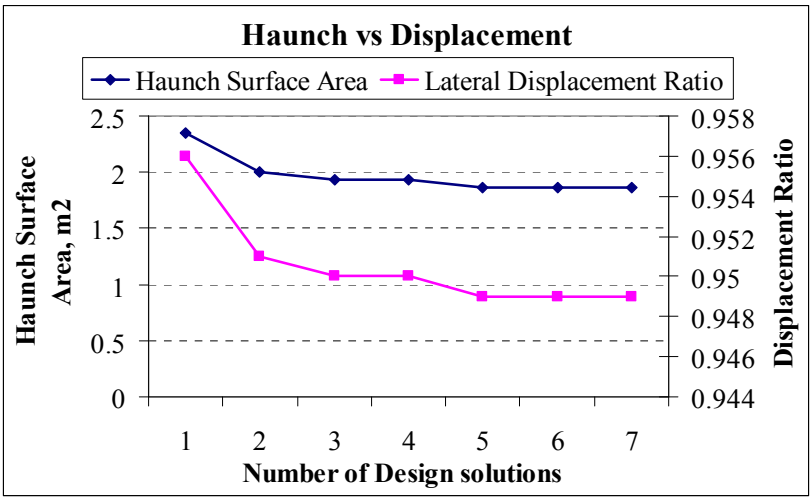

Figure 7-53: Surface triangular area of haunch versus lateral displacement of SPF

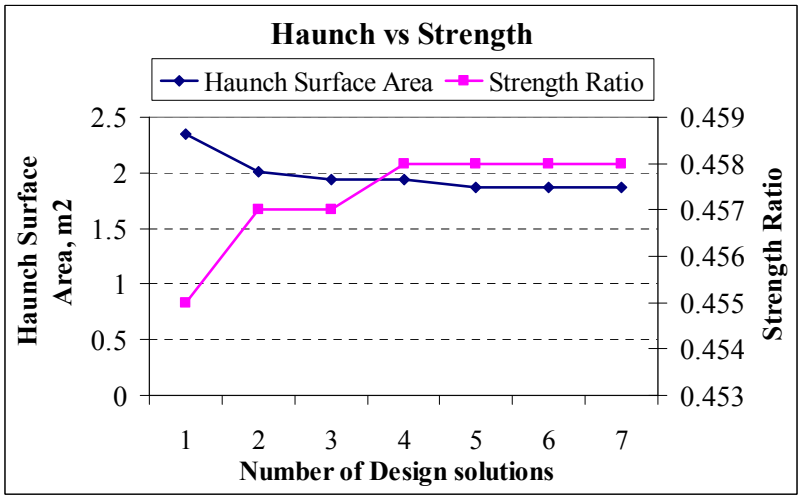

Figure 7-54: Surface triangular area of haunch versus strength ratio of SPF

7.5.2 Weight-load relationships

Figs. 7-55 to 7-58 illustrate the relationship between the applied load, *w*, and the weight of the optimum solution with different pitch angle and span length of SPF. They show that there are no large changes in weight as the load increases for SPF with spans of 5m and 10m. However, there is a noticeable increase in weight for spans greater than 10m, particularly when the weight is switched from 10kN/m to 15kN/m.

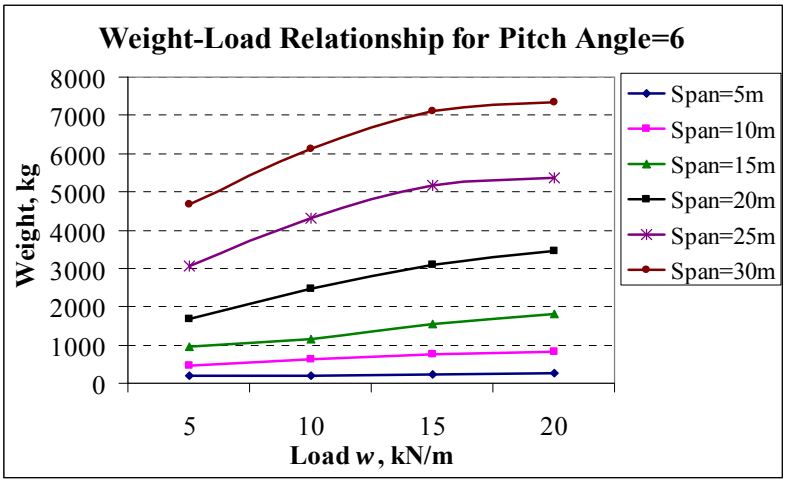

Figure 7-55: Weight-load relationship of SPF for the pitch angle of 6°

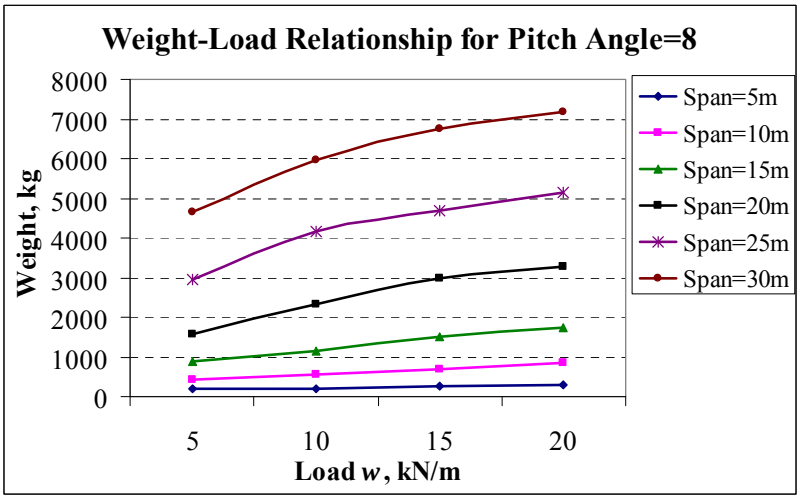

Figure 7-56: Weight-load relationship of SPF for the pitch angle of 8°

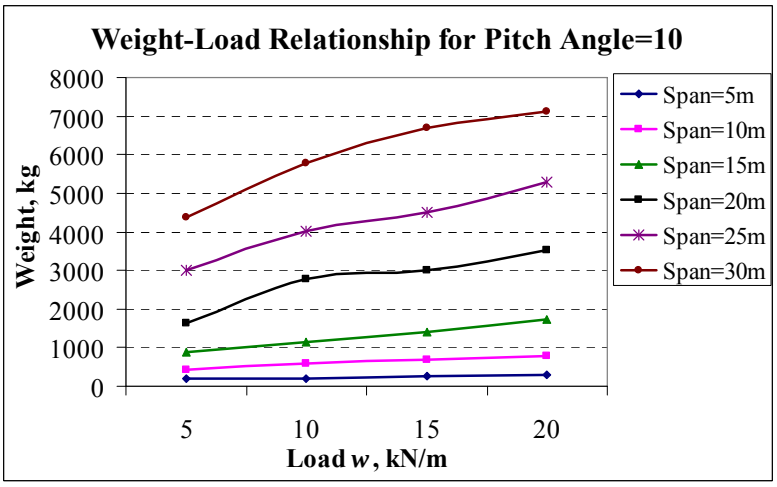

Figure 7-57: Weight-load relationship of SPF for the pitch angle of 10°

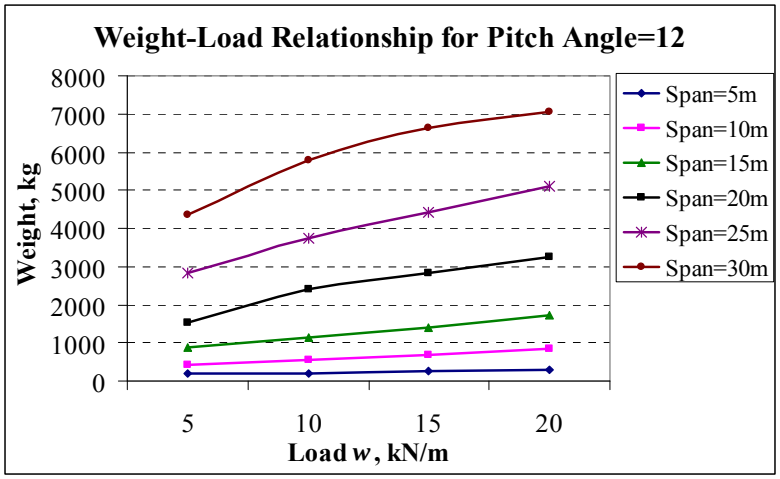

Figure 7-58: Weight-load relationship of SPF for the pitch angle of 12°

7.5.3 Weight-pitch angle relationships

Figs. 7-59 to 7-61 illustrate the relationship between weight of optimum solution and the pitch angle of SPF with different spans and applied loads. In general, they show that increasing pitch angle decreases the weight of the optimum solution. Although the same steel sections are assigned to the member cross-sections, the dimensions of haunch are reduced due to a decrease in displacement made by increasing the pitch angle. This is why the weight is slightly reduced.

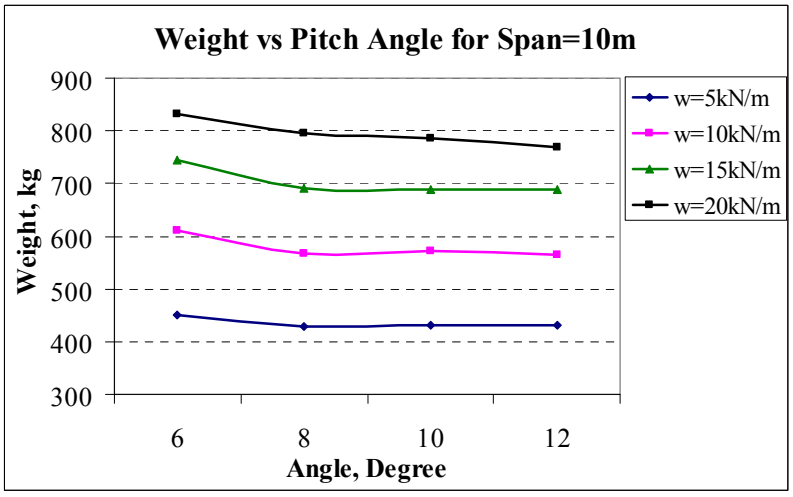

Figure 7-59: Weight-pitch angle relationship of SPF for span of 10m

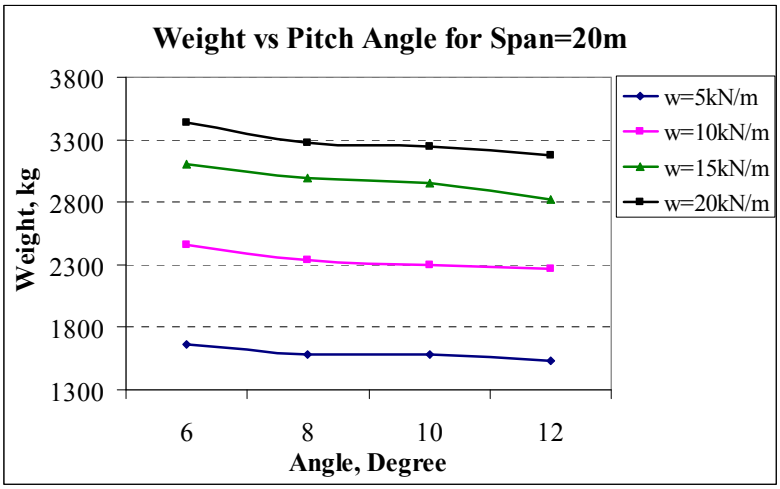

Figure 7-60: Weight-pitch angle relationship of SPF for span of 20m

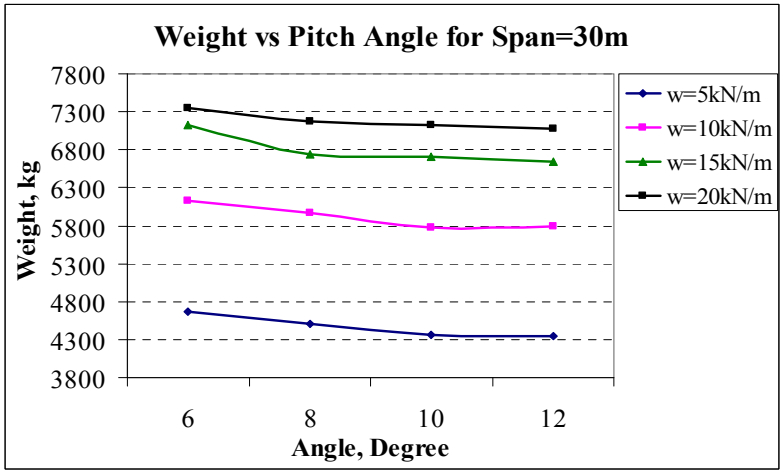

Figure 7-61: Weight-pitch angle relationship of SPF for span of 30m

7.5.4 Bending moment coefficients

Fig. 7-62 depicts the relationship between the span of SPF and the ratio of positive to negative bending moments at the rafter. It can be seen that as the span increases the positive to negative bending moment ratio drops. It can be pointed out that for smaller span the positive moment is critical, whereas for the larger span the negative bending moment will control the design, as clearly shown in Figs. 7-63 and 7-64. The coefficient has to be multiplied by wL^2, where w is the factored applied load and L is the span of SPF, in order to find the bending moments.

7.5.5 Axial and shear forces coefficients

Including the frame's self weight, the relationship between the span and coefficients of maximum axial and shear forces at column and rafter are illustrated in Figs. 7-65 to 7-67 with different pitch angle. There are sharp increases in axial force at column and rafter as length of span increases, whereas this change is smoother for the maximum shear coefficient at the rafter. The pitch angle does not have significant effects on the maximum axial force at column and rafter, but it does affect the value of shear force at the rafter. The coefficient must by multiplied by wL, in order to find the shear and axial forces in structural members.

7.5.6 Haunch length

Fig. 7-68 shows that the role of haunch is substantial when the span of SPF is between 10m and 20m. The role of haunch is less effective for the SPF with the span of less than 10m or greater than 20m. This is because the frame is controlled by strength when the span of SFP is less than 10m or greater than 20m.

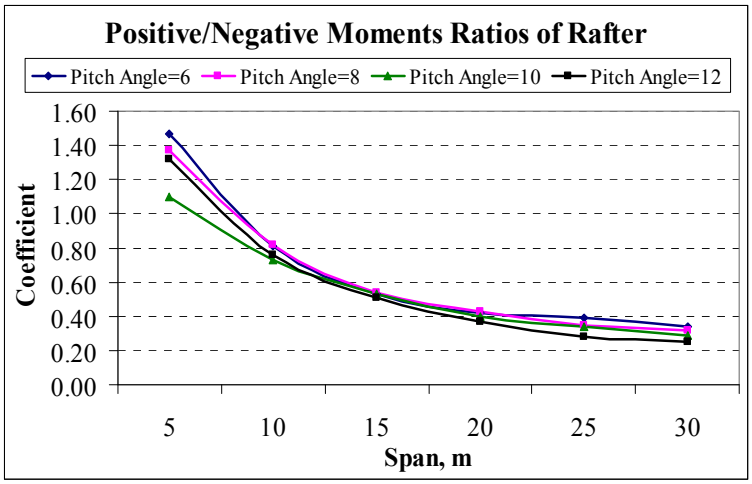

Figure 7-62: Relationships between the rafter positive/negative moments ratio and span

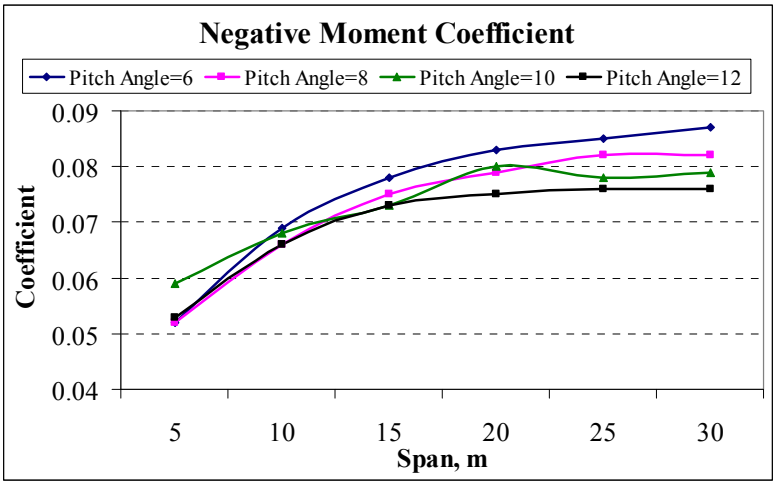

Figure 7-63: Relationships between the coefficient of negative moment and span

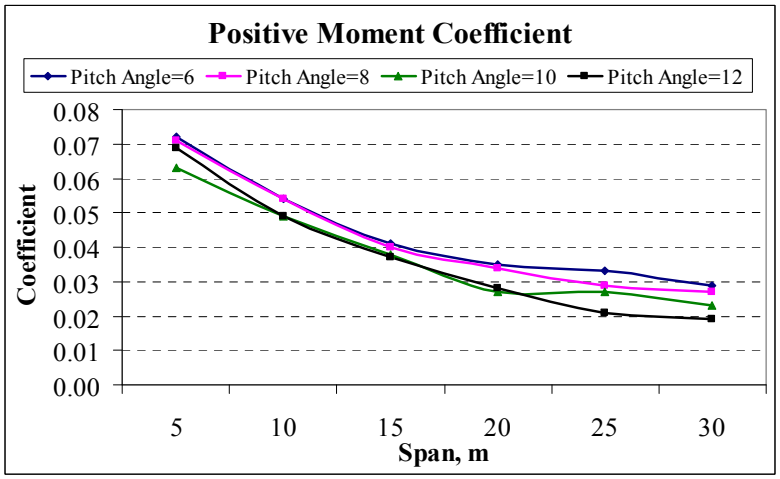

Figure 7-64: Relationships between the coefficient of positive moment and span

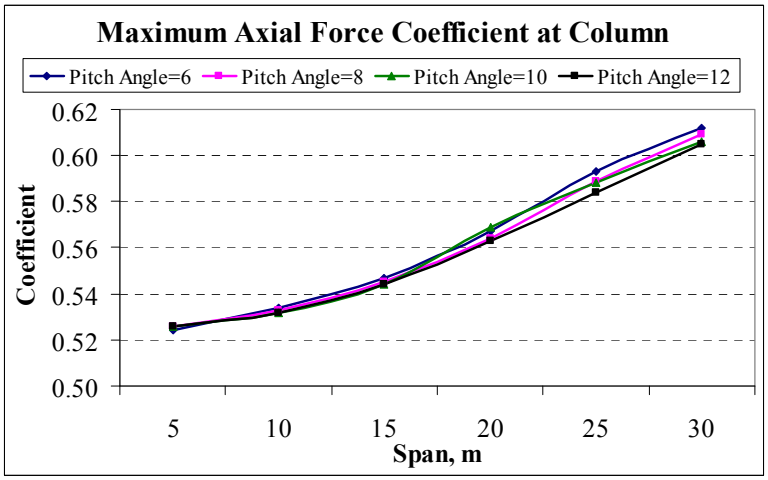

Figure 7-65: Relationships between the coefficient of column axial force and span

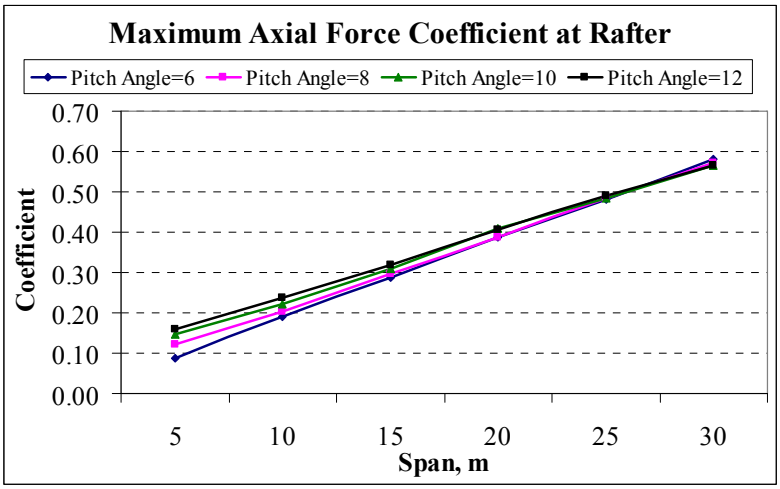

Figure 7-66: Relationships between the coefficient of rafter axial force and span

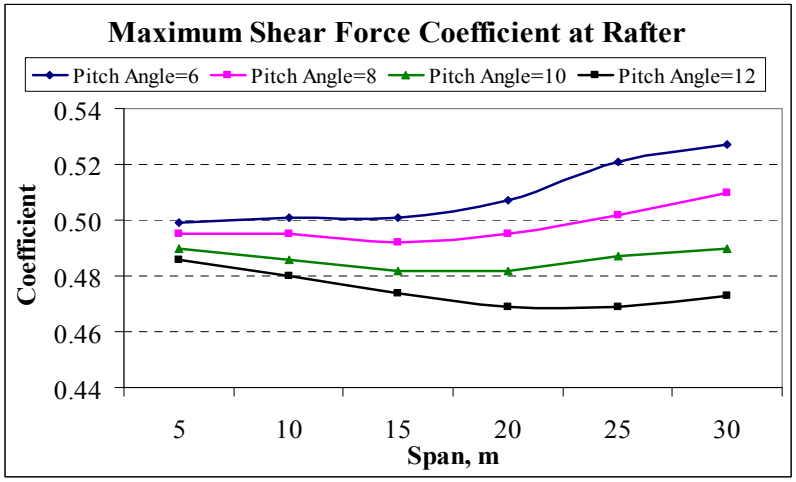

Figure 7-67: Relationships between the coefficient of rafter shear force and span

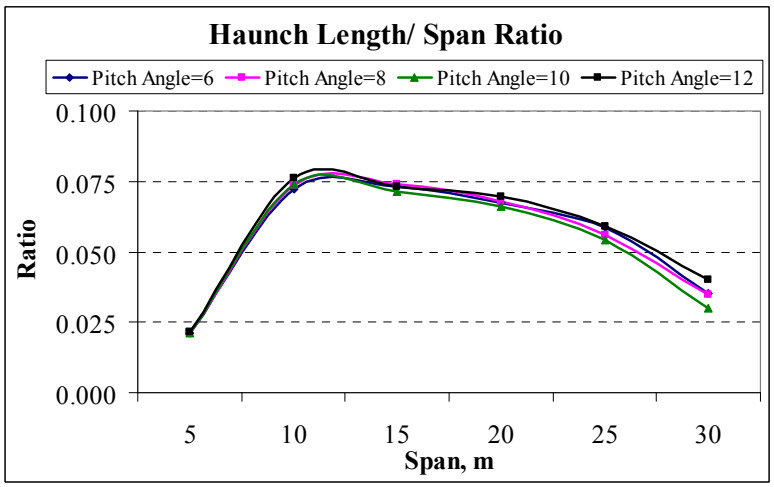

Figure 7-68: Relationships between the span and the haunch length/span ratio

Table 7-14 makes it possible to select the universal beams sections for the cross-section of SPFs' elements, obtained form design optimisation.

Table 7-14: Steel cross-sections of SPFs' elements

Span, m	**Load, kN/m**	**Column, UB**	**Rafter, UB**
5	5	127x76x13	127x76x13
	10	127x76x13	127x76x13
	15	152x89x16	152x89x16
	20	178x102x19	178x102x19
10	5	178x102x19	178x102x19
	10	203x133x25	203x133x25
	15	254x146x31	254x146x31
	20	356x127x33	356x127x39
15	5	254x146x31	254x146x31
	10	305x165x40	305x165x40
	15	406x178x54	305x165x46
	20	406x178x60	406x178x60
20	5	356x171x51	305x165x46
	10	457x191x67	457x191x67
	15	610x229x101	533x210x82
	20	686x254x125	533x210x82
25	5	533x210x92	457x191x67
	10	610x229x101	610x229x101
	15	762x267x134	610x229x101
	20	762x267x134	686x254x125
30	5	610x229x101	533x210x92
	10	686x254x125	686x254x125
	15	686x254x152	686x254x140
	20	610x305x179	610x305x149

7.6 Summary

Three studies with different loads were used to investigate the behaviour of SPFs in the optimisation process; a SPF subjected to gravity loads, one subjected to gravity and lateral wind loads, and one subjected to gravity loads and a large lateral point load. In choosing the cases to study, the attempt was made to use different spans, heights, pitched angles, and loads to undertake a broad investigation of this popular frame. There were two objective functions; weight minimisation to reduce the steel material, and displacement maximisation to increase the lateral displacement as much as possible. While considering the limitations imposed by both BS 5950 and EC3 codes of practice, the models of connections was chosen to be rigid and semi-rigid. A parametric study was conducted to make it easier for the structural engineer to calculate the parameters required for the design of SPFs without measuring the response of frame against the applied load. The results indicate that the exponential mutation scheme, created as a genetic operator, makes the algorithm to converge more quickly than the other two schemes; linear and quadratic. The results of displacement maximisation confirm that there is a benefit of weight minimisation in a steel structure since they did not prove the need for another objective function. Semi-rigid connections failed to yield lighter frames in the design optimisation of SPFs which contradicts findings by other authors. In addition, design according to EC3 gives lighter frames compared with those of BS 5950 due to the smaller factored load in the design according to EC3. However, for the design which is controlled by lateral displacement, the results are almost the same for both codes of practice. The graphs produced by parametric studies are promising since they make it possible to eliminate the complicated structural analysis process.

Chapter 8: Conclusions and Suggestions for Future Works

8.1 Introduction

The main achievements accomplished in this programme of work are summarised in the first section of this chapter. The conclusions that have been drawn with respect to the method that has been developed and for its application in structural optimisation are outlined in the second section. Finally, some recommendations and suggestions are made for possible directions of further work in the third section.

8.2 Contribution to knowledge

The significant achievements of this study can be summarised as follows:

1) Following a regression analysis, a stiffness matrix was developed to include the haunched part of the rafter of SPFs in measuring the structural responses.

2) The design procedures according to BS 5950 and EC3 have been thoroughly presented and the differences between the two codes of practice have been highlighted.

3) The concept of the DGA methodology has been studied in detail and new modifications and techniques for reproduction operator, crossover operator, mutation operator, twin analogy, and penalty function are implemented.

4) A computer based-technique for the structural analysis and design optimisation has been developed without reference to the finite element package existing on the market. The modified DGA has been embedded into the program which was developed.

5) The effects of the new schemes on the technique which was developed have been comprehensively investigated and justified.

6) The different objective functions have been introduced according to the form and behaviour of steel frames with respect to the structural optimisation.

7) The computer-based technique that was developed has been validated by comparing it with other techniques found in the literature using various optimisation techniques applied to different forms of steel structures.

8) A study of displacement maximisation has been conducted separately from the weight minimisation and its effects have been investigated.

9) The design optimisation has been conducted by considering both rigid and semi-rigid connections, and comparisons have been made between both types of connections.

10) A comprehensive study has been conducted on different types of SPFs with different real-life load cases.

11) A parametric study has been carried out to calculate the induced bending moments and forces of SPFs without the need for performing structural analysis.

The main achievement of this study is that the modified DGA contributes to structural optimisation and parametric studies. It is hoped that the DO-DGA program, which involves the modified DGA, can pave the road toward the application of structural optimisation in design practices.

8.3 Conclusions

This study leads to some significant conclusions which are summarised as follows:

1) Implementing the developed stiffness matrix for the non-prismatic member saves computation time for structural analysis by 200% and for structural optimisation by 13%.

2) The optimum solutions for steel structures performed by DO-DGA using the modified DGA are encouraging when compared with those achieved by alternative standard optimisation techniques.

3) The tests conducted to maximise a simple mathematical function have shown the efficiency and correctness of the new schemes of DGA. They have effectively contributed to improve the performance quality of the modified DGA in converging to the optimum solutions.

4) It has been shown that the modified DGA-based search approach is useful in dealing with both discrete and continuous design variables through the design optimisation of SPFs. The cross-sectional area of column and rafter represent the discrete variable, whereas the haunch length and depth represent the continuous variables.

5) Each of the mutation schemes have improved the performance of modified DGA. The linear mutation allows the algorithms to obtain the greatest number of best solutions among the ten runs of DO-DGA. The exponential mutation makes the algorithms converge to the optimum solutions more quickly than others. It also obtains the lightest average weight among ten runs of DO-DGA with the smallest standard deviation for the weights.

6) Use of either of the mutation schemes relies on the structural engineer's judgement. The exponential mutation is the best option if the aim is for quick convergence to an optimum solution. In addition, the exponential mutation gives a number of very similar solutions. This increases options for the structural engineer when deciding on the appropriate design for structural elements. Regardless of time, linear mutation can be the best option for achieving the best set of solutions within a given set of ten runs of DO-DGA.

7) The inverse mutation of linear mutation schemes failed to obtain the optimum solution. This justifies the use of varied mutation. The mutation with constant probability reaches the optimum solution only once in ten runs of DO-DGA.

8) The DO-DGA can handle any design problem related to plane steel structures and gives the promise of using the optimisation technique in the office by a structural engineer. Most importantly, the DO-DGA obtains the optimum solution for SPFs within six minutes in the worst case when using the exponential mutation scheme.

9) All convergences to the optimum solutions occur with the first group of the population. Since the best individuals of the second group in the population are allowed to migrate to the first group, the results demonstrate the effectiveness of the migration idea in improving the performance quality of first group.

10) Due to smaller load factor in EC3 to calculate the load combination, the design optimisation according to EC3 yields a lighter frame than BS 5950 for the SPFs that are subject to gravity and lateral wind loads. There is no difference in weight for the design according to BS 5950 and EC3 if the SPFs experience a heavy lateral concentrated load. This is because the optimum solution is controlled by the lateral displacement, for which the computation is based on working loads.

11) Application of semi-rigid connections leads to larger displacements of joints in SPFs. Since the optimum solutions for SPFs are controlled by displacement, assuming semi-rigid connections does not produce a lighter frame than with rigid connections.

12) By calibrating the finite element model developed by Mohammadi-shooreh and Mofid (2008) to compute the initial stiffness of semi-rigid connections, the same optimum solutions have been obtained as with the Frye-Morris model.

13) The maximum joint displacement of the optimum solutions controlled by displacement is with the vertical displacement of the apex. Due to the continuity that exists between the vertical and lateral displacements, any attempt to maximise the lateral displacement decreases the vertical displacement of the apex. This reduction of the vertical displacement necessitates having a stiff frame which is achieved by using deeper sections for the structural elements. As a result, the weight of frame increases compared with using the technique of weight minimisation.

14) Although the curved rafter SPF gives a better solution than the pitched-roof SPF in aesthetic terms, the design optimisation of SPFs with curved rafters

yields a heavier and more expensive frame than the pitched-roof rafter due to the longer period and cost of manufacturing.

15) The best optimum solutions do not possess the highest average strength and displacement ratios compared with the other solutions. The fully stressed members and fully displaced joints are not indications of the best optimum solution. Having observed that, the displacement maximisation failed to exhibit better results, the weight minimisation is the best criterion for assessing the best optimum solution.

16) The results indicate that the haunch part of the rafter is efficient in controlling excessive displacements rather than controlling the induced stresses by bending moment due to increasing in stiffness.

17) Increasing the span of the SPF will increase the negative bending moment and decrease the positive bending moment in the rafter.

18) The parametric study produced a number of graphs which can be used by the structural engineer to calculate the bending moments, axial and shear forces in rafter and column of SPFs without referring to structural analysis; at least at the initial stage of design. The graphs can be used to find the value to be used as a coefficient which is multiplied by factored applied loads and frame span.

19) And more importantly, the modified DGA can be used in any field of science that seeks to optimise (minimise and/or maximise) a defined objective function. For this purpose, the constraints may be changed to meet the requirements of another particular problem.

8.4 Suggestions for future works

The work conducted in this study has revealed many promising areas for further studies in the field of structural optimisation. Suggestions for areas of study following the current research are as follows:

1) Since the genetic parameters are sensitive, a comprehensive study is worthwhile to find an equation that defines the relationship between the

appropriate design variables, population size, minimum and maximum mutation probabilities, elite rate, migration rate, migration interval, and maximum number of generations so that the genetic parameters can be directly specified for a particular problem.

2) Large gravity loads that are applied to SPFs induce considerable lateral displacements. A geometrical non-linear analysis may be useful for design optimisation.

3) A dynamic analysis can be included in any design optimisation for those areas in the world which are subject to severe earthquakes.

4) The design problem may lead to a lighter frame when applying built-up sections. This makes it necessary to deal with the continuous variables rather than the discrete ones. Since the modified DGA has shown its capability in dealing with continuous variables, it is also able to handle the design problem.

5) A design optimisation can be performed to maximise the load carrying capacity of SPFs with different types of column supports.

6) A topology optimisation using the finite element method can be carried out to investigate the best shape of haunch and the best combination of the span, height of the column, shape of rafter and height of apex, provided that it does not affect the cost of manufacturing.

7) Nonlinear analysis of the SPF due to material plasticity might be worthwhile to consider in the design optimisation.

8) Design optimisation might be carried out for the whole SPF in 3D. This can be done by incorporating the number of frames, purlins, sheeting rails, and braces into the analysis part, as well as the optimisation processes of DO-DGA.

9) Considering semi-rigid connections will give the best optimum solution when the positive and negative bending moments in a steel beam are the same ($wL^2/16$). This will depend on the type of connection. An optimisation

process can be carried out on different types of connections to find the best parameters, such as plate dimensions and bolts, so that the positive bending moment equals to the negative bending moment as much as possible.

The developed algorithm has potential application in fields beyond structural engineering; GA are used in economics, mathematics, and other engineering sciences. Therefore, it is worth for the investigation into these improved algorithms and their potential to contribute to other academic areas.

References and Bibliography

References

Adeli, H., & Cheng, N. T. (1993). Integrated genetic algorithm for optimization of space structures. *ASCE Journal of Aerospace Engineering , 6* (4), 315 – 328.

Adeli, H., & Kumar, S. (1995). Distributed genetic algorithm for structural optimization. *ASCE Journal of Aerospace Engineering , 8* (3), 156 – 163.

Aggarwal, A. K., & Coates, R. C. (1986). Moment-rotation characteristics of bolted beam-column connections. *Journal of Constructional Steel Research , 6*, 303-318.

Akin, J. E., & Arjona-Baez, J. (2001). Enhancing structural topology optimization. *Engineering Computation , 18* (3/4), 663-675.

Al-khatab, Z., & Bouchaïr, A. (2007). Analysis of a bolted T-stub strengthened by backing-plate with regard to Eurocode 3. *Journal of Constructional Steel research , 63*, 1603-1615.

Al-Salloum, Y. A., & Almusallam, T. H. (1995). Optimality and safety rigidly- and flexible-jointed steel frames. *Journal of Constructional Steel Research , 35*, 189-215.

American Institute of Steel Construction (1986) *AISC*, *Load and Resistance Factor Design Specification for Structural Steel Buildings*, Chicago, IL

Aristizábal-Ochoa, J. D. (2001). Stability and second-order analysis of frames with semirigid connections under distributed axial loads. *ASCE Journal of Structural Engineering , 127* (11), 1306-1315.

Arora, J. S. (1989). *Introduction to optimum design* (2nd ed.). San Diego: McGraw Hil.

Arora, J. S., & Govil, A. K. (1977). An efficient method for optimal structural design by substructures. *Computers and Structures , 7*, 507-515.

Arora, J. S., Huang, M. W., & Hsieh, C. C. (1994). Method for optimization of non-linear problems with discrete variables: a review. *Structural Optimization , 8*, 69-85.

Atrek, E., Gallagher, R. H., Ragsdell, K. K., & Zienkiewicz, O. C. (1984). *New directions in optimum structural design.* New York: John Wiley & Sons.

Baddoo, N. R., Morrow, A. W., & Taylor, J. C. (1993). *C-EC3 Concise Eurocode 3 for the design of steel buildings in the United Kingdom.* Ascot: The Steel Construction Institute.

Bahaari, M. R., & Sherbourne, A. N. (1994). Computer modelling of an extended end-plate bolted connection. *Computers and Structures , 52* (5), 879-893.

Balling, R. J., Briggs, R. R., & Gillman, K. (2006). Multiple optimum size/shape/topology designs for skeletal structures using a genetic algorithm. *ASCE Journal of Structural Engineering , 132* (7), 1158 – 1165.

Barakat, M. A., & Chen, W. F. (1991). Design analysis of semi-rigid frames; evaluation and implementation. *Engineering Journal , 28* (2), 55-64.

Bigelow, R. H., & Gaylord, E. H. (1967). Design of steel frames for minimum weight. *ASCE Journal of Structure Division , 93* (6), 109-131.

Bjorhovde, R., Colson, A., & Brozzetti, J. (1990). Classification system for beam-to-column connections. *ASCE Journal of Structural Engineering , 116* (11), 3059-3076.

Boyd, S. W., Blake, J. I., Shenoi, R. A., & Mawella, J. (2007). Optimisation of steel-composite connections for structural marine applications. *Composites Part B: Engineering , 39* (5), 891-906.

British Standard Institution. (1990). *BS 5950: 1990 Structural use of steelworks in building. Part 1. Code of practice for design in simple and continuous construction, hot rolled section.* London.

British Standard Institution. (1995). *BS6399: Part 2 Loading for Building Part2, Code of Practice for Wind Load.* London.

British Standard Institution. (1996). *BS6399: Part 1 Loading for Building Part2, Code of Practice for Dead and Imposed Loads.* London.

Cabrero, J. M., & Bayo, E. (2005). Development of practical design methods for steel structures with semi-rigid connection. *Engineering Structures , 27*, 1125-1137.

Camp, C. V., Bichon, B. J., Stovall, & P, S. (2005). Design of steel frames using ant colony optimization. *ASCE Journal of Structural Engineering , 131* (3), 369-379.

Camp, C., Pezeshk, S., & Cao, G. (1998). Optimum design of two-dimensional structures using a genetic algorithm. *ASCE Journal of Structural Engineering , 124* (5), 551 – 559.

Castro, R. A., da Silva, J. G., da S. Vellasco, P. C., de Lima, L. R., de Andrade, S. A., & da C. Neves, L. F. (2007). Dynamic response of steel portal frames with

semi-rigid joints. In B. H. Topping (Ed.), *Proceeding of the 11th International Conference on Civil, Structural and Environmental Engineering Computing* (pp. 1-20). Stirlingshire: Civil-Comp Press.

CEN (EN 1993-1-1:2005). (2005). EC3: Design of steel structure, Part 1-1: General rules and rules for building.

CEN (EN 1993-1-5:2005). (2005). EC3: Design of steel structure, Part 1-5: Plated structural elements.

CEN (EN 1993-1-8:2005). (2005). EC3: Design of steel structure, Part 1-8: Design of joints.

Chan, C., & Liu, I. W. (1989). Optimal design based on optimality criterion for frame structure including buckling constraints. *Computer and Structures , 31* (4), 535-544.

Chan, C., Sherbourne, A. N., & Grierson, D. E. (1994). Stiffness optimization technique for 3D tall steel building frameworks under multiple lateral loadings. *Engineering Structures , 16* (8), 570-576.

Chan, S. L., Huang, H. Y., & Fang, L. X. (2005). Advanced analysis of imperfect portal frames with semi-rigid base connection. *ASCE Journal of Engineering Mechanics , 131* (6), 633-340.

Chen, W. F., & Lui, E. M. (1991). *Stability design of steel frames.* London: CRC Press.

Chen, W. F., Goto, Y., & Liew, J. Y. (1996). *Stability design of semi-rigid frames.* New York: John Wiley & Sons.

Chui, P. P., & Chan, S. L. (1996). Transit response of moment-resistant steel frames with flexible and hysteretic joints. *Journal of Constructional Steel Research , 39* (3), 221-243.

Cohn, M. Z., & Dinovitzer, A. S. (1994). Application of structural optimisation. *ASCE Journal of Structural Engineering , 120* (2), 617-650.

Coley, D. A. (2005). *An introduction to genetic algorithms for scientist and engineers.* Singapore: World Scientific Publishing Co.

de Andrade, S. A., da S. Vellasco, P. C., Ferreira, L. T., & de Lima, L. R. (2007). Semi-rigid composite frames with perfobond and T-rib connectors Part2: Design models assessment. *Journal of Constructional Steel Research , 63*, 280-292.

Degertekin, S. O., & Hayalioglu, M. S. (2004). Design of non-linear semi-rigid steel frames with semi-rigid column bases. *EJSE Electronic Journal of Structural Engineering , 4*, 1-16.

Degertekin, S. O., Saka, M. P., & Hayalioglu, M. S. (2008). Optimal load and resistance factor design of geometrically nonlinear steel space frames via tabu search and genetic algorithm. *Engineering Structures , 30*, 197-205.

Del Savio, A. A., Martha, L. F., de Andrade, S. A., da Silva Vellasco, P. C., & de Lima, L. R. (2005). Structural modelling of vierendeel beams with semi-rigid joints. *Proceeding of the XXVI Iberain Latin-American Congress on Computational Methods in Engineering.* Espirito Santo: CILAMCE.

Dhillon, B. S., & O'Malley III, J. (1999). Interactive design of semi-rigid steel frames. *ASCE Journal of Structural Engineering , 125* (5), 556-564.

Easton, F. F., & Mansour, N. (1999). Theory and methodology of a distributed genetic algorithm for deterministic and stochastic labour scheduling problems. *European Journal of Operational Research , 188*, 505-523.

Erbatur, F., & Al-Hussainy, M. M. (1992). Optimum design of frames. *Computer and Structures , 45* (5/6), 887-891.

Fang, L. X., Chan, S. L., & Wong, Y. L. (1999). Strength analysis of semi-rigid steel concrete composite frames. *Journal of Constructional Steel Research , 52*, 269-291.

Filho, M. S., Guimarães, M. J., Sahlit, C. L., & Birto, J. L. (2004). Wind pressure in framed structure with semi-rigid connections. *Journal of the Brazilian Society of Mechanical Science and Engineering , XXVI* (2), 180-189.

Foley, C., & Schinler, D. (2003). Automated design of steel frames using advanced analysis and object-oriented evolutionary computation. *ASCE Journal of Structural Engineering , 129* (5), 648 – 660.

Fraser, D. J. (1983). Design of tapered member portal frames. *Journal of Constructional Steel Research , 3* (3), 20-26.

Friedberg, S., & Insel, A. (1986). *Introduction to linear algebraic with applications.* New York: Prentice-Hall.

Frye, M. J., & Morris, G. A. (1975). Analysis of flexibly connected steel frames. *Canadian Journal of Civil Engineering , 2* (3), 280-291.

Garai, G., & Chaudhuri, B. B. (2007). A distributed hierarchical algorithm for efficient optimization and pattern matching. *Pattern Recognition , 40*, 212-218.

Gere, J. M., & Timoshenko, S. P. (1999). *Mechanics of materials* (4 ed.). Cheltenham: Stanley Thornes.

Gero, M. B., García, A. B., & del Coz Díaz, J. J. (2006). Design optimization of 3D steel structures: Genetic algorithms vs. classical technique. *Journal of Constructional Steel Research , 62*, 1303-1309.

Ghali, A., Neville, A. M., & Brown, T. G. (2003). *Structural Analysis; A Unified Classical and Matrix Approach* (5th ed.). New York: Spon Press.

Ghasemi, M. R., Hinton, E., & Wood, R. D. (1999). Optimization of trusses using genetic algorithms for discrete and continuous variables. *Engineering Computation , 16* (3), 273–301.

Goldstein, L. J., Lay, D. C., & Schneider, D. I. (1987). *Calculus and its applications.* New York: Prentice-Hall.

Golub, G. H., & Van Loan, C. F. (1989). *Matrix computation* (2nd ed.). London: The John Hopkins University Press.

Goto, Y., & Miyashita, S. (1998). Classification system for rigid and semi-rigid connections. *ASCE Journal of Structural Engineering , 124* (7), 750-757.

Grawley, S. W., & Dillon, R. M. (1993). *Steel buildings; analysis and design* (4th ed.). New York: John Wiley & Sons.

Grierson, D. E., & Chan, C. M. (1993). Optimality criteria design method for tall steel buildings. *Advances in Engineering Software , 16* (2), 119-125.

Gutkowski, W., Bauer, J., & Zawidzki, J. (2000). An effective method for discrete structural optimization. *Engineering Computation , 17* (4), 417-426.

Gutkowski, W., Zawidzki, J., Laplume, D., Guerlement, G., & Boulanger, S. (2000). Realistic minimum weight design of steel framework. In M. Ivanyi, J. P. Muzeau, & B. H. Topping (Ed.), *Computational Steel Structure Technology* (pp. 147-153). Edinburgh: Civil-Comp Presss.

Hajela, P. (1990). Genetic search-an approach to the nonconvex optimization problem. *AIAA Journal , 28*(*7*), 1205-1210.

Hasançebi, O., & Erbatur, F. (2000). Evaluation of crossover techniques in genetic algorithm based optimum structural design. *Computer and Structures , 78*, 435-448.

Hegazy, T., & Kassab, M. (2003). Resource optimization using combined simulated annealing and genetic algorithms. *Journal of Construction Engineering and Management , 129* (6), 698-705.

Ivany, M., & Baniotopoulos, C. C. (2000). *Semi-rigid joints in structural steelwork.* Udine: Springer-Verlag Wien New York.

Jaspart, J. P. (2000). General report: session on connection. *Journal of Constructional Steel Research , 55*, 69-89.

Joghataie, A., & Asbmarz, M. M. (2008). Vibration Controller Design for Confined Masonry Walls by Distributed Genetic Algorithms. *ASCE Journal of Structural Engineering , 134* (2), 300-309.

Jones, S. W., Kirby, P. A., & Nethercot, D. A. (1980). Effectt of semi-rigid connections on steel column strength. *Journal of Constructional Steel Research , 1* (1), 38-46.

Kameshki, E. S., & Saka, M. P. (2001). Optimum design of non-linear steel frames with semi-rigid connection using a genetic algorithm. *Computer and Structures* , 1593-1604.

Kargahi, M., Anderson, J. C., & Dessouky, M. M. (2006). Structural optimization of frames using tabu search. I: optimization procedure. *Journal of Structural Engineering , 132* (12), 1858-1868.

Kattner, M., & Crisinel, M. (2000). Finite element modelling of semi-rigid composite joints. *Journal Computer and Structures , 78*, 341-353.

Kishi, N., & Chen, W. F. (1990). Moment-rotation relations of semirigid connections with angles. *ASCE Journal of Structural Engineering , 116* (7), 1813-1834.

Krajnc, A., & Beg, D. (2009). Heuristic approach to steel frame structural optimisation. In M. Ivanyi, J. P. Muzeau, & B. H. Topping (Ed.), *Computational Steel Structures Technology* (pp. 155-164). Edinburgh: Civil-Comp Press.

Kripakaran, P., Gupta, A., & Baugh Jr, J. W. (2007). A novel optimization approach for minimum cost design of trusses. *Computers and Structures , 85* (23-24), 1782-1794.

Law, S. S., Wu, D., & Shi, Z. Y. (2001). Model updating of semirigid jointed structure using generic parameters. *ASCE Journal of Engineering Mechanics , 127* (11), 1174-1183.

Lee, Z. J., Su, S. F., Chuang, C. C., & Liu, K. H. (2008). Genetic algorithm with ant colony optimization (GA-ACO) for multiple sequence alighnment. *Applied Soft Computing , 8*, 55-78.

Li, G. Q., & Li, J. J. (2007). *Advanced analysis and design of steel frames.* Chichester: John Wiley & Sons.

Liu, X., Yi, W. J., Li, Q. S., & Shen, P. S. (2007). Genetic evolutionary structural optimization. *Journal of Constructional Steel Research , 5*, 346-358.

Lorenz, R. F., Kato, B., & Chen, W. F. (1993). *Semi-rigid connections in steel frames.* New York: McGraw-Hill.

Machaly, E. S. (1986). Optimum weight analysis of steel frames with semirigid connections. *Computer and Structures , 23* (4), 461-474.

Mahfouz, S.Y. (1999) Design optimization of steelwork structures. *PhD thesis*, University of Bradford.

Majid, K. I., & Elliot, D. W. (1971). Optimum design of frames with deflection constraints by non-linear programming. *Structural Engineer , 49* (4), 179-188.

Man, K. F., & Kwong, S. (1999). *Genetic algorithms; concept and design.* London: Springer.

Majid, K. I. (1974). *Optimum design of structures.* London: Butterworth & Co.

Masika, R. J., & Dunai, L. (1995). Behaviour of bolted end-plate portal frame joints. *Journal of Constructional Steel Research , 32*, 207-225.

McCormac, J. C. (2007). *Structural analysis; using classical and matrix method* (4th ed.). New York: John Wiley & Sons.

McGuire, W., Gallegher, R. H., & Ziemian, R. D. (2000). *Matrix structural analysis.* New York: John Wiley & Sons.

McKenzie, W. M. (1998). *Design of Structural Steelwork.* London: McMillan Press.

Mitchell, M. (1999). *An introduction to genetic algorithms.* New York: Massachusetts Institute of Technology.

Mohammadi-shooreh, M. R., & Mofid, M. (2008). Parametric analysis on the initial stiffness of flush-end-plate splice connection using FEM. *Journal of Constructional Steel Research , 64*, 1129-1141.

Mühlenbein, H., Schomisch, M., & Born, J. (1991). The parallel genetic algorithms as a function optimizer. *Parallel Computing , 17*, 619–632.

Park, H. S., Kwon, H. Y., Seo, J. H., & Woo, B. H. (2006). Journal of Structural Engineering. *Distributed hybrid genetic algorithms for structural optimization on a PC cluster , 132* (12), 1890-1897.

Pease, M. C. (1965). *Method of matrix algebra.* New York: Academic Press.

Pezeshk, S., Camp, C. V., & Chen D. (2000). Design of non-linear framed structures using genetic optimization. *ASCE Journal of Structural Engineering , 126* (3), 382 – 388.

Pyrz, M., & Zawidzka, J. (2001). Optimal discrete truss design using improved sequential and genetic algorithm. *Engineering Computation , 18* (8), 1078-1090.

Rajeev, S., & Krishnamoorthy, C. S. (1992). Discrete optimization of structures using genetic algorithm. *ASCE Journal of Structural Engineering , 118* (5), 1233–50.

Rajeev, S., & Krishnamoorthy, C. S. (1997). Genetic algorithm-based methodologies for design optimization of truss. *Journal of Structural Engineering , 123* (3), 350 – 358.

Sack, R. (1989). *Matrix structural analysis.* PWS-Kent Publishing Company.

Saka, M. P. (2003). Optimum design of pitched roof steel frames with haunched rafter by genetic algorithms. *Computers and Structures , 81*, 1967 – 1978.

Saka, M. P. (2009). Optimum design of steel sway frames to BS5950 using harmony search algorithms. *Journal of Constructional Steel Research , 65* (1), 36-43.

Saka, M. P. (2007). Optimum design of steel sway frames to BS 5950 using search harmony algorithm. In B. H. Topping (Ed.), *Proceeding of the 11th International Conference on Civil, Structural and Environmental Engineering Computing* (pp. 1-20). Stirlingshire: Civil-Comp Press.

Saka, M. P., & Hayalioglu, M. S. (1991). Optimum design of geometrically nonlinear elastic-plastic steel frames. *Computers and Structures , 38* (3), 329-344.

Saka, M. P., & Kameshki, E. S. (1998). Optimum design of un-braced rigid frames. *Computers and Structures , 69* (4), 433-442.

Salter, P. R., Malik, A. S., & King, C. M. (Eds.). (2004). *Design of single-span steel portal frames to BS 5950-1:2000.* Ascot: The steel Construction Institute.

Schneider, D. I. (2004). *An introduction to programming using visual basic 6.0* (4th ed.). New Jersey: Pearson Prentice Hall.

Serna, M. A., López, A., Puente, I., & Yong, D. J. (2006). Equivalent uniform moment factors for lateral-torsional buckling of steel members. *Journal of Constructional steel Research , 62*, 566 – 580.

Sibai, W. A., & Frey, F. (1993). New semi-rigid joint elements for non-linear analysis of flexibly connected frames. *Journal of Constructional Steel research , 25*, 185-199.

Starkweather, T., Whitley, D., & Mathias, K. (1990). Optimization using distributed genetic algorithms. *Springer-Verlag lecture notes in computer science , 496*, 176–185.

Taylor, J. C., Baddoo, N. R., Morrow, A. W., & Gibbons, C. (1999). *Steelwork design guide to Eurocode 3: part 1.1 – introducing Eurocode 3* (3rd ed.). Berkshire: The Steel Construction Institute.

Toropov, V. V., & Mahfouz, S. Y. (2001). Design optimization of structural steelwork using a genetic algorithm, FEM and a system of design rules. *Engineering Computations , 18* (3/4), 437-459.

Tranhair, N. S., Bradford, M. A., Nethercot, D. A., & Gardner, L. (2008). *The behaviour and design of steel structures to EC3*. London: Taylor & Francis.

Vanderplaats, G. N., & Sugimoto, H. (1986). A general-purpose optimization program for engineering design. *Computers and Structures , 24* (1), 13-21.

Wang, Q., & Arora, J. S. (2006). Alternative formulation of structural optimization: an evaluation using frames. *Journal of Structural Engineering , 132* (12), 1880-1889.

Weaver, W., & Gere, J. M. (1980). *Matrix analysis of framed structures* (2nd ed.). New York: Nostrand Company.

White, J. W. (1978). *Advanced structural analysis; worked example examples.* London: William Clowes & Sons.

Willems, N., & Lucas, W. M. (1978). *Structural Analysis for Engineers.* Tokyo: McGraw–Hill.

Yourdan, E., & Constantine, L. L. (1979). *Structural design; foundamentals of a discipline of computer program and systems design.* New Jersey: Prentice-Hall.

Bibliography

Adeli, H., & Cheng, N. T. (1994). Concurrent genetic algorithm for optimization of large structures. *ASCE Journal of Aerospace Engineering , 7* (3), 276–96.

Adeli, H., & Sarma, K. C. (2006). *Cost optimization of structures; fuzzy logic, genetic algorithms, and parallel computing.* Chichester: John Wiley & Sons.

Allwood, R. J., & Chung, Y. S. (1984). Minimum weight design of truss by an optimality criteria method. *International Journal of the Numeric Methods in Engineering , 20*, 697 – 713.

Arora, J. S. (1980). Analysis of optimality criteria and gradient projection methods for optimum structural design. *Computer Method Application in Mechanical Engineering , 23*, 185 – 213.

Barakat, M. A. (1989). Simplified design analysis of frames with semi-rigid connection. *PhD Dissertation* . New York University, Department of Civil Engineering.

Barakat, M. A., & Chen, W. F. (1990). Practical analysis of semi-rigid frames. *Engineering Journal , 28* (2), 55-64.

Bhatt, P. (1986). *Programming the matrix analysis of skeletal structures.* New York: Halsted Press.

Bhatt, P., & Nelson, H. M. (1990). *Marshal and Nelson's structures* (3rd ed.). London: Longman Scientific & Technical Longman Group.

Brant, A. M., Dzieniszewski, W., Jendo, S., Marks, W., Owczarek, S., & Wasiutynski, Z. W. (1984). *Criteria and methods of structural optimization.* Warszawa: PWN-Polish Scientific Publisher.

Bunday, B. D. (1984). *Basic optimisation method.* London: Edward Arnold.

Chang, K. J. (1992). Optimality criteria method using K-S functions. *Structural Optimizatoin , 4*, 213 – 217.

Chen, I. H., & Chen, W. F. (2000). Practical advanced analysis in seismic design of steel building frames and 1997 LRFD evaluation. In M. Ivanyi, J. P. Muzeau, & B. H. Topping (Ed.), *Proceeding of International Conference on Computational Steel Structures Technology* (pp. 131-145). Edinburgh: Civil-Comp Press.

Chen, W. F. (1994). *Advanced analysis of steel frames; theory, software, and applications.* New York: CRC Press.

Chamber, L. (2001). *The practical handbook of genetic algorithms application* (2nd ed.). Washington DC: Chapman & Hall.

Coates, R. C., Couite, F. K., & Kong, F. K. (1997). *Structural analysis.* London:

Chapman & Hall.

Colson, A. (1991). Classification of connection for beam-to-column connections. Tentative document for circulation to members of SSRC.

Davis, L. (1991). *Handbook of Genetic Algorithms.* New York: Van Nostrand Reinhold.

Davison, B., & Owens, G. W. (2003). *Steel designer's manual* (6th ed.). Oxford: Blackwell Scientific Publication.

de Lima, L. R., de Andrade, S. A., Vellasco, P. C., & da Silva, L. S. (2002). Experimental and mechanical model for predicting the behaviour of minor axis beam-to-column semi-rigid joints. *International Journal of Mechanical Sciences , 44*, 1047–1065.

Fisher, C. (2001). Analysis and design of semi-continuous sway and non-sway frames. *PhD Thesis* . University of Southampton.

Fleury, C. (1979). Structural weight optimization by dual methods of convex programming. *International Journal of Numerical Methods in Engineering , 14*, 1761-1783.

Fleury, C., & Geradin, M. (1978). Optimality criteria and mathematical programming in structural weight optimization. *Computer and Structure , 8*, 7-17.

Gellaty, R. A., & Berk, L. (1971). *Optimal structural design.* Air Force Flight Dynamic Laboratory. Ohio: Wright-Patterson Air Force Base.

Goldberg, D. E. (1989). *Genetic Algorithms in search, optimization and machine learning.* New York: Addison-Wesley Publishing Company.

Grierson, D. E., & Pak, W. H. (1993). Optimal sizing, geometrical and topological design using genetic algorithms. *Structure Optimization , 6*, 151-159.

Harrison, H. B. (1980). *Structural analysis and design; some mini-computer application* (Vol. 2). Oxford: Pergamon Press.

Holland, J. H. (1975). *Adaptation in natural and artificial systems.* Michigan: University of Michigan Press.

Horne, M. R., & J, M. L. (1971). *Plastic design of low-rise frames.* London: Granada Publishing.

Khan, M. R., Willmert, K. D., & Thornton, W. A. (1979). An optimality criteria method for large scale structures. *AIAA Journal , 17* (7), 753-761.

Khot, N. S., Venkayya, V. B., & Berke, L. (1973). *Optimization of structures for strength and stability requirements.* Air Force Flight Dynamic Laboratory. Ohio: Wright-Patterson Air Force Base.

Kim, Y., & Chen, W. F. (1998). Practical analysis for partially restrained frame design. *ASCE Journal of Structural Engineering , 124* (7), 736-749.

Kirsch, U. (1981). *Optimum structural design; concepts, methods and applications.* New York: McGraw-Hill.

Krisch, U. (1991). Feasibility and optimality in structural design. *Computer and Structures , 41* (6), 1349 – 1356.

Liew, J. Y. (1992). Advanced analysis for frame design. *PhD Dissertation* . Purdue University, School of Civil Engineering.

Liew, J. Y., White, D. W., & Chen, W. F. (1993b). Limit state design of semi-rigid frames using advanced analysis; II. Analysis and design. *Journal of Constructional Steel research , 26* (1), 29-57.

Liew, J. Y., White, D. W., & Chen, W. (1993a). Limit state design of semi-rigid frames using advanced analysis; I. Connection modelling and classification. *Journal of Constructional Steel research , 26* (1), 1-27.

Lim, J. B., King, C. M., J., R. A., Davis, J. M., & Edmonson, V. (2005). Eurocode 3 and in-plane stability of steel portal frames. *The Structural Engineer , 83*, 43-49.

Lin, C. C., & Liu, I. W. (1999). Optimal design based on optimality criterion for frame structures including buckling constraints. *Computer and Structures , 31* (4), 535 – 544.

Lin, C. Y., & Hajela, P. (1992). Genetic algorithms in optimization problem with discrete and integer variables. *Engineering Optimization , 19*, 309-327.

Luo, Y. Z., Xu, X., & Wu, F. (2007). Accurate stiffness matrix for non-prismatic members. *ASCE Journal of Structural Engineering , 133* (8), 1168-1175.

Mahendran, M., & Moor, C. (1999). Three-dimensional modelling of steel portal frame building. *ASCE Journal of Structural Engineering , 125* (8), 870-878.

Mattheck, C., & Burkhardt, S. (1990). A new method of structural shape optimization based on biological growth. *International Journal of Fatigue , 1*, 36-79.

McGinley, T. J. (2002). *Steel structures; practical design studies* (2nd ed.). London: Spon Press.

McKenzie, W. M. (2006). *Examples in structural analysis.* London: Taylor & Francis.

Meek, J. L. (1991). *Computer method in structural analysis.* London: Chapman & Hall.

Michalewicz, Z. (1996). *Genetic Algorithm + Data Structures = Evolution Programs* (3rd ed.). New York: Springer-Verlag.

Mills, J., & LaBoube, R. (2004). Self-drilling screw joints for cold-formed channel portal frames. *Journal of Structural Engineering , 130* (11), 1799-1806.

Narayanan, R., Lawless, V., Naji, F. J., & Taylor, J. C. (1993). *Introduction to concise Eurocode 3(C-EC3) – with worked examples.* Ascot: The Steel Construction Institute.

Onwubico, C. (2000). *Introduction to engineering design optimization.* New Jersey: Prentice-Hall.

Owens, W. G., Khowels, P. P., & Dowling, P. J. (1992). *Steel designers manual* (5th ed.). Oxford: Blackwell Scientific Publication.

Rajan, S. D. (1995). Sizing, shape and topology design optimization of truss using genetic algorithms. *ASCE Journal of Structural Engineering , 121* (10), 1480-1487.

Rizzi, P. (1976). Optimization of multi-constrained structures based on optimality criteria. *Proeeding AIAA/ASME/SAE 17th Structure Dynamic and Mathematic Conference.* King of Prussia.

Rockey, K., Evans, H., Griffiths, D., & Nethercot, D. A. (1983). *The finite element method* (2nd ed.). London: Collins.

Rozvany, G. I., & Zhou, M. (1993). Continuum-based optimality criteria (COC) methods: an introduction, in optimization of large structural systems. *Proceeding Conference of NATO/DFG ASI*, (pp. 1-26). Dordrecht.

Rozvany, G. I., & Zhou, M. (1991). The COC algorithms, part I: cross section optimization or sizing. *Computer Method in Applied Mechanic and Engineering , 89*, 281-309.

Rozvany, G. I., Zhou, M., & Gollub, W. (1990). Continuum-type optimality criteria methods for large finite element systems with a displacement constraints-part II. *Structure Optimization , 2*, 77-104.

Rozvany, G. I., Zhou, M., Gollub, W., & Spengemann, F. (1989). Continuum-type optimality criteria methods for large finite element systems with a displacement constraints-part I. *Structure Optimization , 1*, 47-72.

Saka, M. P. (1979). Optimum design of rigidly jointed frames. *Computers and Structures , 11*, 411-419.

Saka, M. P. (1991). Optimum design of steel frames with stability constraints. *Computer and Structures , 41* (6), 1365 – 1377.

Saka, M. P. (2007). Optimum topological design of geometrically nonlinear single layer latticed domes using coupled genetic algorithm. *Computers and Structures , 85*, 1635-1646.

Save, M., & Prager, W. (1985). *Structural optimization; volume 1: optimality criteria.* New York: Plenum Press.

Save, M., Prager, W., Borkowski, A., & Jendo, S. (1990). *Structural optimization; volume 2: mathematical programming.* New York: Plenum Press.

Tabak, E. I., & Wright, P. M. (1981). Optimality criteria methods for building frames. *ASCE Journal of Structural Engineering , 107* (7), 1327-1342.

Turner, H. K., & Plaut, R. H. (1980). Optimum design for stability under multiple loads. *ASCE Journal of Engineering Mechanics , 106* (6), 1365-1382.

Utku, S., Norris, C. H., & Wilbur, J. B. (1991). *Elementary structural analysis.* McGraw-Hill.

Wang, H. L., Zhang, Z., Huang, C. L., & Shi, L. (2006). A fuzzy optimum model to asses bridge design options. *Bridge Engineering , 159*, 9-15.

Wang, Z. M. (1996). Behaviour of unstiffened flush end plate beam-to-column connection in structural steelwork. *PhD Thesis* . University of Abertay Dundee.

Weynand, K. (1999). *Semi-rigid behaviour of civil engineering structural connections; Cost C1: column bases in steel building frames.* Brussels: European Commission.

Xie, Y. M., & Steven, G. P. (1992). A simple evolutionary procedure for structural optimization. *Computer and Structures , 149*, 885-896.

Xu, L. (2001). On the minimum-maximum bending moment and the least weight design of semi-rigid beams. *Journal of the International Society for Structural and Multidisciplinary Optimization , 21*, 316-321.

Zalzala, A. M., & Fleming, P. J. (1997). *Genetic algorithms in engineering systems.* Herts: The Institution of Electrical Engineers.

Appendix: List of Publications

A number of papers and posters were presented at different conferences across the world, generated from some parts of the current research study. These are cited as follows:

Issa, H. K. (2008). Investigating the optimum design of steel portal frames with semi-rigid joints. Young Researchers' Conference. London: IStructE.

Issa, H. K., & Mohammad, F. A. (2008). Investigating the optimum design of steel portal frames using genetic algorithms. In M. Casensky, V. Ahmed, D. Eaton, & M. Sutrisna (Ed.), *BuHu 8th International Postgraduate Research Conference. 2*, pp. 35-48. Prague: University of Salford.

Issa, H. K. (2009). Design optimisation of semi-rigidly connected steel portal frames using modified distributed genetic algorithms. The Young Researchers' Conference. London: The Institution of Structural Engineers.

Issa, H. K., & Mohammad, F. A. (2009). Weight and displacement optimizations of steel portal frames to Eurocode 3 using distributed genetic algorithms. In H. C. Rodrigues, J. M. Guedes, P. R. Fernandes, J. O. Folgado, & M. M. Neves (Ed.), *8th World Congress on Structural and Multidisciplinary Optimization.* Lisbon: International Society for Structural and Multidisciplinary Optimization, ISSMO.

Issa, H. K., & Mohammad, F. A. (2009). Displacement maximisation of haunched-raftre pitched-roof steel portal frames. In S. Hernández, & C. A. Brebbia (Ed.), *Computer Aided Optimum Design in Engineering XI* (pp. 143-154). Algarve: WIT Press.

Issa, H. K., & Mohammad, F. A. (2009). Practical non-prismatic stiffness matrix for haunched-rafter of pitched-roof steel portal frames. In N. Ghafoori (Ed.), Challenges, Opportunities, and Solutions in Structural Engineering and Construction, ISEC-5 (pp. 167-171). Las Vegas: CRC Press, Taylor & Francis Group.

Issa, H. K., & Mohammad, F. A. (2010). Effect of mutation schemes on convergence to optimum design of steel frames. *Journal of Constructional Steel Research*. [online] pp. 1-8. Available at: http://www.sciencedirect.com/ doi: 10.1016/j.jscr.2010.02.002

[Accessed 10 March 2010].

A poster entitled as 'Investigating the optimum design of steel portal frames with semi-rigid joints' was presented at 'Young Researchers' Conference 2008' in March 2008. The conference was organised by 'Institute of Structural Engineers' in London, UK. The first page is shown below:

Name of Delegate: **Honar Issa** **Abstract No. 18**
honar.issa@ntu.ac.uk

Research Organisation: **Nottingham Trent University**

Project Title: **Investigating the optimum design of steel portal frames with semi-rigid joints**

Question: Does the minimum weight of steel portal frame give the minimum cost?

Description:
Steel portal frames are common single storey buildings for construction in the UK; it is estimated that 50% of the single storey steel work buildings are constructed by portal frames. The steel portal frame will be the best option for single storey buildings in countries which are at a reconstruction stage. After the war, Iraq and specifically the Kurdistan Region has stepped into a new stage of reconstruction which will require more buildings with steel portal frames; a lot of factories and single storey buildings are necessarily in demand.

The attempt is made to implement different types of steel portal frames and their behaviour will be investigated. The selection criterion relies on their popularity in practice. Pitched roof and curved steel portal frames are the major single storey building in demand. The optimization technique will be implemented on both types of steel portal frames.

A genetic algorithm, which is the recent addition to optimisation technique, will be used for optimum design of different types of steel portal frames. The method is implemented to output the minimum weight of the frames. In addition, a fuzzy optimisation is used to compare with the genetic algorithm for both types of steel portal frames. For both optimization techniques a nonlinear program will be employed. The program will use the design constraints of both BS5950 and EC3 for optimum design.

A mathematical model for semi-rigid joints will be chosen based on previous works achieved in this field. The stiffness matrix for each member will be constructed and then analysis will be performed. On the other hand, an analysis for rigid connections will be done to make a comparison between the semi-rigid and rigid joints.

Results:
1. The output will be two different designed cross sections for both steel portal frames which consequents two different total weight of the frames. As a result, the more efficient frame will be specified.

2. Both optimisation methods will be examined to find out which method is more efficient. The comparison for better convergence to global optimisation will be made between both types of optimisation techniques.

3. Two different results of optimum design using rigid and semi-rigid connection will make it possible to discuss the adopted optimisation techniques concerned with the two steel portal frames. The question of whether optimum design with semi-rigid joint gives the minimum cost for both steel portal frames will be investigated.

A paper entitled as 'Investigating the optimum design of steel portal frames using genetic algorithms' was presented at 'BuHu 8th International Postgraduate Research Conference' in June 2008. The conference was organised by 'University of Salford' in Prague, Czech Republic. The first page is shown below:

In M. Casensky, V. Ahmed, D. Eaton, & M. Sutrisna (Ed.), *BuHu 8th International Postgraduate Research Conference, Vol. 2*

Investigating the Optimum Design of Steel Portal Frame Using Genetic Algorithms

Honar K. Issa[1] and Fouad A. Mohammad[2]

[1] PhD Candidate, Structural Engineering, Nottingham Trent University
[2] Senior Lecturer, Structure Analysis and Design, Nottingham Trent University
Email: honar.issa@ntu.ac.uk & fouad.mohammad@ntu.ac.uk

Abstract

This paper presents a structural optimisation based on modified distributed genetic algorithm (DGA) as a family of parallel genetic algorithm. The technique is developed to deal with discrete optimisation of steel portal frame. In order to have a realistic design and imitate the displacement and strength limitations, the DGA has been linked to BS5950 code of practice. Although the appearance of steel portal frames is simple, many complicated limitations and different structural criteria which are considered in complex structures must be taken into account. As the behaviour of steel portal frames necessitates using universal beam for both column and rafter, the algorithm selects the universal beam cross-sections from a standard table given in code of practice. In addition, it determines the minimum length and depth of haunch satisfying the limitations in order to reduce the weight and reach the most cost-effective form. Formulation of the design is based on elastic method. The objective function is in terms of total weight of frame as it gives a reasonable accurate cost of frame. A pitched roof steel portal frame has been designed to check its practicability.

Keywords: Steel Portal Frames, Optimisation, Distributed Genetic Algorithm

Introduction

Single storey buildings are widely used in the UK; it is estimated that 50% of the single storey steel work buildings are constructed by portal frames (Salter et al, 2004). Because of its economy and versatility for large spans in construction of pitched roofs like shopping centres, warehouses, retail shops, pools, factories, etc, the steel portal frame has become the most often used structure within this sector. Furthermore, those aforementioned places need to have a large span without using intermediate columns and therefore it necessitates using steel portal frames whereas the steel yields economical solution for large spans (Saka, 2003). A number of steel portal frames are commonly available of which the pitched roof type is more popular. The design of steel portal frames can be carried out using either elastic or plastic methods.

Any structural designer attempts to conduct an economical design. This can be achieved by formulating a design problem as an optimisation problem and solving by a systematic way of optimisation and considering the limitations of a code of practice to control the safety of the structure (Toropov and Mahfouz, 2001). However, due to large number of iterations in implementing the optimisation technique, it cannot be achieved by using the designer's experiences and intuition. Optimisation is a mathematical way to seek the minimum and maximum of a certain function. As the major cost of structural steelwork is its own weight, it has been endeavoured to minimise the weight using a systematic way of optimisation. In general, optimisation technique in structural engineering can be categorised into three different approaches: 1) Mathematical programming, 2) Optimality criteria methods and 3) Heuristic search technique (Camp et al. 1998). During the past decades, the attempts have been made to use any of the three aforementioned methods, see for example the work of Rizzi (1976); Arora (1980); Allwood and Chung (1984); Lin and Liu (1989); Krisch (1991); Saka (1991); Chang (1992) and Rozvany & Zhou

A poster entitled as 'Design optimisation of semi-rigidly connected steel portal frames using modified distributed genetic algorithms' was presented at 'Young Researchers' Conference 2009' in March 2009. The conference was organised by 'Institute of Structural Engineers' in London, UK. The first page is shown below:

Design optimisation of semi-rigidly connected steel portal frames using modified distributed genetic algorithms

Honar Issa
honar.issa@ntu.ac.uk
Trent University

14

Poster presenter

Steel portal frame (SPF) is the most popular structure for single storey buildings. Due to its ability to withstand the heavy loads with large span, steel portal frame has frequently been used in shopping and leisure centres, factories, and warehouses, as these kinds of the structures necessitate the elimination of intermediate columns. Considering this fact, performing an optimisation technique on this type of frame will maximise cost-effectiveness.

The nature of structural optimisation necessitates selecting the steel section from standard steel tables which defines the design variables as discrete. In contrast to the other optimisation techniques, a genetic algorithm (GA) can efficiently deal with discrete design variables. However, a conventional genetic algorithm has a low-speed operation and some modifications are required to improve its performance. A distributed genetic algorithm (DGA) is a member of the GA family in which a number of the population group undergo genetic operations in parallel, and the best-fitting individuals are allowed to migrate from one group to another. A modification has been carried out to enhance this performance aspect of the algorithms.

Optimisation in terms of weight is well documented with different optimisation techniques. However, for the frames that are controlled sometime by displacement, it is necessary to formulate a different objective function. In this study, an attempt is made to perform the optimisation in terms of the lateral displacement in addition to minimising the total weight of SPF. To achieve this, a modified DGA maximises the lateral displacement and minimises the total weight of SPF while the constraints meet the requirements of BS 5950 and EC3. The comparison is made between displacement maximisation and weight minimisation to evaluate their efficiency.

The structural response of steel frame is closely related to the behaviour of beam-to-column connections. This necessitates having a realistic connection modelling if an accurate response of the frame is desired. It is common practice to consider either pinned or fully rigid connections in steel framer. However, experiments show that the actual behaviour lies somewhere between these two extremes, which makes the connections somewhat flexible. As a result, in the analysis and design of SPF, it is required to consider semi-rigid joints as a realistic model of the connection. In this study both rigid and semi-rigid joists are considered for frame analysis.

As the value of the moment is relatively high near the columns in steel portal frames, a part of the rafter is haunched to reduce the cost of the steel section. Consequently, this part of the rafter is linearly non-prismatic. In this study, a stiffness matrix is derived for non-prismatic members using a column analogy and a virtual work method to include the haunched part of the rafter in the structural analysis. To eliminate the integration equations of the derived stiffness matrix's elements, it is passed through regression analysis to develop a practical stiffness matrix. The developed stiffness matrix helps to minimise the program iteration and consequently computation time.

For all of above purposes, the DO-DGA (design optimisation with distributed genetic algorithms) software has been developed coded with Visual Basic 6.0. DO-DGA implements the modified DGA and carries out weight minimisation and lateral displacement maximisation according to BS 5950 and EC3 requirements. In addition, it considers both rigid and semi-rigid options as steel connections. A design problem solved by DO-DGA converges to an optimum solution within less than three minutes, which is practicable for daily office-use by structural engineers.

A paper entitled as 'Weight and displacement optimisations of steel portal frames to Eurocode 3 using distributed genetic algorithms' was presented at '8th World Congress on Structural and Multidisciplinary Optimization' in June 2009. The conference was organised by 'International Society for Structural and Multidisciplinary Optimization' in Lisbon, Portugal. The first page is shown below:

8th World Congress on Structural and Multidisciplinary Optimization
June 1 - 5, 2009, Lisbon, Portugal

Weight and displacement optimizations of steel portal frames to Eurocode 3 using distributed genetic algorithms

Honar K. Issa[1] & Fouad A. Mohammad[2]

[1] Nottingham Trent University, Nottingham, UK, honar.issa@ntu.ac.uk
[2] Nottingham Trent University, Nottingham, UK, fouad.mohammad@ntu.ac.uk

1. Abstract
Pitched-roof Steel Portal Frames (SPFs) are common structures used in single storey buildings. It is necessary for this popular steelwork to pass through an optimization process to minimize the total cost of the frame. Optimization in terms of weight is well documented with different optimization techniques. However, approach to displacement maximization is somehow rare. In this paper, an attempt is made to perform optimization in terms of lateral displacements. To achieve this, a modified Distributed Genetic Algorithm (DGA) is used to maximize lateral displacements of the SPF while the constraints meet the requirements of Eurocode 3. Furthermore, software 'DO-DGA' (Design Optimization using DGA) coded by Visual Basic 6.0 has been developed by the authors to loop the optimization process. Although the appearance and form of SPFs are simple, according to Eurocode 3, the same limitations should be checked as in complex structures. A stiffness matrix has been derived for the haunched part of the rafter using a column analogy and a virtual work method to involve this part in the analysis process. Through two benchmark examples, the comparison is made between the results of weight minimization and displacement maximization.
2. Keywords: Distributed genetic algorithm, steel portal frame, optimization, displacement maximization

3. Introduction
Single storey buildings are widely used in the UK; it is estimated that 50% of the single storey steel work buildings are constructed by steel portal frames [1]. Because of its economy and versatility for large spans in construction of pitched roofs such as shopping centers, warehouses, retail shops, pools, factories, etc, the steel portal frame has become the most often used structure within this sector.
Any structural designer attempts to conduct an economical design. This can be achieved by formulating a design problem and solving it by an optimization technique while meeting the requirements of a code of practice to control the safety of the structure [2]. However, due to large number of iterations in implementing the optimization technique, it cannot be achieved by using the designer's experiences and intuition. As it believed that the major cost of structural steelwork is its own weight, approaches to minimizing the weight have become increasingly interesting for the researchers. However, it necessitates choosing different approaches for those types of structure which are controlled by deflection and displacement. Minimizing the weight is relatively well documented in literatures; see for examples [2-7]. To the knowledge of the authors there has not been any attempt to investigate the displacement maximization of the steel structure thus far. In this paper, a modified distributed genetic algorithm (DGA) is implemented to conduct both weight minimization and displacement maximization. Through two benchmark examples, the comparison is made to portray the more effective approach for the design optimization.

4. Distributed genetic algorithms
The basic mechanics of the Genetic Algorithm (GA) is based on randomized procedures of selecting and reproduction of the population of individuals and copying the fittest individuals into the next generation. A GA moves from one generation to another until either a certain individual dominated population or a predetermined maximum number of generations are reached. A basic GA consists of three main operators; reproduction, crossover and mutation. In the reproduction stage, a set of population are selected for mating depending on their fitness values which represent the objective function. If any constraint is violated, a penalty is applied to the objective function. The value of the penalty is related to the degree in which the constraints are violated.
Camp *et al.* [8] used three crossover schemes; fixed, flexible, and uniform to minimize the weight of the structure. The crossover and mutation probabilities were 0.85 and 0.05 and the maximum crossover points was 3. Kameshki and Saka [4] applied a GA for optimum design of unbraced multi-storey frames with semi-rigid beam-to-column connection. They adopted constant values of 0.001 for mutation probability. Toropov and Mahfouz [2] modified GA to improve its rate of convergence. The modified GA was linked to a system of structural design rules, interacting with a finite element package in order to obtain minimum weight designs of plane structural steel

A paper entitled as 'Displacement maximisation of haunched-rafter pitched-roof steel portal frames' was presented at 'Eleventh International Conference on Optimum Design of Structures and Materials in Engineering, OPTI 2009' in June 2009. The conference was organised by 'Wessex Institute of Technology' in Algarve, Portugal. The first page is shown below:

Displacement maximisation of haunched-rafter Pitched-roof Steel Portal Frames

H. K. Issa & F. A. Mohammad
School of Architecture, Design and the Built Environment, Nottingham Trent University, UK

Abstract

Pitched-roof Steel Portal Frames (SPFs) are common structures used in single storey buildings. It is necessary for this popular steelwork to pass through an optimisation process to minimise the total cost of the frame. Optimisation in terms of weight is well documented with different optimisation techniques. However, this approach to displacement maximisation is somehow rare. In this paper, an attempt is made to perform optimisation in terms of lateral displacements. To achieve this, a modified distributed genetic algorithm (DGA) is used to maximise lateral displacements of the SPF while the constraints meet the requirements of BS 5950. Furthermore, software 'DO-DGA' (Design Optimisation using DGA), coded by Visual Basic 6.0, has been developed by the authors to loop the optimisation process. Although the appearance and form of SPFs are simple, according to BS 5950, there are more limitations to be checked than in complex structures. A stiffness matrix has been derived for the haunched part of the rafter using a column analogy and a virtual work method to involve this part in the analysis process. Through two benchmark examples, the comparison is made between the results of weight minimisation and displacement maximisation.

Keywords: distributed genetic algorithm, steel portal frame, optimisation, displacement maximisation.

1 Introduction

Single storey buildings are widely used in the UK; it is estimated that 50% of the single storey steel work buildings are constructed by steel portal frames [12]. Because of its economy and versatility for large spans in the construction of

WIT Transactions on The Built Environment, Vol 106, © 2009 WIT Press
www.witpress.com, ISSN 1743-3509 (on-line)
doi:10.2495/OP090131

A paper entitled as 'Practical non-prismatic stiffness matrix for haunched-rafter pitched-roof steel portal frames' was presented at 'The Fifth International Structural Engineering and Construction Conference' in September 2009. The conference was organised by 'University of Nevada Las Vegas' in Las Vegas, USA. The first page is shown below:

Challenges, Opportunities and Solutions in Structural Engineering and Construction - Ghafoori (ed.)
©Taylor & Francis Group, London, ISBN 978-0-415-56809-8

Practical non-prismatic stiffness matrix for haunched-rafter pitched-roof steel portal frames

Honar K. Issa & Fouad A. Mohammad
Nottingham Trent University, Nottingham, UK

ABSTRACT: Pitched roof steel portal frames are popular structures among single-storey buildings. Since the bending moment at the column-to-rafter joint is very high, the decision is made to haunch a part of the rafter adjacent to the joint. The haunch makes this part of the rafter linear non-prismatic. In this study, a stiffness matrix for non-prismatic members is derived and passed through regression analysis to set up a practical stiffness matrix. A column analogy is used to simulate the bending and shear effects whereas a virtual work method is used to involve axial force effect into the stiffness matrix. After a large amount of data was collected from regression analysis, quadratic coefficients have been obtained to generalize the stiffness matrix for both prismatic and non-prismatic members. The correctness of the obtained stiffness matrix is verified by a simple numerical example.

1. INTRODUCTION

Single-storey frame structures are extensively used in commercial, industrial, and leisure buildings. The nature of those buildings necessitates selecting a structural system which covers the area without intermediate columns. As steel provides an economical solution in those buildings, they are commonly constructed with steel frames (Saka 2003). Pitched roof steel portal frames are the most popular steelwork among the structures used in single-storey buildings. It is estimated that 50% of single-storey buildings are constructed with steel portal frames (Salter et al. 2004). Since the bending moment at the column-to-rafter joint is very high, the decision is made to haunch a part of the rafter adjacent to the joint. The haunch makes this part of the rafter linear non-prismatic. Because of non-uniform distribution of the bending moment in the non-prismatic member, material savings can be achieved, while the cross-section capacity is satisfied. Despite the additional cost of fabrication, the use of a tapered member in structural elements provides a more economical structure than the uniform member (Fraser 1983).

When the direct stiffness method is adopted to fulfill the structure analysis, the stiffness matrix for each element of the structure should be necessarily constituted. The stiffness matrix for prismatic element is well documented in the text books. However, different developed stiffness matrices for non-prismatic members are not somehow practical to use. Saka (2003) implemented the stiffness matrix of non-prismatic member developed by Matheson et al. (1959; cited in Saka 2003) to carry out the optimization process on steel portal frames. Luo et al (2007) adopted the transfer matrix method to a deduced general expression for the components of the stiffness matrix of non-prismatic members. Both developed stiffness matrices require long computation time as the matrices components are in integration form. Hence, in this study, it is attempted to develop a practical and generalized stiffness matrix for both prismatic and non-prismatic members so that it could be brought into office daily use.

A typical pitched roof steel portal frame with a haunched-rafter is depicted in Figure 1.

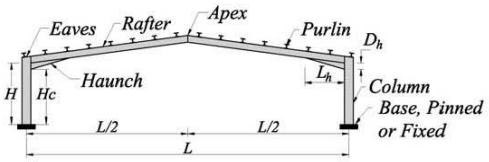

Figure 1. Typical pitched roof steel portal frame

2 STIFFNESS MATRIX

2.1 Prismatic members

The slope deflection method is used to derive the stiffness matrix for prismatic members. For a two-dimensional structure, a prismatic member has six

A paper entitled as 'Effect of mutation schemes on convergence to optimum design of steel frames' has been accepted for publication in the 'Journal of Constructional Steel Research'. The first page is shown below.

ARTICLE IN PRESS

Journal of Constructional Steel Research ▮ (▮▮▮▮) ▮▮▮–▮▮▮

Contents lists available at ScienceDirect

Journal of Constructional Steel Research

journal homepage: www.elsevier.com/locate/jcsr

Effect of mutation schemes on convergence to optimum design of steel frames

Honar K. Issa *, Fouad A. Mohammad

School of Architecture, Design and Built Environment, Nottingham Trent University, UK

ARTICLE INFO

Article history:
Received 27 March 2009
Accepted 4 February 2010

Keywords:
Distributed genetic algorithm
Mutation schemes
Structural optimization

ABSTRACT

In this paper an attempt is made to modify a distributed genetic algorithm (DGA) to minimize the weight of steel frames. The main aspects of modifications include the twin analogy and a number of mutation schemes. Although the mutation is a secondary operator in the GA, it plays an influential role in diversifying the population and exploring more feasible design space. In this research, four different mutation schemes are examined and their effects on convergence to optimum solutions are evaluated. Using three benchmark examples, it is demonstrated that mutation operator can efficiently influence on the speed of convergence and consequently saving computation time. As coding a program is required, the DO-DGA software has been developed to handle the algorithm. DO-DGA applies modified DGA, including different mutation schemes, to obtain the global optimum solution.

1. Introduction

It has been more than three decades that researchers are attempting to implement the optimization techniques to minimize cost of steel structures. During these three decades many techniques have been examined with varied successes. Mathematical programming methods emerged at earlier time, consisting of some different mathematical techniques to launch the optimization process. These techniques are almost based on gradient and deal efficiently with continuous variables. However, most design variables in structural optimization are discrete in nature and using these techniques necessitates discretizing design variables which leads to consuming more time and somewhat inefficient solution. The next generation of optimization technique is optimality criteria method based on Cohen Tucker conditions [1]. Later on, heuristic search methods emerged with different techniques. The main aspect of these methods is to simulate natural phenomena and adopt them in structural optimization.

One of the most efficient techniques is genetic algorithms (GA) which was presented by Goldberg [2]. The core characteristic of the GA is based on the Darwinian "Survival of the Fittest Theory" (survival of the fittest and adaptation). The advantage of GA while dealing with the discrete design variables is the open format for constraint statements and multiple load cases. A GA does not require an explicit relationship between the objective function and the constraints whereas this relationship should be defined when mathematical programming are employed. Another privilege of GA is that there is no need to use the derivative of objective function and constraints. In general, GA has three main operators: reproduction, crossover, and mutation. They launch the operation by first selecting an initial population where each individual is constructed by bringing together the total number of variables respectively in a binary or other code form. Then due to their fitness value, they are selected for a mating pool (reproduction) where the mating of any pairs of individuals takes place (crossover). The next operator to play its role is mutation which is applied to any single gene of individuals with relatively low probability. Mutation is an insurance policy to ensure genetic diversity [2] and allows for the probability that nonexisting features in the parents may be created and passed to the children. Without the mutation operation some of the important region of the solution may never be explored [1]. Although mutation is a secondary operator in GA, it plays an influential role to diversify the population of design variables and explore as much design space as possible.

A probability value should be assigned to both crossover and mutation operators by which the occurrence of both will depend upon. In many recent researches, constant probabilities have been assigned to both operators with varied values. Adeli and Kumar [3] implemented GA to examine its capability to parallelism in a computer system. They made decisions to use a value of 0.0005 as mutation probability. Pezeshk et al. [4] studied design of non-linear framed structure using GA. They used values of 0.85 and 0.01 as crossover and mutation probabilities respectively. Kameshki and Saka [5] adopted constant values of 0.8 for crossover probability and 0.001 for mutation probability. Toropov and Mahfouz [6] made the decision to assign 0.7 and 0.01 to the crossover and mutation probabilities respectively. Saka [7] studied optimum design of pitched-roof steel portal frames. He decided to use crossover and mutation probabilities with values of 0.8 and 0.001 respectively as

* Corresponding author. Tel.: +44 7935424218.
E-mail addresses: honar.issa2@ntu.ac.uk, honar46@yahoo.com (H.K. Issa), fouad.mohammad@ntu.ac.uk (F.A. Mohammad).

0143-974X/$ – see front matter © 2010 Elsevier Ltd. All rights reserved.
doi:10.1016/j.jcsr.2010.02.002

Please cite this article in press as: Issa HK, Mohammad FA. Effect of mutation schemes on convergence to optimum design of steel frames. Journal of Constructional Steel Research (2010), doi:10.1016/j.jcsr.2010.02.002